



Universität Hamburg

DER FORSCHUNG | DER LEHRE | DER BILDUNG

# Total Synthesis of (–)-Aspidospermidine via an Enantioselective Palladium-Catalysed Allylic Substitution Strategy

DISSERTATION

To obtain the academic degree

**DOCTORUM RERUM NATURALIUM**

*Dr. rer. nat.*

Conducted at the Institute of Organic Chemistry, Department of Chemistry,  
Faculty of Mathematics, Informatics and Natural Sciences,

University of Hamburg

Submitted by

**MChem Charlotte O'Donnell**

2024



**Evaluator 1:** Prof. Dr. Christian B. W. Stark

**Evaluator 2:** Prof. Dr. Chris Meier

**Examination committee:** Prof. Dr. Ralph Holl, Prof. Dr. Louisa Temme and Prof. Dr. Christian B. W. Stark

**Date of oral examination:** 13.12.2024

**Date of print release:** 30.12.2024

This thesis was accomplished in the period between October 2019 and March 2024 in the Institute of Organic Chemistry at the University of Hamburg, under the supervision of Prof. Dr. Christian B. W. Stark.

The following publication has resulted from this work:

O'Donnell, C. R., Stark, C. B. W. *Org. Lett.* **2024**, *26*, 9689–9692: Total Synthesis of (–)-Aspidospermidine via an Enantioselective Palladium-Catalyzed Allylic Substitution Strategy

This work has been presented as posters at the following events:

1. 1<sup>st</sup> Berlin MedChem Workshop Nuvisan ICB, Berlin, June 2022
2. ORCHEM 2022, Münster, September 2022
3. GDCh-Wissenschaftsforum Chemie 2023 (WiFo), Leipzig, September 2023
4. HIPS Symposium 2024, Saarbrücken, May 2024
5. 18<sup>th</sup> Belgian Organic Synthesis Symposium (BOSS XVIII), Liège, June 2024



# Table of Contents

<b>Table of Contents</b> .....	<b>VI</b>
<b>Abbreviations, Acronyms and Symbols</b> .....	<b>VIII</b>
<b>Kurzfassung</b> .....	<b>XII</b>
<b>Abstract</b> .....	<b>XIV</b>
1 Introduction.....	1
1.1 Aspidospermidine.....	1
1.1.1 Background.....	1
1.1.2 Isolation and Structural Elucidation.....	2
1.1.3 Biological Activity.....	3
1.1.4 Biosynthetic Hypothesis.....	5
1.1.5 Previous Synthetic Approaches.....	7
1.2 Allylic Substitution Reactions.....	15
1.2.1 General Features.....	15
1.2.2 Pd-Catalysed.....	18
1.2.2.1 Mechanistical Aspects.....	18
1.2.2.2 Ligand Design.....	25
1.2.2.3 Development.....	28
1.2.2.4 3-Substituted Indole Derivatives as Nucleophiles.....	29
2 Planned Synthetic Approach.....	37
2.1 Project Aims.....	39
3 Results and Discussion.....	40
3.1 Preparation of the 3-Substituted Indole Derivative.....	40
3.2 Preparation of the Allylic Alkylation Substrate: Strategy 1.....	42
3.2.1 Approach A.....	43
3.2.1.1 Route 1.....	43
3.2.1.2 Route 2.....	46

3.2.1.3	Route 3.....	49
3.2.2	Approach B .....	53
3.2.2.1	Route 4.....	53
3.2.2.2	Route 5.....	58
3.3	Preparation of the Allylic Alkylation Substrate: Strategy 2 .....	64
3.4	Pd-Catalysed Allylic Substitution Reaction .....	70
3.4.1	Non-Stereoselective Allylic Substitution Reaction.....	70
3.4.2	Enantioselective Allylic Substitution Reaction.....	74
3.5	Mannich Reaction.....	84
3.6	<i>Exo-to-Endo</i> Double Bond Migration .....	86
3.7	Ring-Closing Sequence .....	106
3.8	Deoxygenation.....	111
4	Summary and Outlook .....	115
4.1	Summary.....	115
4.2	Outlook .....	120
5	Experimental.....	124
5.1	General Experimental Conditions .....	124
5.2	Synthetic Procedures .....	126
6	References.....	208
7	Appendices.....	222
7.1	Chiral HPLC Chromatograms .....	222
7.2	List of Hazardous Substances.....	224
7.3	Acknowledgments .....	234
7.4	Statutory Declaration.....	235

## Abbreviations, Acronyms and Symbols

2D	two dimensional	ddt	doublet of doublets of triplets (spectroscopic)
3 Å MS	3 Å molecular sieves	DEAD	diethyl azodicarboxylate
9-BBN	9-borabicyclo[3.3.1]nonane	DIAD	diisopropyl azodicarboxylate
A <sup>1,3</sup>	1,3-allylic strain	DIBAL	diisobutylaluminium hydride
Ac	acetyl	DIP	direct insertion probe
app.	apparent (spectroscopic)	DIPA	diisopropylamine
aq.	aqueous	DIPEA	<i>N,N</i> -diisopropylethylamine
ATR	attenuated total reflectance	DMAP	4-dimethylaminopyridine
BINAP	2,2'-bis(diphenylphosphino) 1,1'-binaphthyl	DMF	dimethylformamide
Bn	benzyl	DMP	Dess–Martin periodinane
Boc	<i>tert</i> -butyloxycarbonyl	DMSO	dimethyl sulfoxide
brsm	based on recovered starting material	dt	doublet of triplets (spectroscopic)
Bu	butyl	DTBMP	2,6-di- <i>tert</i> -butyl-4-methylpyridine
<i>c</i>	concentration in grams per 100 millilitres	DYKAT	dynamic kinetic asymmetric transformation
calcd	calculated	e.r.	enantiomeric ratio
CAN	ceric ammonium nitrate	ee	enantiomeric excess
cm <sup>-1</sup>	wavenumber/s	EI	electron ionisation
cod	1,5-cyclooctadiene	eq.	equivalent
COSY	correlation spectroscopy	ESI	electrospray ionisation
CSA	camphorsulfonic acid	Et	ethyl
d	doublet (spectroscopic)	FT-IR	Fourier-transform infrared spectroscopy
d.r.	diastereomeric ratio	g	gram/s
DAAA	decarboxylative asymmetric allylic alkylation	GCMS	gas chromatography–mass spectrometry
DABCO	1,4-diazabicyclo[2.2.2]octane	Glc	glucosyl
DACH	1,2-diaminocyclohexane	h	hour/s
dba	<i>trans,trans</i> -dibenzylideneacetone	hept	heptet
DBU	1,8 diazabicyclo[5.4.0]undec-7-ene	HMBC	heteronuclear multiple bond correlation
dd	doublet of doublets (spectroscopic)	HMDS	hexamethyldisilazane
ddd	doublet of doublets of doublets (spectroscopic)	HPLC	high-performance liquid chromatography
dddd	doublet of doublets of doublets of doublets (spectroscopic)	HRMS	high resolution mass spectrometry
DDQ	2,3-dichloro-5,6-dicyano- 1,4-benzoquinone	HSQC	heteronuclear single quantum coherence

Hz	hertz	PG	protecting group
<i>i</i> -	<i>iso</i> -	Ph	phenyl
IBX	2-iodoxybenzoic acid	PHOX	phosphinooxazoline
IC <sub>50</sub>	half maximal inhibitory concentration	PMB	<i>p</i> -methoxybenzyl
IR	infrared	ppm	parts per million
<i>J</i>	coupling constant (spectroscopic)	Pr	propyl
LDA	lithium diisopropylamide	q	quartet (spectroscopic)
LG	leaving group	qd	quartet of doublets (spectroscopic)
lit.	literature value	qdd	quartet of doublets of doublets (spectroscopic)
L <sub>n</sub>	ligand (n = number of)	qt	quartet of triplets (spectroscopic)
M	molar (moles per litre)	qtt	quartet of triplets of triplets (spectroscopic)
m	milli	quant.	quantitative
m	multiplet (spectroscopic)	R	alkyl group
m.p.	melting point	R <sub>f</sub>	retention factor (chromatography)
<i>m/z</i>	mass to charge ratio	rt	room temperature
<i>m</i> CPBA	<i>meta</i> -chloroperoxybenzoic acid	s	singlet (spectroscopic)
Me	methyl	SET	single-electron transfer
MEP	non-mevalonate pathway	<i>T</i>	temperature
MHz	megahertz	t	triplet (spectroscopic)
min	minute/s	<i>t</i> -	<i>tert</i> (tertiary)
mol	mole/s	TBAF	tetra- <i>n</i> -butylammonium fluoride
mol%	molar percentage	TBD	1,5,7-triazabicyclo[4.4.0]dec-5-ene
MPO	4-methoxypyridine <i>N</i> -oxide	TBHP	<i>tert</i> -butyl hydroperoxide
MS	mass spectrometry	TBS	<i>tert</i> -butyldimethylsilyl
MTBE	methyl <i>tert</i> -butyl ether	td	triplet of doublets (spectroscopic)
<i>n</i> -	normal-	TES	triethylsilyl
n	nano	TFA	trifluoroacetic acid
n.d.	not determined	TFAA	trifluoroacetic anhydride
Naph	naphthalene	THF	tetrahydrofuran
NBS	<i>N</i> -bromosuccinimide	TIPS	triisopropylsilyl
NMR	nuclear magnetic resonance	TLC	thin layer chromatography
NOE	nuclear Overhauser effect	TMEDA	<i>N,N,N',N'</i> -tetramethylethylenediamine
NOESY	nuclear Overhauser effect spectroscopy	TMS	trimethylsilyl
Nu	nucleophile	t <sub>R</sub>	retention time
OPMP	<i>p</i> -methoxyphenol	TRIS	tris(hydroxymethyl)aminomethane
<i>p</i> -	para	tt	triplet of triplets (spectroscopic)
pfb	perfluorobutyrate	UV	ultraviolet

wt.%	weight percentage	$\lambda$	wavelength
Zn*	Rieke zinc	$\mu$	micro
$\Delta$	heat	$\nu_{\max}$	absorption maxima (wavenumbers)
$\delta$	chemical shift (in parts per million downfield from trimethylsilane)	$[\alpha]_D^{20}$	specific rotation at 589 nm (sodium D line) and at 20 °C

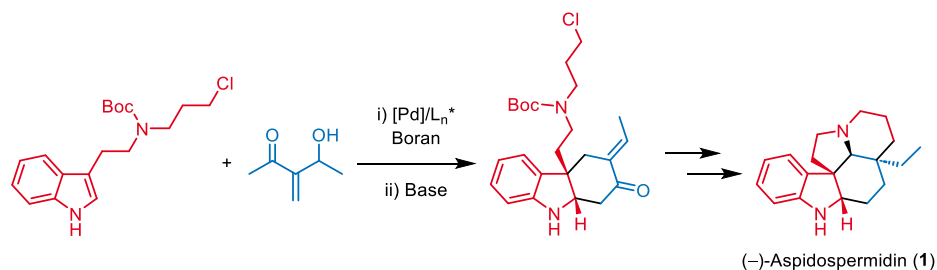


## Kurzfassung

Seit der Isolierung von (+)-Aspidospermidin (**1**) im Jahre 1961, ist der Naturstoff zu einem Prüfstein neuer Synthesemethoden beim Zugang zu *Aspidosperma*-Alkaloiden geworden. Allylische Substitutionsreaktionen sind potente Transformationen in der katalytisch asymmetrischen Chemie. Das Ziel der vorliegenden Arbeit bestand darin, erstmals eine enantioselektive Pd-katalysierte allylische Substitutionsreaktion mit einem 3-substituierten Indolderivat in der Totalsynthese von (-)-Aspidospermidin (**1**) zu etablieren.

Bei der Untersuchung der allylischen Substitutionsreaktion wurde eine neue Klasse von allylischen Alkylierungs substraten entdeckt, die den Anwendungsbereich dieser effizienten Reaktion erweitert. Die allylische Substitutionsreaktion wurde zunächst in racemischer Form entwickelt und im weiteren Verlauf asymmetrisch ausgearbeitet (e.r. von 91:9). Mittels dieser enantioselektiven allylischen Substitutionsreaktion wurde nicht nur das erste quaternäre Kohlenstoff-Stereozentrum des Naturstoffs aufgebaut, sondern auch das Gesamtgerüst von Aspidospermidin (**1**) assembliert. Die pentacyclische Architektur wurde dabei in einer effizienten diastereoselektiven Sequenz bestehend aus einer Redox-getriebenen Doppelbindungsmigration, einer Aza-Michael-Addition und einer Enolatalkylierung aufgebaut. Eine finale Desoxygenierung lieferte erfolgreich den Naturstoff (**1**).

Die hier beschriebene Totalsynthese ist mit sieben linearen Stufen, ausgehend von kommerziell erhältlichen Ausgangsverbindungen, die kürzeste bisher beschriebene enantioselektive Synthese von Aspidospermidin (**1**). Den Schlüsselschritt der Sequenz stellt die allylische Substitutionsreaktion dar: Die weiteren Stereozentren des Naturstoffs wurden unter Substratkontrolle etabliert. Darüber hinaus ist dies die erste Anwendung einer Pd-katalysierten allylischen Substitution mit einem 3-substituierten Indolderivat in der Synthese von Aspidospermidin (**1**) und im weiteren Sinne von *Aspidosperma*-Alkaloiden. In zukünftigen Arbeiten könnte dieser Ansatz für effiziente enantioselektive Synthesen anderer Mitglieder der *Aspidosperma*-Alkaloidfamilie genutzt werden.



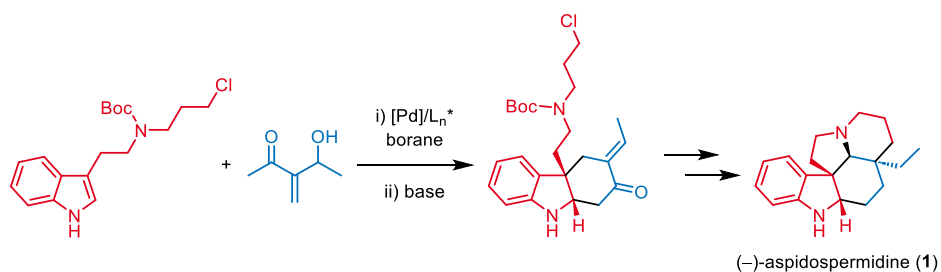


## Abstract

Since the isolation of (+)-aspidospermidine (**1**) in 1961, its synthesis has become the proving ground for the development of novel synthetic methodologies to access members of the *Aspidosperma* alkaloid family. Allylic substitution reactions represent powerful transformations in catalytic asymmetric chemistry. The aim of this work was to apply an enantioselective Pd-catalysed allylic substitution reaction with a 3-substituted indole derivative for the first time in the total synthesis of aspidospermidine (**1**).

From studies into the key allylic substitution reaction, a novel substrate class of allylic alkylation substrates was uncovered, thus expanding the scope of this powerful chemical transformation. The allylic substitution reaction was initially developed in a racemic manner and then rendered enantioselective (e.r. of 91:9). The enantioselective allylic substitution reaction not only constructed the first quaternary carbon stereocentre but also assembled the entire framework of aspidospermidine (**1**). The pentacyclic architecture was then constructed in an efficient and diastereoselective sequence, featuring a redox-driven double bond migration, an *aza*-Michael addition and an enolate alkylation. A final deoxygenation furnished the natural product (**1**).

This culminated in the shortest enantioselective synthesis of aspidospermidine (**1**) reported to date, in seven linear steps from commercially available starting materials. In this pathway, the allylic substitution reaction acted as the key stereo defining step. The remaining stereocenters of the natural product were then established under substrate control. Furthermore, this strategy is the first application of a Pd-catalysed allylic substitution reaction with a 3-substituted indole derivative in the synthesis of aspidospermidine (**1**) and more broadly of *Aspidosperma* alkaloids. It is envisioned that this novel strategy could be employed for efficient enantioselective syntheses of other members of the *Aspidosperma* alkaloid family.





## 1 Introduction

### 1.1 Aspidospermidine

#### 1.1.1 Background

Alkaloids are naturally occurring nitrogen-containing basic compounds. They are mostly of plant origin, but are found to a lesser extent in animals and microorganisms.<sup>[1,2]</sup> Alkaloids are classified according to their nitrogen-containing structures, with those containing indole moieties known as indole alkaloids.<sup>[2,3]</sup> Indole alkaloids are one of the largest alkaloid classes and contain a vast array of natural products with diverse biological activities,<sup>[3,4]</sup> including antimalarial<sup>[5]</sup> and antiviral properties,<sup>[6]</sup> thus representing an area of great synthetic interest.<sup>[7,8]</sup>

*Aspidosperma* alkaloids are the largest family of monoterpene indole alkaloids, with over 250 known compounds.<sup>[9,10]</sup> The *Aspidosperma* family is composed of seven subclasses; the structural framework of each subclass is exemplified by its parent compound: aspidospermidine (**1**), aspidofractinine (**2**), quebrachamine (**3**), vincadifformine (**4**), vindolinine (**5**), meloscine (**6**) and kopsine (**7**) (Figure 1).<sup>[9]</sup>

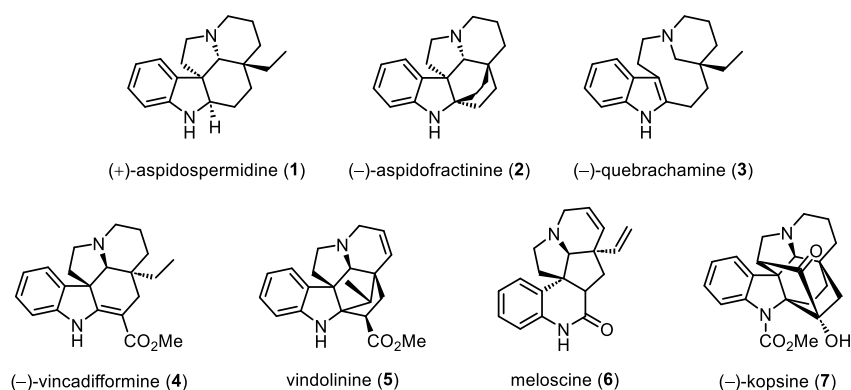


Figure 1. Parent compounds of the *Aspidosperma* alkaloid subclasses.

Aspidospermidine (**1**) is the parent compound of the largest subclass.<sup>[9]</sup> The aspidospermidine subclass has a pentacyclic framework characterised by the [6.5.6.5.6] ABCDE ring system, with four contiguous stereocentres (Figure 2).<sup>[11–13]</sup> The aspidospermidine subclass are composed of a tryptamine (**8**) unit and a C<sub>9</sub> or C<sub>10</sub> unit derived from the terpenoid secologanin (**9**) (Figure 2).<sup>[2,8]</sup>

## Introduction

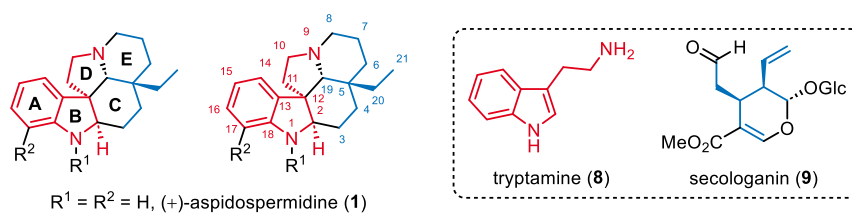


Figure 2. ABCDE pentacyclic framework and numbering of aspidospermidine subclass according to Spiteller and co-workers;<sup>[13]</sup> tryptamine-derived unit in red and C<sub>9</sub> secologanin-derived unit in blue. Structures of tryptamine (**8**) and secologanin (**9**) shown in insert. Glc = glucosyl.

The construction of the pentacyclic framework of the aspidospermidine subclass has attracted significant attention;<sup>[14]</sup> there has been a particularly intense interest in the synthesis of the parent compound, aspidospermidine (**1**).<sup>[12,15,16]</sup> Novel synthetic methodologies towards *Aspidosperma* alkaloids are often exemplified by a synthesis of aspidospermidine (**1**), as the most popular target within the *Aspidosperma* family.<sup>[11,17]</sup>

### 1.1.2 Isolation and Structural Elucidation

Aspidospermidine (**1**) was first isolated from the bark of the South American tree *Aspidosperma quebracho blanco* by Spiteller and co-workers in 1961.<sup>[18,19]</sup> *A. quebracho blanco* is a rich source of *Aspidosperma* alkaloids and approximately twenty alkaloids including (–)-aspidospermine (**10**) and (–)-quebrachamine (**11**) were isolated in the same study (Figure 3). Fifteen of the isolated alkaloids were further investigated with their structural elucidation performed by UV-vis and mass spectroscopy.<sup>[18]</sup> In 1963, Spiteller and co-workers named isolated alkaloid **1** ‘aspidospermidine’. In the same year, Smith and co-workers determined the specific rotation of isolated aspidospermidine (**1**) ( $[\alpha]_D^{20} +17^\circ$ , in ethanol).<sup>[20]</sup> The absolute configuration of the *Aspidosperma* framework was proposed by Schmid and co-workers in 1963, by correlation of the molecular rotations of *Aspidosperma* alkaloids with related strychnine alkaloids.<sup>[21]</sup> This was further supported by optical rotatory dispersion curve studies in 1965.<sup>[22]</sup> The proposed absolute configuration was then confirmed by X-ray diffraction in 1968.<sup>[23]</sup> (+)-Aspidospermidine (**1**) has since been isolated from other plant species, including *Aspidosperma rhombeosignatum*<sup>[24]</sup> and *album*<sup>[25]</sup> and *Melodinus morsei*.<sup>[26]</sup>

## Introduction

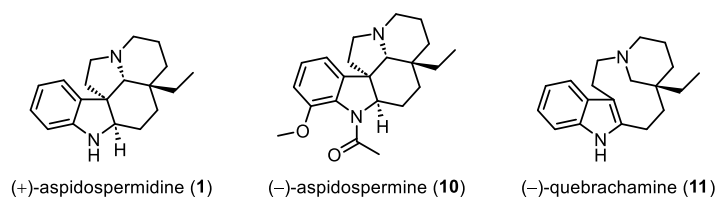


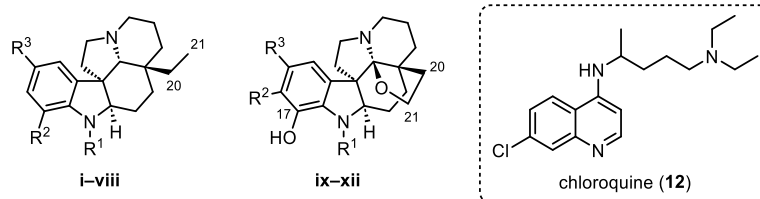
Figure 3. Structures of *Aspidosperma* alkaloids isolated from *Aspidosperma quebracho blanco*: (+)-aspidospermidine (**1**), (-)-aspidospermine (**10**) and (-)-quebrachamine (**11**).

### 1.1.3 Biological Activity

(+)-Aspidospermidine (**1**) (**i** in Table 1) and other structurally-related *Aspidosperma* alkaloids were shown to exhibit antiplasmodial activity against two strains of *Plasmodium falciparum*, the parasite responsible for the most severe forms of malaria.<sup>[27]</sup> The resistance of *P. falciparum* to traditional antimalarial treatments, such as chloroquine (**12**), has driven the search for antimalarial compounds of natural origin. Within this study, the *Aspidosperma* alkaloids with an ethyl group, composed of C20 and C21, (**i–v**, **vii** and **viii**) were found to have lower IC<sub>50</sub> values and hence higher antiplasmodial activities against a chloroquine-resistant and a chloroquine-sensitive strain of *P. falciparum*. Whereas the *Aspidosperma* alkaloids with a fused tetrahydrofuran (THF) ring, containing C20 and C21, and a hydroxy group at C17 (**ix–xii**) were found to have higher IC<sub>50</sub> values and hence lower antiplasmodial activity against both tested strains of *P. falciparum*. In order to determine whether the THF ring, in place of the Et group, or the hydroxy group at C17 was responsible for the lower antiplasmodial activity, the methoxy group at C17 in aspidospermine (**v**) was demethylated giving a phenol group at C17 in derivative **vi**. The antiplasmodial activity of derivative **vi** was found to be similar to that of the more active alkaloids with the free Et group (**i–viii**). Therefore, it was proposed that the replacement of the free Et group by the fused THF ring was responsible for the lower antiplasmodial activity of the alkaloids against the two tested strains of *P. falciparum*. Additionally, alkaloids **iii** and **v** were tested for their chloroquine-potentiating activities and were both found to display a chloroquine-potentiating effect when used together with chloroquine (**12**) against the chloroquine-resistant strain of *P. falciparum*. Zèches-Hanrot and co-workers proposed that the antiplasmodial activity of other *Aspidosperma* alkaloids, and their derivatives, should be evaluated for use as antimalarial agents and, potentially, for use as agents for the reversal of chloroquine-resistance.<sup>[27]</sup>

## Introduction

Table 1. Structures of *Aspidosperma* alkaloids evaluated for their antiplasmodial activity against two strains of *Plasmodium falciparum*. Structure of chloroquine (**12**) shown in insert.



Alkaloid	R <sup>1</sup>	R <sup>2</sup>	R <sup>3</sup>	Chloroquine-resistant (445 nM) <sup>a</sup>		Chloroquine-sensitive (79 nM) <sup>a</sup>	
				IC <sub>50</sub> μM ± sd		IC <sub>50</sub> μM ± sd	
				24 h	72 h	24 h	72 h
<b>i<sup>b</sup></b>	H	H	H	16.3 ± 2.9	3.8 ± 0.7	11.0 ± 1.7	4.6 ± 0.5
<b>ii</b>	H	H	OCH <sub>3</sub>	19.5 ± 7.2	3.2 ± 0.9	13.1	5.1
<b>iii</b>	CHO	H	H	16.1 ± 3.0	5.6 ± 0.7	22.0 ± 7.1	5.9 ± 1.5
<b>iv</b>	CHO	OCH <sub>3</sub>	H	11.8 ± 0.9	4.1 ± 0.6	9.3 ± 2.4	6.6 ± 1.4
<b>v<sup>b</sup></b>	C(O)CH <sub>3</sub>	OCH <sub>3</sub>	H	22.3 ± 11.6	5.6 ± 1.3	n.d.	n.d.
<b>vi</b>	C(O)CH <sub>3</sub>	OH	H	15.1 ± 1.9	12.2 ± 5.2	21.5 ± 6.5	20.3 ± 6.2
<b>vii</b>	C(O)CH <sub>3</sub>	H	H	7.4	6.2	34.0	15.4
<b>viii</b>	C(O)C <sub>2</sub> H <sub>5</sub>	OCH <sub>3</sub>	H	15.4 ± 4.2	12.7 ± 4.2	27.2	8.7
<b>ix</b>	C(O)C <sub>2</sub> H <sub>5</sub>	H	H	17.7 ± 4.9	28.5 ± 13.0	40.8 ± 3.8	22.6 ± 2.5
<b>x</b>	C(O)C <sub>2</sub> H <sub>5</sub>	OCH <sub>3</sub>	H	52.8 ± 7.1	25.6 ± 2.7	113.1	55.3
<b>xi</b>	C(O)C <sub>2</sub> H <sub>5</sub>	OCH <sub>3</sub>	OCH <sub>3</sub>	90.4 ± 43.7	59.2 ± 5.4	44.4	28.0
<b>xii</b>	C(O)CH <sub>3</sub>	OCH <sub>3</sub>	H	149.7 ± 27.6	49.5 ± 3.7	169.3	57.3

<sup>a</sup>Chloroquine-resistant and chloroquine-sensitive strains with IC<sub>50</sub> values for chloroquine of 445 nM and 79 nM, respectively. <sup>b</sup>In the publication alkaloids **i** and **v** were both named as aspidospermine, however according to their substituents alkaloid **i** is in fact (+)-aspidospermidine (**1**) and alkaloid **v** is (-)-aspidospermine (**10**).

Since aspidospermidine (**1**) possesses the core framework of its subclass, its synthesis has become the proving ground for the development of novel synthetic methodology to access other

## Introduction

members of the *Aspidosperma* family,<sup>[11]</sup> which may exhibit important biological activities.<sup>[27]</sup> Bisindole *Aspidosperma* alkaloids (+)-vinblastine (**13**) and (+)-vincristine (**14**), which contain the (–)-aspidospermidine (**1**) and quebrachamine (**11**) frameworks in their ‘monomeric’ units (Figure 4), both display anti-cancer activity and had early clinical success. Unfortunately, (+)-vinblastine (**13**) and (+)-vincristine (**14**) both display serious side-effects. However, the synthesis of vinblastine (**13**) allowed for studies into its mode of action, which led to the development of its derivative: vinorelbine (navelbine) (**15**).<sup>[28]</sup> Vinorelbine (**15**) is used as a chemotherapy drug in the treatment of lung and breast cancers.<sup>[29]</sup>

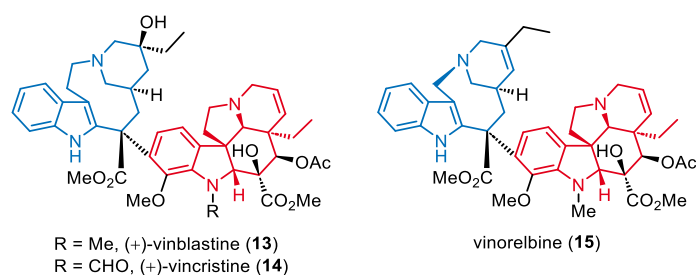
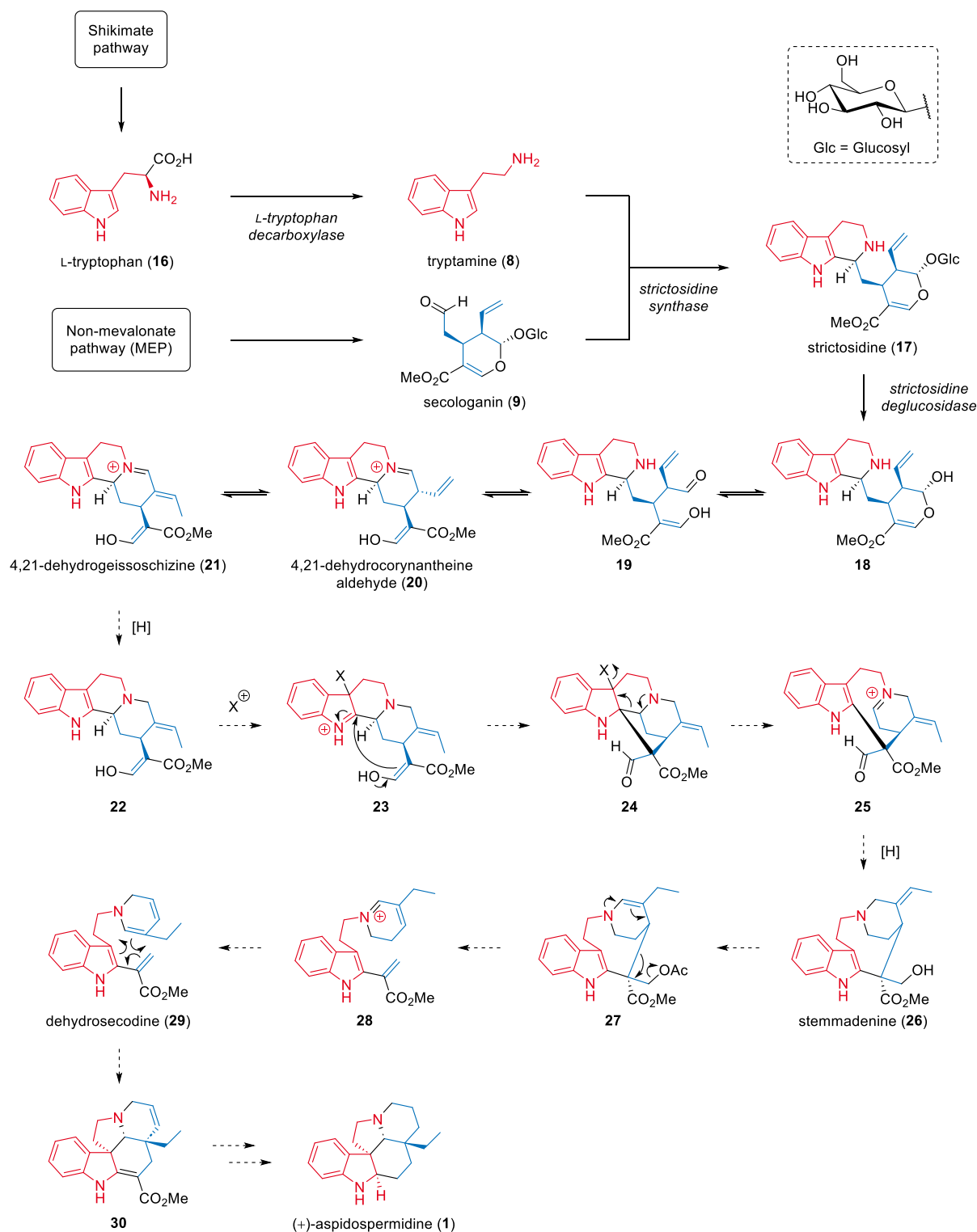


Figure 4. Structures of (+)-vinblastine (**13**), (+)-vincristine (**14**) and vinorelbine (**15**) with the (–)-aspidospermidine (**1**) and quebrachamine (**11**) frameworks shown in red and blue, respectively.

### 1.1.4 Biosynthetic Hypothesis

As aforementioned, the framework of the aspidospermidine subclass is composed of a tryptamine-derived unit and a C<sub>9</sub> or C<sub>10</sub> secologanin-derived unit (Figure 2). The terpenoid secologanin (**9**) is produced from the non-mevalonate pathway (MEP) in plants.<sup>[30,31]</sup> The tryptamine-derived unit originates from the amino acid L-tryptophan (**16**), which is produced from the Shikimate pathway in plants and microorganisms (Scheme 1).<sup>[32]</sup> L-Tryptophan (**16**) is converted to tryptamine (**8**) by the enzyme tryptophan decarboxylase.<sup>[2]</sup>

## Introduction



Scheme 1. Proposed biosynthetic pathway to (+)-aspidospermidine (1). Glc = glucosyl.

A stereoselective Pictet–Spengler condensation between tryptamine (8) and secologanin (9), catalysed by strictosidine synthase, gives the intermediate strictosidine (17).<sup>[33–38]</sup> Strictosidine (17) is then deglycosylated, by strictosidine deglycosidase, forming a reactive hemiacetal intermediate 18 that opens to give the aldehyde intermediate 19. Intramolecular

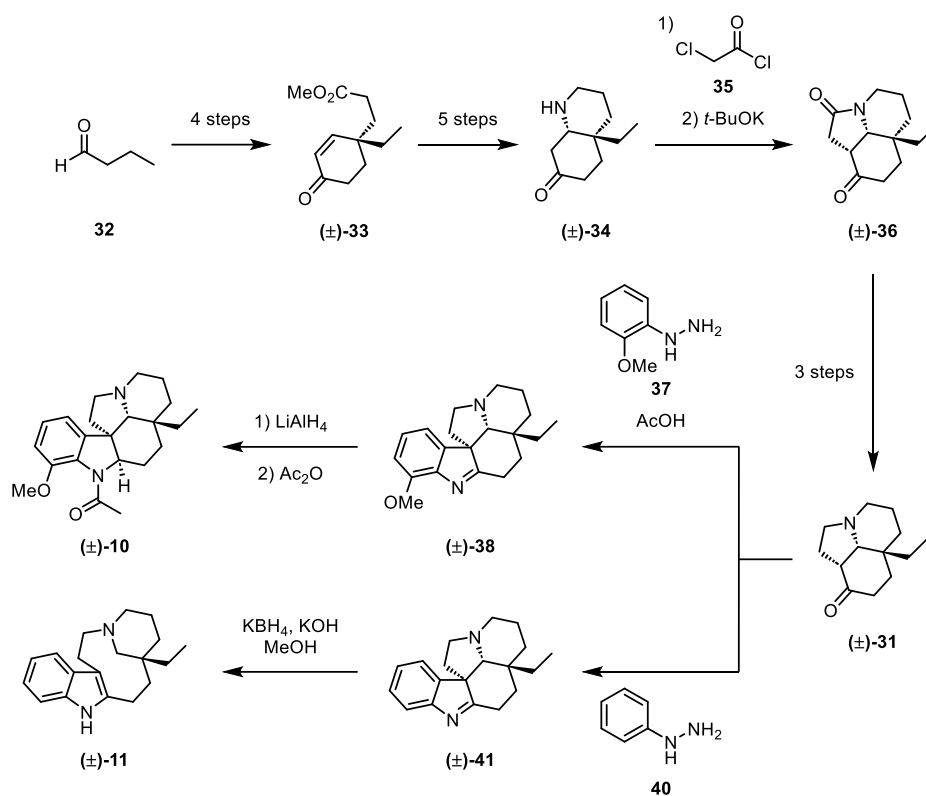
nucleophilic attack from the secondary amine to the aldehyde intermediate **19** gives the iminium ion 4,21-dehydrocorynantheine aldehyde (**20**). Isomerisation of the terminal double bond in 4,21-dehydrocorynantheine aldehyde (**20**) affords the conjugated 4,21-dehydrogeissoschizine (**21**).<sup>[39]</sup> Subsequent reduction would then give intermediate **22**, which would undergo an electrophilic addition at the 3-position of the indole generating indoleninium **23**. An enol addition at the 2-position would then construct the pentacyclic intermediate **24**, the framework is however proposed to spontaneously fragment via a Grob fragmentation thus restoring aromaticity in iminium ion **25**. Reduction of the iminium ion and aldehyde moieties would yield stemmadenine (**26**). Acetylation of the hydroxy group and an *exo*-to-*endo* double bond isomerisation would result in the opening of the macrocycle. An isomerisation would then give the acrylic ester dehydrosecodine (**29**).<sup>[10,40,41]</sup> It is proposed that dehydrosecodine (**29**) could undergo an intramolecular Diels–Alder reaction to construct the *Aspidosperma* pentacyclic framework; however, there is not yet any evidence for this occurring in plants.<sup>[39]</sup> Subsequent ester hydrolysis, decarboxylation and reduction would furnish aspidospermidine (**1**). Although extensive studies into the biosynthetic pathways to *Aspidosperma* alkaloids were conducted in the 1960's and 1970's, no enzymes for the construction of the *Aspidosperma* framework from 4,21-dehydrogeissoschizine (**21**) were identified.<sup>[39,42]</sup>

From the *Aspidosperma* framework, all *Aspidosperma* alkaloids can be obtained through appropriate transformations. This biosynthetic pathway exemplifies the efficiency and elegance of nature's divergent strategy towards *Aspidosperma* alkaloids; thus, there has been substantial interest in harnessing these aspects in a divergent, biomimetic route towards *Aspidosperma* alkaloids.<sup>[10]</sup>

### 1.1.5 Previous Synthetic Approaches

The foundations for the synthesis of *Aspidosperma* alkaloids were laid by Stork and Dolfini in 1963, with their total syntheses of (±)-aspidospermine (**10**) and (±)-quebrachamine (**11**) (Scheme 2).<sup>[43,44]</sup> Their strategy of constructing the pentacyclic framework through a Fischer indole synthesis with phenylhydrazine derivatives and aminoketone intermediate **31**—the Stork intermediate—has dominated synthetic routes to *Aspidosperma* alkaloids.<sup>[45]</sup>

## Introduction



Scheme 2. Total synthesis of (±)-aspidospermine (**10**) and (±)-quebrachamine (**11**) reported by Stork and Dolfini.<sup>[43]</sup>

In this synthesis, aminoketone **31** was produced from butanal (**32**) in 14 steps. Two sequential Stork enamine alkylations of butanal (**32**) with methyl acrylate and methyl vinyl ketone afforded ester **33**, crucially with the first quaternary carbon stereocentre formed. Ester **33** was converted to the corresponding *cis*-fused amine **34**, via an aminolysis, amide reduction and *aza*-Michael addition sequence. A piperidine *N*-acylation with chloroacetyl chloride (**35**) and subsequent cyclisation constructed the tricyclic framework in amide **36**. An amide reduction then yielded the aminoketone **31**, which was submitted to the key Fischer indole synthesis. In which, employing 2-methoxyphenylhydrazine (**37**) gave pentacycle **38**, which upon imine reduction and acetylation afforded (±)-aspidospermine (**10**). Whereas, using phenylhydrazine (**40**) gave pentacycle **41**, which upon reductive cleavage furnished (±)-quebrachamine (**11**).

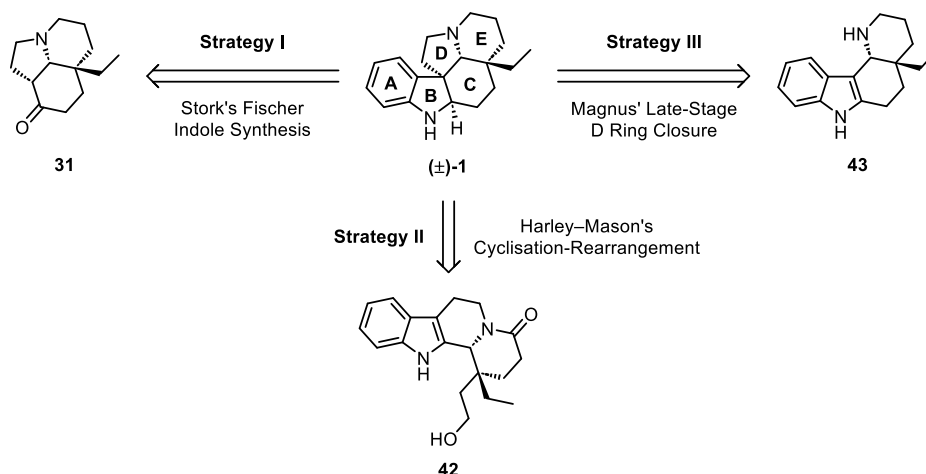
## Introduction

Since the seminal work of Stork and Dolfini, the related compound aspidospermidine (**1**) has become a popular synthetic target within *Aspidosperma* alkaloids, with over fifty reported syntheses in both racemic and enantioselective fashion.<sup>[17,44–48]</sup> Many of these syntheses can be broadly divided into three main strategies (Scheme 3):<sup>[15,16]</sup>

Strategy I: Stork's Fischer indole synthesis

Strategy II: Harley–Mason's cyclisation-rearrangement

Strategy III: Magnus' late-stage D ring closure

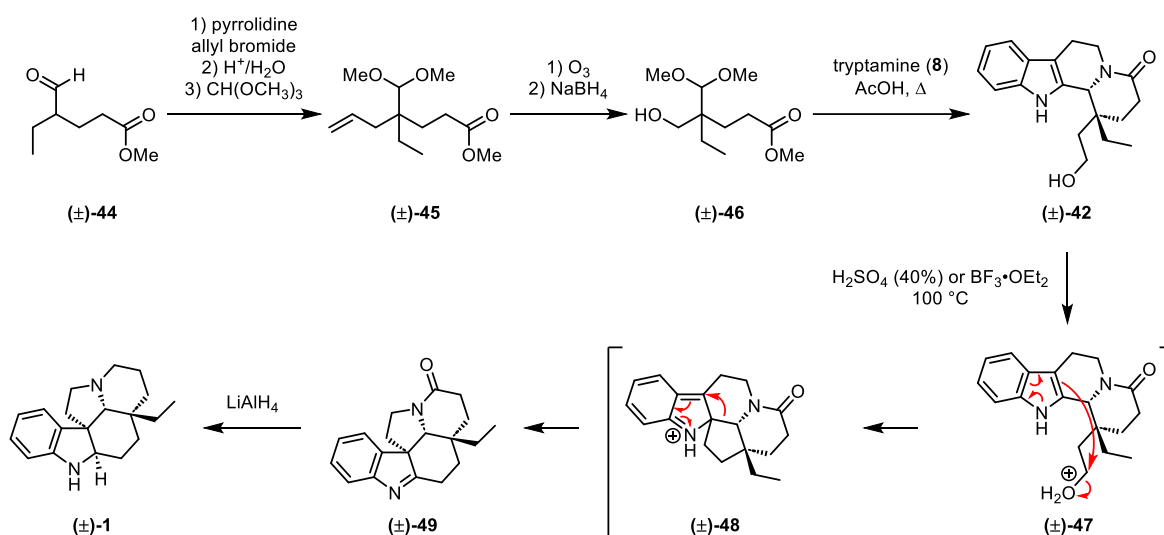


Scheme 3. Three main strategies for the synthesis of aspidospermidine (**1**). Adapted from <sup>[15,16]</sup>.

Strategy I has been employed in numerous total syntheses of aspidospermidine (**1**), with alternative routes to preparing Stork intermediate **31**, followed by the Fischer indole synthesis with phenylhydrazine (**40**) and subsequent reduction to afford aspidospermidine (**1**).<sup>[12,14,49–62]</sup>

Strategy II was first reported in 1967 by Harley–Mason and co-workers in the synthesis of  $(\pm)$ -aspidospermidine (**1**) from prepared aldehyde **44** (Scheme 4).<sup>[63,64]</sup> Aldehyde **44** was alkylated with allyl bromide via the pyrrolidine enamine and then converted to the corresponding dimethyl acetal **45**. Ozonolysis followed by borohydride reduction gave alcohol **46**. An acid-promoted cyclisation-rearrangement sequence between alcohol **46** and tryptamine (**8**) was performed, in which the carbon directly bonded to the activated hydroxy group underwent an  $S_N2$  displacement from the 2-position of the indole. A 1,2-shift then constructed the CDE rings in pentacycle **49**. A final reduction furnished  $(\pm)$ -aspidospermidine (**1**).<sup>[47,64]</sup> Strategy II has since been utilised in other syntheses of aspidospermidine.<sup>[65–70]</sup>

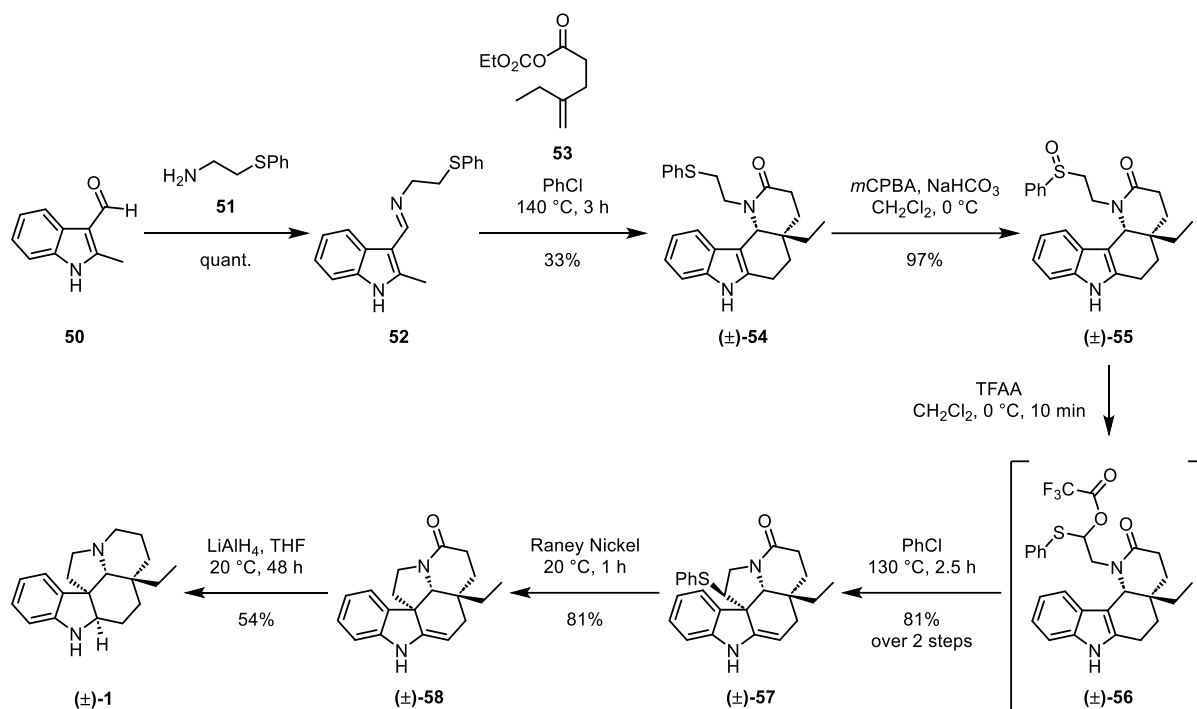
## Introduction



Scheme 4. Synthesis of (±)-aspidospermidine (**1**) via Strategy II.<sup>[64]</sup>

Strategy III features late-stage D ring formation, after construction of the ABCE ring system. Strategy III was originally reported by Magnus and co-workers in 1982 in their total synthesis of (±)-aspidospermidine (**1**) (Scheme 5). Their synthesis began with the condensation of 3-formyl-2-methylindole (**50**) with 2-(phenylthio)ethylamine (**51**), giving imine **52**. Treatment of imine **52** with the mixed anhydride **53** resulted in a nucleophilic acyl substitution followed by a Diels–Alder reaction, stereoselectively constructing the *cis*-fused E ring in tetracycle **54**. Oxidation of the sulfide in tetracycle **54** afforded the corresponding sulfoxide **55** as a mixture of diastereomers. Upon treatment with trifluoroacetic anhydride, sulfoxide **55** underwent a Pummerer rearrangement, forming the  $\alpha$ -acyloxy-thioether **56**, which cyclised *in situ* via a nucleophilic attack from the indole 3-position, thus installing the D ring in intermediate **57**. A desulfurisation and final reduction then yielded (±)-aspidospermidine (**1**).<sup>[71]</sup> Strategy III has been employed in various syntheses of aspidospermidine (**1**), with alternative strategies for constructing the ABCE ring system and for late-stage installation of the D ring.<sup>[11,72–83]</sup>

## Introduction



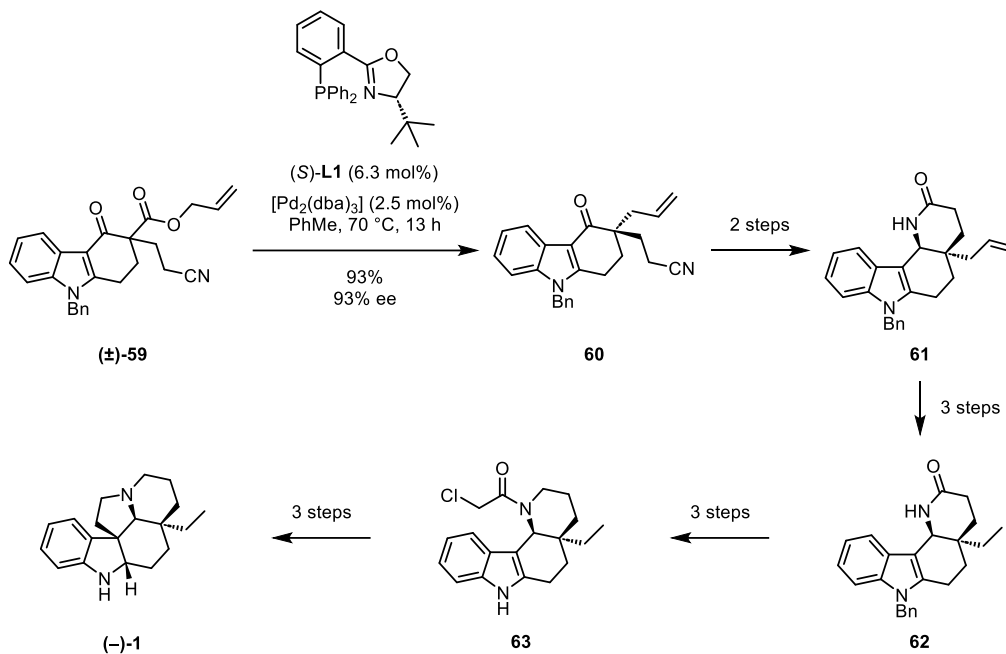
Scheme 5. Total synthesis of (±)-aspidospermidine (**1**) via Strategy III.<sup>[71]</sup>

There are also reported syntheses of aspidospermidine (**1**) that do not fall into strategies I, II or III.<sup>[28,84–88]</sup> Remarkably, out of all of the reported syntheses to aspidospermidine (**1**), relatively few employ catalytic enantioselective strategies.<sup>[51,53,73,74,78,81,89–91]</sup> Examples that employ asymmetric transition-metal catalysed transformations include Pd-catalysed decarboxylative asymmetric allylic alkylation (DAAA) strategies<sup>[73,81,92,93]</sup> and Zhang and co-workers' Ir-catalysed allylic substitution and homo-Mannich sequence.<sup>[94]</sup>

The first enantioselective synthesis of aspidospermidine (**1**) that employed the Pd-catalysed DAAA methodology was reported by Shao and co-workers in 2013. In which the Pd-catalysed DAAA methodology was adapted for carbazolone substrates using the chiral phosphinooxazoline (PHOX) ligand (*S*)-**L1**. Upon submitting carbazolone **59** to their Pd-catalysed DAAA procedure, the tricyclic intermediate **60** was obtained, with the key quaternary carbon stereocentre set (Scheme 6). A mild hydrolysis of the nitrile group to the corresponding amide, followed by a chemoselective ketone reduction selectively constructed the *cis*-fused tetracycle **61**. The ethyl chain was then installed by a sequential oxidation, mercaptalation and desulfurisation to give intermediate **62**. Amide reduction, deprotection and selective piperidine *N*-acylation with chloroacetyl chloride (**35**) provided tetracycle **63**.<sup>[81]</sup> The endgame of Heathcock and Toczko was then applied.<sup>[11]</sup> In which a Finkelstein reaction of the acyl chloride **63** with sodium iodide gave the corresponding acyl iodide. Treatment with silver triflate then induced a S<sub>N</sub>2 displacement from the indole 3-position to the alkyl iodide resulting

## Introduction

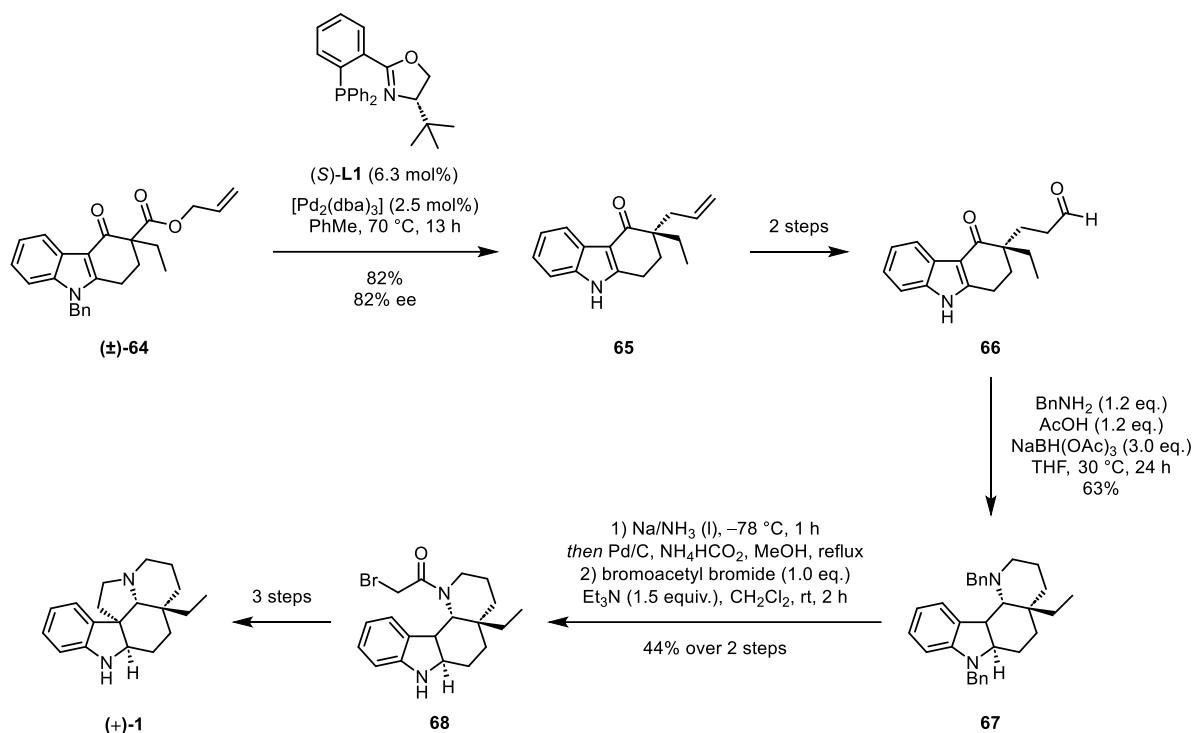
in the late-stage construction of the D ring. A final reduction furnished (–)-aspidospermidine (**1**).<sup>[11,81]</sup>



Scheme 6. Pd-catalysed decarboxylative asymmetric allylic alkylation with carbazolone substrates applied in the total synthesis of (–)-aspidospermidine (**1**).<sup>[81]</sup> dba = *trans,trans*-dibenzylideneacetone.

In 2019, Chang and co-workers employed the conditions of Shao and co-workers with carbazolone **64** to obtain tricyclic intermediate **65** (Scheme 7). A hydroboration-oxidation of the double bond in tricyclic intermediate **65** with subsequent oxidation gave keto-aldehyde **66**. This was followed by a key reductive amination-carbonyl reduction-dehydration-intramolecular conjugate addition cascade to give tetracycle **67**. Deprotection and selective piperidine *N*-acylation with bromoacetyl bromide then afforded intermediate **68**, which was also subjected to the endgame of Heathcock and Toczko to give (+)-aspidospermidine (**1**).<sup>[11,73]</sup>

## Introduction

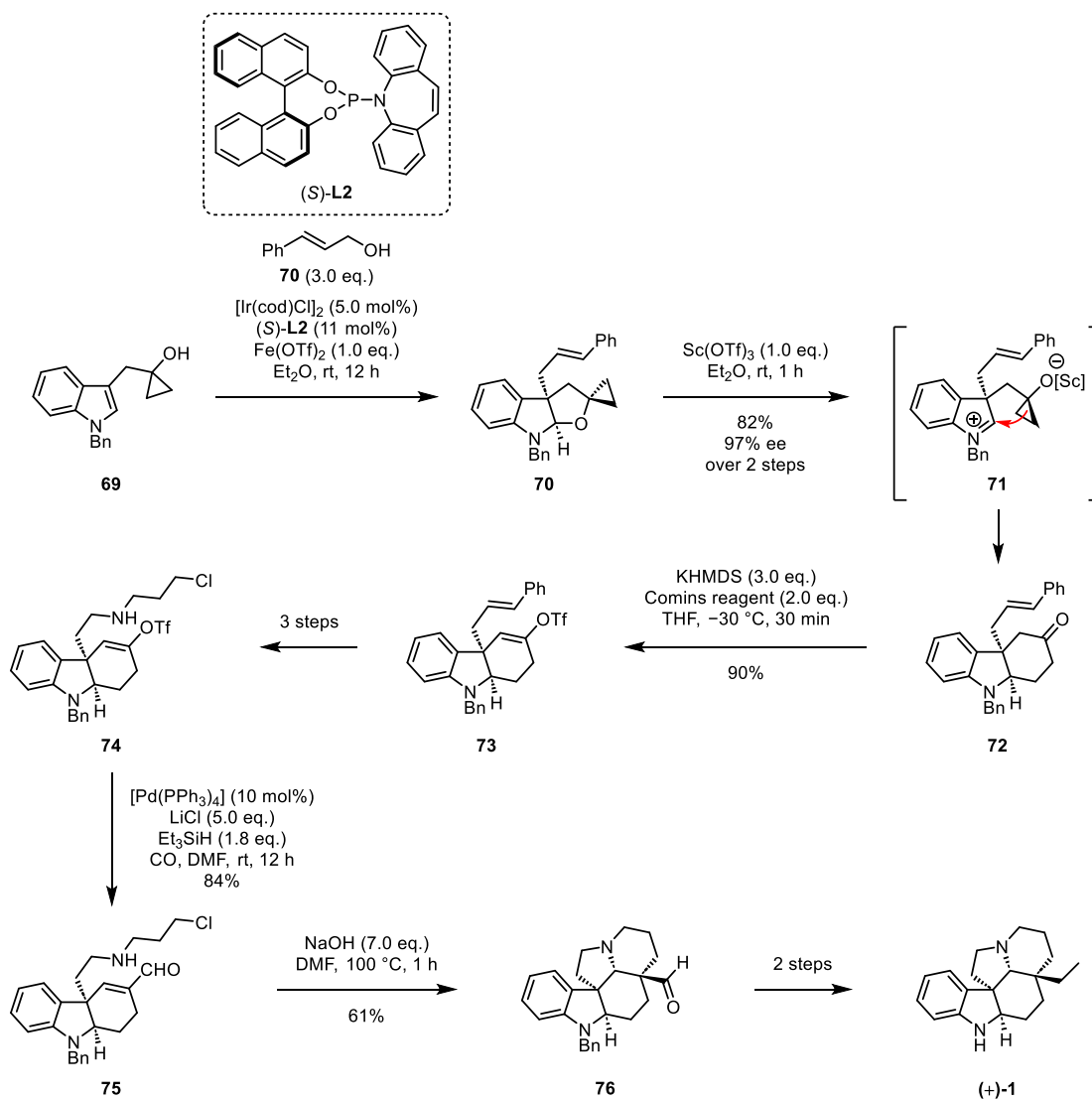


Scheme 7. Total synthesis of (+)-aspidospermidine (**1**), via a Pd-catalysed decarboxylative asymmetric allylic alkylation and a reductive animation-carbonyl reduction-dehydration-intramolecular conjugate addition cascade.<sup>[73]</sup>

Zhang and co-workers' work was of particular interest to us as they employed an Ir-catalysed allylic substitution reaction with 3-substituted indole derivative **69**, followed by a homo-Mannich reaction, in which the *in situ* generated indoline iminium ion **71** was trapped by the tethered cyclopropanol (Scheme 8).<sup>[91]</sup> They applied conditions reported by You and co-workers for the asymmetric allylic substitution step and used scandium(III) triflate for promotion of the sequential homo-Mannich reaction to give hydrocarbazole **72**, thus stereoselectively constructing the quaternary carbon stereocentre at the 3-position and the vicinal stereocentre at the 2-position.<sup>[94,95]</sup> Treatment of hydrocarbazole **72** with Comins' reagent afforded the enol triflate **73**. An Upjohn dihydroxylation of the double bond in enol triflate **72** followed by oxidative cleavage and reductive animation gave intermediate **74**, which was submitted to a Pd-catalysed hydroformylation to give enal **75**. Under basic conditions, enal **75** underwent a 1,4-conjugate-addition-alkylation for concurrent *cis*-construction of the D and E rings in pentacycle **76**. A Wittig methylenation and deprotection then afforded (+)-aspidospermidine (**1**) over two steps from pentacycle **76**. This work from Zhang and co-workers was pivotal in the field of allylic substitution chemistry with 3-substituted indole derivatives, as it was the first example of an unactivated methylene nucleophile cyclising onto

## Introduction

the *in situ* generated indoline iminium ion **71**.<sup>[94]</sup> As in allylic substitution reactions with 3-substituted indole derivatives, the generated indoline iminium ion is typically trapped by pendant nitrogen and oxygen nucleophiles or under basic conditions by activated methylene nucleophiles, such as at the  $\alpha$ -position in a malonic ester.<sup>[95–102]</sup>



Scheme 8. Total synthesis of (+)-aspidospermidine (**1**), by an Ir-catalysed allylic substitution and homo-Mannich sequence.<sup>[94]</sup>

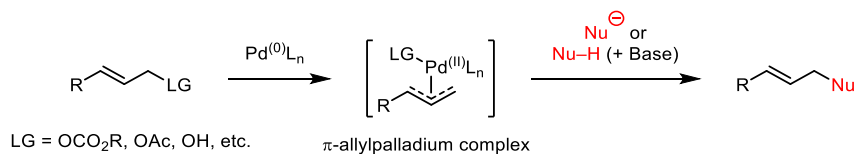
The broad variety of synthetic approaches to aspidospermidine (**1**) reported over the past 60 years, demonstrates that aspidospermidine (**1**) remains the gold standard within *Aspidosperma* alkaloids for the application of emerging synthetic methodologies.

## 1.2 Allylic Substitution Reactions

### 1.2.1 General Features

Transition-metal catalysed reactions are key for the formation of carbon-carbon and carbon-heteroatom bonds.<sup>[103]</sup> Of these, allylic substitution reactions have emerged as powerful transformations in catalytic asymmetric chemistry and have consequently found many applications in natural product synthesis.<sup>[93,103]</sup>

The general components of an allylic substitution reaction are a transition-metal catalyst such as Pd, an allylic substrate as the electrophile and a carbon or heteroatom nucleophile (Scheme 9). Depending on the system, other additives such as bases, for generation of the nucleophile, maybe be required.<sup>[104]</sup> Additionally, chiral ligands can be employed to render this transformation asymmetric.



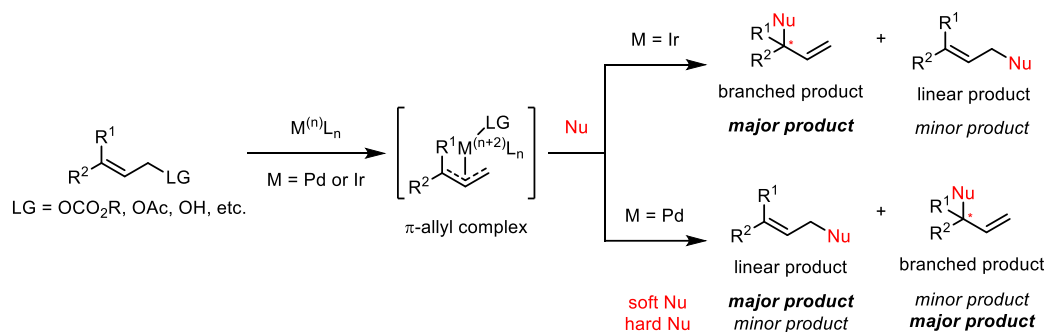
Scheme 9. General scheme of Pd-catalysed allylic substitution reaction.

The allylic substrate has a leaving group at an allylic position (Scheme 9). Allylic substrates with a good leaving group such as carbonate or acetate are called activated allylic substrates. Whereas, allylic substrates with a poor leaving group such as hydroxy groups, as in allylic alcohols, are called unactivated allylic substrates and require activation by additives such as Lewis acids.<sup>[93]</sup> Based on the nucleophile employed,<sup>[93]</sup> a diverse range of bonds can be constructed in an allylic substitution reaction. This is a unique feature amongst asymmetric metal-catalysed reactions, which are typically limited to forming only one type of bond, for example C–H or C–O.<sup>[105]</sup> The net result of an allylic substitution reaction is the substitution of a leaving group at an allylic position by a nucleophile.<sup>[106]</sup> This net reaction at an  $\text{sp}^3$  centre is not commonly encountered in asymmetric metal-catalysed reactions, which typically feature net reactions at  $\text{sp}^2$  centres.<sup>[107]</sup>

Although other transition-metals such as Ni, Rh and Fe have been applied as catalysts in allylic substitution reactions,<sup>[108]</sup> the use of Pd- and Ir-catalysis has dominated. The key difference between Pd- and Ir-catalysed allylic substitution reactions is the regioselectivity of the nucleophilic attack on the  $\pi$ -allyl complex. Under Pd-catalysis, the nucleophilic attack preferentially occurs at the least substituted allyl terminus giving the linear product. Whereas

## Introduction

under Ir-catalysis, the nucleophilic attack preferentially occurs at the most substituted allyl terminus to give the branched product, thus generating a new stereocentre when  $R^1 \neq R^2$  (Scheme 10).<sup>[103,109]</sup> Notably, under Pd-catalysis the nature of the nucleophile can also affect the linear to branched product ratio; with soft nucleophiles, such as malonates and amines, giving higher ratios of linear to branched product compared to hard nucleophiles.<sup>[110]</sup> Other factors may also affect the linear to branched ratio of the product, such as the bulkiness of the nucleophile,<sup>[111]</sup> the rigidity of the ligand<sup>[112]</sup> or even the solvent choice.<sup>[112–114]</sup>



Scheme 10. Regioselectivity of allylic substitution under Ir- or Pd-catalysis. Adapted from <sup>[110]</sup>.

It was originally proposed that the linear regioselectivity obtained in Pd-catalysed allylic substitution reactions was due to the nucleophilic attack preferentially occurring at the least sterically hindered allyl terminus and was therefore due to steric factors. Whereas the branched regioselectivity observed under Ir-catalysis was proposed to be due to electronic effects, in which the positive charge formed upon ionisation is better stabilised at the most substituted allyl terminus, hence nucleophilic attack occurring preferentially at this terminus to afford the branched product.<sup>[98]</sup>

Many studies have been conducted to uncover the origin of this observed regioselectivity. Theories for the linear regioselectivity obtained under Pd-catalysis include nucleophilic attack at the terminus with the longer carbon-metal bond,<sup>[115]</sup> with the greater positive charge,<sup>[116]</sup> or *trans* to the softer P donor when using bidentate ligands with P and N donors.<sup>[115,117–123]</sup> Furthermore, in systems with amine nucleophiles it has been shown that the kinetic branched product can be initially formed and then isomerised to the thermodynamic linear product during the allylic substitution reaction.<sup>[124,125]</sup> Early theories for the branched regioselectivity under Ir-catalysis similarly included nucleophilic attack at the terminus with the longer carbon-metal bond<sup>[126]</sup> or with the greater positive charge.<sup>[127,128]</sup> The Helmchen Group carried out DFT studies to investigate the origin of the regioselectivity for allylic animations under Ir-catalysis.<sup>[129,130]</sup> Whilst the DFT calculations supported the expected branched

## Introduction

regioselectivity, no evidence was found to explain the preferential formation of the branched product.

In 2015, Hartwig and co-workers conducted detailed investigations into the origin of the regioselectivity of allylic substitution reactions with oxygen-containing nucleophiles under Ir- and Pd-catalysis. Experimental and computational studies with Ir-complexes with cod ligands suggested that non-covalent attractive C–H···O interactions between the vinyl C–H bond of the cod ligands and the O atom of malonate ester and alkoxide nucleophiles played a major role in the preferential nucleophilic attack at the most substituted allyl terminus. These non-covalent attractive C–H···O interactions were observed in the transition state to form the branched product and were proposed to dominate over other factors such as the carbon-metal bond length or the presence of a *trans* P-donor. Computational studies of allylpalladium complexes with PPh<sub>3</sub> ligands and either trifluoroacetate as a hard nucleophile or the dimethyl malonate anion as a soft nucleophile were then conducted to investigate whether these stabilising C–H···O interactions played a role in determining the regioselectivity under Pd-catalysis. DFT calculations showed that a higher linear to branched ratio was obtained with the dimethylmalonate soft nucleophile compared to with the hard trifluoroacetate nucleophile. NBO second-order perturbation analysis was employed to measure the attractive C–H···O interactions between C–H bonds of the PPh<sub>3</sub> ligands and the O atom of the nucleophiles present in the transition states leading to branched or linear products. With trifluoroacetate as the hard nucleophile, the attractive interactions in the transition state leading to the branched product were larger than those in the transition state leading to the linear product. Whereas with dimethyl malonate as the soft nucleophile, the attractive interactions in the transition state leading to the linear product were larger. These results suggested that the non-covalent attractive C–H···O interactions are also a major factor in determining the regioselectivity of allylic substitution reactions under Pd-catalysis with oxygen-containing nucleophiles.<sup>[110]</sup>

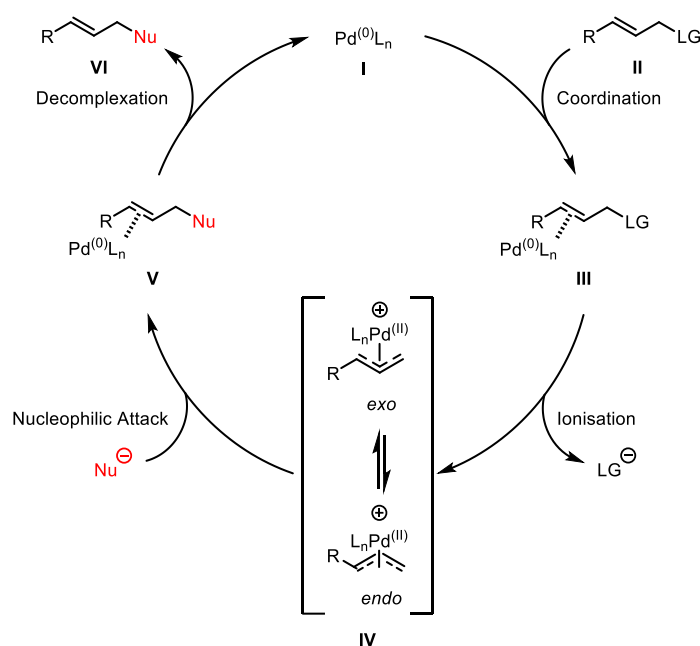
However, the corresponding non-covalent attractive C–H···N interactions were not observed in the allylic animation studies by the Helmchen group.<sup>[129,130]</sup> Thus, a general explanation for the difference in the experimentally observed regioselectivity under Pd- or Ir-catalysis remains to be found.

In our system, the linear product from the allylic substitution reaction was required, as shown in Planned Synthetic Approach, we therefore focused on Pd-catalysis.

## 1.2.2 Pd-Catalysed

### 1.2.2.1 Mechanistical Aspects

The general catalytic cycle of a Pd-catalysed allylic substitution reaction is shown in Scheme 11. The active Pd<sup>(0)</sup> catalyst **I** coordinates to the double bond in the allylic substrate **II**, generating the η<sup>2</sup>-π-allylpalladium<sup>(0)</sup> complex **III**. Oxidative addition then occurs with dissociation of the leaving group to give two equilibrating *endo/exo* η<sup>3</sup>-π-allylpalladium<sup>(II)</sup> complexes **IV**, which can exist as *syn* or *anti* isomers (shown as *syn* in Scheme 11).<sup>[93,107,131]</sup> The oxidative addition and leaving group dissociation step is commonly referred to as an “ionisation” in the literature, due to the generation of the ionic η<sup>3</sup>-π-allylpalladium<sup>(II)</sup> complex **IV**.<sup>[111]</sup> The ionisation occurs with inversion, in which the Pd metal is on the opposite face of the π-allyl unit to the leaving group.<sup>[131]</sup> Nucleophilic attack to the η<sup>3</sup>-π-allylpalladium<sup>(II)</sup> complex **IV** forms the η<sup>2</sup>-π-allylpalladium<sup>(0)</sup> complex **V**. Decomplexation then releases the substituted product **VI** and regenerates the Pd<sup>(0)</sup> catalyst.<sup>[131]</sup>

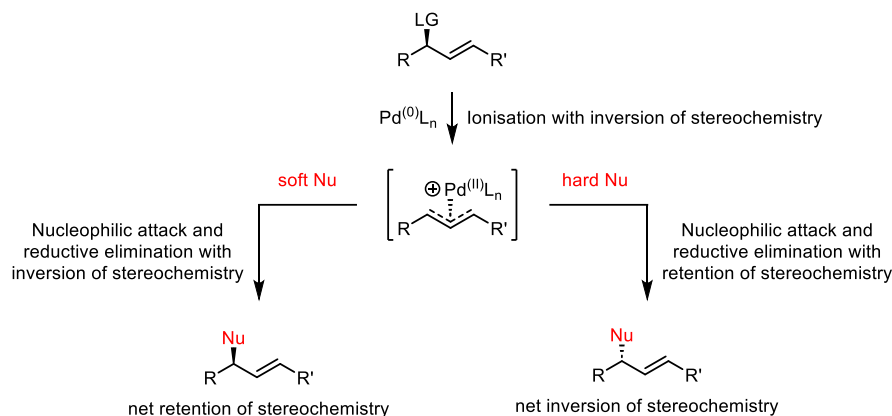


Scheme 11. General catalytic cycle of Pd-catalysed allylic substitution reaction. Adapted from <sup>[107]</sup>.

With soft nucleophiles, those with conjugate acids with a  $pK_a < 25$ , the nucleophilic attack occurs at the opposite face of the π-allyl unit to the Pd<sup>(II)</sup> metal via an outer-sphere mechanism. This nucleophilic attack therefore proceeds with inversion of stereochemistry, resulting in a net retention of the stereochemistry (Scheme 12). Whereas, hard nucleophiles, those with conjugate acids with a  $pK_a > 25$ , attack the Pd<sup>(II)</sup> metal directly and the subsequent reductive

## Introduction

elimination proceeds via an inner-sphere mechanism with retention of stereochemistry, resulting in a net inversion of stereochemistry in the allylic substitution reaction.<sup>[108,131]</sup>



Scheme 12. Mechanism for the net stereochemistry of the allylic substitution reaction with soft or hard nucleophiles. Adapted from <sup>[104]</sup>.

The *syn/anti* nomenclature of the  $\eta^3$ - $\pi$ -allylpalladium<sup>(II)</sup> complex **IV** refers to the configuration of the substituents at the 1- and 3-positions on the  $\eta^3$ - $\pi$ -allyl ligand relative to the 2-substituent, as illustrated in Figure 5.<sup>[107]</sup> For 1,3-disubstituted  $\eta^3$ - $\pi$ -allylpalladium<sup>(II)</sup> complexes the *syn/syn* conformation is usually the more stable and hence dominant conformation, due to reduced steric interactions between the 1-, 3-substituents and with the Pd metal.<sup>[111,114]</sup>

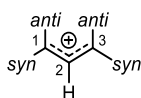


Figure 5. *Syn/anti* nomenclature in  $\eta^3$ - $\pi$ -allyl ligands relative to the 2-substituent. Adapted from <sup>[132]</sup>.

The  $\eta^3$ - $\pi$ -allylpalladium<sup>(II)</sup> complex **IV** has a square planar geometry at the metal centre, with two coordination sites occupied by the  $\eta^3$ - $\pi$ -allyl ligand and the remaining two coordination sites occupied by Lewis-basic ligands. This complex **IV** may have various stereogenic elements, depending on the substitution of the allyl ligand and/or the Lewis-basic ligands used (Figure 6). When the Lewis-basic ligands that are coordinated to the Pd are identical, as shown in A, then the  $\eta^3$ - $\pi$ -allylpalladium<sup>(II)</sup> complex **IV** has no stereogenic element. Whereas when the coordinated Lewis-basic ligands are different as in B, then the Pd atom is the stereogenic element in the  $\eta^3$ - $\pi$ -allylpalladium<sup>(II)</sup> complex **IV**, which exists as enantiomers. When the allyl ligand is unsymmetrically substituted, as in C, then the allyl plane is the stereogenic element and the  $\eta^3$ - $\pi$ -allylpalladium<sup>(II)</sup> complex **IV** exists as enantiomers. When both the coordinated

## Introduction

Lewis-basic ligands are different and the allyl ligand is unsymmetrically substituted, then there are two stereogenic elements: the Pd atom and the allyl plane as in D. The  $\eta^3$ - $\pi$ -allylpalladium<sup>(II)</sup> complex **IV** then exists as four isomers: two diastereomeric pairs of enantiomers. Furthermore, the allyl ligand itself can also act as the stereogenic element as *endo* and *exo* isomers as in E, therefore the complex **IV** exists as two diastereomers.<sup>[111]</sup> Crucially, when chiral ligands are applied, the enantiomeric complexes exist as diastereomeric complexes.<sup>[113]</sup>

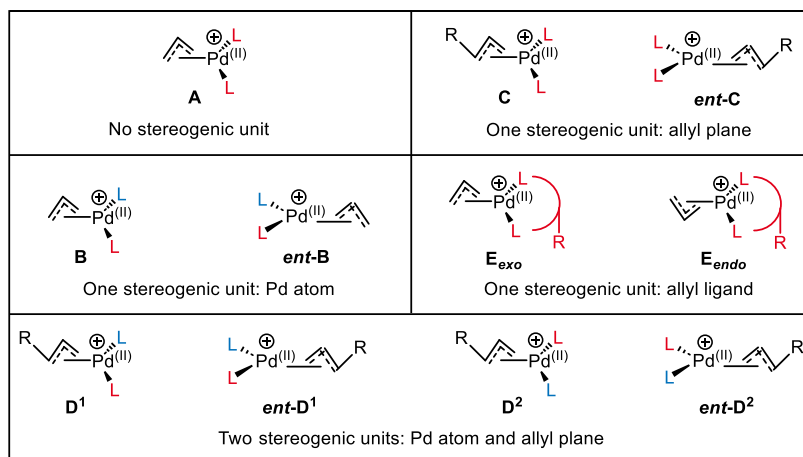


Figure 6. Stereogenic elements present in  $\eta^3$ - $\pi$ -allylpalladium<sup>(II)</sup> complexes and possible isomers thereof. **L** and **L'** represent different ligands. Adapted from <sup>[111]</sup>.

The  $\eta^3$ - $\pi$ -allylpalladium<sup>(II)</sup> complexes **IV** can interconvert between their respective isomeric forms by various mechanisms:<sup>[111]</sup>

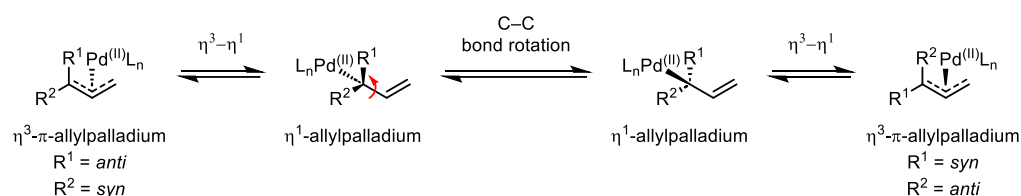
- i.  $\eta^3$ - $\eta^1$ - $\eta^3$  isomerisation
- ii. ligand association
- iii. ligand dissociation
- iv. nucleophilic attack by Pd<sup>(0)</sup>

The occurrence of these isomerisation mechanisms depends upon the reaction conditions. These mechanisms can result in a switch of the face of the allyl ligand that is coordinated to the Pd metal—with or without a *syn-anti* switch of the allyl substituents—or an apparent allyl rotation of the allyl ligand with respect to the Pd–allyl axis.<sup>[111]</sup> These various isomerisation mechanisms can play a significant role in the stereoselectivity of the allylic substitution reaction when their rate constants are faster than that of the nucleophilic attack.

During the  $\eta^3$ - $\eta^1$ - $\eta^3$  isomerisation, the  $\pi$ -allyl ligand undergoes a hapticity change from  $\eta^3$  to  $\eta^1$ , followed by a rotation around the C–C bond of the allyl ligand, before reforming the

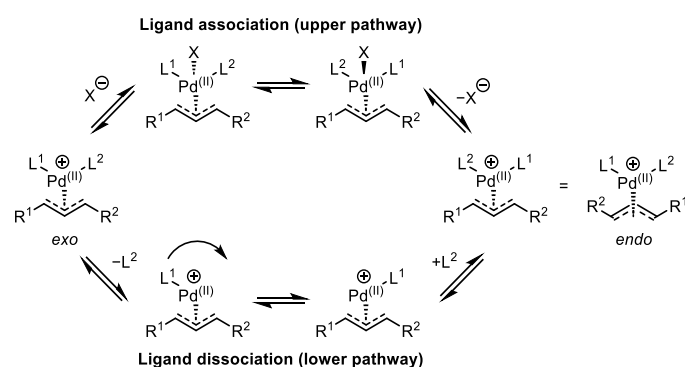
## Introduction

$\eta^3$ - $\pi$ -allylpalladium complex<sup>(II)</sup> (Scheme 13). This isomerisation results in a *syn-anti* isomerisation of the substituents at the allyl terminus that was coordinated to the Pd in the  $\eta^1$ -allylpalladium<sup>(II)</sup> complex and a switch of the allyl ligand face that is coordinated to the Pd metal. This isomerisation is particularly prevalent when both  $R^1$  and  $R^2 = H$ .<sup>[111]</sup> Notably, this *syn-anti* isomerisation is not possible for cyclic substrates, as they are locked as the *anti,anti* isomer.<sup>[107]</sup>



Scheme 13.  $\eta^3$ - $\eta^1$ - $\eta^3$  Isomerisation of a  $\eta^3$ - $\pi$ -allylpalladium complex resulting in *syn-anti* isomerisation of  $R^1$  and  $R^2$ . Adapted from <sup>[111]</sup>.

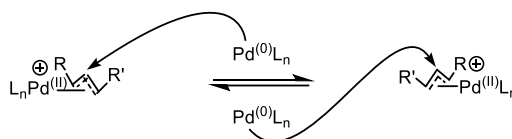
During ligand association an incoming ligand adds to the complex forming an intermediate with an increased coordination number, thus changing the coordination geometry (Scheme 14). An outgoing ligand then dissociates from the intermediate, regenerating the original coordination number of the complex, but with the coordinated ligands in inverted positions. Whereas during ligand dissociation the outgoing ligand first dissociates from the complex, forming an intermediate with a decreased coordination number. The remaining ligands can then switch between the coordination sites. An incoming ligand then adds to this intermediate and thus regenerates the original coordination number of the complex, but with the coordinated ligands in inverted positions.<sup>[133]</sup>



Scheme 14. Mechanisms of ligand association (upper pathway) and ligand dissociation (lower pathway). Adapted from <sup>[93]</sup>.

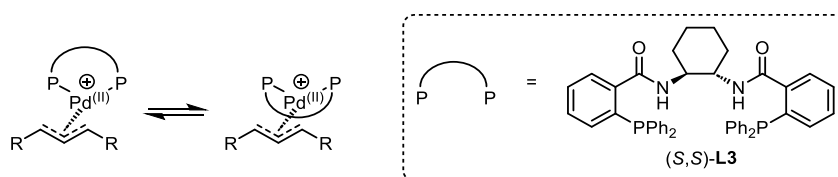
## Introduction

The electrophilic  $\eta^3$ - $\pi$ -allylpalladium<sup>(II)</sup> complex can also undergo nucleophilic attack from  $\text{Pd}^{(0)}$  complexes, effectively resulting in a switch of the allyl ligand face that is coordinated to the Pd metal (Scheme 15).<sup>[111,134]</sup> If the faces of the allyl ligand are enantiotopic then nucleophilic attack to the different faces affects the enantioselectivity of the reaction.<sup>[111]</sup> This phenomenon was reported by Tsuji and co-workers, when they observed that higher Pd-catalyst loading led to a reduced enantioselectivity.<sup>[135]</sup> This isomerisation event can be mitigated by using low Pd-catalyst loadings and is generally assumed to be slower than the nucleophilic attack to the electrophilic  $\eta^3$ - $\pi$ -allylpalladium<sup>(II)</sup> complex.<sup>[111]</sup>



Scheme 15.  $\text{Pd}^{(0)}$ -catalysed allyl exchange. Adapted from <sup>[106]</sup>.

The  $\eta^3$ - $\pi$ -allylpalladium<sup>(II)</sup> complexes **IV** can also interconvert between their *endo/exo* isomers, in an apparent allyl rotation.<sup>[93]</sup> This apparent allyl rotation can occur via three different mechanisms: ligand association, ligand dissociation or an  $\eta^3$ - $\eta^1$ - $\eta^3$  isomerisation, in which the  $\pi$ -allyl ligand undergoes a hapticity change from  $\eta^3$  to  $\eta^1$ , subsequent rotation around the C–Pd bond occurs before reforming the  $\eta^3$ - $\pi$ -allylpalladium<sup>(II)</sup> complex.<sup>[111]</sup> Additionally, *endo-exo* isomerisation can also occur when a bidentate Lewis-basic ligand exists as two separate rotamers above and below the Pd–allyl axis, for example this phenomenon has been reported with the Trost DACH-phenyl ligand **L3** (Scheme 16).<sup>[136]</sup> The *endo* isomers are generally more stable.<sup>[137]</sup> Crucially, the *endo/exo* isomers may display different reactivities to nucleophilic attack, potentially leading to enantioenriched product formation.<sup>[111]</sup>

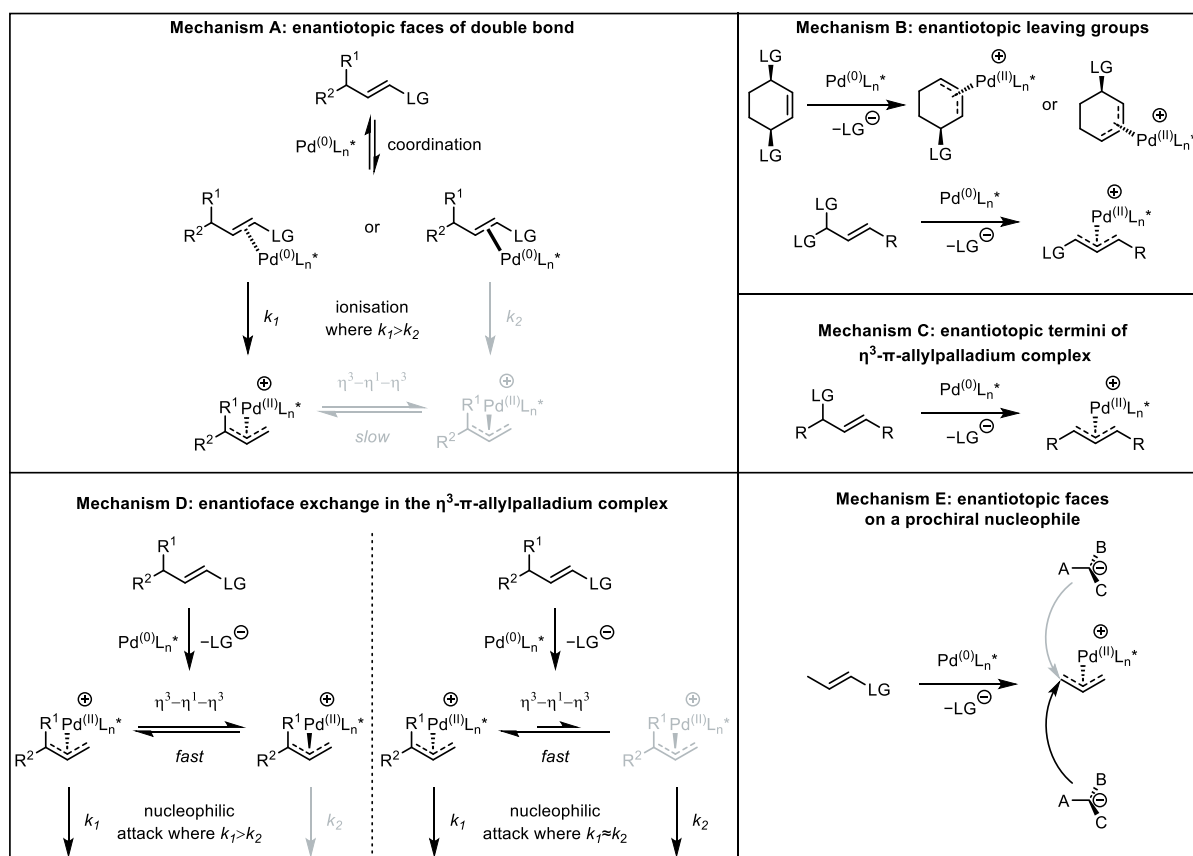


Scheme 16. *Exo/endo* isomerisation with the Trost DACH-phenyl ligand (*S,S*)-**L3** as a bidentate ligand existing as two separate rotamers. Adapted from <sup>[111]</sup>.

In addition to the interconversion of the  $\eta^3$ - $\pi$ -allylpalladium<sup>(II)</sup> complexes affecting the stereoselectivity of the allylic substitution reaction, there are five different opportunities for enantiodiscrimination in a Pd-catalysed asymmetric allylic substitution reaction when using chiral ligands (Scheme 17).<sup>[138]</sup> These opportunities for enantiodiscrimination occur at each of

## Introduction

the stages in the allylic substitution catalytic cycle, apart from the reductive elimination step, as the stereochemistry is already set prior to this step.<sup>[107]</sup> The multiple enantiodiscrimination opportunities are a unique feature of allylic substitution reactions; as other asymmetric metal-catalysed reactions are typically limited to one source of enantiodiscrimination, for instance differentiation of enantiotopic faces of  $\pi$ -unsaturation, as in a carbonyl group or a double bond.<sup>[138]</sup>



Scheme 17. Mechanisms of enantiodiscrimination in Pd-catalysed allylic substitution reactions. Adapted from <sup>[131,139]</sup>.

In mechanism A, coordination to one enantiotopic face of the allyl substrate forms a diastereomeric  $\eta^2$ - $\pi$ -allylpalladium(0) complex that has a faster rate of ionisation than the diastereomeric complex formed from coordination to the opposite enantiotopic allyl face. Additionally, the rate of the nucleophilic attack to the  $\eta^3$ - $\pi$ -allylpalladium(II) complexes is faster than that of the  $\eta^3$ - $\eta^1$ - $\eta^3$  isomerisation between the diastereomeric  $\eta^3$ - $\pi$ -allylpalladium(II) complexes.<sup>[107]</sup> Mechanism B occurs when the allyl substrate is *meso* or gem-disubstituted with two enantiotopic leaving groups, which become diastereotopic in the presence of a chiral ligand.<sup>[111]</sup> In mechanism C, the allyl substrate is a chiral racemate that upon ionisation forms

## Introduction

a *meso*  $\eta^3$ - $\pi$ -allylpalladium<sup>(II)</sup> complex.<sup>[107]</sup> In the presence of a chiral ligand, the termini of the allyl ligand are diastereotopic and consequently exhibit different reactivities to the nucleophilic attack. Therefore, the regioselectivity of the nucleophilic attack can be controlled by a chiral ligand, to form the desired enantioenriched product. This mechanism therefore allows for enantioenriched product to be obtained from a chiral racemic starting material, via a dynamic kinetic asymmetric transformation (DYKAT).<sup>[111]</sup> In mechanism D, upon ionisation two diastereomeric  $\eta^3$ - $\pi$ -allylpalladium<sup>(II)</sup> complexes are formed, whose interconversion via the  $\eta^3$ - $\eta^1$ - $\eta^3$  isomerisation is faster than the rate of the nucleophilic attack. The asymmetric induction is determined from either the different rates of nucleophilic attack to the two diastereomeric  $\eta^3$ - $\pi$ -allylpalladium<sup>(II)</sup> complexes or when these rates are approximately equal then by the equilibrium ratio of the diastereomeric complexes. In this mechanism, the allyl substrate can be either achiral or chiral. When a chiral racemate is applied, enantioenriched product can be obtained and thus constitutes a DYKAT.<sup>[138]</sup> Finally, the nucleophilic attack from one of the enantiotopic faces of the prochiral nucleophile can also act as the enantiodiscriminating mechanism as in mechanism E.<sup>[107]</sup> This generates a new stereocentre on the prochiral nucleophile. Since for soft nucleophiles, the nucleophilic attack occurs via an outer-sphere mechanism and the nucleophile is outwith the coordination sphere of the metal, it can be challenging to achieve high asymmetric induction via this enantiodiscriminating mechanism.<sup>[131]</sup>

In mechanisms A and B, the ionisation step is the enantiodiscriminating step, with often a faster rate of nucleophilic attack compared to the isomerisation of the diastereomeric  $\pi$ -allyl complexes.<sup>[111,138]</sup> Whereas in mechanisms C, D and E the nucleophilic attack is the enantiodiscriminating step.<sup>[138]</sup> Furthermore, these mechanisms show that the enantiodiscrimination event can occur at either the electrophile or the nucleophile or both.<sup>[107]</sup>

Mechanism C requires a chiral allyl substrate and mechanism D can involve one.<sup>[138]</sup> The ability of allylic substitution reactions to convert chiral racemic starting material into enantioenriched or even enantiopure material, through either a *meso* intermediate, as in mechanism C, or a DYKAT, as in mechanism D, is rarely observed in other asymmetric metal-catalysed reactions.<sup>[107]</sup>

### 1.2.2.2 Ligand Design

As aforementioned, the stereo defining ionisation and nucleophilic attack for soft nucleophiles occurs on the opposite face of the  $\pi$ -allyl unit to the Pd metal and thus outwith the chiral environment of the ligand. This presented a challenge when designing chiral ligands for asymmetric allylic substitutions. To this end, inspiration was sought from nature. Trost and co-workers hypothesised that to induce high asymmetric induction, the ligand required a chiral pocket to embrace the substrates, analogous to that of an enzyme active site. They postulated that this could be achieved by using a bidentate ligand that creates a constricted chiral space.<sup>[139]</sup>

For the Lewis-basic ligands in the Pd-catalysed allylic substitution reaction, donor ligands such as phosphines are required to increase the electron density on the Pd centre, for promotion of the oxidative addition.<sup>[111]</sup> Hence Pd-catalysed asymmetric allylic substitution reactions often employ chiral phosphine ligands.<sup>[131]</sup> Thereof, Trost's ligands have arguably enjoyed the most success, with the DACH-phenyl ligand **L3**—the standard Trost ligand—being the ligand of choice for total syntheses featuring Pd-catalysed asymmetric allylic substitution reactions (Figure 7a).<sup>[106]</sup> The Trost ligands coordinate to the metal centre through their two phosphorous atoms and are thus bidentate (Figure 7b).<sup>[106]</sup> The phenyl groups attached to the phosphorus atoms form the walls and flaps of the chiral pocket and the chiral N–C–C–N scaffold the roof thereof,<sup>[138]</sup> as reminiscent of an enzyme active site.<sup>[139]</sup>

Structural modifications to the standard Trost ligand **L3** have been made over the years, in attempts to enhance its asymmetric induction.<sup>[106]</sup> These modifications included increasing the N–C–C–N dihedral angle, as in the DACH-anthracene **L5** and stilbene diamine **L6** derivatives (Figure 7a), which resulted in a larger P–Pd–P bite angle.<sup>[139]</sup> A larger P–Pd–P bite angle is often associated with a deeper chiral pocket, which was postulated to enhance the chiral recognition and thus the asymmetric induction through more effectively embracing the substrates.<sup>[108,140]</sup>

Studies to investigate the asymmetric induction of the Trost ligands in Pd-catalysed allylic substitution reactions through direct characterisation of the intermediates by NMR spectroscopy or X-ray crystallography were unsuccessful. Therefore, the working model for the stereoselectivity proposed by Trost and co-workers is based on indirect experimental evidence. The wall-and-flap model of the Trost ligands as shown in Figure 7b was based on molecular modelling studies of  $\pi$ -allylpalladium complexes with the Trost ligands.<sup>[113]</sup>

## Introduction

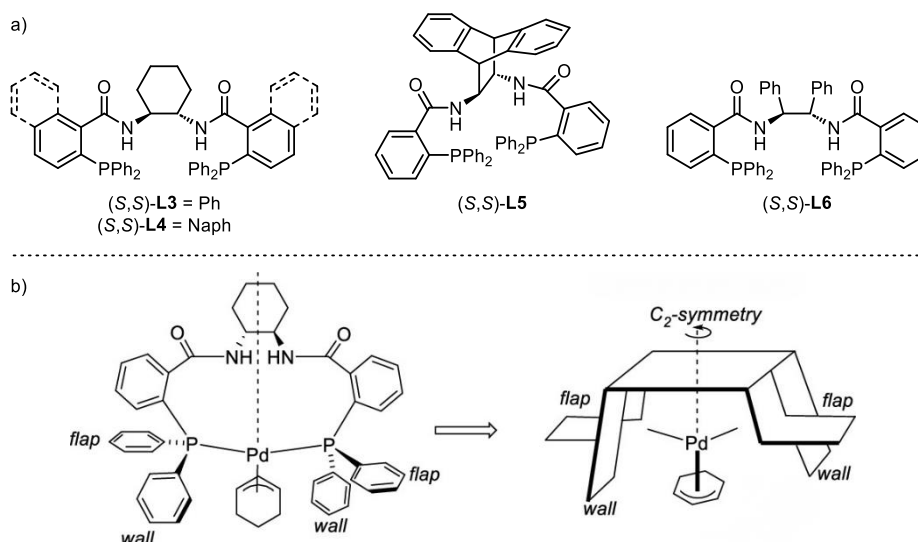


Figure 7. a) Selected Trost ligands; b) Trost's wall-and-flap model with the (*R,R*)-DACH-phenyl ligand **L3**.<sup>[93]</sup>

In the  $\pi$ -allylpalladium complex, the Pd metal is located above the *anti*-substituents of the  $\pi$ -allyl ligand, consequently the allyl ligand cants away from the Pd metal at an angle of 5–15° to reduce unfavourable steric interactions between its *anti*-substituents and the Pd metal (Figure 8 top).<sup>[113]</sup> In the allylic substitution reaction, both the ionisation and nucleophilic attack are proposed to occur *exo* to the Pd metal, as this allows for an angle close to 180° between the leaving group and the incoming nucleophile to the Pd metal. Notably, in the ionisation step, Pd<sup>(0)</sup> is the nucleophile whereas in the substitution step, Pd<sup>(II)</sup> is the leaving group. With the Trost ligands, the nucleophilic attack must occur through one of the front quadrants, for it to be *exo* to the Pd metal. Of the two possible front quadrants, entry of the nucleophile under the flap is sterically favoured as opposed to beside the wall (Figure 8 middle). In the case of the unsymmetrically substituted  $\pi$ -allyl ligand **I**, upon ionisation the kinetically preferred diastereomeric  $\pi$ -allylpalladium complex **II** is formed, which can undergo  $\eta^3$ - $\eta^1$ - $\eta^3$  isomerisation to the thermodynamically preferred diastereomeric  $\pi$ -allylpalladium complex **III** (Figure 8 bottom). The diastereomeric  $\pi$ -allylpalladium complex **III** is thermodynamically favoured as the R substituent is located close to the flap, as opposed to beside the wall as in the  $\pi$ -allylpalladium complex **II**. For the diastereomeric  $\pi$ -allylpalladium complex **II**, favoured *exo* attack of the nucleophile under the flap in the front right-hand quadrant would give the favoured or 'matched' linear product **IV**, whereas unfavoured *exo* nucleophile attack along the wall would give the branched unfavoured or 'mismatched' product **V**. Favoured *exo* attack of the

## Introduction

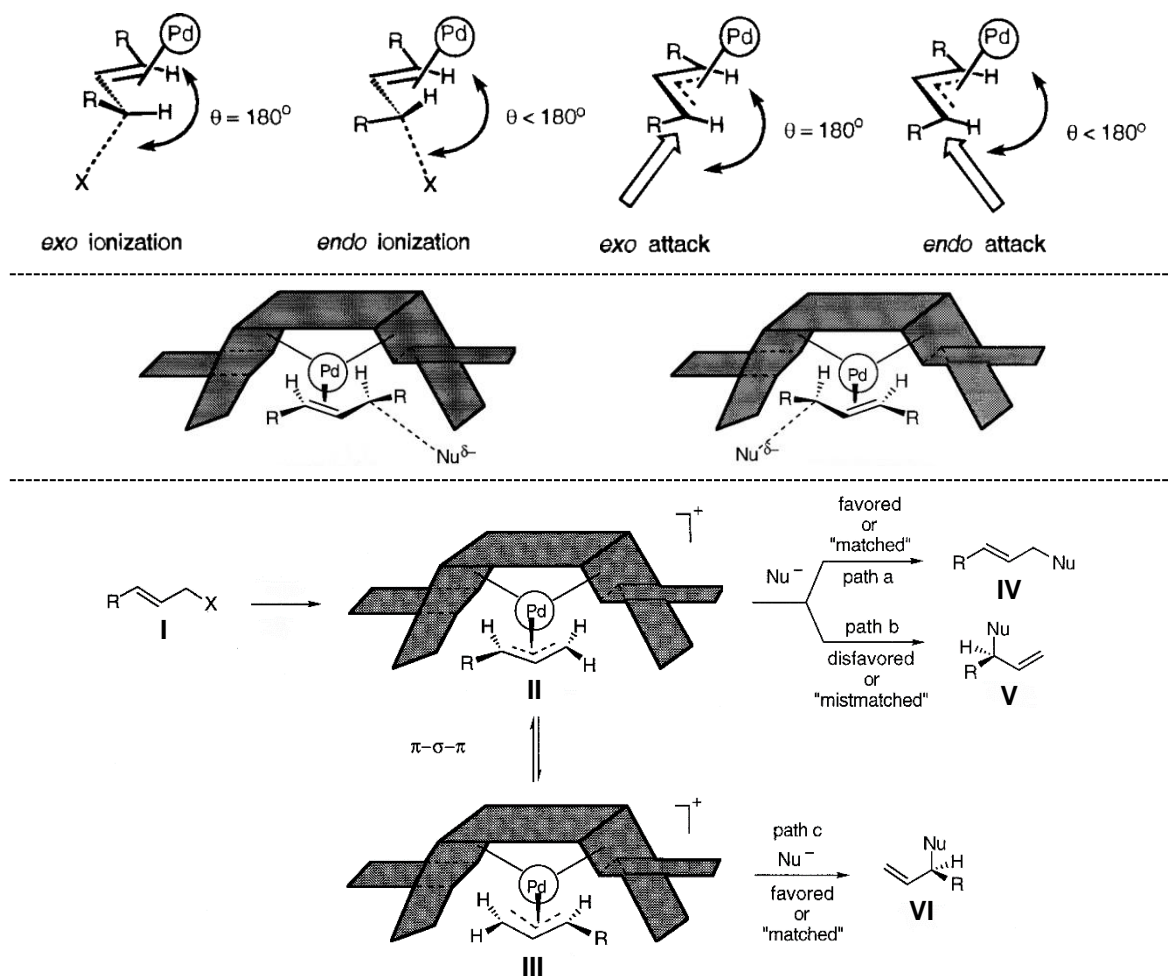
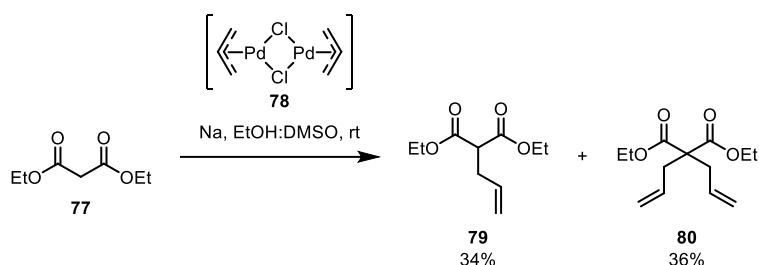


Figure 8. *Exo* and *endo* ionisation and nucleophilic attack in  $\pi$ -allylpalladium complexes (top); possible *exo* nucleophilic attack in  $\pi$ -allylpalladium complexes with the (*R,R*)-Trost ligands (middle); matched and mismatched nucleophilic attack pathways between the diastereomeric  $\pi$ -allylpalladium complexes with the (*R,R*)-Trost ligands (bottom).<sup>[113]</sup>

nucleophile under the flap in the front right-hand quadrant of the diastereomeric complex **III** would give the favoured or 'matched' branched product **VI**. This difference in product formation highlights the importance of the relative rate of the  $\eta^3$ - $\eta^1$ - $\eta^3$  isomerisation between the diastereomeric  $\pi$ -allylpalladium complexes compared to that of the nucleophilic attack. Furthermore, this model shows how the Trost chiral ligands affect not only the stereoselectivity but also the regioselectivity of the allylic substitution reaction.<sup>[113]</sup>

## 1.2.2.3 Development

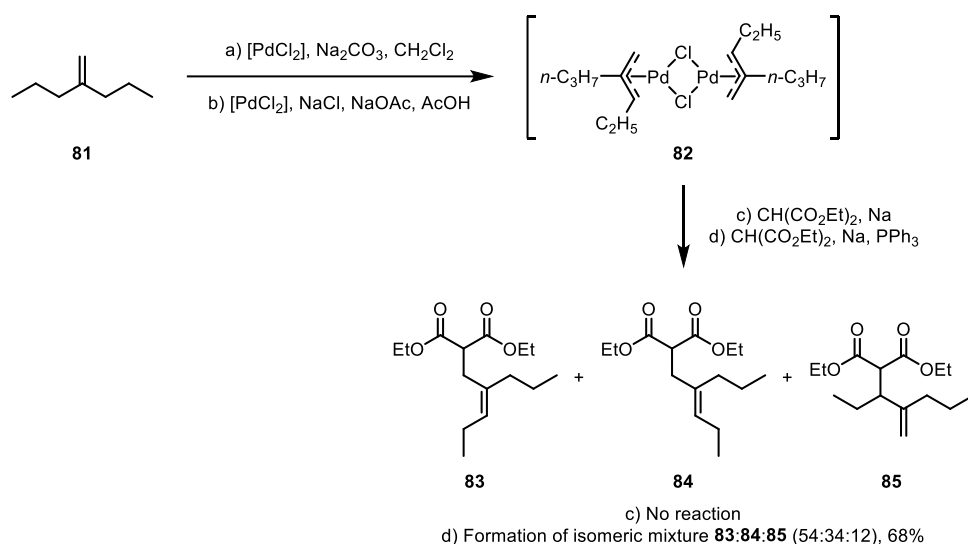
The seminal publication on Pd-catalysed allylic substitution reactions was reported by Tsuji and co-workers in 1965, in which they reported that  $[\text{Pd}(\text{allyl})\text{Cl}]_2$  (**78**) underwent nucleophilic attack by carbanions of diethyl malonate (**77**) and acetoacetate to yield the respective  $\alpha$ -mono- and di-allylated products **79** and **80** (as demonstrated with diethyl malonate (**77**) in Scheme 18). Additionally, it was shown that an enamine could be employed as a carbon nucleophile in the allylic substitution reaction in which the enamine was allylated and then hydrolysed to afford the respective  $\alpha$ -allylated ketone. This work demonstrated that  $\pi$ -allylpalladium complexes, such as  $[\text{Pd}(\text{allyl})\text{Cl}]_2$  (**78**), could undergo nucleophilic attack with carbon nucleophiles to form a carbon-carbon bond and give the allylated derivatives.<sup>[141]</sup>



Scheme 18. Nucleophilic attack of diethyl malonate (**77**) to  $[\text{Pd}(\text{allyl})\text{Cl}]_2$  (**78**) to give the mono- and di-allylated derivatives **79** and **80**.<sup>[141]</sup>

This work was then further developed by Trost and co-workers in 1973. In which, they prepared various alkyl-substituted  $\pi$ -allylpalladium complexes from the corresponding alkenes and  $[\text{PdCl}_2]$  (conditions a or b in Scheme 19); however, no reaction with the diethyl malonate carbanion was observed (conditions c in Scheme 19). Upon addition of triphenylphosphine the reaction proceeded within minutes (conditions d in Scheme 19). Interestingly, the nucleophilic attack was shown to occur preferentially at the less substituted terminus of the  $\pi$ -allylpalladium complex **82** to give linear alkylated derivatives **83** and **84**, over the branched alkylated derivative **85** that resulted from nucleophilic attack at the more substituted allyl terminus.<sup>[142]</sup>

## Introduction



Scheme 19. Allylic alkylation reaction of alkyl-substituted  $\pi$ -allylpalladium complex **82** with diethyl malonate (**77**).<sup>[142]</sup>

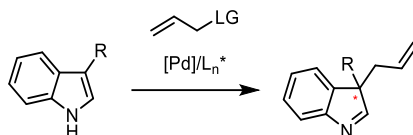
Due to these pioneering contributions of Tsuji and Trost, the Pd-catalysed allylic substitution reaction with soft carbon nucleophiles, via a  $\pi$ -allylpalladium complex, is called the Tsuji–Trost reaction.<sup>[104,111]</sup> Allylic substitution methodology remains a research area of significant interest and is thus continuously advancing.<sup>[93]</sup>

### 1.2.2.4 3-Substituted Indole Derivatives as Nucleophiles

Over the last two decades, 3-substituted indole derivatives have emerged as attractive nucleophiles in allylic substitution reactions. As when they are applied as nucleophiles at their 3-positions, a quaternary carbon stereocentre can be generated in the 3,3-disubstituted indolenine product (Scheme 20). The asymmetric construction of quaternary carbon stereocentres remains a significant challenge within synthetic chemistry, with limited methods to accomplish this.<sup>[143,144]</sup> Notably, when using 3-substituted indole derivatives in allylic substitution reactions the N1-position may also act as a nucleophile. This competing C3 and N1 nucleophilicity is an issue of chemoselectivity.<sup>[100]</sup> The regioselectivity of the nucleophilic attack on the  $\pi$ -allylpalladium complex, to deliver the branched or linear substituted product also needs to be considered. Furthermore, in asymmetric protocols the stereoselectivity has to be induced by an appropriate chiral ligand. Consequently, the need for the precise control of the chemo-, regio- and stereoselectivity means that this transformation with 3-substituted indole derivatives is not straightforward. Furthermore, when 3-substituted indole derivatives are used as nucleophiles at their 3-positions, this results in a dearomatisation of the indole system, which has a thermodynamic cost.<sup>[145]</sup> Nonetheless, allylic substitution reactions

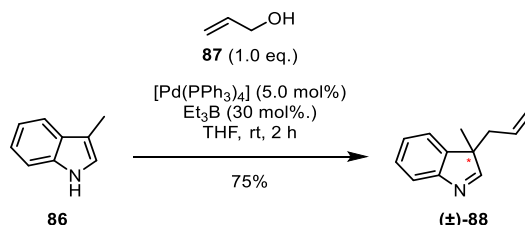
## Introduction

employing 3-substituted indole derivatives as nucleophiles at their 3-positions have been reported, both in a non-stereoselective and asymmetric manner. Thus, paving the way for efficient access to indole alkaloid natural products, which display interesting biological activities.<sup>[146]</sup>



Scheme 20. 3-Substituted indole derivatives as nucleophiles at their 3-positions in allylic substitutions reactions.

The first use of a 3-substituted indole derivative in a Pd-catalysed allylic substitution reaction was reported by Tamaru and co-workers in 2005. They reported that a [Pd(PPh<sub>3</sub>)<sub>4</sub>]-Et<sub>3</sub>B system with simple alkyl substituted allyl alcohols and substituted indole derivatives selectively gave the corresponding 3-allylated indole derivatives. Crucially, 3-methylindole (**86**) was one of their substrates, which afforded the corresponding 3-methyl-3-allylated-indolenine **88** in a yield of 75% (Scheme 21).<sup>[146]</sup> In their previous related work, Tamaru and co-workers had proposed that the coordination of Et<sub>3</sub>B to the hydroxy group in allyl alcohol (**87**), activates the allylic substrate to oxidative addition by Pd<sup>(0)</sup> to give the corresponding  $\pi$ -allylpalladium complex.<sup>[147]</sup>

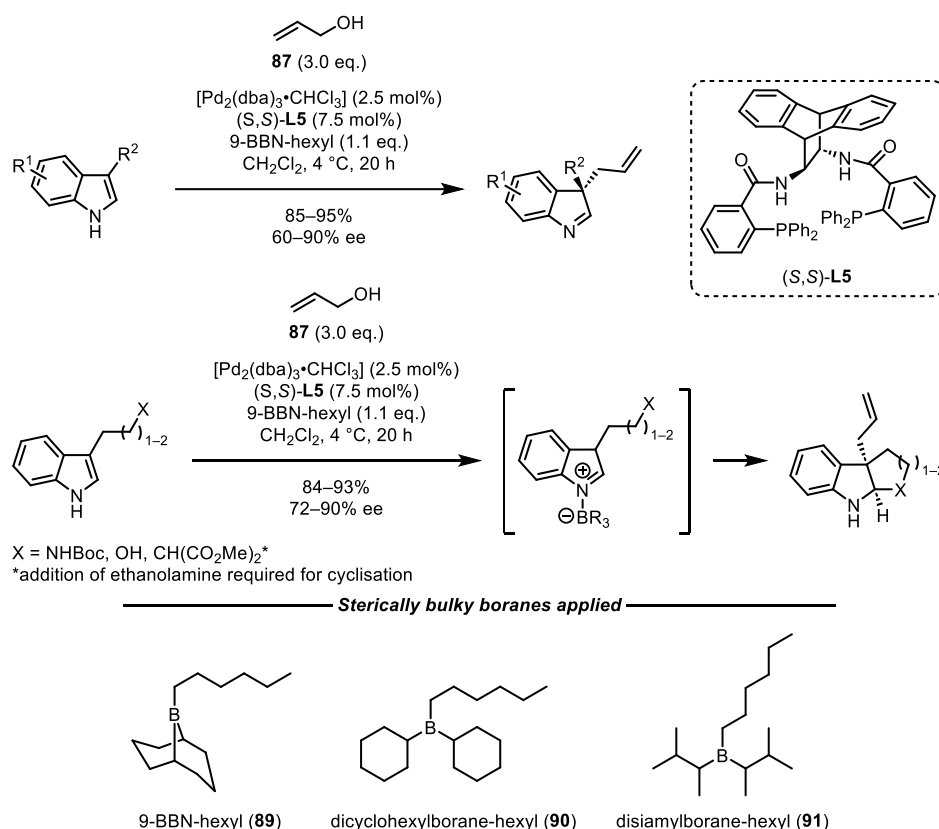


Scheme 21. First reported Pd-catalysed allylic substitution reaction with a 3-substituted indole derivative.<sup>[146]</sup>

This work attracted the attention of Trost and co-workers, who hypothesised that their Trost ligands could be used to render this transformation enantioselective, as the reaction appeared to go via a  $\pi$ -allylpalladium complex. They employed a [Pd<sub>2</sub>(dba)<sub>3</sub>•CHCl<sub>3</sub>]-DACH-anthracene ligand **L5** system, with 3-substituted indole derivatives and allyl alcohol (**87**) to give the corresponding 3,3-disubstituted indolenines in high yields and enantiomeric excesses (Scheme 22). Substrates with a pendent nucleophile cyclised onto the *in situ* generated indoline iminium ions furnishing the corresponding *cis*-fused indolines. In their optimisation studies, it was

## Introduction

shown that increasing the steric bulk of the borane additive from Et<sub>3</sub>B to 9-BBN-hexyl (**89**) and performing the reaction at a lower temperature of 4 °C both resulted in higher enantioselectivities. Interestingly, further increasing the steric bulk of the borane additive to dicyclohexylborane-hexyl (**90**) decreased the yield and enantioselectivity, or in the case of disiamylborane-hexyl (**91**) inhibited the reaction completely. They believed that this suggested that the borane played a role in the enantiodiscriminating step through its coordination to the indole nitrogen—in addition to activating the allyl alcohol (**87**). This coordination was also thought to explain the chemoselectivity for C3-allylation over N1-allylation.<sup>[96]</sup>

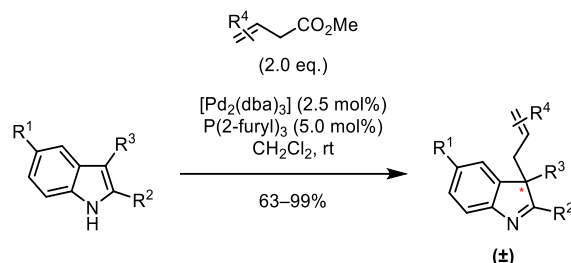


Scheme 22. First reported enantioselective Pd-catalysed allylic substitution reaction with 3-substituted indole derivatives.<sup>[96]</sup>

Rawal and co-workers sought conditions for the Pd-catalysed allylic substitution with 2,3-disubstituted indoles. They initially tested the conditions reported by Tamaru and Trost with a 2,3-fused indole and allyl alcohol (**87**); however, the corresponding 3-allylated indolenine was only obtained in modest yields of 20% and 52%, respectively. From their optimisation studies, they found that a [Pd<sub>2</sub>(dba)<sub>3</sub>]-P(2-furyl)<sub>3</sub> system with activated allyl methyl carbonate selectively gave the 3-allylated indolenine in quantitative yield. These conditions were then shown to be applicable to a broad scope of 2,3-disubstituted indole

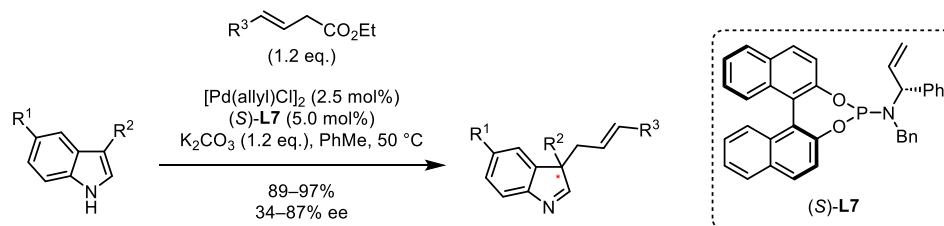
## Introduction

derivatives (Scheme 23), with additional 5-substituents and varying carba- and heterocycle fused rings tolerated. The allyl substrates were also extended to various alkyl substituted allyl methyl carbonates.<sup>[148]</sup>



Scheme 23. Pd-catalysed allylic substitution reaction with 2,3-disubstituted indoles and activated allyl methyl carbonates.<sup>[148]</sup>

Du and co-workers then employed their expertise on chiral olefin ligands to develop a suitable chiral ligand for the Pd-catalysed enantioselective allylic substitution with 3-substituted indole derivatives and activated allyl carbonates (Scheme 24). From their optimisation studies, chiral phosphoramidite olefin ligand (*S*)-**L7** was shown to give the indolenine product in the highest yield and with the highest enantioselectivity. The substrate scope was then expanded in terms of the R<sup>3</sup>-substituent in the allyl carbonate and the 3- and 5-substituents on the indole derivative. When the indole derivative had a pendent nucleophile, cyclisation onto the initially formed indolenine occurred. The undesired N1-allylated products were also observed under these basic conditions. When a 2,3-fused indole derivative was submitted to these conditions, the corresponding indolenine was only obtained with 34% ee.<sup>[97]</sup>

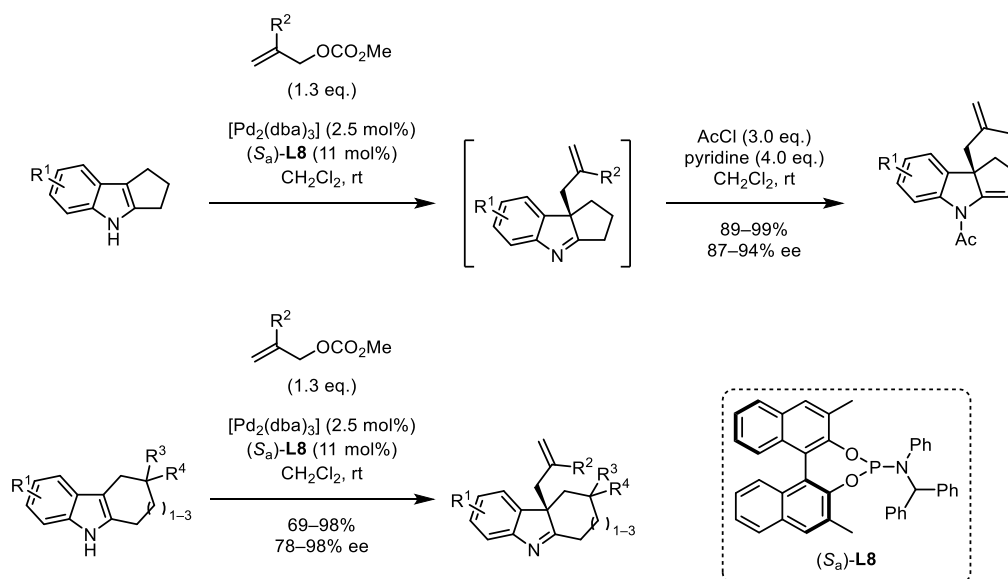


Scheme 24. Enantioselective Pd-catalysed allylic substitution of 3-substituted indole derivatives with activated allyl carbonates.<sup>[97]</sup>

You and co-workers therefore sought chiral ligands to enable high enantioselectivities in Pd-catalysed allylic substitution reactions with 2,3-fused indole derivatives. From their studies, allyl methyl carbonates and 2,3-disubstituted indole derivatives with fused cyclopentane units were found to give indolenines that were unstable to silica gel column chromatography (Scheme 25). The indolenines were therefore protected *in situ* and subsequently isomerised to

## Introduction

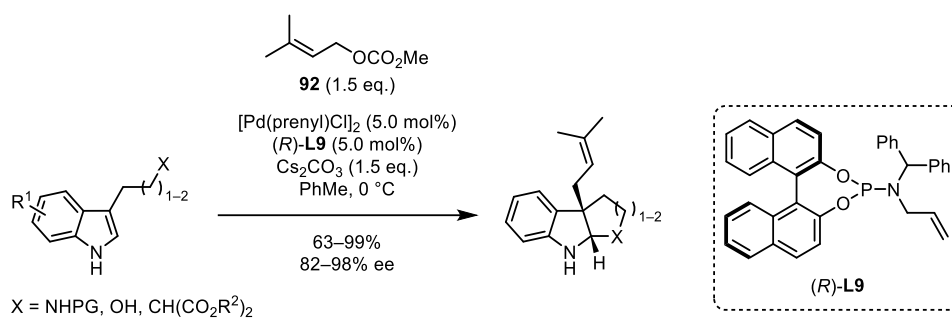
give the corresponding stable enamines. The chiral phosphoramidite ligand (*S<sub>a</sub>*)-**L8** was reported to give the enamines with the highest enantioselectivities. The substrate scope was then evaluated. Sterically hindered 2-phenyl allyl carbonates were shown to be well-tolerated. With respect to the 2,3-fused indole derivative, additional substituents at the 4-, 5- and 6-positions and larger fused carbacycles, from cyclohexane to cyclooctane, were tolerated. Interestingly, the indolenines with 6-, 7- and 8-membered fused carbacycles were stable to purification.<sup>[149]</sup>



Scheme 25. Enantioselective allylic substitution reaction with 2,3-fused indole derivatives with 2-substituted allyl methyl carbonates.<sup>[149]</sup>

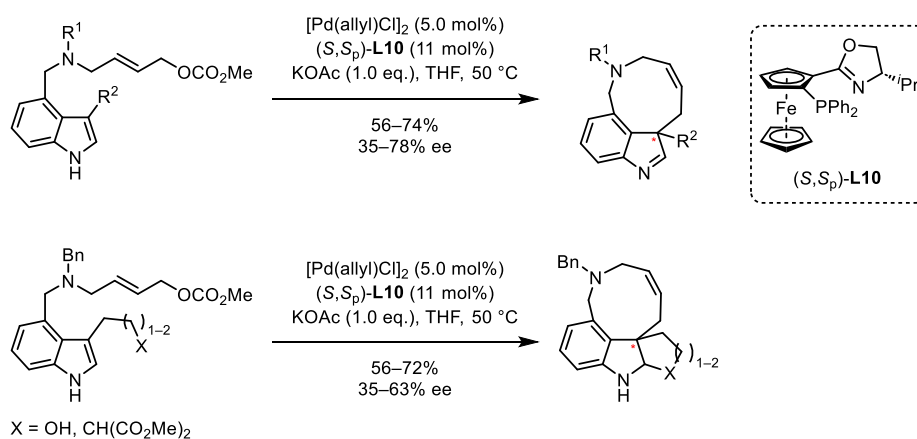
In the same year, You and co-workers reported a  $[\text{Pd}(\text{prenyl})\text{Cl}]_2$  and chiral phosphoramidite olefin ligand (*R*)-**L9** system with basic conditions for the enantioselective allylic substitution and subsequent cyclisation of 3-substituted indole derivatives with a pendent nucleophile to give the fused polycyclic indoline products (Scheme 26). Methyl prenyl carbonate (**92**) was used as the allyl substrate, thus introducing a prenyl group at the 3-positions of the indole derivatives. Nitrogen, oxygen and activated carbon pendent nucleophiles were successfully employed to give the polycyclic prenylated products in high yields and with high enantioselectivities. With the indole derivatives containing a nitrogen pendent nucleophile, various *N*-protecting groups and 4-, 5- and 6-substituents were well-tolerated.<sup>[199]</sup>

## Introduction



Scheme 26. Enantioselective Pd-catalysed allylic substitution and subsequent cyclisation with 3-substituted indoles derivatives with a pendent nucleophile.<sup>[99]</sup>

You and co-workers also reported an enantioselective intramolecular Pd-catalysed allylic substitution reaction with 3-substituted indole derivatives with an allyl methyl carbonate tethered at the 4-position (Scheme 27). From their optimisation studies,  $[\text{Pd}(\text{allyl})\text{Cl}]_2$  with chiral PHOX ferrocene-based ligand ( $S,S_p$ )-**L10** under basic conditions, was shown to give the C3–C4 fused indolenine derivatives in the highest yields and with the highest enantioselectivities. The substrate scope of the reaction was shown to tolerate methyl, allyl and substituted-benzyl groups at the 3-position. When a pendent nucleophile was present at the 3-position, subsequent cyclisation onto the initially formed C3–C4 fused indolenine products occurred to afford the polycyclic indoline derivatives.<sup>[98]</sup>

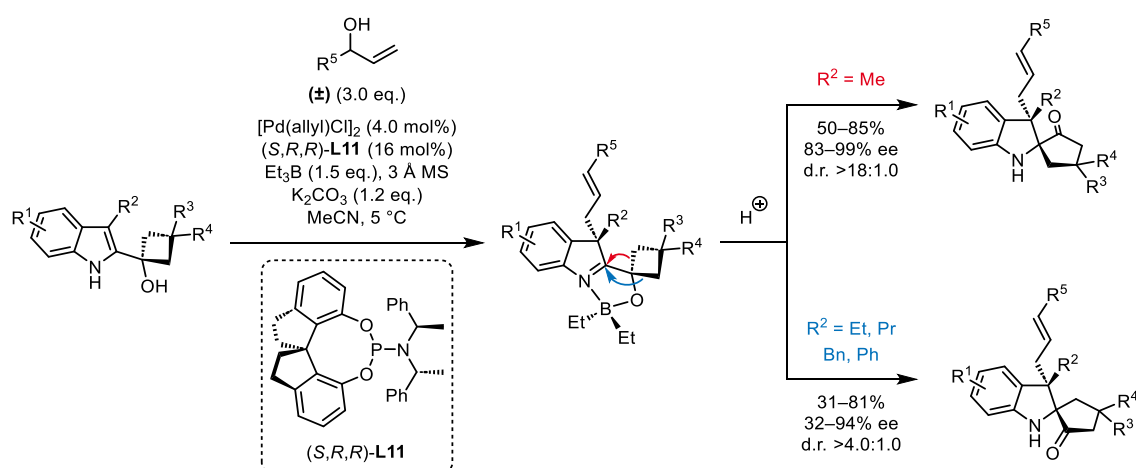


Scheme 27. Enantioselective intramolecular Pd-catalysed allylic substitution reaction with 3-substituted indole derivatives with an allyl methyl carbonate tethered at the 4-position.<sup>[98]</sup>

Wang and co-workers recently reported a sequential Pd-catalysed asymmetric substitution and  $\alpha$ -iminol rearrangement with 3-substituted indole derivatives possessing a cyclobutanol tethered at the 2-position to afford 2-spirocyclic-3,3-disubstituted indoline derivatives (Scheme 28). This elegant sequence constructed two vicinal quaternary carbon stereocentres. From their

## Introduction

optimisation studies, they developed a  $[\text{Pd}(\text{allyl})\text{Cl}]_2\text{-Et}_3\text{B}$  system with chiral phosphoramidite ligand (*S,R,R*)-**L11** and a racemic branched allylic alcohol for enantioselective C3-allylation of the indole derivative, thus generating an isolable tetrahedral boron complex.<sup>[150]</sup> The role of the  $\text{Et}_3\text{B}$  was threefold: to activate the allylic alcohol,<sup>[147]</sup> to coordinate to the N and O atoms in the boron complex thus inhibiting competing N/O-allylation and to enhance the  $\pi$ -nucleophilicity of the indole substrate.<sup>[145]</sup> Subsequent  $\alpha$ -iminol rearrangement of the boron complex under acidic conditions diastereoselectively yielded the 2-spirocyclic-indoline. The substrate scope was investigated. A variety of aryl- and heteroaryl-substituted branched racemic allylic alcohols were shown to be compatible. Notably, substituents at all positions on the indole benzene ring were tolerated. Whereas, in the trialkylborane-promoted Trost procedure no conversion was observed for indole derivatives with 7-substituents; this was assumed to be due to the 7-substituent preventing the coordination of the borane to the indole nitrogen.<sup>[96]</sup> In Wang and co-workers' method, various substituents on the cyclobutanol ring and at the 3-position of the indole derivative were also compatible. Interestingly, when the 3-substituents were larger than methyl the  $\alpha$ -iminol derivatives with opposite diastereoselectivity were obtained. Studies revealed that the allylation step proceeded with the same enantioselectivity; however, the  $\alpha$ -iminol rearrangement proceeded with the opposite facial selectivity. This was attributed to the larger 3-substituents directing the 1,2-shift in the  $\alpha$ -iminol rearrangement to occur on the opposite face. To gain mechanistical insight into the allylic substitution, control experiments were conducted, which supported a kinetic resolution of the racemic branched allylic alcohol rather than a dynamic kinetic resolution.<sup>[150]</sup>



Scheme 28. Sequential enantioselective Pd-catalysed allylic substitution and diastereoselective  $\alpha$ -iminol rearrangement with 3-substituted indole derivatives possessing a cyclobutanol tethered at the 2-position.<sup>[150]</sup>

## *Introduction*

From examination of the conditions employed in the reported systems for the Pd-catalysed allylic substitution with 3-substituted indole derivatives, it can be seen that the Trost Ligands and phosphoramidite ligands are most commonly used. It appears that the Trost ligands are more effective in systems with unactivated allylic alcohols together with trialkylborane additives, whereas phosphoramidite ligands are more suitable with activated allylic substrates, such as allyl carbonates.<sup>[151]</sup>

## 2 Planned Synthetic Approach

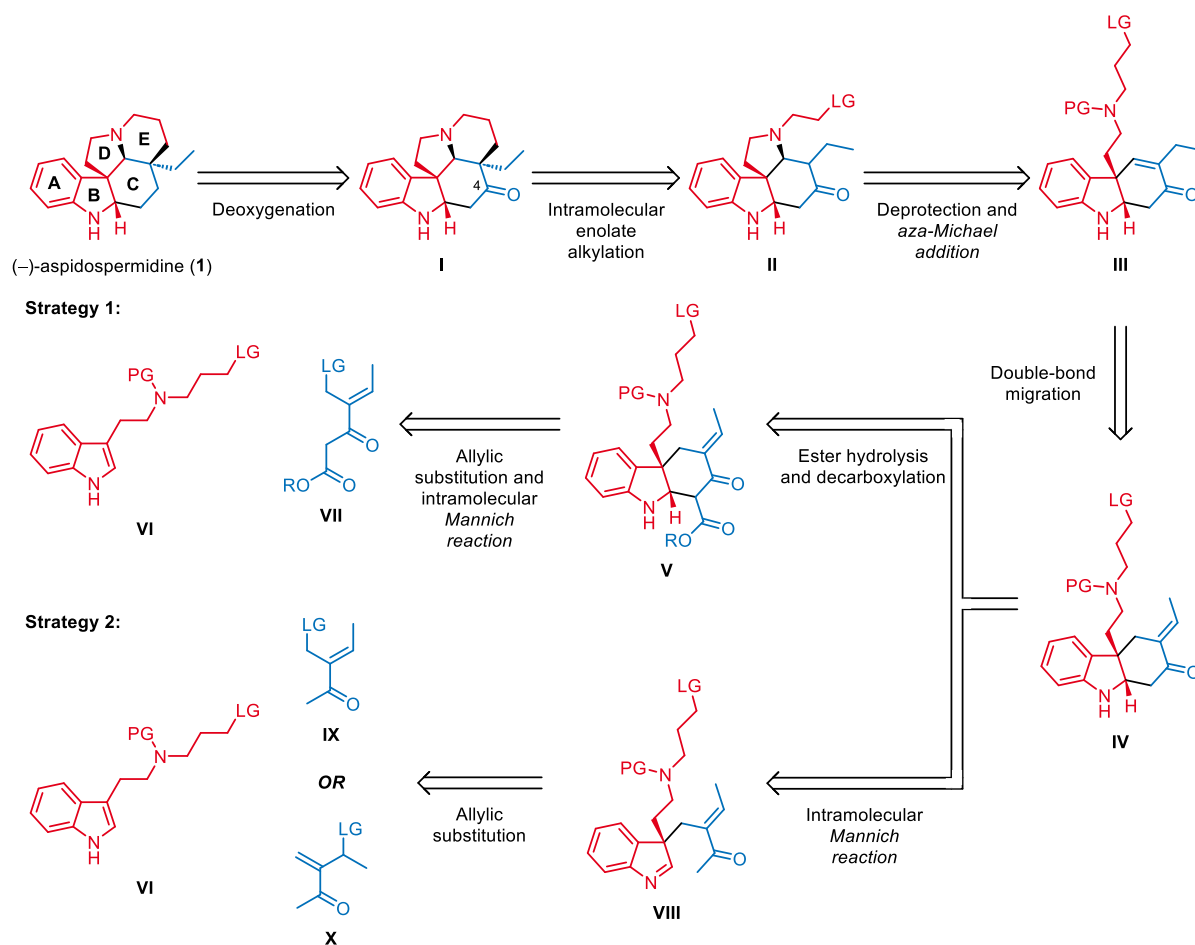
Based on the ongoing interest in asymmetric allylic substitution methodology with 3-substituted indole derivatives<sup>[102]</sup> as well as natural product synthesis in the Stark Group, a novel enantioselective Pd-catalysed allylic substitution strategy for the total synthesis of aspidospermidine (**1**) was proposed.

The retrosynthetic analysis is outlined in Scheme 29. Aspidospermidine (**1**) would be obtained from a deoxygenation of 4-oxo-aspidospermidine **I**. The keto-group in 4-oxo-aspidospermidine **I** would be a residual functionality from the preceding  $\alpha,\beta$ -unsaturated ketone **III**, which would be the bipolar functional handle for establishing both the D and E rings of aspidospermidine (**1**). The E ring in 4-oxo-aspidospermidine **I** would be installed via an intramolecular enolate alkylation from ketone **II**. The D ring in ketone **II** would be established via a *N*-deprotection and concomitant *aza*-Michael addition from the preceding  $\alpha,\beta$ -unsaturated ketone **III**. Importantly, both the D and E rings should be installed in a diastereoselective *cis*-manner. The essential endocyclic enone functionality should arise from an *exo-to-endo* double bond migration from the exocyclic enone **IV**. Two strategies were devised to obtain *exo*-enone **IV**. In the first strategy, the *exo*-enone **IV** would be formed from an ester hydrolysis and decarboxylation of tricycle **V**. The tricycle **V** would be obtained from the key enantioselective allylic substitution reaction between tryptamine derivative **VI**, as the 3-substituted indole derivative, and  $\beta$ -keto ester **VII** as the allylic alkylation substrate. Crucially, under the non-neutral conditions of the allylic substitution reaction, an *in situ* trapping of the generated indoline iminium ion (not shown) by the activated methylene should occur via an intramolecular diastereoselective Mannich reaction to construct the *cis*-fused C ring in tricycle **V**. Thus, two vicinal stereocentres would be installed in this key step. In the second strategy, the *exo*-enone **IV** would be formed from an intramolecular Mannich reaction of indolenine **VIII**. Indolenine **VIII** would be obtained from the key enantioselective allylic substitution reaction between the tryptamine derivative **VI** and either of the regioisomeric  $\alpha,\beta$ -unsaturated ketones **IX** or **X** as the allylic alkylation substrate.

It is worth noting that in both strategies the key enantioselective allylic substitution reactions should not only construct the first quaternary carbon stereocentre, but also assemble the entire framework of aspidospermidine (**1**) in a single step. Since the four stereocentres in aspidospermidine (**1**) are contiguous, it is theoretically possible to establish the correct absolute stereochemistry by defining the first stereocentre and using this to guide the correct stereochemistry at the vicinal positions.<sup>[28]</sup> However, the formation of quaternary carbon

## Planned Synthetic Approach

stereocentres—especially in a catalytic manner—remains an challenging transformation in synthetic chemistry.<sup>[92,144]</sup>



Scheme 29. Retrosynthetic analysis of (+)-aspidospermidine (**1**) via two enantioselective Pd-catalysed allylic substitution strategies.

There are, however, several challenges associated with key allylic substitution reaction. First, there is the chemoselectivity issue, in which both the N1- and C3-positions in the tryptamine derivative **VI** may act as competing nucleophiles. Second, the regioselectivity of the nucleophilic attack on the  $\pi$ -allylpalladium complex, to afford the desired linear substituted product, needs to be considered. Third, there is the challenge of asymmetric induction in which the stereo dictating quaternary carbon stereocentre should be constructed on the prochiral nucleophile **VI**, which may be outwith the chiral environment of the ligand. Finally, there is the unprecedented application of a carbonyl-containing allylic alkylation substrate with a 3-substituted indole derivative; as reported Pd-catalysed allylic substitution methods with 3-substituted indole derivatives employ simple allyl carbonates<sup>[97–99,148,149]</sup> or allyl alcohols<sup>[96,146,150]</sup> as the allylic substrates.

## **2.1 Project Aims**

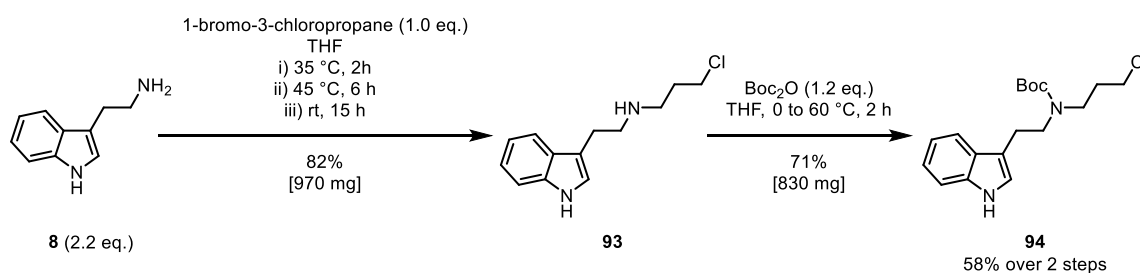
Herein, we report the development of a novel enantioselective Pd-catalysed allylic substitution strategy for the construction of *Aspidosperma* alkaloids, as exemplified by an efficient asymmetric total synthesis of (-)-aspidospermidine (**1**). This required the following milestones:

1. Preparation of the tryptamine derivative **VI** and allylic alkylation substrates **VII**, **IX** and **X**
2. Screening of the allylic alkylation substrates and optimisation of conditions for the Pd-catalysed allylic substitution reaction
3. Screening of chiral ligands and optimisation of conditions to render the Pd-catalysed allylic substitution reaction enantioselective
4. Investigation of alternative pathways for the *exo*-to-*endo* double bond migration from *exo*-enone **IV** to *endo*-enone **III**
5. Performing the diastereoselective D/E ring-closing sequence
6. Performing the deoxygenation reaction to afford aspidospermidine (**1**)

### 3 Results and Discussion

#### 3.1 Preparation of the 3-Substituted Indole Derivative

The synthesis commenced with the preparation of the tryptamine derivative **94** as reported by Zheng and co-workers (Scheme 30).<sup>[152]</sup> In this procedure tryptamine (**8**) was used in slight excess (2.2 eq.) and 1-bromo-3-chloropropane was the limiting reagent. Tryptamine (**8**) was selectively mono-alkylated with 1-bromo-3-chloropropane to give the alkylated intermediate **93** in a yield of 82%. A subsequent *N*-Boc-protection afforded the tryptamine derivative **94** in a yield of 71%. The tryptamine derivative **94** was therefore obtained in an overall yield of 58% over two steps from commercially available tryptamine (**8**). For the Boc-protection step, standard conditions with di-*tert*-butyl dicarbonate, Boc<sub>2</sub>O, and Et<sub>3</sub>N in CH<sub>2</sub>Cl<sub>2</sub> at room temperature were also tested. Under these conditions, the tryptamine derivative **94** was obtained in a lower yield of 59% from the alkylated tryptamine **93**, potentially due to elimination of the primary chloride via an E2 mechanism.

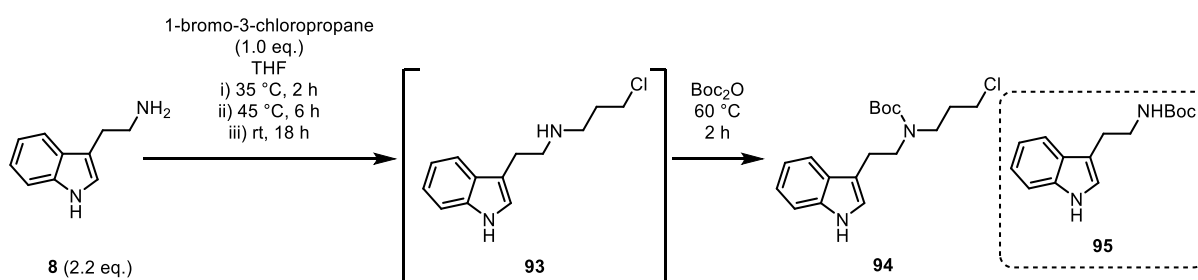


Scheme 30. Preparation of tryptamine derivative **94** over two steps from tryptamine (**8**).

We were intrigued to see whether the alkylation and Boc-protection sequence could be performed as a one-pot transformation (Table 2). Notably, it was not possible to monitor the conversion of the 1-bromo-3-chloropropane limiting reagent by thin layer chromatography (TLC) analysis; therefore, after the reaction was stirred at room temperature for 15 h, the presence of the alkylated tryptamine intermediate **93** was confirmed by TLC analysis, prior to addition of Boc<sub>2</sub>O for the protection step. The conditions reported by Zheng and co-workers were initially applied for the one-pot transformation; the tryptamine derivative **94** was obtained in a yield of 57% over two steps from tryptamine (**8**) (Table 2, entry 1). In this one-pot sequence, Boc-tryptamine (**95**) was formed as a side product. The separation of this side product **95** from the tryptamine derivative **94** required repeated column chromatography purification. Therefore, to reduce the amount of Boc-tryptamine (**95**) produced, and hence facilitate the purification process, fewer equivalents of Boc<sub>2</sub>O were used to test whether the alkylated tryptamine intermediate **93** was preferentially Boc-protected compared to the excess

tryptamine (**8**). Although the alkylated tryptamine **93** was more sterically hindered due to its two alkyl substituents, the electron-donating inductive effect of these two alkyl substituents meant that the pendent nitrogen atom in the alkylated tryptamine intermediate **93** should be more nucleophilic than the pendent nitrogen atom in tryptamine (**8**). However, using fewer  $\text{Boc}_2\text{O}$  equivalents resulted in a lower yield of the tryptamine derivative **94** of 41% (Table 2, entry 2). Another idea to facilitate the purification was to use fewer equivalents of tryptamine (**8**), by replacing the excess tryptamine (**8**) with  $\text{Et}_3\text{N}$  (Table 2, entry 3). Unfortunately, the tryptamine derivative **94** was then obtained in an even lower yield of 33%. Therefore, the conditions reported by Zheng and co-workers were further used in the modified one-pot procedure. Pleasingly, upon scale-up the tryptamine derivative **94** was obtained in a yield of 72% (Table 2, entry 4).

Table 2. Screening of conditions for the one-pot alkylation and Boc-protection of tryptamine (**8**).

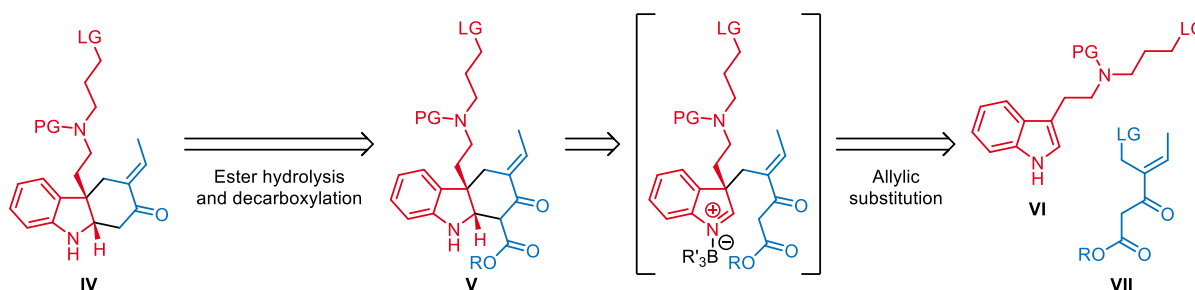


Entry	Reagents (eq.)	Yield (%)
1	<b>8</b> (2.2), $\text{Boc}_2\text{O}$ (2.5)	57
2	<b>8</b> (2.2), $\text{Boc}_2\text{O}$ (1.3)	41
3	<b>8</b> (1.1), $\text{Et}_3\text{N}$ (1.1), $\text{Boc}_2\text{O}$ (1.3)	33
4 <sup>a</sup>	<b>8</b> (2.3), $\text{Boc}_2\text{O}$ (2.8)	72

Unless stated otherwise, all reactions were performed on a scale of 0.5 mmol. <sup>a</sup>Reaction scale of 12 mmol.

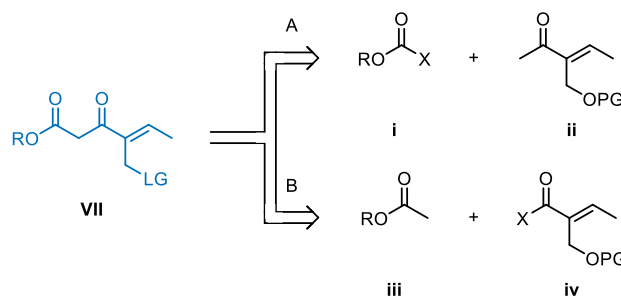
### 3.2 Preparation of the Allylic Alkylation Substrate: Strategy 1

With the tryptamine derivative **94** in hand, we then turned our attention to the synthesis of the  $\beta$ -keto ester **VII** as the allylic alkylation substrate in strategy 1. Notably, the  $\beta$ -keto ester **VII** contains an additional carbon atom, incorporated within the ester group, than is present in aspidospermidine (**1**) (Scheme 31). The additional ester group in the  $\beta$ -keto ester **VII** was required for activation of the methylene group at the  $\alpha$ -position to the ketone in the indoline iminium ion. Under the non-neutral conditions of the allylic substitution reaction, deprotonation of the activated methylene group was proposed to result in an *in situ* trapping of the generated indoline iminium ion. Thus, two vicinal stereocentres would be installed in this key step. The superfluous ester group in tricycle **V** would then be cleaved through an ester hydrolysis and decarboxylation to give the *exo*-enone **IV**.



Scheme 31. Retrosynthetic analysis of *exo*-enone **IV** according to strategy 1.

There are two main approaches to the synthesis of the  $\beta$ -keto ester **VII** as shown in Scheme 32. In approach A, an electrophilic chloroformate ester **i** would be used with a nucleophilic  $\alpha,\beta$ -unsaturated methyl ketone **ii**. In approach B the electrophilic and nucleophilic components are reversed, in which a nucleophilic acetate ester **iii** would be applied with an electrophilic  $\alpha,\beta$ -unsaturated compound **iv**. Approach A was first investigated for the synthesis of the  $\beta$ -keto ester **VII**.

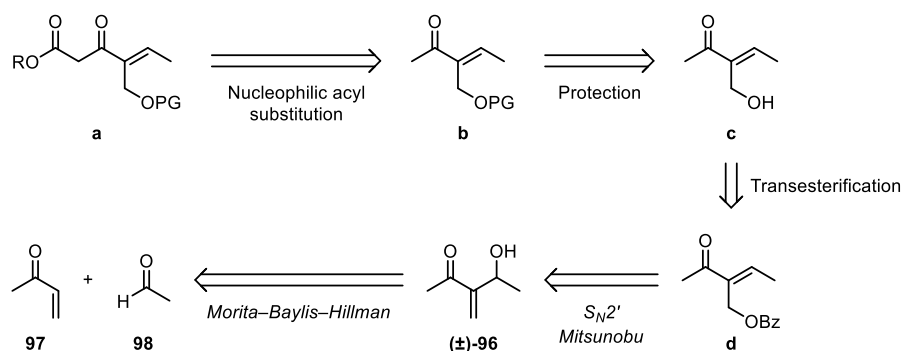


Scheme 32. Retrosynthetic analysis of  $\beta$ -keto ester **VII** via approaches A and B. Where LG = OPG.

## 3.2.1 Approach A

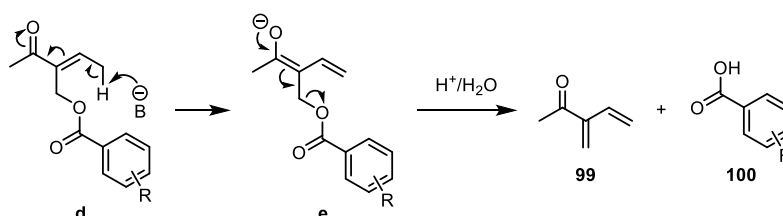
## 3.2.1.1 Route 1

The retrosynthetic analysis of the  $\beta$ -keto ester **VII** according to approach A is outlined in Scheme 33. The  $\beta$ -keto ester **a** would be obtained from a nucleophilic acyl substitution of a chloroformate ester with the  $\alpha,\beta$ -unsaturated methyl ketone **b**. The protected  $\beta$ -hydroxy ketone **b** would be prepared in a deprotection-reprotection sequence from the benzoate-protected  $\beta$ -hydroxy ketone **d**. The benzoate-protected allylic alcohol **d** would be obtained from a  $S_N2'$  Mitsunobu reaction of the allylic alcohol **96** with a benzoic acid. A Morita–Baylis–Hillman reaction between methyl vinyl ketone (**97**) and acetaldehyde (**98**) would afford the adduct **96**.



Scheme 33. Retrosynthetic analysis of the  $\beta$ -keto ester **a** in route 1.

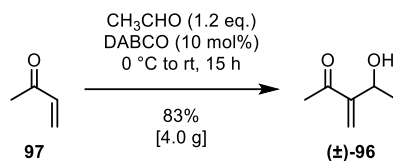
Under the basic conditions of the nucleophilic acyl substitution reaction, it was proposed that the  $\gamma$ -position of the allylic benzoate **d** could be deprotonated to form the thermodynamic dienolate **e**, which would eliminate the benzoate (Scheme 34). This elimination should be prevented by exchanging the benzoate ester with another hydroxy protecting group that is not a good leaving group via a deprotection-reprotection sequence.



Scheme 34. Proposed elimination from the allylic benzoate **d**, via the thermodynamic dienolate **e** upon  $\gamma$ -deprotonation.

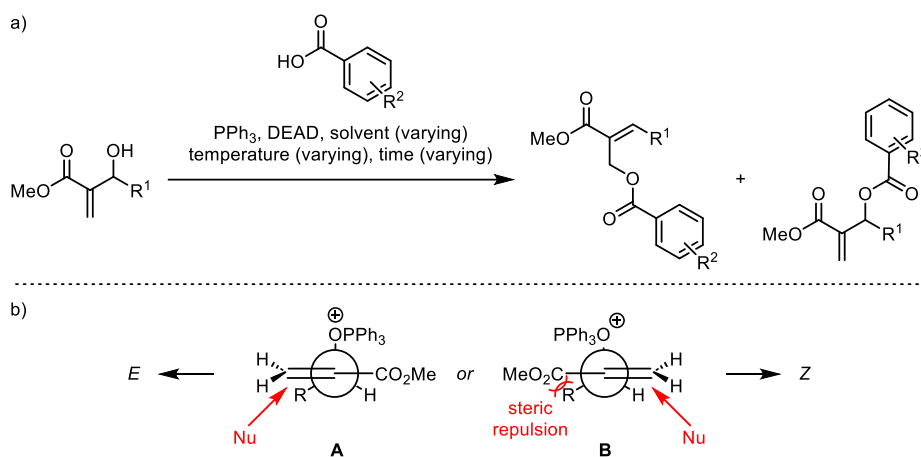
## Results and Discussion

The synthesis began with the Morita–Baylis–Hillman reaction to afford the adduct **96** in a high yield of 83% (Scheme 35).<sup>[153]</sup>



Scheme 35. Preparation of Morita–Baylis–Hillman adduct **96** from methyl vinyl ketone (**97**) and acetaldehyde (**98**).

The proposed  $\text{S}_{\text{N}}2'$  Mitsunobu reaction was based on a regio- and stereoselective  $\text{S}_{\text{N}}2'$  Mitsunobu method reported by Charette and co-workers. Their procedure used various 3-hydroxy-2-methylenealkanoates and benzoic acids to give the regioisomeric  $\text{S}_{\text{N}}2'$  and  $\text{S}_{\text{N}}2$  products (Scheme 36a). The  $\text{S}_{\text{N}}2'$  products were exclusively formed as the (*E*)-stereoisomers, which was accounted for by the proposed transition state shown in Scheme 36b. In which the oxophosphonium leaving group is located perpendicular to the double bond for maximal  $\pi \rightarrow \sigma^*$  overlap upon nucleophilic addition, giving two possible models **A** and **B**. Model **B** is disfavoured due to steric repulsion between the methyl ester and R substituent. This repulsion is reduced in model **A**, which is therefore favoured and results in the stereoselective formation of the (*E*)-isomer.<sup>[154,155]</sup>

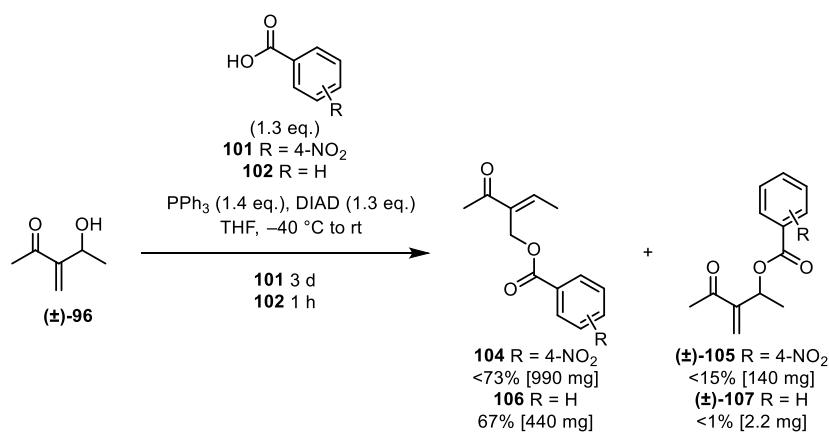


Scheme 36. Mitsunobu reaction reported by Charette and co-workers: a) between 3-hydroxy-2-methylenealkanoates and benzoic acids to give  $\text{S}_{\text{N}}2'$  and  $\text{S}_{\text{N}}2$  products;<sup>[154,155]</sup> b) proposed transition state, adapted from <sup>[155]</sup>. DEAD = diethyl azodicarboxylate.

In our studies into the Mitsunobu reaction, diethyl azodicarboxylate (DEAD) was replaced with diisopropyl azodicarboxylate (DIAD) as a safer azodicarboxylate. Additionally, Charette and

## Results and Discussion

co-workers reported that yields and selectivities were not affected upon switching from DEAD to DIAD.<sup>[155,156]</sup> Although it was reported that employing 4-nitrobenzoic acid (**101**) in the Mitsunobu reaction gave the lowest  $S_N2'$ : $S_N2$  product ratios, the products were reported to be easier to purify compared to when benzoic acid (**102**) or 2,4,6-trimethylbenzoic acid (**103**) were used. Therefore, 4-nitrobenzoic acid (**101**) was initially applied in our system. The low temperature control that Charette and co-workers had reported to give the highest  $S_N2'$ : $S_N2$  product ratios in their system with 4-nitrobenzoic acid (**101**) was also employed to favour formation of the desired  $S_N2'$  product (Scheme 37).<sup>[155]</sup> Unfortunately, when submitting allylic alcohol **96** under these conditions, the desired  $S_N2'$  product **104** was obtained in a yield of <73% with reduced DIAD as an inseparable impurity after repeated column chromatography. Attempts to further purify the  $S_N2'$  product **104** by recrystallisation from petroleum ether 40–65/EtOAc (1:1), as described by Charette and co-workers for their related compounds,<sup>[155]</sup> were ineffective. The undesired  $S_N2$  product **105** was obtained in a yield of <15%, with inseparable impurities after column chromatography and subsequent recrystallisation from petroleum ether 40–65/EtOAc (1:1). Benzoic acid (**102**) was then used in place of 4-nitrobenzoic acid (**101**), as Charette and co-workers had reported that benzoic acid (**102**) gave the highest  $S_N2'$  product yields in their system.<sup>[154,155]</sup> Fortunately, the pure desired  $S_N2'$  product **106** was then obtained in a yield of 67%, with the undesired  $S_N2$  product **107** obtained in trace amounts (Scheme 37).

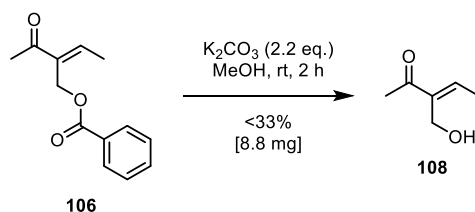


Scheme 37. Mitsunobu reaction between allylic alcohol **96** and 4-nitrobenzoic acid (**101**) or benzoic acid (**102**) to give the  $S_N2'$  products **104** and **106** and  $S_N2$  products **105** and **107**, respectively.

Transesterification of the allylic benzoate **106** gave the allylic alcohol **108**, albeit in a low yield with inseparable impurities, which were presumed to be from methoxide addition to the Michael system of the  $\alpha,\beta$ -unsaturated ketone **106**. Therefore, an alternative route to the  $\beta$ -keto

## Results and Discussion

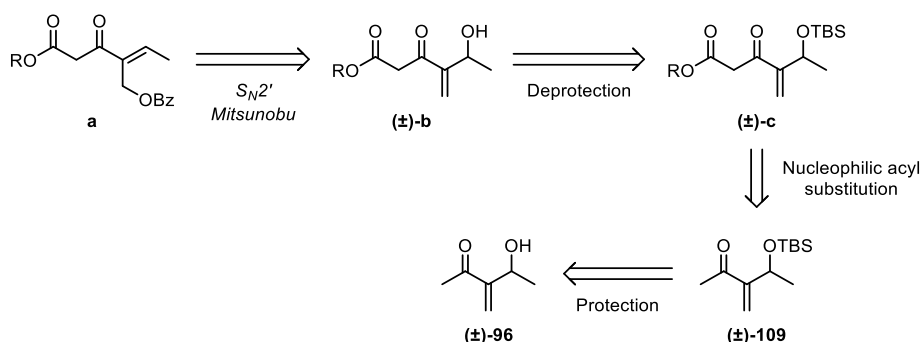
ester **VII** according to approach A, which circumvented the transesterification of an  $\alpha,\beta$ -unsaturated compound was sought.



Scheme 38. Transesterification of the allylic benzoate **106** to give the allylic alcohol **108**.

### 3.2.1.2 Route 2

By reversing the order of the nucleophilic acyl substitution and Mitsunobu reactions, as shown in the retrosynthetic analysis of the  $\beta$ -keto ester **a** in route 2 (Scheme 39), the transesterification step could be avoided. Furthermore, benzoates have been reported as leaving groups in allylic substrates in Pd-catalysed allylic substitution reactions.<sup>[93]</sup> The  $\beta$ -keto ester **a** would be obtained from an  $S_N2'$  Mitsunobu reaction of allylic alcohol **b** with a benzoic acid. The allylic alcohol **b** would be provided from a deprotection of the TBS-protected allylic alcohol **c**, which in turn would be obtained from a nucleophilic acyl substitution of a chloroformate ester with the  $\alpha,\beta$ -unsaturated methyl ketone **109**. The *tert*-butyldimethylsilyl (TBS) ether **109** would be provided from a protection of the hydroxy group in the allylic alcohol **96**. Protection of the hydroxy group as the base-stable TBS ether **109** was required to prevent side reactions with the nucleophilic alkoxide that would otherwise be generated under the basic conditions of the nucleophilic acyl substitution reaction.

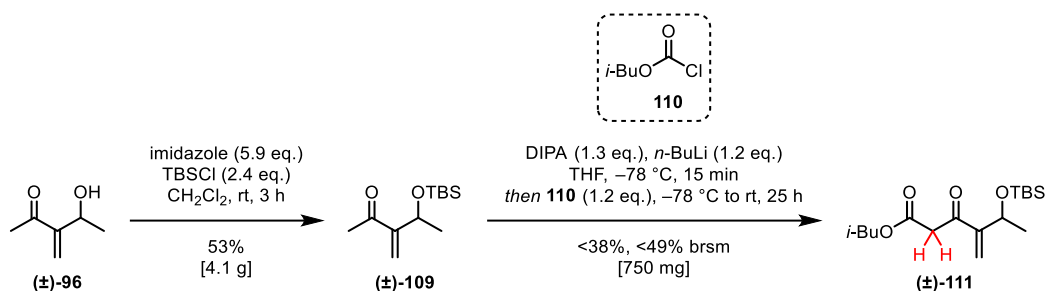


Scheme 39. Retrosynthetic analysis of the  $\beta$ -keto ester **a** in route 2.

The hydroxy group in the allylic alcohol **96** was protected with *tert*-butyldimethylsilyl chloride, TBSCl, to afford the TBS ether **109** (Scheme 40). In the subsequent nucleophilic acyl substitution reaction, isobutyl chloroformate (**110**) was applied as the electrophile. The desired

## Results and Discussion

$\beta$ -keto ester **111** was obtained in a yield of <38%, <49% brsm (brsm = based on recovered starting material), with impurities that were non-trivial to separate even after repeated column chromatography. It was proposed that the low yield of the nucleophilic acyl substitution was due to quenching of the lithium diisopropylamide (LDA) base by the  $\beta$ -keto ester product **111**, as its  $\alpha$ -hydrogens atoms (shown in red in Scheme 40) were more acidic than the  $\alpha$ -hydrogen atoms to the ketone in the starting material **109**. Using more than two equivalents of the base may have resulted in complete conversion of the TBS ether **109**. However, as we had sufficient quantities of the  $\beta$ -keto ester **111** in hand, we proceeded with the next steps.

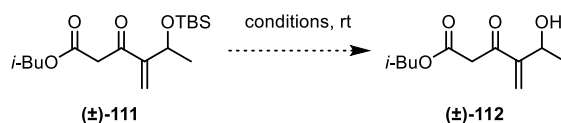


Scheme 40. TBS-protection of allylic alcohol **96** and subsequent nucleophilic acyl substitution to give  $\beta$ -keto ester **111**. DIPA = diisopropylamine.

Conditions for the deprotection of the TBS-protected allylic alcohol **111** were then sought (Table 3). Tetra-*n*-butylammonium fluoride (TBAF) was first used as a fluoride source (Table 3, entry 1), however decomposition was observed. A mixture of TBAF and acetic acid (1:1) was then applied (Table 3, entry 2), to neutralise the basicity of the TBAF.<sup>[157]</sup> Decomposition was again observed. When acetic acid was employed alone, no reaction was observed (Table 3, entry 3).<sup>[158]</sup> Camphorsulfonic acid (CSA) was then used as a stronger acid (Table 3, entry 4).<sup>[159]</sup> Unfortunately, decomposition was observed. Applying sodium periodate also resulted in decomposition (Table 3, entry 5).<sup>[160]</sup> HF-pyridine was then employed (Table 3, entry 6).<sup>[161]</sup> From TLC analysis, a new product and complete conversion of the TBS-protected allylic alcohol **111** were observed. From analysis of the  $^1\text{H}$  NMR spectrum of the crude product, an upfield shift of the methylenes signals was observed that was suggestive of formation of the deprotected product **112**. After purification by silica gel column chromatography the upfield shifted methylenes signals were only observed as trace signals, which suggested decomposition of the allylic alcohol **112** on the silica gel, despite 2D TLC analysis of the crude product indicating that it was stable to silica.

## Results and Discussion

Table 3. Screening of conditions for the deprotection of the TBS-protected allylic alcohol **111**.



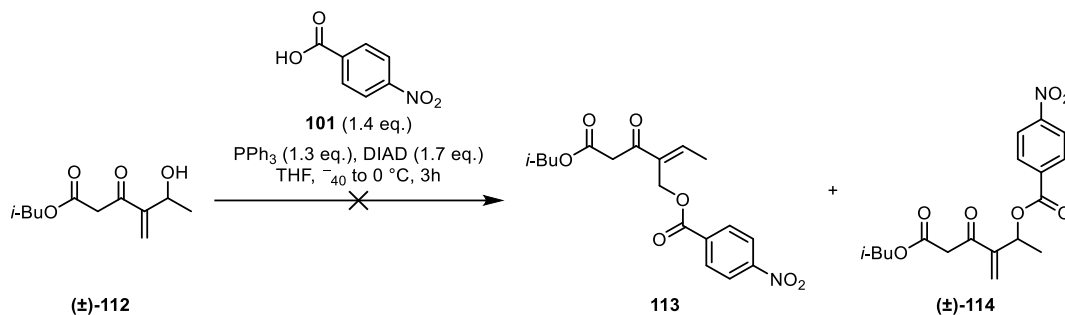
Entry	Reagent (eq.)	Solvent	Time	Scale ( $\mu\text{mol}$ )	Result
1	TBAF (1.2)	THF	23 h	120	decomposition
2	TBAF:AcOH (1.2; 1:1)	THF	3 d	60	decomposition
3	AcOH (1.7)	MeOH	3 d	60	no reaction
4	CSA (1.0)	CH <sub>2</sub> Cl <sub>2</sub> :MeOH (1:1)	21 h	60	decomposition
5	NaIO <sub>4</sub> (3.2)	THF	4 d	60	decomposition
6	HF-pyridine (0.15 mL <sup>a</sup> )	THF	3 h	60	crude <b>112</b> <sup>b</sup>
7	HCOOH (67)	THF:H <sub>2</sub> O (6:1)	18 h	60	crude <b>112</b> <sup>b</sup>
8	BF <sub>3</sub> ·OEt <sub>2</sub> (2.0)	CH <sub>2</sub> Cl <sub>2</sub>	3 h	60	crude <b>112</b> <sup>b</sup>
9	BF <sub>3</sub> ·OEt <sub>2</sub> (2.1)	CH <sub>2</sub> Cl <sub>2</sub>	2 h	150	crude <b>112</b> <sup>b</sup>

<sup>a</sup>Not possible to determine equivalents as HF-pyridine is a complex. <sup>b</sup>Observed by TLC analysis and by analysis of the <sup>1</sup>H NMR spectrum of the crude product.

To circumvent the silica gel column chromatography purification, it was decided to use the crude product **112** directly in the subsequent Mitsunobu reaction. Although signals indicative of the allylic alcohol **112** were observed in the <sup>1</sup>H NMR spectrum of the crude product when using HF-pyridine (Table 3, entry 6), large quantities of pyridine were also observed. Therefore, alternative deprotection conditions were sought. Formic acid (HCOOH) (Table 3, entry 7)<sup>[162]</sup> and BF<sub>3</sub>·OEt<sub>2</sub> (Table 3, entry 8) were then tested in parallel.<sup>[163]</sup> Under both of these conditions, a new product that was presumed to be the allylic alcohol **112** was observed by TLC analysis. Additionally, from <sup>1</sup>H NMR analysis of both of the crude products, the upfield shifted methylenes signals were observed and the spectra contained fewer impurities than under the HF-pyridine conditions. Under the BF<sub>3</sub>·OEt<sub>2</sub> conditions, full assignment of the signals from the deprotected product **112** was possible by analysis of the <sup>1</sup>H and <sup>13</sup>C NMR spectra of the crude product. The deprotection using BF<sub>3</sub>·OEt<sub>2</sub> was then repeated on a larger scale (Table 3, entry 9), to obtain material for the subsequent Mitsunobu reaction. Notably, the

cyclic  $\beta$ -keto ester, from a lactonisation of the allylic alcohol **112**, was not observed under any of the deprotection conditions.

The crude allylic alcohol **112** was then submitted to the  $S_N2'$  Mitsunobu reaction, with 4-nitrobenzoic acid (**101**) and the low temperature control as employed in route 1 (Scheme 41). Although there was complete conversion of the allylic alcohol **112**, neither of the Mitsunobu products **113** nor **114** were obtained.



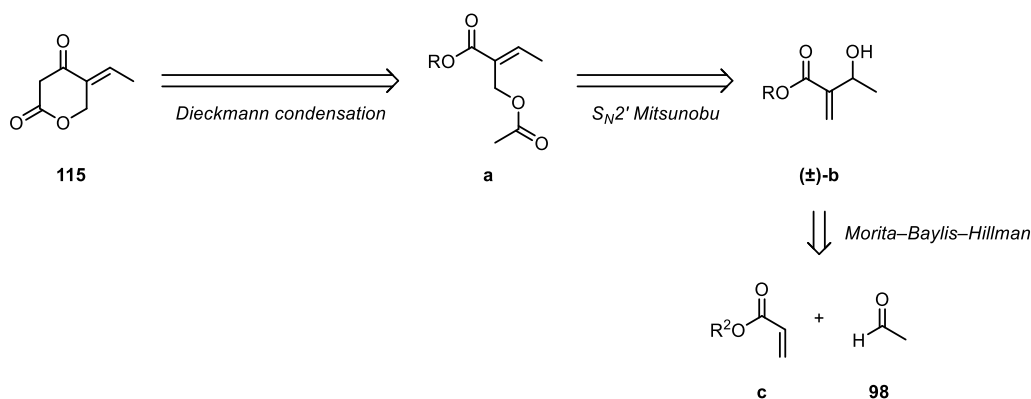
Scheme 41. Unsuccessful Mitsunobu reaction between crude allylic alcohol **112** and 4-nitrobenzoic acid (**101**).

Due to challenges associated with the purification of the allylic alcohol **112** and the unsuccessful Mitsunobu reaction, we attempted to synthesise a cyclic  $\beta$ -keto ester as an alternative allylic alkylation substrate.

### 3.2.1.3 Route 3

The retrosynthetic analysis of the cyclic  $\beta$ -keto ester **115** is outlined in Scheme 42. The cyclic  $\beta$ -keto ester **115** would be obtained from a Dieckmann condensation of the acyclic diester **a**. Under the basic conditions of the Dieckmann condensation, the acetate group in the acyclic diester **a** would be deprotonated, generating the corresponding enolate, which would then act as the nucleophile in the condensation reaction. The alkyl ester group in the acyclic diester **a** would be the electrophile in the condensation reaction, compared to a chloroformate ester as in routes 1 and 2. The acetate ester **a** would be formed from an  $S_N2'$  Mitsunobu reaction with acetic acid as the pronucleophile, from the allylic alcohol **b**. The allylic alcohol **b** would be prepared from a Morita–Baylis–Hillman reaction between an alkyl acrylate **c** and acetaldehyde (**98**).

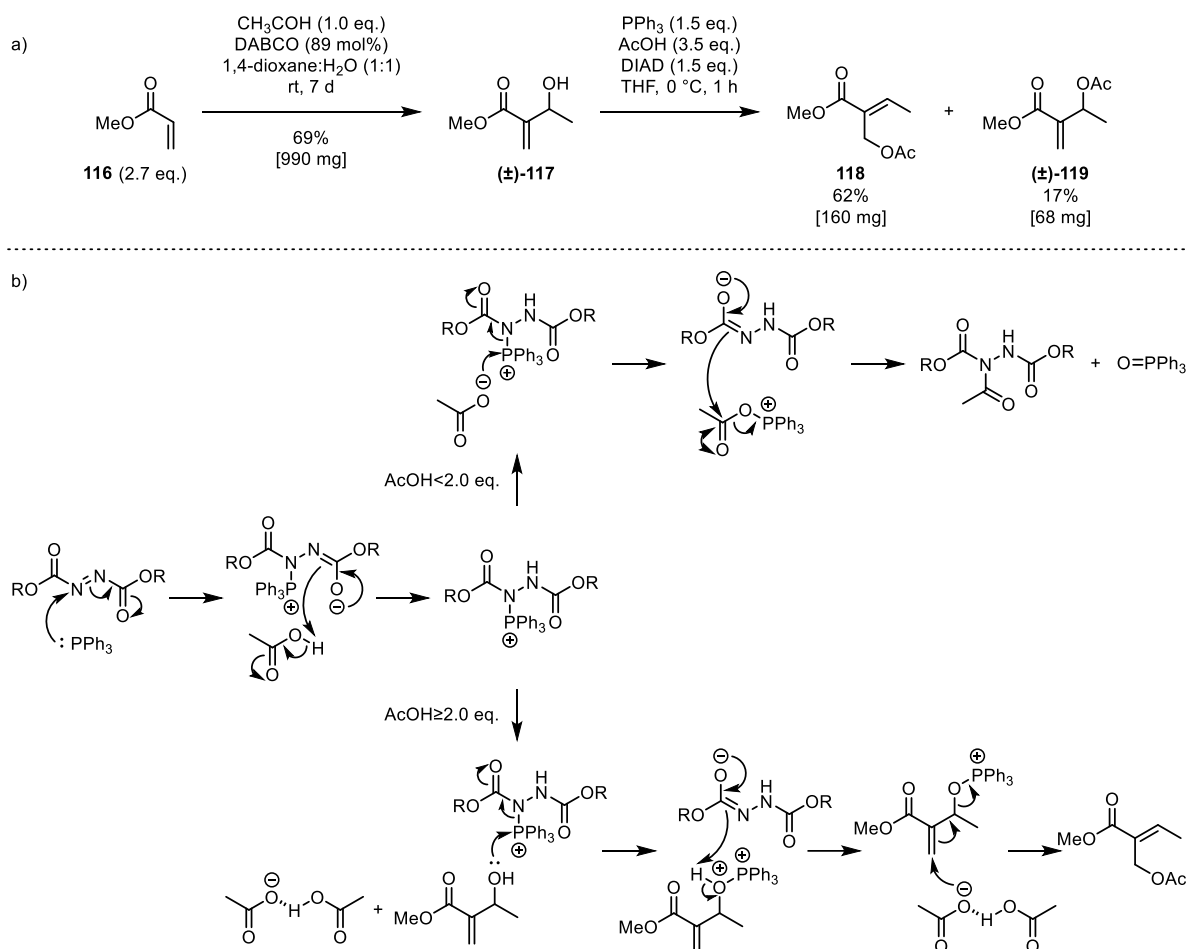
## Results and Discussion



Scheme 42. Retrosynthetic analysis of the cyclic  $\beta$ -keto ester **115** in route 3.

The methyl ester Morita–Baylis–Hillman adduct **117** was prepared from methyl acrylate (**116**) and acetaldehyde (**98**) and then submitted to the Mitsunobu reaction, giving the desired  $S_{N2'}$  product **118** in a yield of 62% (Scheme 43a).<sup>[154,155,164]</sup> Crucially, in the Mitsunobu reaction more than two equivalents of acetic acid were required. The Mitsunobu reaction commences with nucleophilic attack of the triphenylphosphine on the azodicarboxylate, generating a zwitterionic intermediate. When only one equivalent of acetic acid is applied, it is fully deprotonated by the zwitterionic intermediate forming the acetate ion, which then attacks the phosphonium ion (Scheme 43b). The newly formed O-acyl phosphonium ion undergoes nucleophilic acyl substitution from the partially reduced azodicarboxylate, resulting in *N*-acetylation of the azodicarboxylate. Consequently, the Mitsunobu reaction does not proceed. However, when two or more equivalents of acetic acid are used, only one equivalent is fully deprotonated and a H-bonded species between the acetate ion and the second equivalent of acetic acid is proposed to form. This H-bonded species is proposed to be less nucleophilic than the acetate ion and therefore does not attack the phosphonium ion. Thus, *N*-acetylation of the azodicarboxylate is prevented and the desired Mitsunobu reaction proceeds.<sup>[156]</sup> Notably, when less than two equivalents of 4-nitrobenzoic acid (**101**) were later applied with the analogous ethyl ester Morita–Baylis–Hillman adduct **121** (Scheme 45), *N*-benzoylation of the azodicarboxylate was not observed. It was proposed that the electron-withdrawing 4-nitrophenyl substituent in 4-nitrobenzoic acid (**101**) renders it less nucleophilic than acetic acid, consequently the 4-nitrobenzoate does not attack the phosphonium ion.

## Results and Discussion

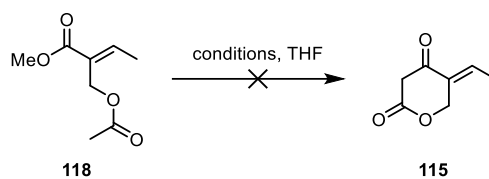


Scheme 43. a) Morita–Baylis–Hillman and Mitsunobu reaction sequence to give the desired  $S_N2'$  and undesired  $S_N2$  products **118** and **119**, respectively. b) Mechanism of the Mitsunobu reaction of the allylic alcohol **116** with acetic acid, as dependent on the equivalents of acetic acid used, formation of the  $S_N2$  product is not shown; adapted from <sup>[156]</sup>.

Basic conditions for the Dieckmann condensation of the acyclic diester **118** were then screened (Table 4). Unfortunately, none of the applied conditions gave the desired lactone **115** nor the recovered starting material **118**. It was proposed that under the applied basic conditions, the  $\gamma$ -carbon of the allylic acetate **118** could have been deprotonated to form the thermodynamic dienolate, which could then eliminate the acetate, comparable with the analogous benzoate compound in Scheme 34.

## Results and Discussion

Table 4. Screening of conditions for the Dieckmann condensation of the acyclic diester **118**.



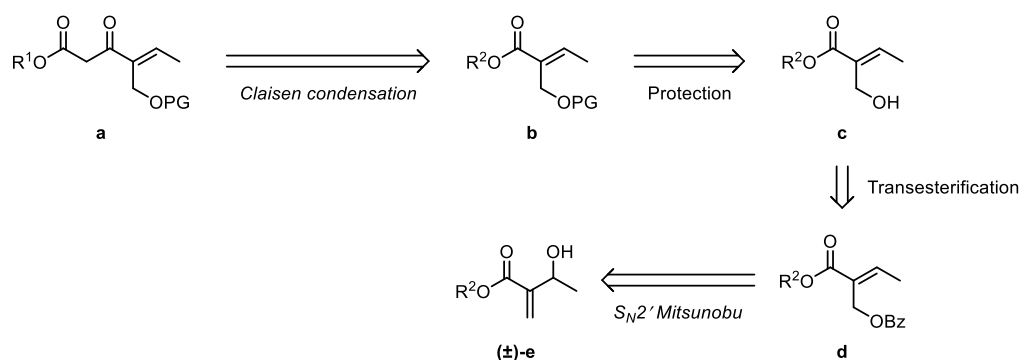
Entry	Base (eq.)	<i>T</i> (°C)	Time (h)	Scale (mmol)	Result
<b>1</b>	<i>t</i> -BuOK (2.3)	0	0.5	0.15	decomposition
<b>2</b>	LiHMDS (1.3)	-78 to 0	1	0.12	decomposition
<b>3</b>	LiHMDS (2.2)	-78 to 0	1	0.12	decomposition
<b>4</b>	DIPA (2.4) <i>n</i> -BuLi (2.2)	-78 to 0	3	0.17	decomposition

Due to the unsuccessful synthesis of the  $\beta$ -keto ester **VII** by routes 1–3 in approach A, approach B was then investigated for synthesis of the  $\beta$ -keto ester **VII**.

### 3.2.2 Approach B

#### 3.2.2.1 Route 4

The initial retrosynthetic analysis of the  $\beta$ -keto ester **VII** according to approach B is outlined in Scheme 44. The  $\beta$ -keto ester **a** would be obtained from a Claisen condensation between the  $\alpha,\beta$ -unsaturated ester **b** and an alkyl acetate. The protected  $\beta$ -hydroxy ester **b** would be formed by a deprotection-reprotection sequence from the benzoate-protected  $\beta$ -hydroxy ester **d**. In the benzoate-protected  $\beta$ -hydroxy ester **d**, the benzoate ester would be the more electrophilic than the  $\alpha,\beta$ -unsaturated ester, therefore a deprotection-reprotection sequence of the hydroxy group with a non-electrophilic protecting group was required for the desired chemoselectivity at the  $\alpha,\beta$ -unsaturated ester in the Claisen condensation. The  $\alpha,\beta$ -unsaturated ester **d** would be formed from a  $S_N2'$  Mitsunobu reaction of the allylic alcohol **e** with a benzoic acid.

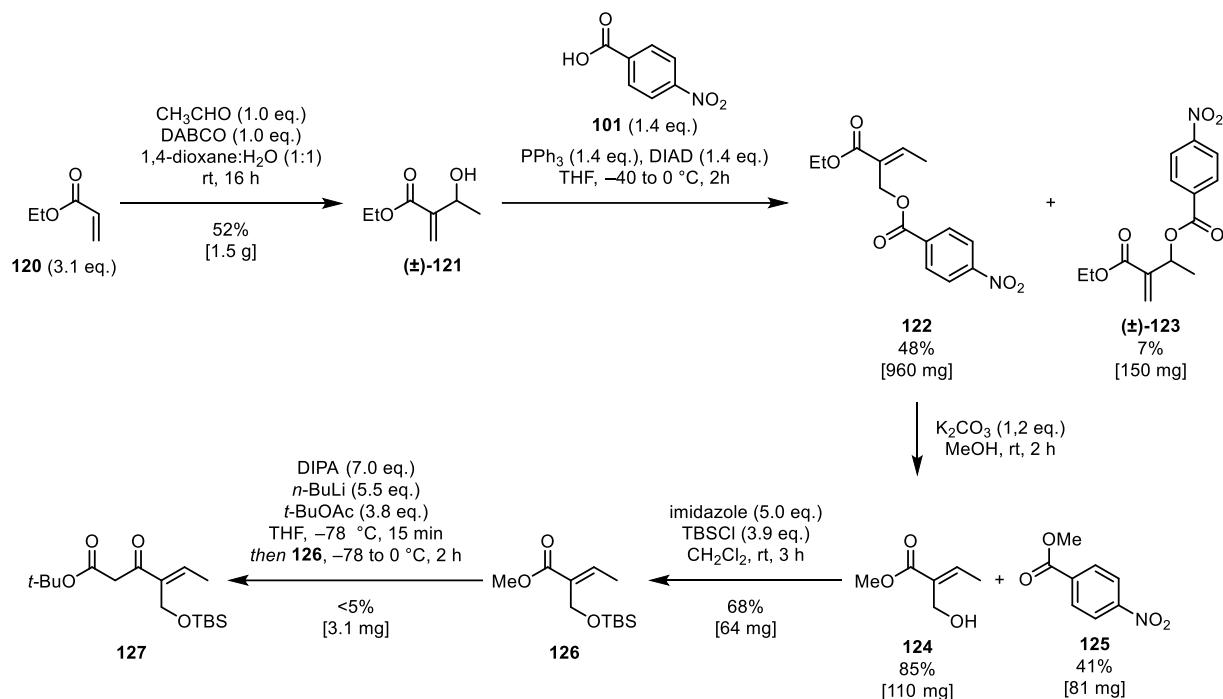


Scheme 44. Retrosynthetic analysis of the  $\beta$ -keto ester **a** in route 4.

The ethyl ester Morita–Baylis–Hillman adduct **121** was prepared from ethyl acrylate (**120**) and acetaldehyde (**98**) in a yield of 52% (Scheme 45).<sup>[165]</sup> The Mitsunobu reaction between the allylic alcohol **121** and 4-nitrobenzoic acid (**101**) afforded the desired  $S_N2'$  Mitsunobu product **122** in 48% yield. The undesired  $S_N2$  Mitsunobu product **123** was obtained in 7%. The transesterification of the 4-nitrobenzoate ester **122** afforded the  $\alpha,\beta$ -unsaturated methyl ester **124**.<sup>[154]</sup> Notably, the transesterification of the 4-nitrobenzoic ester **122** proceeded in higher yield than when the related benzoate ester **106** was cleaved (Scheme 38), due to the better 4-nitrobenzoate leaving group.<sup>[166]</sup> The hydroxy group in the ester **124** was then protected as a TBS ether **126**. Notably, for the allylic substitution reaction the silyl group would have to be exchanged for an appropriate leaving group or alternatively deprotection of the TBS ether **126** after the Claisen condensation would give an unactivated allylic alkylation substrate. For the subsequent Claisen condensation, *t*-butyl acetate, *t*-BuOAc, was selected as the alkyl acetate as the steric bulk of the *t*-butyl group should prevent its self-condensation.<sup>[167]</sup>

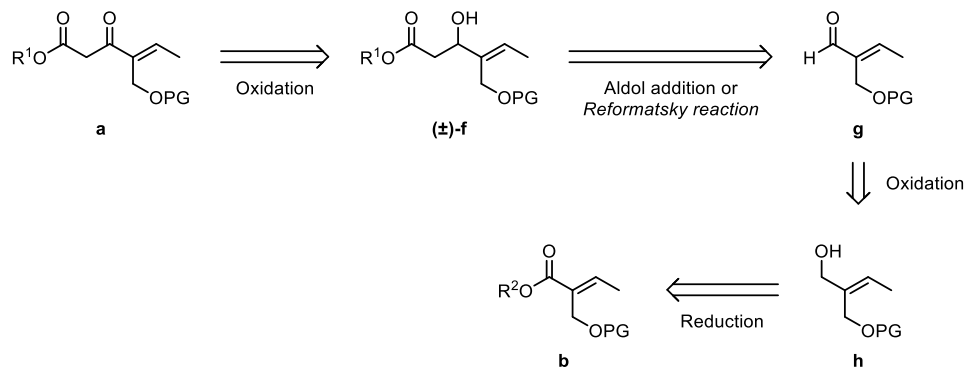
## Results and Discussion

Unfortunately, the desired  $\beta$ -keto ester **127** was only obtained in trace amounts in the Claisen condensation.



Scheme 45. Synthesis of  $\beta$ -keto ester **127** in route 4.

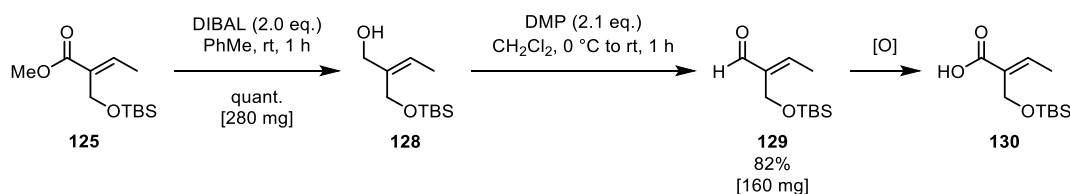
It was proposed that the yield of the key carbon-carbon bond forming step could be increased by using the more electrophilic corresponding  $\alpha,\beta$ -unsaturated aldehyde **g** in place of the ester **b** (Scheme 46). Notably, when employing the aldehyde **g** as the electrophile, other carbon-carbon bond forming reactions such as an aldol addition or a Reformatsky reaction would be required. These reactions would give the  $\beta$ -hydroxy ester **f**. A subsequent oxidation would then provide the corresponding  $\beta$ -keto ester **a**. It was proposed that the aldehyde **g** would be obtained by an oxidation-reduction sequence from the ester **b**.



Scheme 46. Retrosynthetic analysis of the  $\beta$ -keto ester **a** via aldehyde **g**.

## Results and Discussion

The reduction of the  $\alpha,\beta$ -unsaturated ester **125** using diisobutylaluminium hydride (DIBAL) gave the allylic alcohol **128** in quantitative yield (Scheme 47). Oxidation with Dess–Martin periodinane (DMP) provided the desired  $\alpha,\beta$ -unsaturated aldehyde **129** in a yield of 82%. Unfortunately, the aldehyde **129** was prone to rapid autoxidation to the corresponding carboxylic acid **130**. Therefore, the aldehyde **129** had to be used immediately after purification.



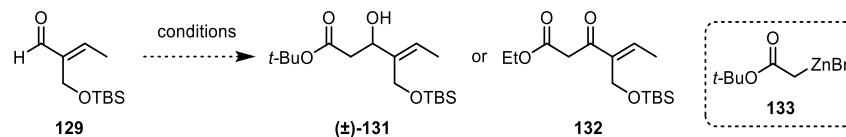
Scheme 47. Reduction-oxidation sequence to afford the  $\alpha,\beta$ -unsaturated aldehyde **129** and subsequent autoxidation to the carboxylic acid **130**.

We then turned our efforts to the carbon-carbon bond forming reactions to give the  $\beta$ -hydroxy ester **131** (Table 5). LDA was initially used as the base in the crossed aldol addition with *t*-butyl acetate. Unfortunately, decomposition was observed (Table 5, entry 1). LiHMDS was then used as a weaker base and the desired  $\beta$ -hydroxy ester **131** was obtained, albeit in traces amounts (Table 5, entry 2). Notably, prior to performing the aldol addition, we were not aware of the susceptibility of the aldehyde **129** to autoxidation. Therefore, the yield of the  $\beta$ -hydroxy ester **131** obtained from the aldol addition was most likely inaccurate, if the aldehyde **129** had already partly oxidised to the corresponding carboxylic acid **130**.

In addition to the aldol addition, a Reformatsky reaction between the  $\alpha,\beta$ -unsaturated aldehyde **129** and the zinc enolate **133** of *t*-butyl bromoacetate was proposed to afford the  $\beta$ -hydroxy ester **131**. The zinc enolate **133** was prepared by addition of *tert*-butyl bromoacetate to a solution of the Rieke zinc. The Rieke zinc (Zn\*) was prepared based on a reported procedure, in which ZnCl<sub>2</sub> was substituted for ZnBr<sub>2</sub>.<sup>[168]</sup> Typically, the Reformatsky reaction is performed under reflux. However, Rathke and co-workers proposed that base-catalysed side reactions of the carbonyl substrate with the zinc alkoxides, generated in the Reformatsky reaction, could lower the yield of the  $\beta$ -hydroxy ester, particularly at elevated temperatures. They proposed that Lewis acids, such as trimethyl borate, B(OMe)<sub>3</sub>, could be used in room temperature Reformatsky reactions to provide a weakly acidic medium, thus avoiding side reactions by neutralising the basic zinc alkoxides (Scheme 48).<sup>[169]</sup>

Results and Discussion

Table 5. Screening of conditions for the carbon-carbon bond forming reactions to give either the  $\beta$ -hydroxy ester **131** or the  $\beta$ -keto ester **132**.

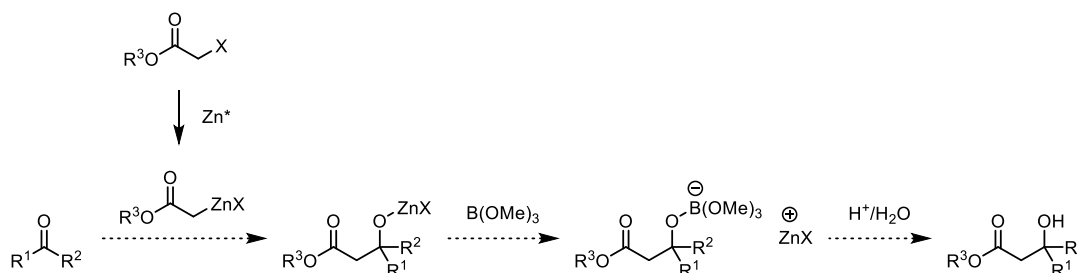


Entry	Reaction Type	Reagents (eq.)	Solvent	$T$ ( $^{\circ}\text{C}$ )	Time (h)	Scale ( $\mu\text{mol}$ )	Result (%)
<b>1</b>	aldol addition	DIPA (1.2), <i>n</i> -BuLi (1.1) <i>t</i> -BuOAc (1.2)	THF	-78 to 0	2	40	decomposition
<b>2</b>	aldol addition	LiHMDS (5.0) <i>t</i> -BuOAc (3.0)	THF	-78 to 0	21	110	<b>131</b> (8)
<b>3</b>	Reformatsky	zinc enolate <b>133</b> (3.0) <sup>a</sup>	THF	rt to reflux	50	80	decomposition
<b>4</b>	Reformatsky	zinc enolate <b>133</b> (3.0) <sup>a</sup> BF <sub>3</sub> •OEt <sub>2</sub> (2.0)	THF	rt to reflux	50	130	decomposition
<b>5</b>	cat. SnCl <sub>2</sub>	SnCl <sub>2</sub> (1.3) ethyl diazoacetate (1.4)	CH <sub>2</sub> Cl <sub>2</sub>	rt	4	100	<b>132</b> (<3)
<b>6</b>	cat. SnCl <sub>2</sub>	SnCl <sub>2</sub> (1.0) ethyl diazoacetate (1.2)	CH <sub>2</sub> Cl <sub>2</sub>	rt	23	240	decomposition

<sup>a</sup>Formed from Rieke zinc (Zn\*) and *t*-butyl bromoacetate.

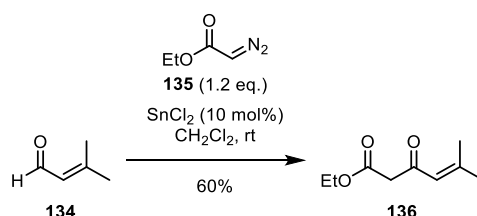
## Results and Discussion

Therefore, two Reformatsky reactions were performed in parallel, with the Lewis acid  $\text{BF}_3 \cdot \text{OEt}_2$  added to one reaction for neutralisation of the basic zinc alkoxide **133** (Table 5, entries 3 and 4). Notably, in the presence of  $\text{BF}_3 \cdot \text{OEt}_2$  the deprotection of the TBS group could have occurred, as the deprotection of the TBS group in the  $\beta$ -keto ester **111** had previously been performed with  $\text{BF}_3 \cdot \text{OEt}_2$  (Table 3, entries 8 and 9).<sup>[163]</sup> In both Reformatsky reactions, formation of the desired  $\beta$ -hydroxy ester **131** was not observed when performing the reactions at room temperature nor under reflux.



Scheme 48. Reformatsky reaction generating a basic zinc alkoxide, which is proposed to be neutralised by the  $\text{B}(\text{OMe})_3$  Lewis acid according to Rathke and co-workers.<sup>[169]</sup>

Since the aldol addition and Reformatsky reactions either afforded the  $\beta$ -hydroxy ester **131** in trace amounts or not at all, alternative carbon-carbon bond forming reactions were sought. We were inspired by conditions reported by Roskamp and co-workers for the direct conversion of aldehydes to  $\beta$ -keto esters with ethyl diazoacetate (**135**) and tin<sup>(II)</sup> chloride,  $\text{SnCl}_2$ , as a Lewis acid catalyst.<sup>[170]</sup> Furthermore, the substrate library included the  $\alpha,\beta$ -unsaturated aldehyde **134** (Scheme 49).<sup>[170]</sup> Upon applying these conditions, the desired  $\beta$ -keto ester **132** was obtained, albeit in trace amounts with impurities remaining after column chromatography (Table 5, entry 5). Due to the small amount of material obtained, further purification was not performed. Upon repeating the reaction on a larger scale, the desired  $\beta$ -keto ester **132** was not obtained (Table 5, entry 6).

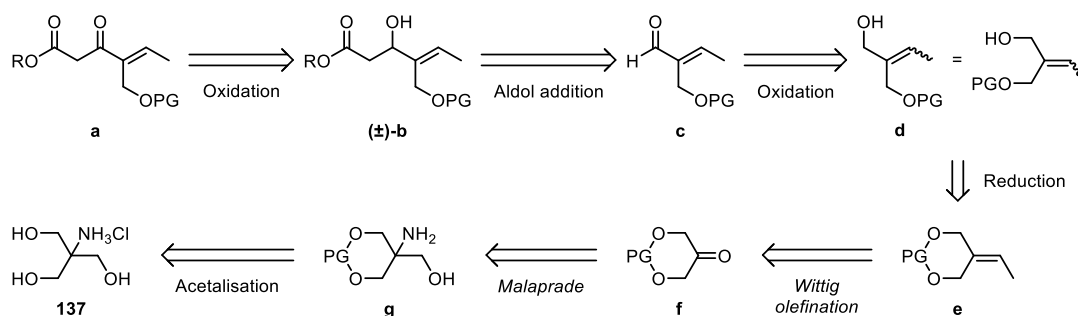


Scheme 49. Direct conversion of  $\alpha,\beta$ -unsaturated aldehyde **134** to  $\beta$ -keto ester **136**, with ethyl diazoacetate (**135**), reported by Roskamp and co-workers.<sup>[170]</sup>

Although the yield of the key carbon-carbon bond forming reaction was increased by applying the more electrophilic aldehyde **129** in place of the ester **126**, the rapid autoxidation of the aldehyde **129** meant that it was not a viable intermediate. It was thought that the autoxidation of the  $\alpha,\beta$ -unsaturated aldehyde **129** to the corresponding carboxylic acid **130** was the reason for the low yield obtained in the aldol addition (Table 5, entry 2). Therefore, neither further optimisation of the aldol addition nor investigation of alternative reactions to afford either the  $\beta$ -hydroxy ester **131** or the  $\beta$ -keto ester **132** were performed.

### 3.2.2.2 Route 5

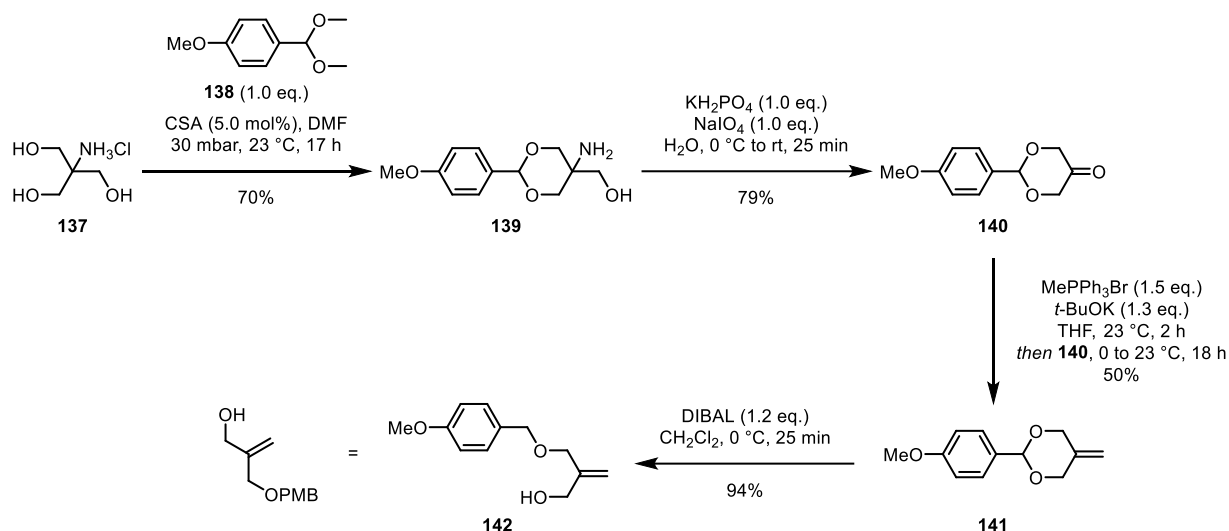
In parallel to route 4, an alternative route to the  $\alpha,\beta$ -unsaturated aldehyde **c** was investigated as shown in the retrosynthetic analysis of route 5 in Scheme 50. As in route 4, the  $\beta$ -keto ester **a** would be obtained from an oxidation of the corresponding  $\beta$ -hydroxy ester **b**, which would in turn be formed from the  $\alpha,\beta$ -unsaturated aldehyde **c** by a carbon-carbon bond forming reaction, such as a crossed aldol addition. The  $\alpha,\beta$ -unsaturated aldehyde **c** would again be provided from an oxidation of the allylic alcohol **d**. However, the allylic alcohol **d** would be formed from a partial deprotection of the diol **e**. The olefin **e** would be afforded from a Wittig olefination of the ketone **f**. The ketone **f** would be formed by a Malaprade reaction of the  $\beta$ -amino alcohol **g**, which would be furnished from an acetalisation of tris(hydroxymethyl)aminomethane hydrochloride (TRIS hydrochloride) (**137**).



Scheme 50. Retrosynthetic analysis of the  $\beta$ -keto ester **a** via  $\alpha,\beta$ -unsaturated aldehyde **c** in route 5.

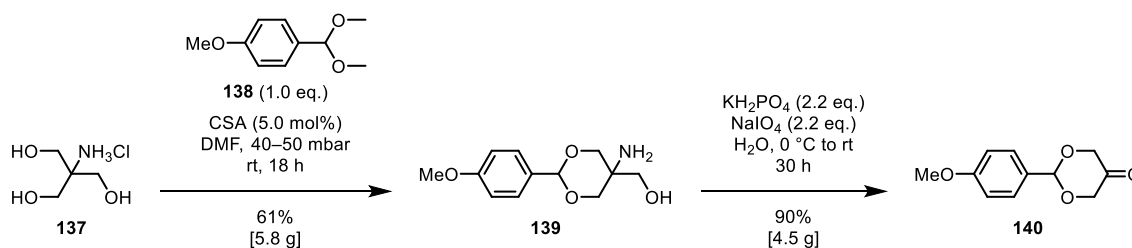
The acetalisation, Malaprade reaction and Wittig olefination sequence was based upon related work by Ritter (Scheme 51).<sup>[171]</sup> In which TRIS hydrochloride (**137**) was acetalised with *p*-anisaldehyde dimethyl acetal (**138**) under acid catalysis to give the  $\beta$ -amino alcohol **139**; oxidative cleavage by a Malaprade reaction with sodium periodate and subsequent hydrolysis afforded the ketone **140**. A Wittig olefination with ketone **140** introduced the methylidene group to give olefin **141**. A partial reduction of acetal **141** with DIBAL gave allylic alcohol **142**.

## Results and Discussion



Scheme 51. Synthesis of allylic alcohol **142** reported by Ritter.<sup>[171]</sup>

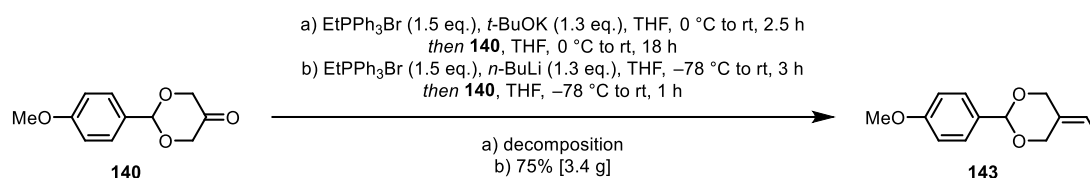
This reported route was therefore adapted for the preparation of analogous allylic alcohol **144**, which had an ethylidene group in place of the methylidene group. The acetalisation of TRIS hydrochloride (**137**) with *p*-anisaldehyde dimethyl acetate (**138**) gave  $\beta$ -amino alcohol **139** in a yield of 61% (Scheme 52). Notably, this reaction was performed under reduced pressure with a rotary evaporator to remove the methanol by-product. The Malaprade reaction and subsequent hydrolysis afforded the ketone **140** in excellent yield.



Scheme 52. Synthesis of ketone **140** from TRIS hydrochloride (**137**).

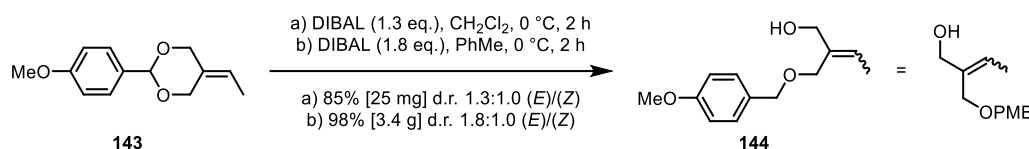
The Wittig olefination of ketone **140** with ethyltriphenylphosphonium bromide was then performed. *t*-BuOK was initially applied as the base (Scheme 53), as in the analogous Wittig reaction reported by Ritter. However, neither the desired product **143** nor the starting material **140** were obtained. It was thought that the aged *t*-BuOK had absorbed atmospheric moisture. *n*-Butyllithium, *n*-BuLi, was then employed as the base and the desired olefin **143** was obtained in a yield of 75%.

## Results and Discussion



Scheme 53. Wittig olefination of ketone **140** to give olefin **143**.

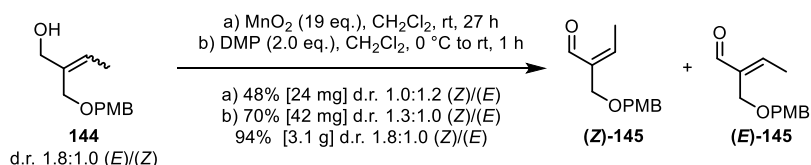
The partial reduction of acetal **143** with DIBAL was initially carried out in CH<sub>2</sub>Cl<sub>2</sub> as reported by Ritter and afforded the allylic alcohol **144** in a very good yield of 85% (Scheme 54). Since DIBAL was used as a PhMe solution, the partial reduction was also performed in PhMe. Pleasingly, the allylic alcohol **144** was obtained in a near quantitative yield. The allylic alcohol **144** was obtained as an inseparable mixture of *E/Z* diastereomers. However, as a double bond migration of the ethylidene double bond was required at a later stage, as discussed in the Planned Synthetic Approach, the configuration of the double bond was irrelevant.



Scheme 54. The partial reduction of acetal **143** to afford allylic alcohol **144**.

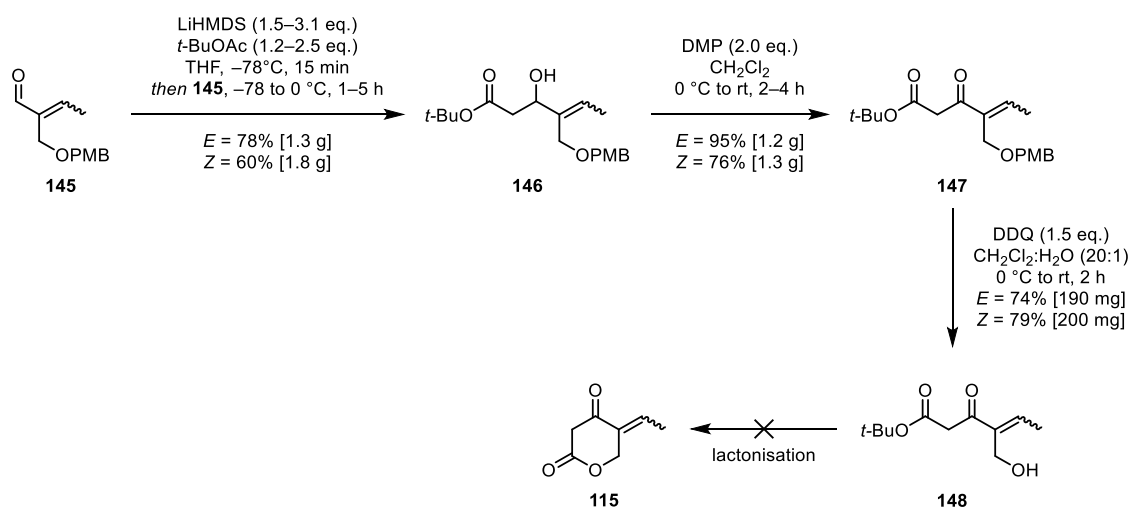
The oxidation of the allylic alcohol **144** to the corresponding  $\alpha,\beta$ -unsaturated aldehyde **145** was then carried out. Manganese dioxide, MnO<sub>2</sub>, was initially used as the oxidising agent (Scheme 55). The desired  $\alpha,\beta$ -unsaturated aldehyde **145** was obtained as separable *E/Z* diastereomers in a combined moderate yield of 48%. When DMP was employed as the oxidising agent, the  $\alpha,\beta$ -unsaturated aldehydes **145** were obtained in a higher combined yield of 83%. Upon scale-up, the  $\alpha,\beta$ -unsaturated aldehydes **145** were obtained in an excellent combined yield of 94% with a d.r. of 1.8:1.0 (*Z*)/(*E*). It is worth noting that the *E/Z* assignment of the diastereomers is reversed between the allylic alcohol **144** and the  $\alpha,\beta$ -unsaturated aldehyde **145**, as the aldehyde group has a higher priority than the PMB-protected hydroxymethyl group. Importantly, autoxidation of the PMB-protected  $\alpha,\beta$ -unsaturated aldehydes **145** to the corresponding carboxylic acids was not observed. Therefore, it was proposed that the TBS protecting group in the  $\alpha,\beta$ -unsaturated aldehyde **129** was responsible for the autoxidation. The  $\alpha,\beta$ -unsaturated aldehydes **145** were therefore viable intermediates for the synthesis of the  $\beta$ -keto ester **a**.

## Results and Discussion



Scheme 55. Oxidation of allylic alcohols **144** to the corresponding  $\alpha,\beta$ -unsaturated aldehydes **145**.

The subsequent reactions were performed with the separated diastereomers of the  $\alpha,\beta$ -unsaturated aldehydes **145**. The aldol addition with the  $\alpha,\beta$ -unsaturated aldehydes **145** gave the  $\beta$ -hydroxy esters **146** in good yields (Scheme 56). This further supports the hypothesis that the low yield obtained in the aldol addition with the TBS-protected  $\alpha,\beta$ -unsaturated aldehyde **129** was due to its prior autoxidation to the carboxylic acid **130**. The subsequent oxidation with DMP to the corresponding  $\beta$ -keto esters **147** proceeded in good to excellent yields. Since there was no literature precedence of PMB-protected alcohols as allylic alkylation substrates in Pd-catalysed allylic substitution reactions,<sup>[93,151]</sup> a deprotection-derivatisation of the hydroxy group in the  $\beta$ -keto esters **147** was required. The PMB-protected  $\beta$ -keto esters **147** were deprotected with 2,3-dichloro-5,6-dicyano-1,4-benzoquinone (DDQ) to give the allylic alcohols **148**. Unfortunately, the allylic alcohols **148** were observed to be unstable and quickly decomposed as observed by TLC analysis and analysis of the  $^1\text{H}$  NMR spectra. The material that was obtained after purification was therefore directly submitted to the subsequent derivatisation step. Notably, no formation of the cyclic  $\beta$ -keto ester **115** from lactonisation of the allylic alcohols **148** was observed (Scheme 56).



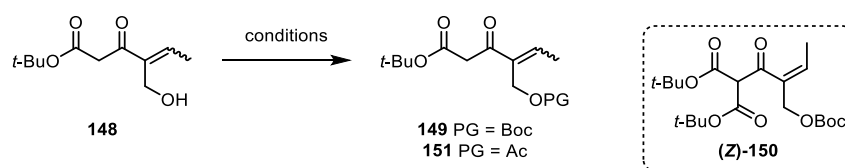
Scheme 56. Synthesis of  $\beta$ -keto esters **148** from the  $\alpha,\beta$ -unsaturated aldehydes **145**.

## Results and Discussion

In Pd-catalysed allylic substitution reactions with 3-substituted indole derivatives, unactivated allylic substrates such as allylic alcohols<sup>[96,147,150]</sup> and activated allylic substrates with good leaving groups such as carbonates<sup>[97–99,148,149]</sup> or acetates<sup>[93,151]</sup> have been applied. Therefore, the allylic alcohols **148** could have been applied as an unactivated allylic alkylation substrates in the allylic substitution reaction. However, since the use of activated allylic substrates is more commonly reported, we attempted to prepare the carbonate and acetate derivatives of the allylic alcohols **148** (Table 6).

For formation of the *t*-butyl carbonate **149**, basic conditions were employed. Two equivalents of LiHMDS were used, due to the more acidic  $\alpha$ -hydrogens atoms in the allylic alcohol **148** quenching the first equivalent of the base (Table 6, entry 1). Under these conditions, the Boc-protected tricarbonyl compound **150** was obtained. Although, there was a lot of steric hinderance at the  $\alpha$ -position in the product (*Z*)-**150**, it was proposed to still be a suitable allylic alkylation substrate for the allylic substitution reaction; in fact, the additional *t*-butyl ester group was expected to enhance the acidity of the  $\alpha$ -hydrogen atom. This would be beneficial as deprotonation at the  $\alpha$ -position is required for the intramolecular Mannich reaction onto the indoline iminium ion to construct the C ring of aspidospermidine (**1**). When the Boc-protection was repeated with the allylic alcohol (*Z*)-**148** but with 1 equivalent of Boc<sub>2</sub>O, to see if the more accessible alkoxide could be preferentially Boc-protected, formation of the Boc  $\beta$ -keto ester (*Z*)-**150** was observed with incomplete conversion of the starting material (*Z*)-**148** (Table 6, entry 2). Unfortunately, decomposition of the crude product was observed by TLC analysis and the Boc-protected tricarbonyl (*Z*)-**150** was not obtained. Only the starting material (*Z*)-**148** was recovered in trace amounts. The original conditions were then repeated with freshly purified allylic alcohol (*Z*)-**148** (Table 6, entry 3). Unfortunately, the Boc-protected tricarbonyl product (*Z*)-**150** was only obtained in a yield of <16%, with impurities.

The preparation of the acetate derivative of the allylic alcohol **148** was then attempted. Standard conditions of acetic anhydride (Ac<sub>2</sub>O) and 4-dimethylaminopyridine (DMAP) were first employed (Table 6, entry 4), unfortunately neither the Ac-protected allylic alcohol **151** nor the allylic alcohol **148** were obtained. Sub-stoichiometric scandium<sup>(III)</sup> triflate, Sc(OTf)<sub>3</sub>, was then applied as a Lewis acid catalyst with Ac<sub>2</sub>O (Table 6, entry 5),<sup>[172,173]</sup> again neither the desired product **151** nor starting material **148** were obtained. Classical conditions, with Ac<sub>2</sub>O in pyridine were tested (Table 6, entry 6); however, decomposition was observed.<sup>[174]</sup> An enzymatic acylation of the allylic alcohol **148** was also attempted using rizolipase and vinyl acetate (Table 6, entry 7);<sup>[175]</sup> which also resulted in decomposition.

Table 6. Screening of conditions for the derivatisation of the allylic alcohols **148**.

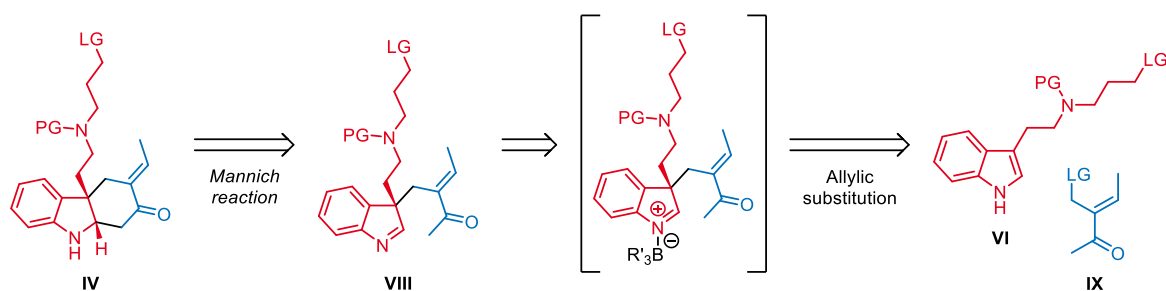
Entry	<i>E/Z</i>	Reagents (eq.)	Solvent	<i>T</i> (°C)	Time (h)	Scale (μmol)	Result (%)
<b>1</b>	<i>Z</i>	LiHMDS (2.2) Boc <sub>2</sub> O (2.6)	THF	-78 to rt	18	97	<b>150</b> (42)
<b>2</b>	<i>Z</i>	LiHMDS (2.2) Boc <sub>2</sub> O (1.0)	THF	0 to rt	1	93	<b>148</b> (4)
<b>3</b>	<i>Z</i>	LiHMDS (2.4) Boc <sub>2</sub> O (2.4)	THF	-78 to rt	15	99	<b>150</b> (<16)
<b>4</b>	<i>Z</i>	Ac <sub>2</sub> O (1.5) DMAP (1.4)	CH <sub>2</sub> Cl <sub>2</sub>	rt	1	94	decomposition
<b>5</b>	<i>E</i>	Ac <sub>2</sub> O (1.5) Sc(OTf) <sub>3</sub> (0.10)	MeCN	rt	3	95	decomposition
<b>6</b>	<i>E</i>	Ac <sub>2</sub> O (50)	C <sub>5</sub> H <sub>5</sub> N	rt	24	110	decomposition
<b>7</b>	<i>E</i>	Rizolipase (10 wt.%) vinyl acetate (2.0)	THF:MTBE (1:1)	21	25	98	decomposition

MTBE = methyl *tert*-butyl ether.

Although route 5 furnished the stable  $\alpha,\beta$ -unsaturated aldehydes **146**, which gave the  $\beta$ -keto esters **148**, the multi-step synthesis and instabilities of the  $\beta$ -keto esters **148** and the Boc-protected tricarboxyl product (Z)-**150** rendered them unfeasible allylic alkylation substrates. Consequently, an alternative strategy for the synthesis of the key *exo*-enone **IV** intermediate en route to aspidospermidine (**1**) was sought.

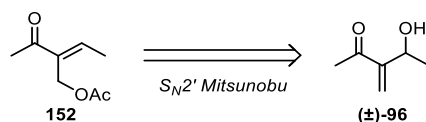
### 3.3 Preparation of the Allylic Alkylation Substrate: Strategy 2

In strategy 2, an alternative pathway for the synthesis of the *exo*-enone **IV** was envisioned. To this end, we aimed to prepare the  $\alpha,\beta$ -unsaturated ketone **IX** as the allylic alkylation substrate in the key Pd-catalysed allylic substitution reaction (Scheme 57). In comparison to the  $\beta$ -keto ester **VII** in strategy 1, the  $\alpha,\beta$ -unsaturated ketone **IX** contains the correct number of carbon atoms for construction of the aspidospermidine (**1**) framework. Moreover, the synthetic route to the  $\alpha,\beta$ -unsaturated ketone **IX** was expected to be significantly shorter than to the  $\beta$ -keto ester **VII**. The allylic substitution reaction between tryptamine derivative **VI** and the allylic alkylation substrate **IX** would afford indolenine **VIII**. Notably, without the superfluous ester group, the  $\alpha$ -position to the ketone in the generated indoline iminium ion is not sufficiently activated for the *in situ* trapping to occur. A subsequent intramolecular Mannich reaction of the indolenine **VIII** would however give the *exo*-enone **IV**, thus constructing the C ring of aspidospermidine (**1**).



Scheme 57. Retrosynthetic analysis of *exo*-enone **IV** according to strategy 2.

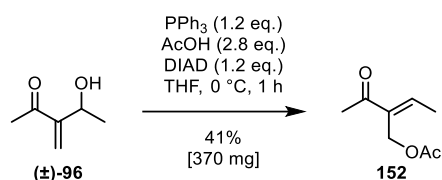
The allylic acetate **152** was initially proposed as the allylic alkylation substrate **IX**. The allylic acetate **152** would be formed in a  $S_N2'$  Mitsunobu reaction from the allylic alcohol **96**, with acetic acid as the pronucleophile, as shown in Scheme 58.



Scheme 58. Retrosynthetic analysis of the allylic acetate **152**.

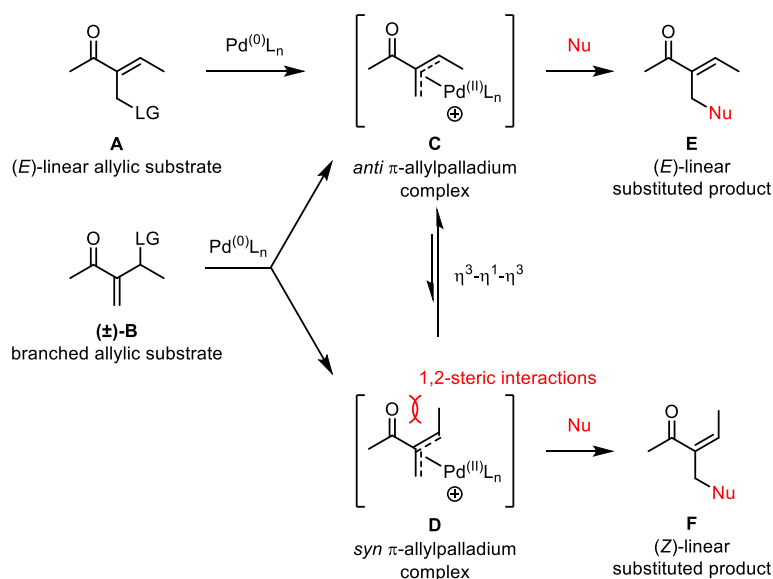
The  $S_N2'$  Mitsunobu reaction with the allylic alcohol **96** and acetic acid gave the allylic acetate **152** in a yield of 41% (Scheme 59).

## Results and Discussion



Scheme 59. Preparation of allylic acetate **152** by an  $\text{S}_{\text{N}}2'$  Mitsunobu reaction with allylic alcohol **96**.

It was proposed that the allylic alcohol **96** itself could also be used as a regioisomeric allylic alkylation substrate in the Pd-catalysed allylic substitution reaction. As upon ionisation, it was hypothesised that both the allylic alcohol **96** and allylic acetate **152** would preferentially form the *anti*  $\eta^3$ - $\pi$ -allylpalladium<sup>(II)</sup> complex **C** (Scheme 60). Under achiral Pd-catalysis with a soft nucleophile, as is the case in our system with an indole derivative ( $\text{p}K_{\text{a}} < 25$ ),<sup>[176]</sup> nucleophilic attack would then preferentially occur at the least substituted allyl terminus of the *anti*  $\pi$ -allylpalladium complex **C** to afford the (*E*)-linear substituted product **E**.<sup>[111]</sup>



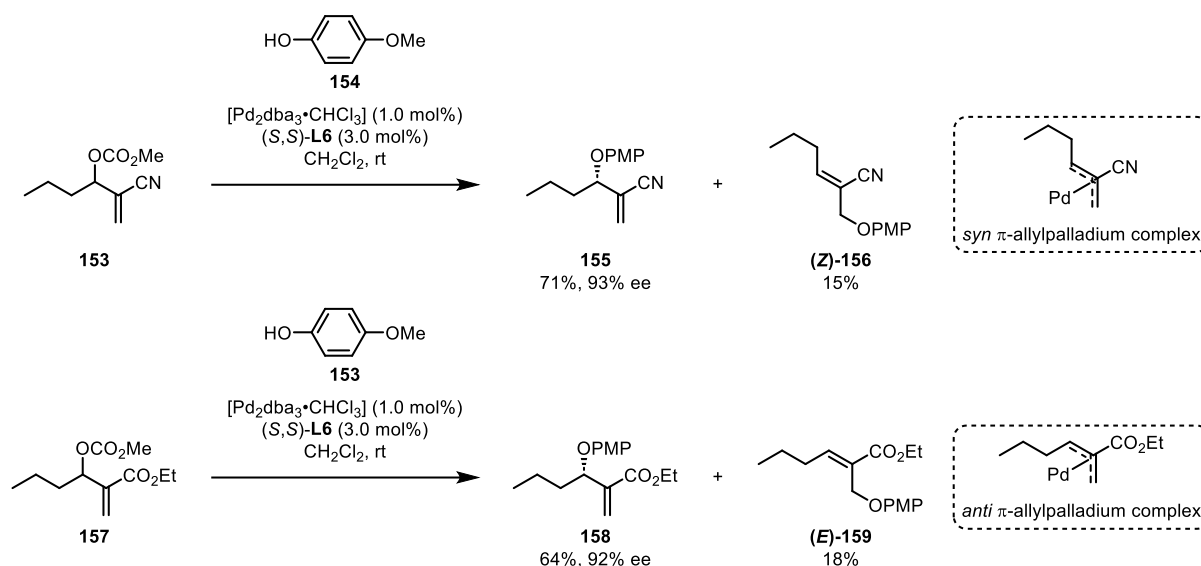
Scheme 60. Proposed preferential formation of the *anti*  $\eta^3$ - $\pi$ -allylpalladium<sup>(II)</sup> complex **C** from either the linear or branched allylic alkylation substrates **A** and **B**, respectively.

Allylic acetate **152** is a linear allylic substrate (**A** in Scheme 60), as the leaving group is on the carbon atom that becomes the least substituted allyl terminus upon ionisation. Whereas the allylic alcohol **96** is a branched allylic substrate (**B** in Scheme 60), as the leaving group is on the carbon atom that becomes the most substituted allyl terminus upon ionisation. The (*E*)-linear allylic substrate **A** would be expected to initially form the *anti*  $\pi$ -allylpalladium complex **C**. Whereas the branched allylic substrate **B** would be expected to initially give a

mixture of *anti* and *syn*  $\pi$ -allylpalladium complexes **C** and **D**, respectively. In both cases the *syn* and *anti*  $\pi$ -allylpalladium complexes would be expected to rapidly interconvert through the  $\eta^3$ - $\eta^1$ - $\eta^3$  isomerisation.<sup>[111]</sup> For allylic substrates without a 2-substituent, the *syn*  $\pi$ -allylpalladium complex is generally favoured due to the destabilising allylic strain ( $A^{1,3}$ ) between the allyl termini substituents in the *anti* complex.<sup>[177]</sup> Whereas, when the allylic substrate has a 2-substituent, destabilising 1,2-steric interactions between the 2-substituent and the allyl termini substituents in the *syn*  $\pi$ -allylpalladium complex may dominate and thus favour formation of the *anti* complex.<sup>[112,177]</sup> Crucially, the size of the 2-substituent plays a role in the ratio of the *syn/anti*  $\pi$ -allylpalladium complexes.<sup>[177]</sup>

Trost and co-workers reported that with allylic substrate **153** with a 2-cyano substituent, the linear product **156** was obtained exclusively with *Z*-configuration (Scheme 61). This configuration is expected to be obtained from nucleophilic attack to the *syn*  $\pi$ -allylpalladium complex. Whereas, with allylic substrate **157** with an ester 2-substituent, the (*E*)-linear substituted product **159** was obtained, which is expected to be formed from nucleophilic attack to the *anti*  $\pi$ -allylpalladium complex. This switch in *syn/anti* conformation between the  $\pi$ -allylpalladium complexes of the 2-cyano and 2-ester substituted allylic substrates was explained by the difference in size between the cyano and ester substituents. In the  $\pi$ -allylpalladium complex with the smaller, linear 2-cyano substituent, the allylic strain in the *anti* complex was more destabilising, thus favouring formation of the *syn* complex. Whereas in the  $\pi$ -allylpalladium complex with the larger ester group, the 1,2-steric interactions between the ester and the 1-propyl substituent in the *syn* complex were more destabilising and consequently the *anti* complex dominated.<sup>[177]</sup> Importantly, the rate of the nucleophilic attack relative to the rate of the *syn-anti* isomerisation also affects the product outcome. When the rate of nucleophilic attack is slower than that of the *syn-anti* isomerisation then the product distribution will represent the equilibrium ratio of the *syn/anti* isomers.

## Results and Discussion



Scheme 61. Pd-catalysed allylic substitution of 2-substituted allylic substrates **153** and **157** as reported by Trost and co-workers. Adapted from <sup>[177]</sup>. OPMP = *para*-methoxyphenol.

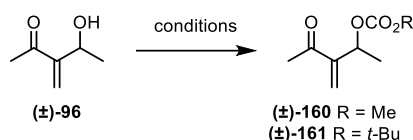
It was therefore proposed that the allylic alcohol **96** could serve as an unactivated branched allylic alkylation substrate to also give the desired indolenine product **VIII** in the allylic substitution reaction. Pd-catalysed allylic substitution reactions between activated allylic carbonates<sup>[112,114,178]</sup> and acetates<sup>[179–181]</sup>, derived from Morita–Baylis–Hillman adducts, with nucleophiles: phenol derivatives,<sup>[112,114]</sup> amines,<sup>[178]</sup> Meldrum’s acid,<sup>[114]</sup> enamines<sup>[181]</sup> and indole derivatives<sup>[179–181]</sup> have been reported. However, to the best of our knowledge Morita–Baylis–Hillman adducts or carbonate or acetate derivatives thereof have never been applied in a Pd-catalysed allylic substitution reaction with a 3-substituted indole nucleophile. Morita–Baylis–Hillman adducts are unique allylic alkylation substrates as they form 2-acceptor substituted  $\pi$ -allylpalladium complexes, in which it is proposed that the 2-carbonyl substituent can coordinate to the Pd metal.<sup>[114,177]</sup>

Since activated allylic substrates are more commonly reported in Pd-catalysed allylic substitution reactions,<sup>[93]</sup> conditions for preparation of the carbonate derivatives of the allylic alcohol **96** were sought (Table 7), to produce an activated branched allylic alkylation substrate for screening, in addition to the allylic alcohol **96** and allylic acetate **152**. To this end, conditions inspired by Trost and co-workers were applied for preparation of the allylic methyl carbonate **160** (Table 7, entry 1).<sup>[114]</sup> After 1 h at 0 °C, a new product with a higher  $R_f$  value than the allylic alcohol **96** was observed, which was presumed to be the desired methyl carbonate derivative **160**. However, incomplete conversion of the starting material **96** was also observed. Upon warming to room temperature, decomposition of the presumed allylic methyl

## Results and Discussion

carbonate **160** was observed. The reaction was then repeated under the same conditions while maintaining a temperature of 0 °C (Table 7, entry 2). Formation of the presumed product **160** was observed after 30 min and 1 h; however, decomposition was already observed at 1 h. Upon purification, the allylic methyl carbonate **160** was obtained in a low yield of 20%.

Table 7. Screening of conditions for the derivatisation of the allylic alcohol **96**.



Entry	Reagents (eq.)	Solvent	T (°C)	Time (h)	Result (%)
<b>1<sup>a</sup></b>	DMAP (8 mol%), pyridine (1.1) methyl chloroformate (1.6)	CH <sub>2</sub> Cl <sub>2</sub>	0 to rt	17	<b>96</b> and decomposition
<b>2</b>	DMAP (10 mol%) pyridine (1.1) methyl chloroformate (1.6)	CH <sub>2</sub> Cl <sub>2</sub>	0	1	<b>160</b> (20)
<b>3</b>	DIPEA (1.2) methyl chloroformate (1.2)	THF	0 to rt	18	no reaction
<b>4</b>	DMAP (1.2) methyl chloroformate (1.4)	CH <sub>2</sub> Cl <sub>2</sub>	0 to rt	18	<b>96</b> and decomposition
<b>5</b>	<i>t</i> -BuOK (0.20) dimethyl carbonate (5.0)	—	0 to 80	40	no reaction
<b>6</b>	<i>t</i> -BuOK (1.2) dimethyl carbonate (5.0)	—	rt	2	decomposition
<b>7</b>	TBD (0.10) dimethyl carbonate (7.5)	—	80	1	decomposition
<b>8</b>	DMAP (0.10), Boc <sub>2</sub> O (1.2)	CH <sub>2</sub> Cl <sub>2</sub>	0 to rt	19	unknown side product

Unless stated otherwise, all reactions were performed on a scale of 0.50 mmol. <sup>a</sup>Reaction scale of 2.0 mmol.

Alternative bases for deprotonation of the secondary oxonium ion formed after nucleophilic acyl substitution were applied, such as *N,N*-diisopropylethylamine (DIPEA) and DMAP (Table 7, entries 3 and 4). Neither of these conditions gave the desired product **160**. Stronger bases were then used for deprotonation of the alcohol **96**, with dimethyl carbonate used in place of

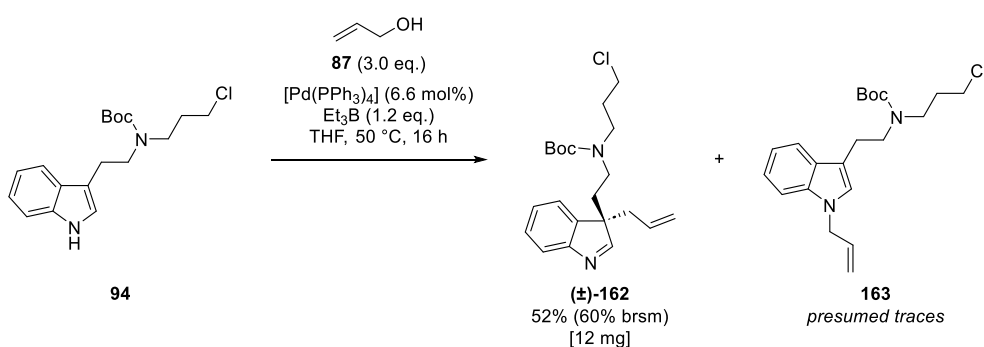
## Results and Discussion

methyl chloroformate. Applying 0.20 equivalents of *t*-BuOK resulted in no reaction at room temperature nor upon heating (Table 7, entry 5).<sup>[182]</sup> However, using 1.2 equivalents of *t*-BuOK at room temperature led to rapid decomposition (Table 7, entry 6). Applying sub-stoichiometric 1,5,7-triazabicyclo[4.4.0]dec-5-ene (TBD) also resulted in decomposition (Table 7, entry 7).<sup>[183]</sup> It is worth noting that if the allylic methyl carbonate **160** was generated under these strong basic conditions (Table 7, entries 6 and 7), rapid elimination of the methyl carbonate via an E2 mechanism may have occurred. Conditions to afford the allylic *tert*-butyl carbonate **161** with Boc<sub>2</sub>O and DMAP were also tried (Table 7, entry 8). However, this resulted in the formation of an unknown side product. Although preparation of the allylic methyl carbonate **160** proved non-trivial, we had material in hand for a test allylic substitution reaction with an activated branched allylic alkylation substrate.

### 3.4 Pd-Catalysed Allylic Substitution Reaction

#### 3.4.1 Non-Stereoselective Allylic Substitution Reaction

To investigate the general feasibility of the Pd-catalysed allylic substitution reaction, non-stereoselective conditions with achiral ligands were initially sought. Due to the ease of the preparation of the allylic alcohol **96**, we were interested to see if it could be applied as an unactivated allylic alkylation substrate with the tryptamine derivative **94** in the allylic substitution reaction. For which, conditions reported by Tamaru and co-workers for the Pd-catalysed allylic substitution reaction between indole derivatives and unactivated allyl alcohols were envisioned (Scheme 21 on page 30).<sup>[146]</sup> A test reaction was first performed between allyl alcohol (**87**), as the model allylic substrate reported by Tamaru and co-workers, and the tryptamine derivative **94** (Scheme 62), to assess if the tryptamine derivative **94** was a suitable nucleophile under these conditions. The desired 3-allylated indolenine product **162** was obtained in a reasonable yield of 52% (60% brsm). The borane additive, Et<sub>3</sub>B, was applied as a Lewis acid for activation of the allyl alcohol (**87**), but also to suppress competing *N*-allylation.<sup>[147]</sup> The borane was proposed to tightly coordinate to the indole nitrogen atom, thus preventing the N1 position from serving as a nucleophile in the allylic substitution reaction.<sup>[145,184]</sup> Although stoichiometric equivalents of the borane were used, traces of the presumed *N*-allylated product **163** were observed by analysis of the <sup>1</sup>H NMR spectrum of the by-product.



Scheme 62. Test allylic substitution reaction between tryptamine derivative **94** and allyl alcohol (**87**).

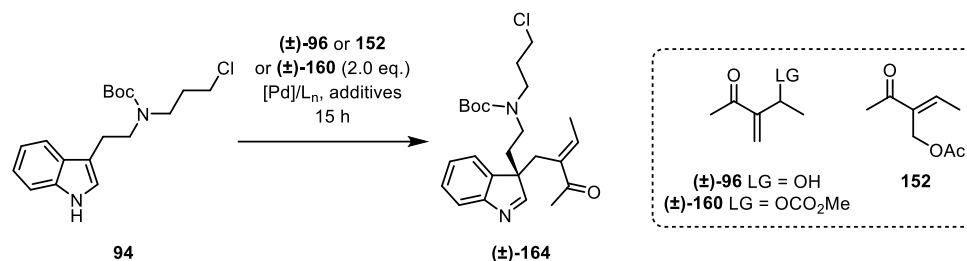
The allylic alcohol **96** was then applied in the allylic substitution reaction (Table 8). Upon applying the conditions reported by Tamaru and co-workers, the desired indolenine **164** was obtained in trace amounts (Table 8, entry 1). The reaction was initially performed at room temperature as Tamaru and co-workers had performed their reaction with 3-methylindole (**86**)

## Results and Discussion

at room temperature, whereas the reactions with the other indole derivatives had been performed at 50 °C. Upon performing the reaction at 50 °C, the indolenine **164** was obtained in an increased yield of 33% (Table 8, entry 2). In both of these reactions, 3.6 equivalents of the borane were used, as Tamaru and co-workers, had reported that with sterically hindered allyl alcohols excess amounts of the borane were required to give the 3-allylated product in reasonable yields.<sup>[146]</sup> However, under neither of these conditions was full conversion of the tryptamine derivative **94** observed (Table 8, entries 2 and 3). When the allylic acetate **152** was applied under the same conditions (Table 8, entry 3), the indolenine product **164** was obtained in a comparable yield of 31%. Again, incomplete conversion of the tryptamine derivative **94** was observed. Therefore, the use of the allylic methyl carbonate **160** was investigated. Conditions reported by Rawal and co-workers for the Pd-catalysed allylic substitution reaction with activated allyl methyl carbonates were applied, but with 1,2-dichloroethane as the solvent in place of CH<sub>2</sub>Cl<sub>2</sub>, in case heating above 40 °C was required (Table 8, entry 4).<sup>[148]</sup> Full conversion of the allylic methyl carbonate **160** was observed; however there was no formation of the desired indolenine product **164**. Furthermore, incomplete conversion of the tryptamine derivative **94** was observed. Although the allylic alkylation substrates **96** and **152** afforded the indolenine **164** in comparable yields, the allylic alcohol **96** was selected as the allylic alkylation substrate best suited for our system due to its ease of preparation. The allylic alcohol **96** was prepared in a single step with a high yield of 83%. Whereas the allylic acetate **152** was prepared in an overall yield of 34% over two steps. Furthermore, using the allylic acetate **152** in place of the allylic alcohol **96** in the substitution reaction would have increased the longest linear sequence of the synthesis of aspidospermidine (**1**) by one step. Upon performing the allylic substitution reaction on a larger scale with the allylic alcohol **96**, the indolenine **164** was obtained in a preparatively useful yield of 67% (86% brsm) (Table 8, entry 5).

## Results and Discussion

Table 8. Screening of conditions for the allylic substitution reaction between tryptamine derivative **94** and allylic alkylation substrates **96**, **152** and **160**.



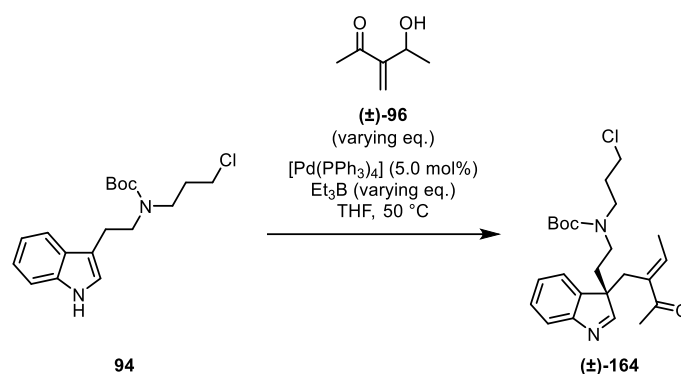
Entry	Allylic substrate	[Pd]/L <sub>n</sub> and additives	Solvent	T (°C)	Result (%)
1	<b>96</b>	[Pd(PPh <sub>3</sub> ) <sub>4</sub> ], Et <sub>3</sub> B <sup>a</sup>	THF	rt	6
2	<b>96</b>	[Pd(PPh <sub>3</sub> ) <sub>4</sub> ], Et <sub>3</sub> B <sup>a</sup>	THF	50	33
3	<b>152</b>	[Pd(PPh <sub>3</sub> ) <sub>4</sub> ], Et <sub>3</sub> B <sup>a</sup>	THF	50	31
4	<b>160</b>	[Pd <sub>2</sub> (dba) <sub>3</sub> ], P(2-furyl) <sub>3</sub> <sup>b</sup>	(CH <sub>2</sub> Cl) <sub>2</sub>	rt	—
5 <sup>c</sup>	<b>96</b>	[Pd(PPh <sub>3</sub> ) <sub>4</sub> ], Et <sub>3</sub> B <sup>a</sup>	THF	50	67 (86 brsm)

Unless otherwise stated, all reactions were performed on a 0.1 mmol scale. <sup>a</sup>[Pd(PPh<sub>3</sub>)<sub>4</sub>] (5.0 mol%), Et<sub>3</sub>B (3.6 equiv.). <sup>b</sup>[Pd<sub>2</sub>(dba)<sub>3</sub>] (5.0 mol%), P(2-furyl)<sub>3</sub> (10 mol%). <sup>c</sup>Reaction scale of 1.0 mmol.

Notably, the (*E*)-indolenine product **164** was obtained in all cases, indicating that the nucleophilic attack had occurred to the *anti* π-allylpalladium complex.<sup>[177]</sup> This supported our hypothesis that the same *anti* π-allylpalladium complex would be preferentially formed from either the (*E*)-linear allylic substrate **A** or branched allylic substrate **B** (Scheme 60).

Since full conversion of the tryptamine derivative **94** was not observed under any of these conditions (Table 8), optimisation through varying the equivalents of the reagents was attempted (Table 9). The ratio of the borane additive to the combined equivalents of the tryptamine derivative **94** and the allylic alcohol **96** was maintained at 1.2:1.0. Increasing or decreasing the equivalents of the allylic alkylation substrate **96** resulted in lower yields, even with prolonged reaction times (Table 9, entries 2 and 3). Therefore, 2.0 equivalents of the allylic alcohol **96** was found to be optimal. Reducing the relative equivalents of the borane additive led to a lower yield (Table 9, entry 4). When the reaction was performed on a larger scale, the indolenine product **164** was obtained in a reduced yield (Table 9, entry 5).

Table 9. Optimisation of reagent equivalents in the allylic substitution reaction.



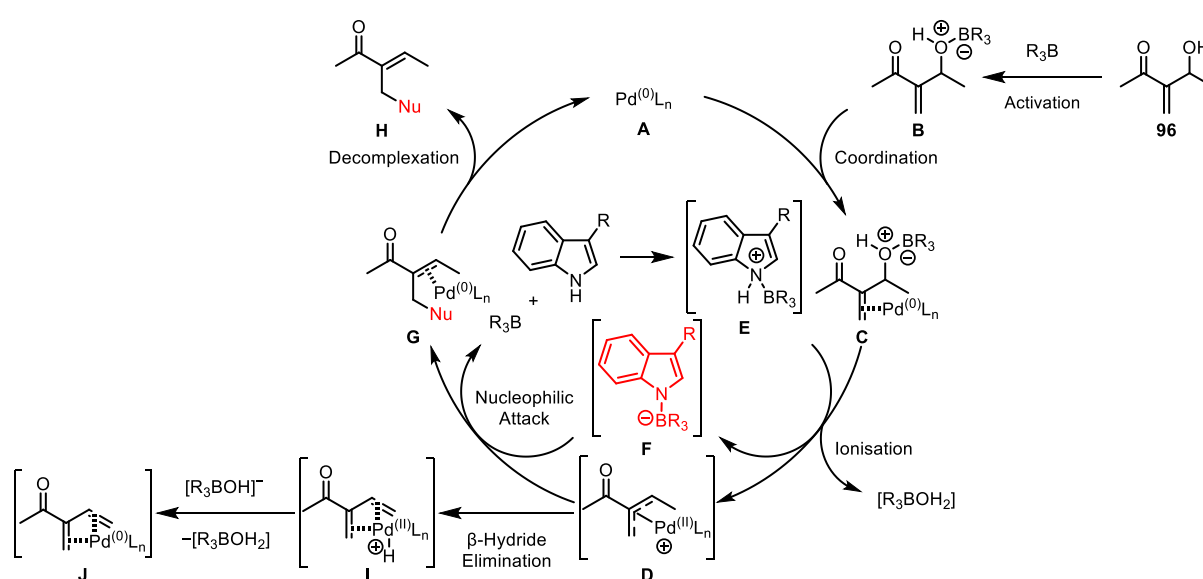
Entry	96 (eq.)	Et <sub>3</sub> B (eq.)	Time (h)	Scale (mmol)	Yield (%)
1	2.0	3.6	15	1.0	67 (86 brsm)
2	4.0	7.2	42	1.4	56 (86 brsm)
3	1.2	2.4	40	1.2	38 (72 brsm)
4	2.0	2.4	22	0.63	40 (n.d. brsm)
5	2.0	3.6	22	7.5	43 (54 brsm)

n.d. = not determined.

Upon repetition of the allylic substitution reaction with the optimal conditions, the indolenine product **164** was obtained in varying yields. It was proposed that a competing  $\beta$ -hydride elimination from the  $\pi$ -allylpalladium complex **D** could occur (Scheme 63). The  $\beta$ -hydride elimination product **J** was proposed to exhibit an enhanced chelating ability to the Pd metal, due to its additional coordinating carbonyl group.<sup>[114,177,184]</sup> Thus, effectively deactivating the Pd-catalyst and inhibiting further conversion of the tryptamine derivative **94**.<sup>[185]</sup> In an attempt to circumvent this, the allylic alcohol **96** was added as a diluted solution over 2.5 h to the reaction mixture. This was intended to maintain a high relative concentration of the nucleophile with respect to the  $\pi$ -allylpalladium complex **D** and thus favour the nucleophilic attack. Although this was found to give more reproducible yields of the indolenine **164**, full conversion of the tryptamine derivative **94** was still not observed. Further addition of the Pd catalyst, also did not result in full conversion of the tryptamine derivative **94**.

The proposed catalytic cycle for the allylic substitution reaction shows the dual role of the borane additive, BR<sub>3</sub> (Scheme 63). First, one equivalent of the borane coordinates to the hydroxy group in the allylic alcohol **96**, activating the allylic alkylation substrate **96** to oxidative addition by Pd<sup>(0)</sup> into the allylic C–O bond.<sup>[147]</sup> Second, another equivalent of the borane coordinates to the nitrogen atom of the indole derivative giving intermediate **E**, in which

the acidity of the N1 hydrogen atom is significantly increased.<sup>[96,184]</sup> Deprotonation of intermediate **E** by the  $[\text{Et}_3\text{BOH}]^-$  complex then affords the activated nucleophile: *N*-indolyltrialkylborate **F**.<sup>[184]</sup> The coordination of the borane to the indole nitrogen atom is also proposed to be key to the chemoselectivity of the reaction, through suppressing the competing *N*-alkylation.<sup>[145,184]</sup> Furthermore, the formation of this Lewis acid-base complex increases the  $\pi$ -nucleophilicity of the indole derivative.<sup>[145]</sup> Regioselective nucleophilic attack of the bulky *N*-indolyltrialkylborate **F** to the least substituted allyl terminus of the *anti*  $\pi$ -allylpalladium complex **D** then affords the (*E*)-linear substituted product **G**, which is released upon decomplexation.



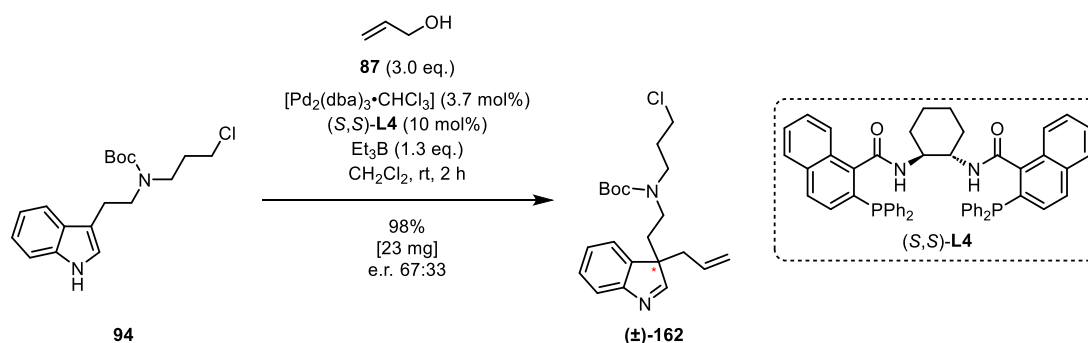
Scheme 63. Proposed catalytic cycle with allylic alcohol **96** and a 3-substituted indole derivative.

### 3.4.2 Enantioselective Allylic Substitution Reaction

We then attempted to render the key allylic substitution reaction enantioselective by applying chiral ligands. We were initially drawn to the related system reported by Trost and co-workers in which the (*S,S*)-DACH-anthracene ligand **L5** was applied with 3-substituted indole derivatives and allyl alcohol (**87**) (Scheme 22 on page 31). It was reported that the DACH-anthracene ligand **L5** gave the highest enantioselectivities in preliminary experiments.<sup>[96]</sup> At the outset of the enantioselective studies, we did not have the DACH-anthracene ligand **L5**, but instead the (*S,S*)-DACH-phenyl **L3** and (*S,S*)-DACH-naphthyl **L4** ligands. A test reaction was first performed between allyl alcohol (**87**), as the model allylic substrate reported by Trost and co-workers, and tryptamine derivative **94**, to investigate the feasibility of the tryptamine derivative **94** as the nucleophile

## Results and Discussion

under these conditions (Scheme 64). The indolenine **164** was obtained in near quantitative yield, albeit with low enantioselectivity.

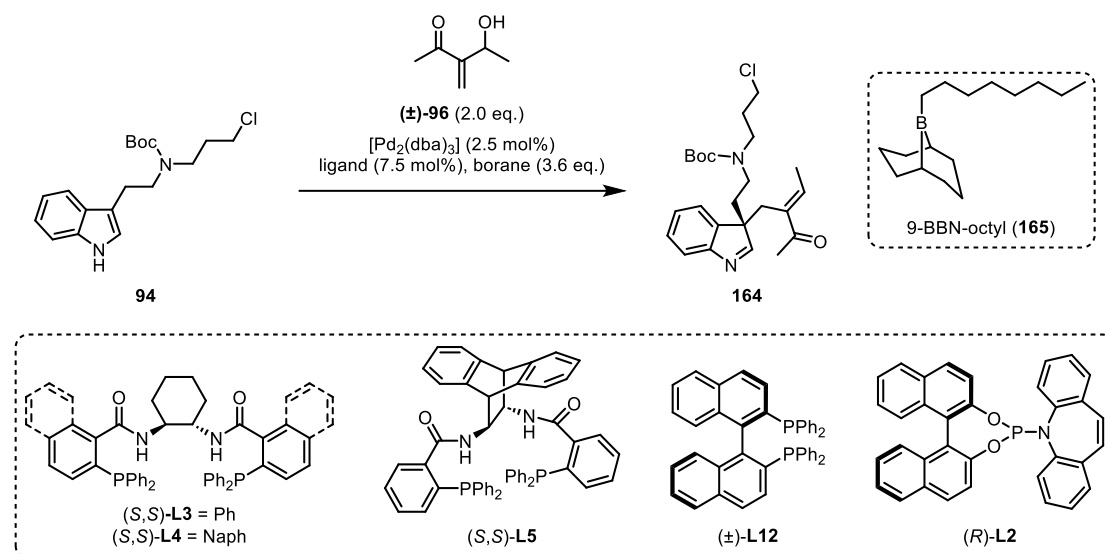


Scheme 64. Test enantioselective allylic substitution reaction between tryptamine derivative **94** and allyl alcohol (**87**).

The allylic alcohol **96** was then used in the enantioselective allylic substitution reaction (Table 10). The conditions as reported by Trost and co-workers with 1.1 equivalents of the borane,  $Et_3B$ , at room temperature but with the  $(S,S)$ -DACH-phenyl **L3** and  $(S,S)$ -DACH-naphthyl **L4** Trost ligands were initially applied (Table 10, entries 1 and 2). However, no formation of the indolenine product **164** was observed after prolonged reaction time, increasing the borane equivalents nor upon heating the reaction to 35 °C. Therefore, alternative ligands were screened.  $(±)$ -2,2'-bis(diphenylphosphino)-1,1'-binaphthyl (BINAP)  $(±)$ -**L12** was chosen as a bidentate diphosphine ligand that served as a donor ligand for promotion of the oxidation addition step and with the potential to render the reaction enantioselective through the use of the enantiopure ligand **L12**.<sup>[111]</sup> No formation of the indolenine **164** was observed upon performing the reaction at room temperature nor upon heating at 50 °C (Table 10, entry 3). The Carreira phosphoramidite olefin ligand  $(R)$ -**L2** was then selected as a chiral phosphoramidite olefin ligand.<sup>[186]</sup> As hemilabile chiral phosphoramidite olefin ligands have been employed in allylic substitution reactions with 3-substituted indole derivatives and activated allylic substrates under Pd-catalysis<sup>[97,99]</sup> and under Ir-catalysis.<sup>[102]</sup> Again, no formation of the indolenine **164** was observed upon performing the reaction at room temperature nor upon heating to 50 °C (Table 10, entry 4). Notably, the reactions with the  $(±)$ -**L12** and  $(R)$ -**L2** ligands were performed in THF, as this allowed for heating to 50 °C, as in the optimised non-stereoselective conditions, and as the non-stereoselective allylic substitution reactions had been performed in THF.

Results and Discussion

Table 10. Optimisation of reaction conditions for the enantioselective allylic substitution of allylic alcohol **96** with tryptamine derivative **94**.



Entry	Ligand	Borane	Solvent	$T$ ( $^{\circ}\text{C}$ )	Time (h)	Yield (%)	e.r. ( $R:S$ )
<b>1<sup>a</sup></b>	$(S,S)\text{-L3}$	$\text{Et}_3\text{B}$	$\text{CH}_2\text{Cl}_2$	rt to 35	71	—	—
<b>2<sup>a</sup></b>	$(S,S)\text{-L4}$	$\text{Et}_3\text{B}$	$\text{CH}_2\text{Cl}_2$	rt to 35	71	—	—
<b>3<sup>b</sup></b>	$(\pm)\text{-L12}$	$\text{Et}_3\text{B}$	THF	rt to 50	18	—	—
<b>4<sup>c</sup></b>	$(R)\text{-L2}$	$\text{Et}_3\text{B}$	THF	rt to 50	23	—	—
<b>5<sup>d</sup></b>	$(S,S)\text{-L3}$	$\text{Et}_3\text{B}$	THF	50	48	49	26:74
<b>6<sup>d</sup></b>	$(S,S)\text{-L4}$	$\text{Et}_3\text{B}$	THF	50	48	23	19:81
<b>7</b>	$(S,S)\text{-L3}$	<b>165</b>	THF	50	15	22	14:86
<b>8</b>	$(S,S)\text{-L3}$	<b>165</b>	THF	rt	15	37	9:91
<b>9</b>	$(S,S)\text{-L3}$	<b>165</b>	THF	4	15	18	30:70
<b>10<sup>e</sup></b>	$(S,S)\text{-L3}$	<b>165</b>	THF	rt	15	23	18:82
<b>11<sup>f</sup></b>	$(S,S)\text{-L3}$	<b>165</b>	THF	rt	15	25	14:86
<b>12<sup>g</sup></b>	$(R,R)\text{-L3}$	<b>165</b>	THF	rt	15	12	56:44
<b>13</b>	$(S,S)\text{-L3}$	<b>165</b>	$\text{CH}_2\text{Cl}_2$	rt	15	0	—
<b>14</b>	$(R,R)\text{-L3}$	<b>165</b>	PhMe	rt	15	0	—
<b>15</b>	$(R,R)\text{-L3}$	<b>165</b>	THF	rt	24	36	90:10
<b>16</b>	$(S,S)\text{-L5}$	<b>165</b>	THF	rt	15	26	37:63
<b>17<sup>h</sup></b>	$(R,R)\text{-L3}$	<b>165</b>	THF	rt	15	42	91:9

## Results and Discussion

Unless stated otherwise, all reactions were performed on a 0.1 mmol scale. <sup>a</sup>(±)-**96** (3.0 eq.), Et<sub>3</sub>B in THF (3.3 eq.). <sup>b</sup>(±)-**L12** (5.0 mol%), Et<sub>3</sub>B in THF (2.4 eq.). <sup>c</sup>[Pd<sub>2</sub>(dba)<sub>3</sub>] (5.0 mol%), (*R*)-**L2** (10 mol%), Et<sub>3</sub>B in THF (2.4 eq.). <sup>d</sup>Additional (±)-**96** (2.0 eq.) were added after 15 h. <sup>e</sup>(±)-**96** (4.0 eq.). <sup>f</sup>(±)-**96** (1.5 eq.). <sup>g</sup>(*R,R*)-**L3** (15 mol%) and [Pd<sub>2</sub>(dba)<sub>3</sub>] (5 mol%). <sup>h</sup>Reaction scale of 1.0 mmol.

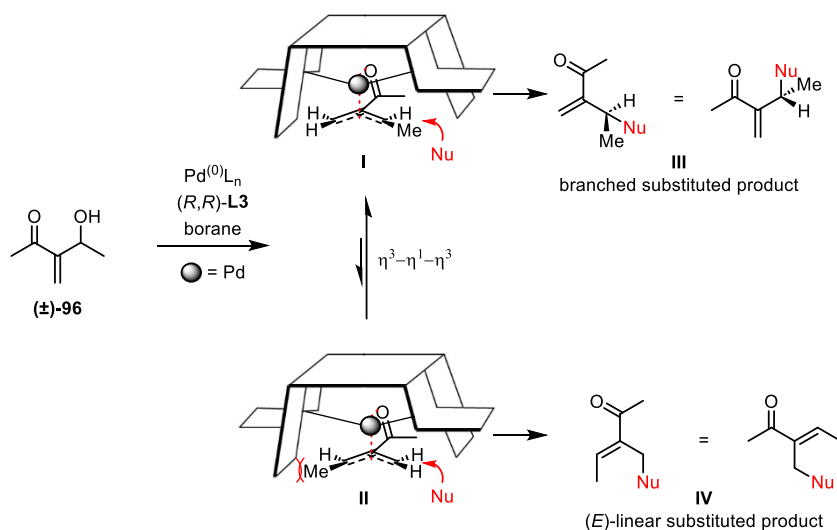
The conditions inspired by Trost and co-workers when again tested but with THF as the solvent in place of CH<sub>2</sub>Cl<sub>2</sub>.<sup>[96]</sup> To our surprise, the enantioenriched indolenine product **164** was obtained (Table 10, entries 5 and 6). After 15 h, incomplete conversion of the tryptamine derivative **94** but near-complete conversion of the allylic alcohol **96** was observed. Therefore, an additional 2.0 equivalents of the allylic alcohol **96** were added to each reaction. From TLC analysis of the reaction mixture directly after the second addition of the allylic alcohol **96** and 31 h later, no further conversion of the tryptamine derivative **94** nor of the allylic alcohol **96** was observed. However, it is worth noting that TLC analysis is only a qualitative measurement of reaction progress. Although Trost and co-workers reported formation of the indolenine product in their related system in comparable yields in solvents other than CH<sub>2</sub>Cl<sub>2</sub>, including THF, they reported that non-coordinating solvents such as PhMe and CH<sub>2</sub>Cl<sub>2</sub> gave the best enantioselectivities.<sup>[96]</sup> It was proposed that coordinating solvents, such as THF, may competitively coordinate to the borane additive and thus disrupt the formation of the Lewis acid-base complex between the borane additive and the indole nitrogen atom,<sup>[187]</sup> which is not only essential for the chemo- and stereoselectivity of the reaction,<sup>[96,145,184]</sup> but also for promoting the reaction through increasing the  $\pi$ -nucleophilicity of the indole derivatives.<sup>[145]</sup> With non-coordinating solvents such as CH<sub>2</sub>Cl<sub>2</sub>, this competitive coordination between the solvent and the borane would not be present.<sup>[187]</sup> Since the indolenine **164** was obtained in comparable enantiomeric ratios (e.r.) with the DACH-phenyl **L3** and DACH-naphthyl **L4** Trost ligands, but in a higher yield with the DACH-phenyl **L3** ligand, ligand **L3** was taken forward in the optimisation studies, due to difficulties previously encountered in yield optimisation when performing the reaction non-stereoselectively.

In their related system, Trost and co-workers had reported that increasing the steric bulk of the borane additive from Et<sub>3</sub>B to 9-BBN-hexyl (**89**) had resulted in an enhanced enantioselectivity.<sup>[96]</sup> This was also observed in our system, as replacing Et<sub>3</sub>B with 9-BBN-octyl (**165**) led to an increased enantioselectivity but a reduced yield (Table 10, entry 7).

Trost and co-workers had initially performed their related allylic substitution reaction at room temperature and reported that performing the reaction at 4 °C resulted in an increased enantioselectivity.<sup>[96]</sup> While in our system, lowering the temperature from 50 °C to room temperature was found to increase both the enantioselectivity and yield, further cooling to 4 °C was shown to be detrimental with respect to both the yield and enantioselectivity (Table 10, entries 8 and 9). Since the allylic alcohol **96** forms an unsymmetrically substituted allyl ligand upon ionisation (Scheme 60 on page 65), the allyl plane is a stereogenic element in the  $\eta^3$ - $\pi$ -allylpalladium<sup>(II)</sup> complex, which exists as enantiomers in the presence of an achiral ligand (C in Figure 6 on page 20).<sup>[111]</sup> However when a chiral ligand, such as the DACH-phenyl **L3** Trost ligand, is applied then the  $\pi$ -allylpalladium complexes exist as diastereomers **I** and **II** in Scheme 65. Out of the potential enantiodiscriminating methods in Pd-catalysed allylic substitution reactions, it was initially proposed that mechanism D was present in our system (Scheme 17 on page 23). In which the rate of interconversion between the two diastereomeric  $\pi$ -allylpalladium complexes, via the  $\eta^3$ - $\eta^1$ - $\eta^3$  isomerisation, is faster than the rate of the nucleophilic attack.<sup>[138]</sup> The asymmetric induction can then be under kinetic control and determined from the different rates of the nucleophilic attack to the two diastereomeric  $\pi$ -allylpalladium complexes, or when the rates of nucleophilic attack are approximately equal then the asymmetric induction can be under thermodynamic control. In which, the equilibrium distribution of the diastereomeric  $\pi$ -allylpalladium complexes determines the stereoselectivity of the reaction.<sup>[138]</sup> In our system, the allylic alcohol **96** was employed as a racemate. Therefore, the diastereomeric *anti*  $\pi$ -allylpalladium complexes **I** and **II** were initially formed in equal amounts. However, upon  $\eta^3$ - $\eta^1$ - $\eta^3$  isomerisation the distribution of the diastereomeric complexes **I** and **II** varies from the initial 50:50 ratio, due to either kinetic or thermodynamic control. Upon cooling the reaction from 50 °C to room temperature, it was proposed that the rate of the nucleophilic attack was decreased relative to that of the  $\eta^3$ - $\eta^1$ - $\eta^3$  isomerisation. Hence allowing the diastereomeric  $\pi$ -allylpalladium complexes **I** and **II** to equilibrate via  $\eta^3$ - $\eta^1$ - $\eta^3$  isomerisation, prior to nucleophilic attack, thus resulting in a higher enantioselectivity. Whereas upon further cooling of the reaction to 4 °C, the rate of the  $\eta^3$ - $\eta^1$ - $\eta^3$  isomerisation was proposed to be slowed relative to the rate of the nucleophilic attack. Therefore the nucleophilic attack would occur before the diastereomeric  $\pi$ -allylpalladium complexes **I** and **II** were able to equilibrate via the  $\eta^3$ - $\eta^1$ - $\eta^3$  isomerisation, hence decreasing the enantioselectivity of the reaction.<sup>[177]</sup> While this could explain the difference in the enantioselectivity of the reaction when the stereocentre would be generated on the electrophilic allylic substrate, for example if the branched substituted product **III** in Scheme 65 would be formed; at this stage it is unclear

## Results and Discussion

how the temperature-dependent relative rates of the  $\eta^3$ - $\eta^1$ - $\eta^3$  isomerisation and the nucleophilic attack would affect the enantioselectivity of the reaction, when the stereocentre is generated on the prochiral nucleophile—as is the case in our system. In which the quaternary stereocentre is constructed at the 3-position of the nucleophilic indole derivative. It was therefore revised that mechanism E is in fact the enantiodiscriminating mechanism in our system (Scheme 17 on page 23). In this mechanism, the stereoselectivity of the reaction is determined from which enantiotopic face of the prochiral nucleophile undergoes the nucleophile attack. While temperature variation could account for the difference in the relative rates of the  $\eta^3$ - $\eta^1$ - $\eta^3$  isomerisation and the nucleophilic attack, it remains unclear how it would affect the facial selectivity of the nucleophilic attack from the prochiral nucleophile and hence the enantioselectivity of our system.



Scheme 65. Wall-and-flap model of the *anti* diastereomeric  $\pi$ -allylpalladium complexes **I** and **II** with the  $(R,R)$ -Trost ligands and allylic alcohol **96**. The analogous less favoured *syn* complexes are not shown.

Varying the equivalents of the allylic alcohol **96** from the previously optimised 2.0 equivalents was found to decrease both the yield and enantioselectivity (Table 10, entries 10 and 11). Doubling the catalyst and ligand loading significantly decreased the yield and enantioselectivity (Table 10, entry 12). This was initially believed to be due to nucleophilic attack from the  $\text{Pd}^{(0)}$  complexes to the diastereomeric  $\pi$ -allylpalladium complexes, effectively resulting in an isomerisation of the  $\pi$ -allylpalladium complexes (Scheme 15 on page 22).<sup>[111,134]</sup> When the faces of the allyl ligand in the  $\pi$ -allylpalladium complexes are enantiotopic then nucleophilic attack to the different faces results in the substituted product being obtained as

## Results and Discussion

enantiomers, and consequently affects the enantioselectivity of the reaction.<sup>[111]</sup> Notably, this isomerisation can be mitigated by using low Pd-catalyst loadings and is generally assumed to be slower than the nucleophilic attack to the  $\pi$ -allylpalladium complex.<sup>[111]</sup> However, it is unclear how the isomerisation of the diastereomeric  $\pi$ -allylpalladium complexes by nucleophilic attack from the Pd<sup>(0)</sup> complexes would affect which enantiotopic face of the prochiral nucleophile attacks the  $\pi$ -allylpalladium complex, thereby inducing the asymmetric induction in this reaction.

The use of CH<sub>2</sub>Cl<sub>2</sub> and PhMe as non-coordinating solvents with the optimised conditions resulted in no formation of the desired indolenine **164** (Table 10, entries 12 and 13). Extending the reaction time of the optimised conditions to 24 h was shown to have no significant effect on the yield nor on the enantioselectivity (Table 10, entry 15). Further supporting the hypothesis that the Pd-catalyst is deactivated by the  $\beta$ -hydride elimination product **J** (Scheme 63). Switching to the DACH-anthracene Trost ligand **L5**, which was reported to give the highest enantioselectivities for the related system reported by Trost and co-workers,<sup>[96]</sup> led to a diminished yield and enantioselectivity (Table 10, entry 16). Finally, the optimised enantioselective conditions were shown to be scalable with the indolenine **164** obtained in a reasonable yield of 42% with high enantioselectivity (e.r. 91:9) (Table 10, entry 17).

The optimisation of the enantioselective allylic substitution reaction was initially performed with the (*S,S*)-configured Trost ligands. However, to synthesise (+)-aspidospermidine (**1**) we switched to the (*R,R*)-configured ligand, (*R,R*)-**L3**, based on extrapolation of the stereochemical results reported by Trost and co-workers.<sup>[96]</sup> As when the (*S,S*)-**L5** ligand was applied in the related system of Trost and co-workers, the indolenine products from nucleophilic attack of the *Si* face of the prochiral nucleophile to the  $\pi$ -allylpalladium complex were obtained. Therefore, upon extrapolating these stereochemical results to our system it was expected that by switching from the (*S,S*)- to the (*R,R*)-configured Trost ligands, that the nucleophilic attack would then come from the *Re* face of the prochiral nucleophile. To synthesise (+)-aspidospermidine (**1**), the nucleophilic attack should come from the *Re* face of the prochiral nucleophile. Therefore, we switched to the (*R,R*)-configured ligand, (*R,R*)-**L3** to synthesise the natural enantiomer of aspidospermidine (**1**). However, upon completion of the synthesis of (–)-aspidospermidine (**1**), the enantiomer of the natural product was obtained. Therefore, it was determined that using the (*R,R*)-configured ligands in our allylic substitution reaction gave (*R*)-indolenine **164**, from nucleophilic attack of the *Si* face of the prochiral

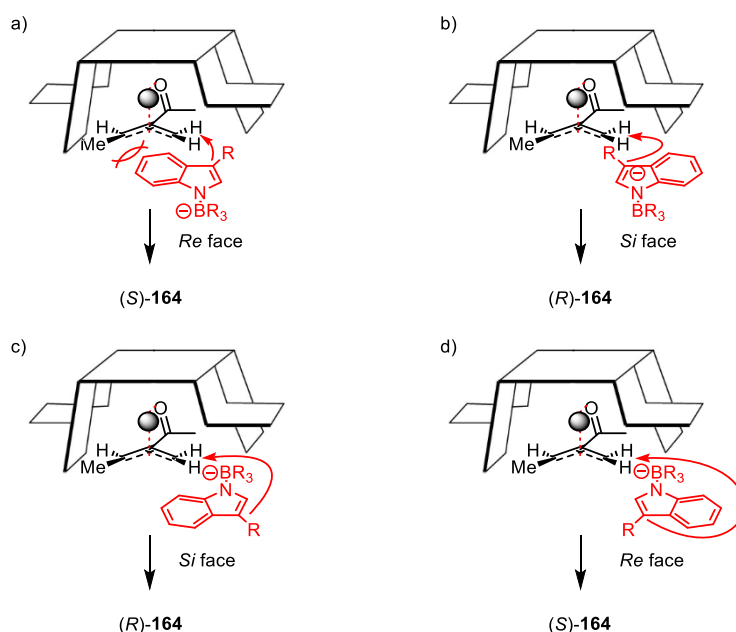
nucleophile. Therefore, it was not possible to extrapolate the stereochemical results from Trost and co-workers to our system.<sup>[96]</sup>

Trost and co-workers had reported that the products obtained from the allylic substitution reaction with cyclohexenyl carbonates and 2-substituted ester cyclohexenyl carbonates had the opposite absolute stereochemistry.<sup>[188]</sup> In the  $\pi$ -allylpalladium complex, the 2-position of the allyl ligand normally cants away from the Pd metal. However, when there is a coordinating group at the 2-position, for example an ester group, this group is proposed to coordinate to the Pd metal, thus changing the cant of the  $\pi$ -allyl ligand. This would then result in a switch in the facial selectivity of the  $\pi$ -allyl ligand to the nucleophilic attack.<sup>[114,177,184]</sup> It was initially thought that this could explain the switch in enantioselectivity in our system to that reported by Trost and co-workers, as the allylic alkylation substrate **96** employed in our system has a coordinating ketone at the 2-position which is absent in the allyl alcohol (**87**) used by Trost and co-workers.<sup>[96]</sup> While this could explain the switch in the enantioselectivity of the allylic substitution reaction when the stereocentre would be created on the electrophilic allylic substrate—as in the example with the cyclohexenyl carbonates—at this stage it is unclear how this change in the cant of the  $\pi$ -allyl ligand would switch which enantiotopic face of the prochiral nucleophile attacks the  $\pi$ -allyl ligand and hence reverse the configuration of the stereocentre generated on the nucleophile—as is the case in our system.

It was proposed that by applying the wall-and-flap model for the Trost ligands to our system, the enantiotopic facial selectivity of the nucleophilic attack—and hence the enantioselectivity of the allylic substitution reaction—could be explained. From which it was determined that there are four different possible approaches of the prochiral *N*-indolyltrialkylborate nucleophile to the  $\pi$ -allylpalladium complex (Scheme 66). It was thought that approach **a** would be disfavoured due to steric repulsion between the phenyl ring of the nucleophile and the front left wall of the Trost ligand.<sup>[189]</sup> With sterically bulky borane additives in the *N*-indolyltrialkylborate, it was believed that steric repulsion between the borane additive and back right wall of the Trost ligand would disfavour approaches **c** and **d**. Therefore, it was proposed that approach **b** would be the least disfavoured, in which the *Si* face of the prochiral nucleophile attacks the  $\pi$ -allylpalladium complex and gives the (*R*)-indolenine product **164**. While this model could account for the enantioselectivity obtained in our allylic substitution reaction; this alone still does not explain why the opposite stereochemistry was obtained in our system as would be expected from extrapolation of the results reported by Trost and co-workers.<sup>[96]</sup> Notably, when we applied the (*S,S*)-configured Trost ligands, the formation of

## Results and Discussion

the (*S*)-indolenine **164** was favoured (Table 10, entries 8 and 15). Therefore, in our system switching between the enantiomers of the Trost ligands switched the enantioselectivity of the allylic substitution reaction, by switching which enantiotopic face of the prochiral nucleophile attacked the  $\pi$ -allylpalladium complex. It remains unclear how applying the (*R,R*)-Trost ligands in our system and the (*S,S*)-Trost ligands in the related system reported by Trost and co-workers both resulted in nucleophilic attack from the *Si* face of the prochiral indole nucleophiles.



Scheme 66. Possible approaches of the prochiral *N*-indolyltrialkylborate nucleophile to the  $\pi$ -allylpalladium complex with the (*R,R*)-configured Trost ligand. Where R = (CH<sub>2</sub>)<sub>2</sub>NBoc(CH<sub>2</sub>)<sub>3</sub>Cl and therefore has lowest priority upon assignment of *Re* and *Si* faces of the prochiral *N*-indolyltrialkylborate nucleophile.

It was proposed that the wall-and-flap model of the Trost ligands could also be used to explain the regioselectivity of our system (Scheme 65). Upon ionisation of the allylic alcohol **96**, two diastereomeric *anti*  $\pi$ -allylpalladium complexes with the keto group at the 2-position coordinating to the Pd metal are generated.<sup>[114,177,184]</sup> These diastereomeric  $\pi$ -allylpalladium complexes can interconvert via the  $\eta^3$ - $\eta^1$ - $\eta^3$  isomerisation. Complex **I** is thermodynamically favoured as the methyl substituent is located close to the flap, as opposed to beside the wall as in complex **II**. However, the location of the methyl substituent in the front right quadrant in complex **I** may impede the *exo* approach of the nucleophile under this flap. Although in complex **II** the location of the methyl substituent beside the wall may result in unfavourable steric interactions, there is less steric hinderance to the *exo* approach of the nucleophile. Therefore, complex **II** is kinetically favoured. Since the methyl group is a relatively small

## *Results and Discussion*

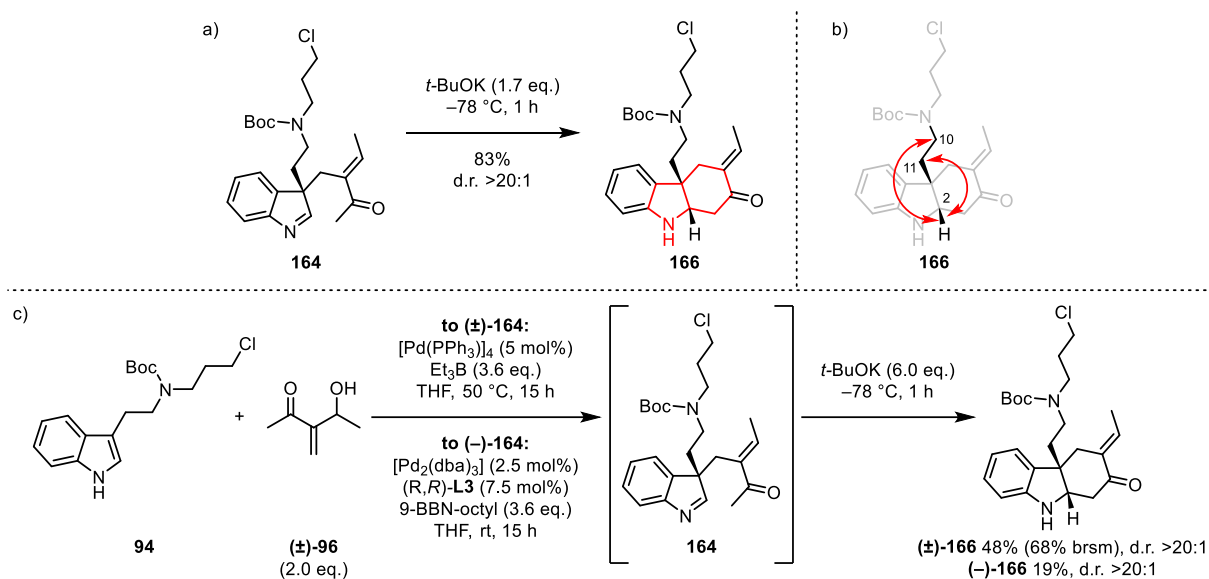
substituent, it was proposed that the steric interactions in complex **II** were not significant and that the regioselectivity of the allylic substitution was instead under kinetic control, in which steric hinderance to the *exo* nucleophilic attack was the determining factor. Therefore, less steric hinderance to the nucleophilic attack of complex **II**, results in a faster rate of the nucleophilic attack to this complex and the linear substituted product **IV** is preferentially formed over the branched product **III**, which would result from nucleophilic attack to the thermodynamic complex **I**. While this model could explain the obtained regioselectivity of the allylic substitution when applying the chiral Trost ligands, it is worth noting that the linear substituted product **IV** was also obtained when the achiral triphenylphosphine ligands were used. Therefore, it is proposed that the regioselectivity of the allylic substitution reaction was rather controlled by the attack of the soft, bulky *N*-indolyltrialkylborate nucleophile to the least substituted allyl terminus of the  $\pi$ -allylpalladium complex, to give the linear substituted product **164**.

### 3.5 Mannich Reaction

With the key Pd-catalysed enantioselective allylic substitution successfully performed, we turned our attention to the next steps in the synthetic route. Indolenine **164** was cyclised to the *cis*-fused tricycle **166** in a high yield of 83% using *t*-BuOK (Scheme 67a). Applying 1,8-diazabicyclo[5.4.0]undec-7-ene (DBU) as the base resulted in no conversion of the indolenine **164**. Whereas using LiHMDS gave the tricycle **166** in a much lower yield of 18% along with side products with lower R<sub>f</sub> values, presumably from elimination of the primary chloride via an E2 mechanism. Upon construction of the C ring in tricycle **166** a [4.3.0] fused bicyclic system was formed (shown in red in Scheme 67a), for which *cis* stereochemistry is more stable.<sup>[167]</sup> Furthermore, from analysis of the NOESY spectrum of tricycle **166**, the strongest NOE correlations were observed between H2 and H10 and between H2 and H11, which indicated the expected *cis* stereochemistry between H2 and the alkyl chain at C3 and hence the formation of the *cis*-fused tricycle **166** (Scheme 67b). Thus, the C ring was established in a highly diastereoselective intramolecular Mannich reaction.

We were interested to see if the allylic substitution and Mannich reaction could be performed as a one-pot process, in which *t*-BuOK would be added after observed formation of the indolenine product **164** by TLC analysis after 15 h. This was shown to be successful when performing the allylic substitution reaction both non-stereoselectively and enantioselectively (Scheme 67c). However, the tricycle **166** was obtained in a higher yield when the allylic substitution and Mannich reaction were performed separately. This allylic substitution and cyclisation sequence between tryptamine derivative **94** and allylic alcohol **96** installed two vicinal stereocentres of aspidospermidine (**1**). In addition, it is worth noting that this approach offers a fairly general and straightforward access to densely functionalised chiral hexahydro carbazoles from simple 3-substituted indole derivatives and Morita–Baylis–Hillman adducts.

## Results and Discussion

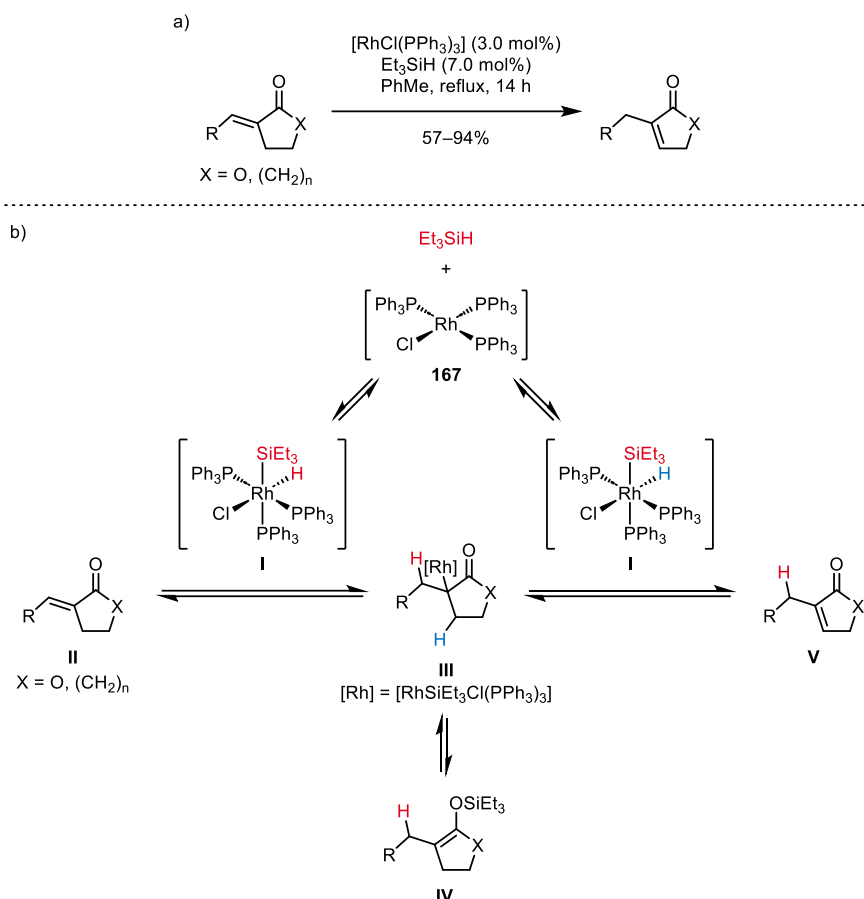


Scheme 67. Synthesis of tricycle **166**: a) Mannich reaction from indolenine **164**, with [4.3.0] *cis*-fused bicyclic system shown in red; b) one-pot allylic substitution and Mannich reaction sequence from tryptamine derivative **94**; c) Strongest NOE correlations observed from analysis of the NOESY spectrum of tricycle **166**.

### 3.6 *Exo-to-Endo* Double Bond Migration

The ensuing *exo-to-endo* double-bond migration presented a significant challenge. With reported methods for direct *exo-to-endo* enone double bond migration being scarce. Wakamatsu and co-workers reported using Wilkinson's catalyst (**167**), [RhCl(PPh<sub>3</sub>)<sub>3</sub>], and sub-stoichiometric triethylsilane for the *exo-to-endo* double bond migration of  $\alpha$ -alkylidene cyclic carbonyl compounds (Scheme 68a). Notably, when superstoichiometric triethylsilane was used, the corresponding hydrogenated compound was obtained as the major product. This transformation was proposed to occur via a hydrosilylation-dehydrosilylation sequence (Scheme 68b). Oxidative additive of triethylsilane to Wilkinson's catalyst (**167**) generates the active complex **I**. Hydrosilylation of *exo*-enone **II** with complex **I** gives silyl enol ether **IV**, via intermediate **III**. This system is in equilibrium and when the concentration of Et<sub>3</sub>SiH is low, the equilibrium position shifts to favour regeneration of Et<sub>3</sub>SiH. Therefore, dehydrosilylation of silyl enol ether **IV** via intermediate **III** occurs. Crucially, upon formation of intermediate **III**, the dehydrosilylation can occur by either elimination of **H** to regenerate the *exo*-enone **II** or with elimination of **H** to form the thermodynamically favoured *endo*-enone **V**.<sup>[190]</sup>

## Results and Discussion

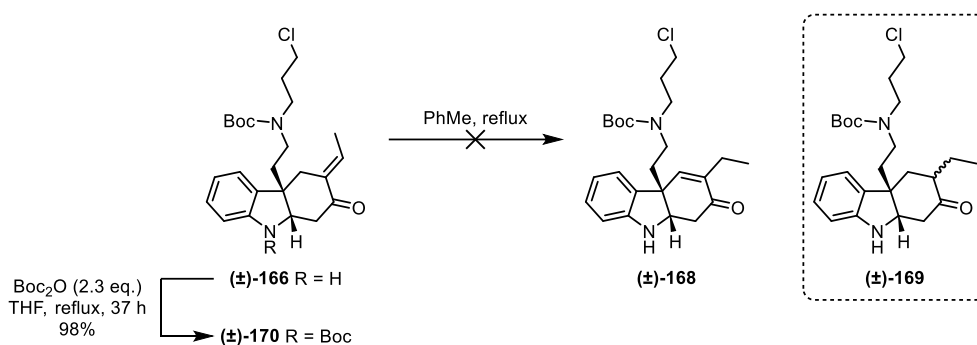


Scheme 68. *Exo*-to-*endo* double bond migration reported by Wakamatsu and co-workers: a) with  $\alpha$ -alkylidene cyclic carbonyl compounds; b) proposed mechanism thereof, adapted from <sup>[190]</sup>.

When these conditions were applied to *exo*-enone **166**, no conversion was observed (Table 11, entry 1). It was thought that the active complex **I** may be too sterically demanding to coordinate to the double bond in *exo*-enone **166**. However, upon increasing the loading of the  $\text{Et}_3\text{SiH}$ , the hydrogenated side product **169** was obtained (Table 11, entry 2), which suggested that the active complex **I** was able to coordinate to the double bond in *exo*-enone **166**. It was then thought that competing coordination of the indoline nitrogen atom in *exo*-enone **166** to the Rh centre in the active complex **I** could be problematic. Therefore, the indoline nitrogen atom in *exo*-enone **166** was Boc-protected to give *N*-Boc *exo*-enone **170**, which was then submitted to the double-bond migration reaction (Table 11, entry 3). Unfortunately, no reaction occurred.

## Results and Discussion

Table 11. Screening of conditions for the Rh-catalysed *exo-to-endo* double bond migration.

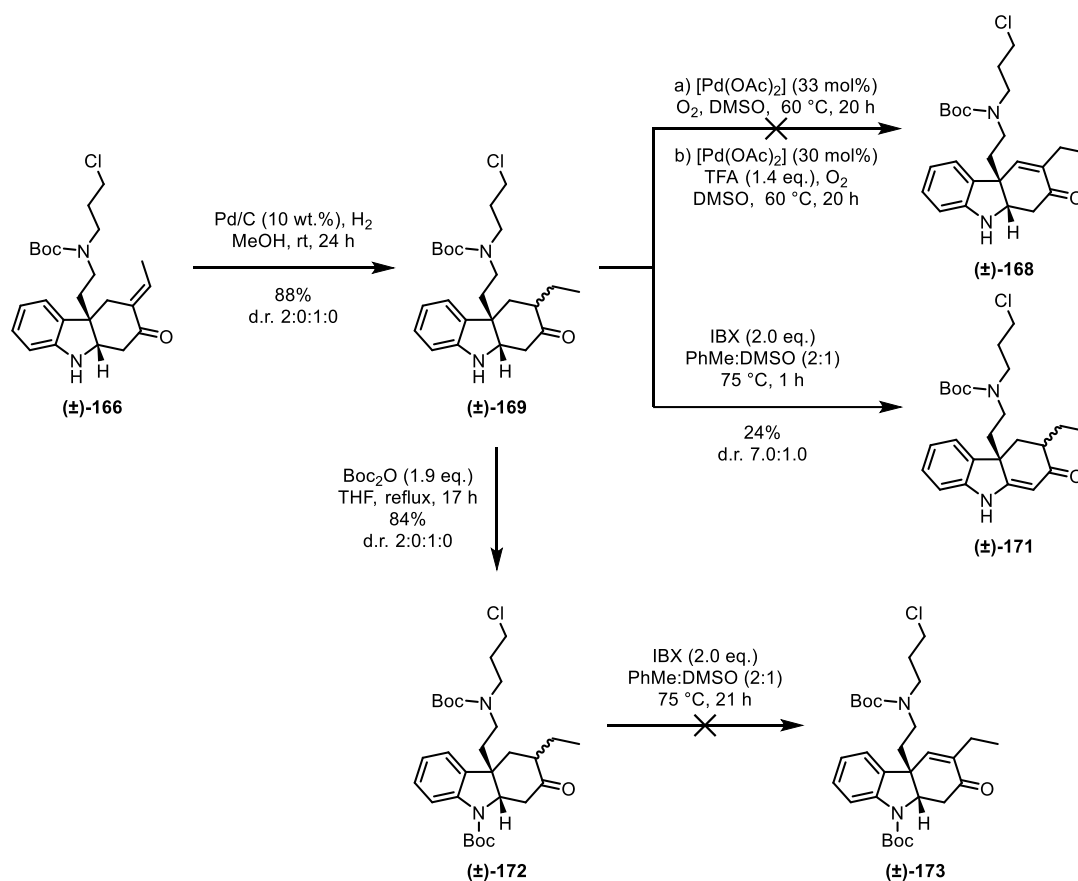


Entry	<i>Exo</i> -enone	Reagents (mol%)	Time (h)	Scale (μmol)	Result (%)
1	166	[RhCl(PPh <sub>3</sub> ) <sub>3</sub> ] (3.0)	4	50	no reaction
		Et <sub>3</sub> SiH (8.0)			
2	166	[RhCl(PPh <sub>3</sub> ) <sub>3</sub> ] (8.0)	20	140	<b>169</b> (36, d.r. 1.2:1.0)
		Et <sub>3</sub> SiH (51)			
3	170	[RhCl(PPh <sub>3</sub> ) <sub>3</sub> ] (4.0) Et <sub>3</sub> SiH (8.0)	4	42	no reaction

A multi-step redox strategy for the *exo-to-endo* double bond migration was therefore sought. A hydrogenation-dehydrogenation sequence was initially investigated. Hydrogenation of the *exo*-enone **166** with Pd/C under a hydrogen atmosphere delivered the saturated ketone **169** in a yield of 88% (Scheme 69). Dehydrogenation methods of cyclic ketones to enones typically require multi-step sequences or the stoichiometric use of reagents.<sup>[191]</sup> For this reason, we were initially drawn to a catalytic direct dehydrogenation method of cyclic ketones to the corresponding enones under Pd<sup>(II)</sup>-catalysis as reported by Stahl and Diao (Scheme 70a).<sup>[191]</sup> The optimised reaction conditions used acetic acid as the solvent. Under these acidic conditions, Boc-deprotection would have been expected with the saturated ketone **169**. Although, Boc-deprotection was required for the subsequent *aza*-Michael addition, milder conditions with [Pd(OAc)<sub>2</sub>] in DMSO at 80 °C under an oxygen atmosphere were initially applied (conditions a in Scheme 69). As Stahl and Diao reported that these conditions also gave the dehydrogenated product **175**, albeit in a lower yield (conditions b in Scheme 70a). Under these conditions, complete conversion of the saturated ketone **169** was observed but the desired product **168** was not obtained. We were then attracted to conditions reported by Wang and co-workers (Scheme 70b). In which [Pd(OAc)<sub>2</sub>] and stoichiometric trifluoroacetic acid (TFA) were used in DMSO.<sup>[185]</sup> These conditions had been employed in the total synthesis of

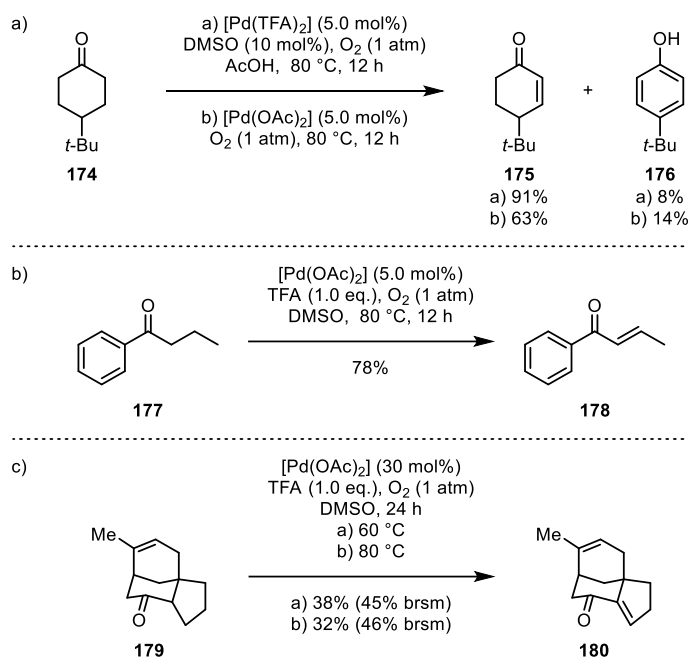
## Results and Discussion

penicibilaenes A and B, in which performing the reaction at 60 °C instead of 80 °C was found to give the dehydrogenated product **180** in higher yield (Scheme 70c).<sup>[192]</sup> Upon applying these conditions at 60 °C with saturated ketone **169**, decomposition was observed (conditions b in Scheme 69).



Scheme 69. Attempted hydrogenation-dehydrogenation sequences from *exo*-enone **166**.

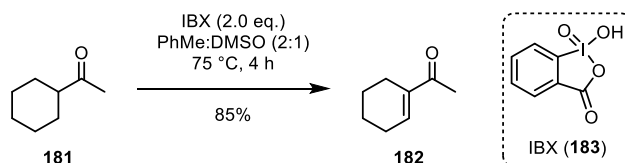
## Results and Discussion



Scheme 70. Direct Pd<sup>(II)</sup>-catalysed dehydrogenation methods of cyclic ketones to enones: a) reported by Stahl and co-workers;<sup>[191]</sup> b) reported by Wang and co-workers;<sup>[185]</sup> c) employed in the total synthesis of penicibilaenes A and B.<sup>[192]</sup>

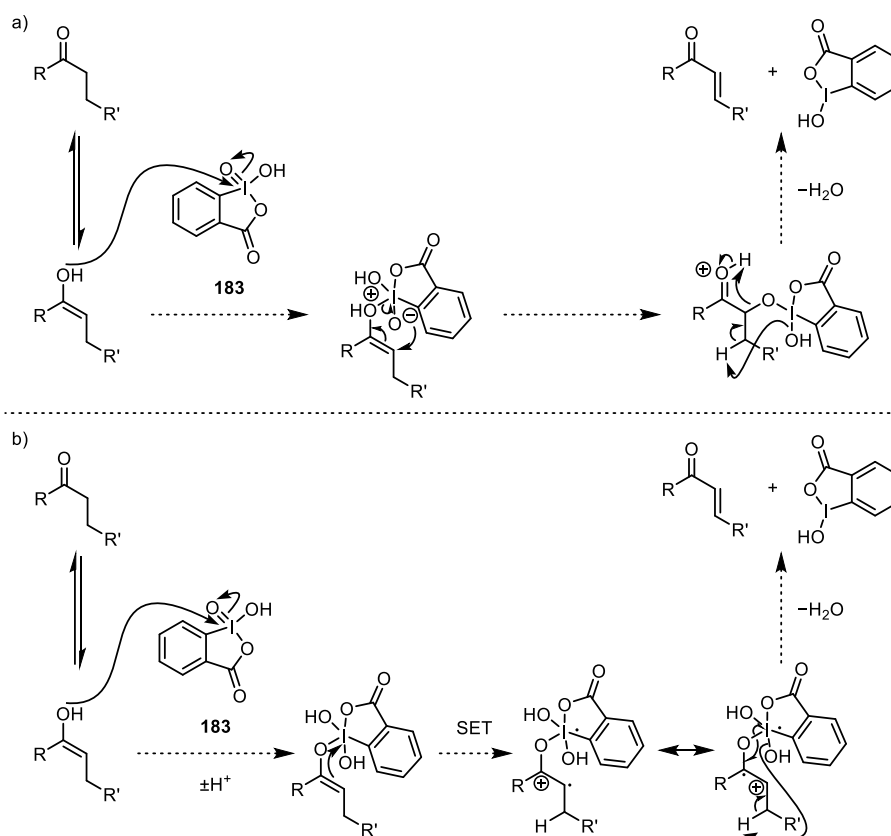
Alternative dehydrogenation conditions were therefore sought. Nicolaou and co-workers had reported a direct dehydrogenation method of carbonyl compounds to the corresponding  $\alpha,\beta$ -unsaturated compounds using 2-iodoxybenzoic acid (IBX) (**183**) as a stoichiometric oxidant. Notably, this method was reported for substrates with  $\alpha$ -substitution and nitrogen-containing functional groups (Scheme 71).<sup>[193]</sup> When saturated ketone **169** was submitted to these conditions, the undesired—but thermodynamically favoured—regioisomeric *endo*-enone **171** was obtained (Scheme 69). During this reaction there was a significant change in the diastereomeric ratio from 2.0:1.0 in the starting material **169** to 7.0:1.0 in the product **171**. This was proposed to be due to an enolisation of either the saturated ketone **169** or the *endo*-enone **171** by the acidic IBX (**183**).<sup>[194]</sup> The *N*-Boc saturated ketone **172** was synthesised to withdraw electron density from the indoline nitrogen atom, to disfavour the formation of the thermodynamic *endo*-enone regioisomer **171**. Interestingly, when the *N*-Boc saturated ketone **172** was submitted to the IBX-mediated dehydrogenation conditions, there was no conversion.

## Results and Discussion



Scheme 71. IBX-mediated dehydrogenation of carbonyl compounds to the corresponding  $\alpha,\beta$ -unsaturated compounds as reported by Nicolaou and co-workers.<sup>[193]</sup>

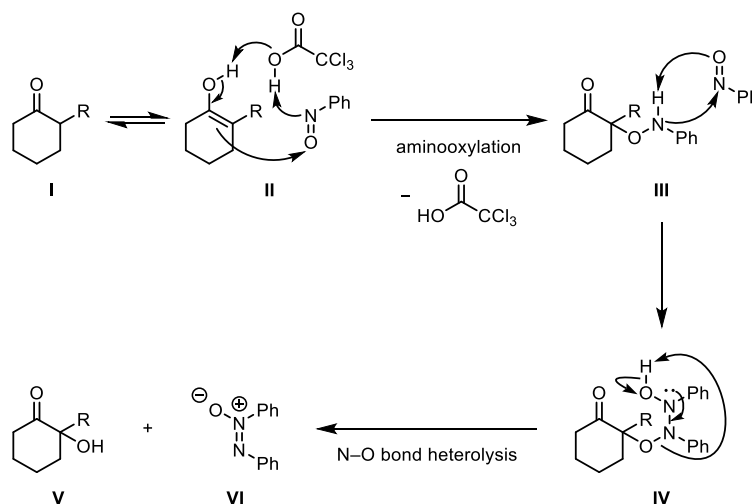
An ionic mechanism (Scheme 72a) was originally proposed for the IBX-mediated Nicolaou oxidation; however, due to mechanistic investigations of other IBX-mediated reactions at elevated temperature, a single-electron transfer (SET) mechanism was then proposed to be more likely (Scheme 72b). This was supported by a ring-opening radical clock experiment with a  $\beta$ -cyclopropyl aldehyde substrate and by a Hammett analysis. The SET-based mechanism shown in Scheme 72b was proposed by Nicolaou and co-workers;<sup>[195]</sup> however, other mechanistic pathways may be possible.



Scheme 72. Proposed mechanisms for the IBX-mediated dehydrogenation of carbonyl compounds to the corresponding  $\alpha,\beta$ -unsaturated compounds by Nicolaou and co-workers: a) ionic mechanism; b) SET-based mechanism. Adapted from <sup>[195]</sup>.

## Results and Discussion

Multi-step dehydrogenation methods were then sought. The first thereof was a regioselective  $\alpha$ -substitution of the saturated ketone **169** followed by elimination. For this, a method for the direct  $\alpha$ -hydroxylation of branched cyclic ketones with nitrosobenzene as reported by List and co-workers was of interest.<sup>[196]</sup> The proposed mechanism begins with the chloroacetic acid selectively protonating the nitrogen atom of the nitrosobenzene,<sup>[197]</sup> thereby activating the oxygen atom of the nitrosobenzene to nucleophilic addition from the thermodynamically favoured enol **II** (Scheme 73). The chloroacetate then deprotonates the enol **II**, forming the  $\alpha$ -aminoxy ketone **III**. The second equivalent of the nitrosobenzene undergoes nucleophilic addition from the nitrogen atom of the  $\alpha$ -aminoxy ketone **III**. A subsequent proton transfer affords the intermediate **IV**, which undergoes N–O bond heterolysis to afford the  $\alpha$ -hydroxy ketone **V** and the *trans*-azoxybenzene **VI**. The nitrosobenzene oxidant was therefore proposed to have a dual role in this transformation, the first equivalent thereof oxidises the  $\alpha$ -position of the ketone **I** through an aminoxylation and the second equivalent reduces the N–O bond in intermediate **IV** via a heterolytic cleavage.<sup>[198]</sup>

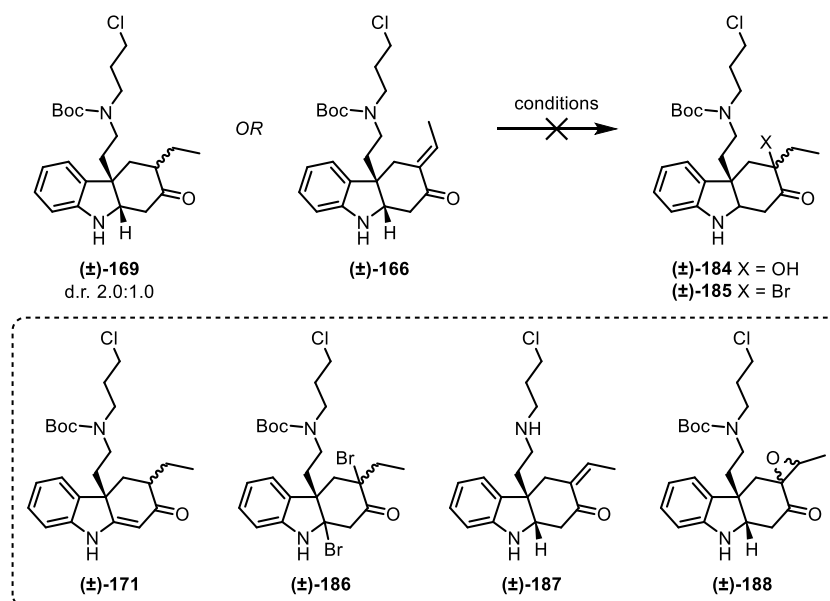


Scheme 73. Proposed reaction mechanism of direct  $\alpha$ -hydroxylation of branched cyclic ketones. Based upon <sup>[197,198]</sup>.

It was proposed that this method would regioselectively install a hydroxy group at the branched  $\alpha$ -position to the ketone in the saturated ketone **169** and that a subsequent elimination would then generate the desired *endo*-enone **168**. However, upon submitting saturated ketone **169** to these conditions, the undesired *endo*-enone **171** was obtained (Table 12, entry 1). It was believed that the hydroxylation instead occurred via the kinetically favoured enol of **169**, with subsequent elimination under the acidic reaction conditions giving the undesired *endo*-enone **171**.

## Results and Discussion

Table 12. Screening of conditions for the regioselective  $\alpha$ -substitution of saturated ketone **169** or from *exo*-enone **166**.



Entry	Starting Material	Reagents (eq.)	Solvent	<i>T</i> (°C)	Time (h)	Scale ( $\mu$ mol)	Result (%)
1	<b>169</b>	Cl <sub>3</sub> CCOOH (3.3) PhNO (2.6)	PhMe	rt	22	57	<b>171</b> (24, d.r. 2:0:1:0) mixture of
2	<b>169</b>	NBS (1.1)	C <sub>6</sub> H <sub>5</sub> Cl	80 to reflux	22	45	dibrominated products <sup>a</sup>
3	<b>166</b>	HBr 33 wt.% in AcOH (20 $\mu$ L) <sup>b</sup>	CH <sub>2</sub> Cl <sub>2</sub>	0	0.5	46	unknown product
4	<b>166</b>	30 % H <sub>2</sub> O <sub>2</sub> (10) aq. LiOH (0.50 M) (0.10)	MeOH	rt	66	47	presumed <b>188</b> <sup>a</sup>
5	<b>166</b>	30 % H <sub>2</sub> O <sub>2</sub> (60) aq. LiOH (0.50 M) (0.60)	MeOH	rt	142	140	unknown products

<sup>a</sup>Observed by ESI-MS analysis of the purified material. <sup>b</sup>Not possible to determine equivalents as is a solution.

Conditions for regioselective  $\alpha$ -bromination at the branched position were then sought. For this, conditions reported for  $\alpha$ -bromination at the branched position of 2-methylcyclohexanone with

## Results and Discussion

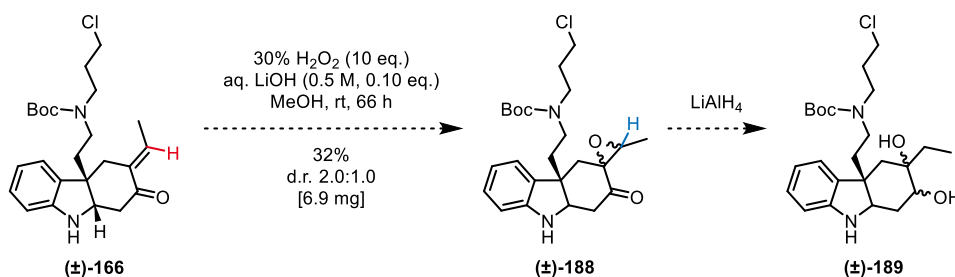
*N*-bromosuccinimide (NBS) were employed.<sup>[199]</sup> In which, NBS was a bromine radical source under heating.<sup>[200]</sup> Applying these conditions with saturated ketone **169** resulted in a complex mixture of dibrominated products (Table 12, entry 2). It was assumed that bromination also occurred at the 2-position of the saturated ketone **169** to afford the dibrominated compound **186**, due to stabilisation of the tertiary radical at the 2-position by lone pair resonance from the adjacent indoline nitrogen atom. In spite of this, the double elimination reaction with K<sub>2</sub>CO<sub>3</sub> at 80 °C in DMF was attempted with the complex mixture.<sup>[199]</sup> Under these conditions, no reaction was observed.

Methods for the regioselective  $\alpha$ -substitution from the *exo*-enone **166** were also investigated. Treatment of the *exo*-enone **166** with HBr was proposed as an alternative strategy for regioselective  $\alpha$ -bromination at the branched position (Table 12, entry 3). However, from electrospray ionisation mass spectrometry (ESI-MS) analysis of the purified material the characteristic bromine isotope peak pattern was not observed. Instead a base peak that would correspond to the [M+H]<sup>+</sup> peak of the Boc-protected *exo*-enone **187** was observed. However, the <sup>1</sup>H NMR spectrum of the purified material did not match that of the Boc-protected *exo*-enone **187**, which was obtained under standard Boc-deprotection conditions (see page 195 for the method).

Epoxidation of *exo*-enone **166** followed by reductive opening of the epoxides **188** at the least substituted position with LiAlH<sub>4</sub> was proposed as an alternative  $\alpha$ -hydroxylation strategy (Scheme 74).<sup>[201,202]</sup> Notably, the LiAlH<sub>4</sub> would also reduce the ketone in 2,3-epoxyketones **188** to give the vicinal diol **189**. Upon performing a test epoxidation reaction on a small scale,<sup>[203]</sup> two products with lower R<sub>f</sub> values than the *exo*-enone **166** were observed, which were presumed to be the two diastereomers of the 2,3-epoxyketone **188** (Table 12, entry 4). Additionally, the [M+H]<sup>+</sup> peaks corresponding to the 2,3-epoxyketones **188** were observed in the ESI spectra of the purified products. From analysis of the <sup>1</sup>H NMR spectra of both of the products, the signal of the vinylic hydrogen atom of the *exo*-enone **166** at 6.59 ppm was absent (highlighted in red in Scheme 74), and a new signal at 2.20 ppm with an integral of 1 was observed, which could correspond to the hydrogen atom at the least hindered position of the epoxide in the 2,3-epoxyketones **188** (highlighted in blue in Scheme 74). Therefore, the characterisation data strongly suggested the formation of the 2,3-epoxyketones **188**; however, since these products were obtained in small quantities, full NMR characterisation was not performed at this stage. Upon repeating the reaction on a larger scale, excess reagents and prolonged reaction times were required for complete conversion of the *exo*-enone **166**. Upon

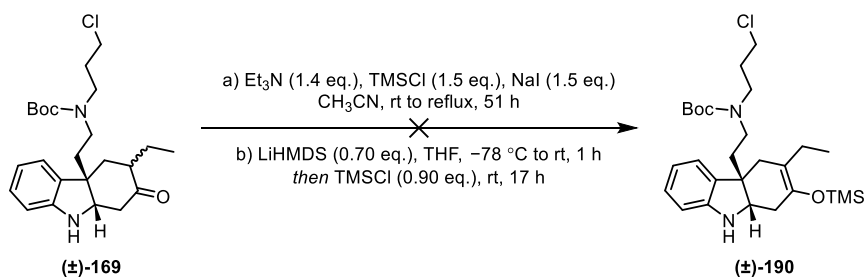
## Results and Discussion

purification, the two products were only isolated in trace amounts and their  $^1\text{H}$  NMR spectra did not match those from when the reaction was performed on a small scale. Due to the difficulties associated with the scale-up of the epoxidation reaction, this strategy was not further pursued.



Scheme 74. Proposed epoxidation and reductive epoxide-opening sequence for regioselective  $\alpha$ -hydroxylation from *exo*-enone **166**.

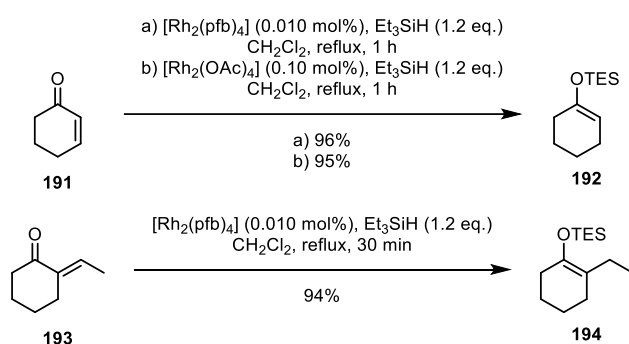
An alternative strategy to the desired *endo*-enone **168** from the saturated ketone **169**, via an oxidation of the intermediate thermodynamic silyl enol ether **190** was then envisaged (Scheme 75). To this end, conditions for the regioselective formation of the thermodynamic silyl enol ether **190** were required. For this, conditions reported by Dunogues and co-workers were applied with the saturated ketone **169** (conditions a in Scheme 75).<sup>[204]</sup> No conversion of the saturated ketone **169** was observed at room temperature nor upon heating under reflux. Thus, a different strategy to the thermodynamic silyl enol ether **190** was sought. Treatment of the saturated ketone **169** with a sub-stoichiometric quantity of  $\text{LiHMDS}$  at  $-78^\circ\text{C}$  should generate the corresponding kinetic enolate, which upon warming to room temperature, should then deprotonate the residual ketone **169** to give the thermodynamic enolate and regenerate the ketone **169**.<sup>[205]</sup> Subsequent addition of trimethylsilyl chloride,  $\text{TMSCl}$ , should then yield the thermodynamic silyl enol ether **190**. However, no conversion of the saturated ketone **169** was observed under these conditions (conditions b in Scheme 75).



Scheme 75. Unsuccessful conditions for the regioselective formation of the thermodynamic silyl enol ether **190**.

## Results and Discussion

An alternative 1,4-hydrosilylation strategy to the thermodynamic silyl enol ether that made use of the existing double bond in the *exo*-enone **166** was then proposed. This was inspired by a method reported by Hashimoto and co-workers, in which dirhodium<sup>(II)</sup> catalysts were employed for the 1,4-hydrosilylation of  $\alpha,\beta$ -unsaturated carbonyl compounds to give the corresponding silyl enol ethers (Scheme 76). From their studies, dirhodium(II) tetrakis(perfluorobutyrate),  $[\text{Rh}_2(\text{pfb})_4]$ , was found to be the most effective dirhodium<sup>(II)</sup> catalyst in terms of activity. Other dirhodium<sup>(II)</sup> catalysts including  $[\text{Rh}_2(\text{OAc})_4]$  were also shown to be effective but required a higher catalyst loading for completion of the reaction. Within the substrate scope, (*E*)-2-ethylidenecyclohexanone (**193**) was of particular interest as this resembled the substructure of our substrate **166**.<sup>[206]</sup>



Scheme 76. 1,4-Hydrosilylation of  $\alpha,\beta$ -unsaturated carbonyl compounds to the corresponding silyl enol ethers, as reported by Hashimoto and co-workers.<sup>[206]</sup>

The conditions reported by Hashimoto and co-workers with  $[\text{Rh}_2(\text{OAc})_4]$  as the catalyst were initially applied with *exo*-enone **166** (Table 13, entry 1). Under these conditions, there was incomplete conversion of *exo*-enone **166**; however, two products with higher  $R_f$  values than *exo*-enone **166** were observed. The product with the highest  $R_f$  value was presumed to be the desired thermodynamic silyl enol ether **195** and the intermediate product was presumed to be the saturated ketone **169** from hydrolysis of the silyl enol ether **195**. From ESI-MS analysis of the crude product,  $[\text{M}+\text{H}]^+$  peaks corresponding to the *exo*-enone **166**, the silyl enol ether **195** and the saturated ketone **169** were observed. After purification of the crude product by silica gel column chromatography, the *exo*-enone **166** and the saturated ketone **169** were obtained, but not the silyl enol ether **195**. It was thought that the silyl enol ether **195** had decomposed on the acidic silica gel. Since incomplete conversion of the *exo*-enone **166** was observed under these conditions, it was proposed that a higher reaction temperature may be required for full conversion. Therefore, the solvent was changed to 1,2-dichloroethane, as it had also been shown to be an effective solvent for the 1,4-hydrosilylation in the optimisation studies

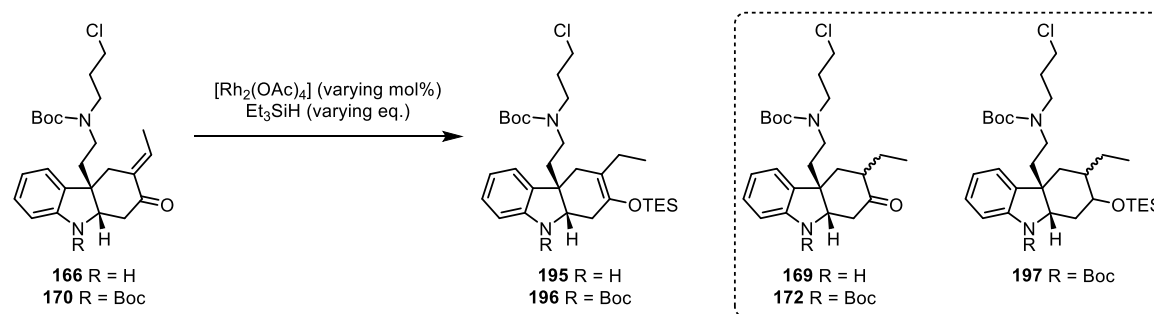
## Results and Discussion

performed by Hashimoto and co-workers.<sup>[206]</sup> When performing the reaction at 40 °C, no conversion of the *exo*-enone **166** was observed. Upon heating under reflux, the saturated ketone **169** was observed via TLC analysis and ESI-MS analysis of the crude product (Table 13, entry 2).

It was proposed that coordination of the indoline nitrogen atom in *exo*-enone **166** to the Rh atom in the catalyst could be problematic for the reaction. Therefore, the *N*-Boc *exo*-enone **170** was submitted under the same reaction conditions (Table 13, entry 3). Upon performing the reaction at 40 °C, no conversion was observed. The reaction was then heated under reflux, and after 4 h a product with a higher  $R_f$  value that was presumed to be the *N*-Boc silyl enol ether **196** was observed; however, incomplete conversion of the *N*-Boc *exo*-enone **170** was observed. After a further 17 h, new products with intermediate  $R_f$  values were observed, which were presumed to be the *N*-Boc saturated ketone **172** and the *N*-Boc silyl ether **197**, from hydrolysis and transfer hydrogenation of the *N*-Boc silyl enol ether **196**, respectively. Furthermore, the  $[M+Na]^+$  peaks corresponding to the *N*-Boc silyl enol ether **196**, the *N*-Boc saturated ketone **172** and the *N*-Boc silyl ether **197** were observed in the ESI mass spectrum of the crude product. It was then proposed that the reaction should be directly heated to reflux to afford the *N*-Boc silyl enol ether **196**, which should then be immediately isolated to prevent its hydrolysis and hydrogenation. Furthermore, column chromatography should be performed on aluminium oxide to prevent decomposition of the silyl enol ether **196** on silica gel. This was employed in entry 4 in Table 13 in which the *N*-Boc silyl enol ether **196** was obtained in a high yield of 83%. Notably, at least 2 equivalents of the  $Et_3SiH$  were required for full conversion of the *N*-Boc *exo*-enone **170**. Finally, these conditions were shown to be scalable with a lower catalyst loading, in which the *N*-Boc silyl enol ether **196** obtained in a yield of 82% on a gram-scale (Table 13, entry 5).

Results and Discussion

Table 13. Optimisation of reaction conditions for Rh-catalysed 1,4-hydrosilylation of *exo*-enones **166** and **170**.

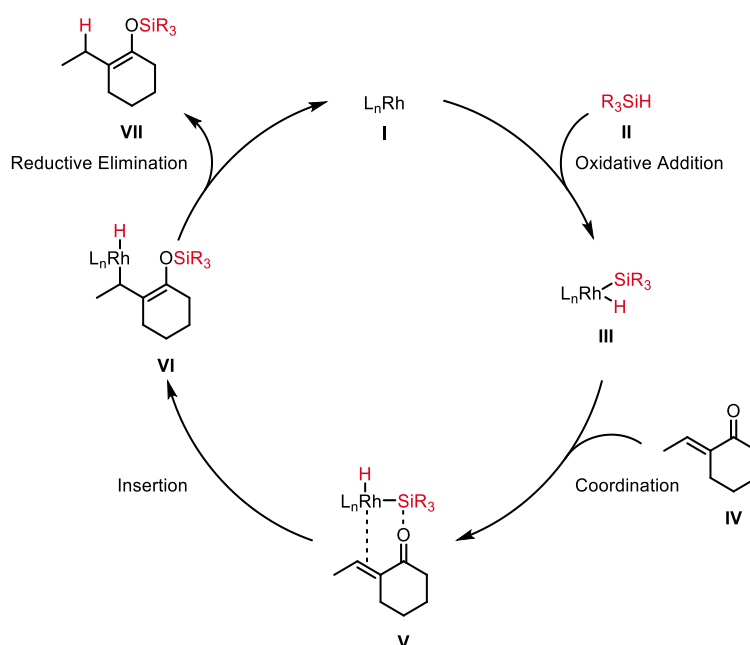


Entry	<i>Exo</i> -enone	Catalyst Loading (mol%)	$\text{Et}_3\text{SiH}$ (eq.)	Solvent	$T$ ( $^\circ\text{C}$ )	Time (h)	Scale (mmol)	Result (%)
1	<b>166</b>	10	2.4	$\text{CH}_2\text{Cl}_2$	reflux	47	0.050	<b>169</b> (18%, 23% brsm, d.r. 1.0:1.0), presumed <b>195</b> <sup>a</sup>
2	<b>166</b>	21	2.3	$(\text{CH}_2\text{Cl})_2$	40 to reflux	30	0.054	<b>169</b> <sup>a</sup>
3	<b>170</b>	10	1.3	$(\text{CH}_2\text{Cl})_2$	40 to reflux	22	0.035	presumed <b>196:172:197</b> <sup>a</sup>
4	<b>170</b>	15	2.6	$(\text{CH}_2\text{Cl})_2$	reflux	1	0.41	<b>196</b> (83)
5	<b>170</b>	2.5	2.5	$(\text{CH}_2\text{Cl})_2$	reflux	1	3.0	<b>196</b> (82)

<sup>a</sup>Observed by TLC analysis and ESI-MS analysis of the crude product.

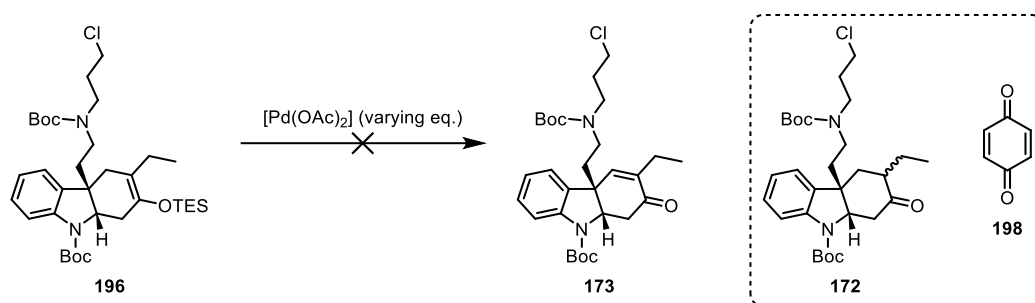
## Results and Discussion

A catalytic cycle for the Rh<sup>(I)</sup>-catalysed selective 1,4-hydrosilylation of  $\alpha,\beta$ -unsaturated ketones with monohydrosilanes was proposed by Zheng and Chan (Scheme 77).<sup>[207]</sup> Oxidative addition of the monohydrosilane **II** to the Rh<sup>(I)</sup> metal **I** occurs, generating species **III**. The  $\alpha,\beta$ -unsaturated ketone **IV** coordinates to species **III** through  $\sigma$ -coordination of the oxygen atom to the silicon atom and  $\pi$ -coordination of the double bond to the Rh metal in intermediate **V**. Insertion of the carbonyl into the Rh–Si bond results in a rearrangement that affords the silyl enol ether species **VI**. Reductive elimination releases the silyl enol ether **VII** and regenerates the active Rh<sup>(I)</sup> catalyst **I**.<sup>[207,208]</sup> It was proposed that in the method reported by Hashimoto and co-workers the monohydrosilane Et<sub>3</sub>SiH also served as a hydride source and thus reduced the Rh<sup>(II)</sup> from the [Rh<sub>2</sub>(OAc)<sub>4</sub>] complex to the active Rh<sup>(I)</sup> catalyst.<sup>[209]</sup>



Scheme 77. Proposed catalytic cycle for the Rh<sup>(I)</sup>-catalysed 1,4-hydrosilylation of  $\alpha,\beta$ -unsaturated ketones with monohydrosilanes by Zheng and Chan. Adapted from <sup>[208]</sup>.

With the thermodynamic silyl enol ether **196** in hand, the ensuing oxidation reaction was investigated. A Saegusa–Ito oxidation was initially envisaged. Saegusa–Ito oxidation protocols typically use trimethylsilyl (TMS) enol ethers, however triethylsilyl (TES) enol ethers have also been reported as substrates.<sup>[210–214]</sup> The conditions originally reported by Saegusa and co-workers with stoichiometric [Pd(OAc)<sub>2</sub>] were first applied (Table 14, entry 1).<sup>[215]</sup> No conversion of the silyl enol ether **196** was observed at room temperature, nor upon heating to 60 °C.<sup>[210]</sup> Saegusa and co-workers had also reported that substoichiometric [Pd(OAc)<sub>2</sub>] could be used with 1,4-benzoquinone (**198**) as a co-oxidant to regenerate the active Pd<sup>(II)</sup> catalyst.<sup>[215]</sup>

Table 14. Screening of reaction conditions for the Saegusa–Ito oxidation of silyl enol ether **196**.

Entry	[Pd(OAc) <sub>2</sub> ] (eq.)	Reagents (eq.)	Solvent	T (°C)	Time (h)	Scale (μmol)	Result (%)
1	1.0	—	MeCN	rt to 60	24	49	no reaction
2	0.67	<b>198</b> (0.57)	MeCN	rt	23	30	no reaction
3	1.7	Na <sub>2</sub> CO <sub>3</sub> (1.4)	MeCN	rt to reflux	75	30	<b>196</b> with presumed <b>172</b> traces <sup>a</sup>
5	1.2	—	DMSO	rt to 80	47	75	<b>172</b> (69, d.r. 1.3:1.0)
6	1.8	O <sub>2</sub> (1 atm)	DMSO	80	26	30	presumed <b>172</b> <sup>ab</sup>

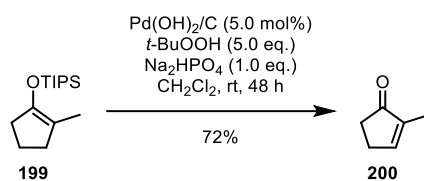
<sup>a</sup>Observed by TLC analysis. <sup>b</sup>Observed by ESI-MS analysis of the crude product.

Under these conditions, no conversion of the silyl enol ether **196** was observed (Table 14, entry 2). The addition of base was then tested (Table 14, entry 3).<sup>[216]</sup> This had been reported to be successful when the standard procedure had failed,<sup>[217]</sup> presumably by neutralisation of the acetic acid formed in the reaction.<sup>[104]</sup> When performing the reaction at room temperature, no conversion was observed. Upon heating under reflux, the presumed saturated ketone **172** was observed by TLC analysis.<sup>[218]</sup> However, incomplete conversion of the silyl enol ether **196** was also observed. A solvent change to DMSO was tested (Table 14, entry 5), as this had been reported for when the reaction failed to proceed in MeCN.<sup>[219]</sup> No conversion was observed when performing the reaction at room temperature. The reaction was then heated to 80 °C, as Larock and co-workers reported that trisubstituted silyl enol ethers that were unreactive at room temperature underwent conversion at 80 °C.<sup>[219]</sup> Unfortunately the saturated ketone **172** was obtained, presumably due to hydrolysis of the silyl enol ether **196**, despite great care being taken to perform the reaction under anhydrous conditions. Finally, the Larock modification

## Results and Discussion

using oxygen as the co-oxidant was tried (Table 14, entry 6).<sup>[219]</sup> However, the presumed saturated ketone **172** was obtained.

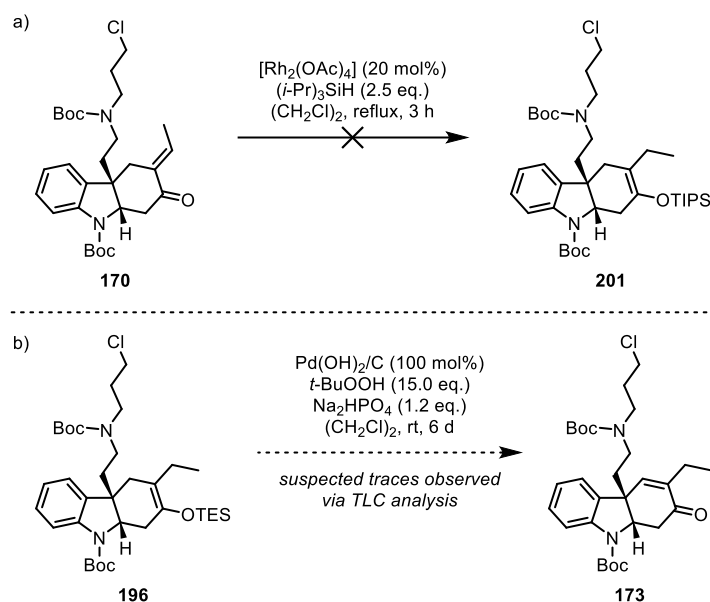
A Pd<sup>(II)</sup>-catalysed oxidation method of silyl enol ethers to the corresponding enones reported by Corey and co-workers was then investigated. Crucially the substrate scope included the  $\alpha$ -substituted thermodynamic silyl enol ether **199**, which regioselectively gave the thermodynamic *endo*-enone **200** (Scheme 78). In this method, the triisopropylsilyl (TIPS) enol ethers were employed due to their stability under the basic reaction conditions.<sup>[220]</sup>



Scheme 78. Pd<sup>(II)</sup>-catalysed oxidation method of silyl enol ethers to the corresponding enones, reported by Corey and co-workers.<sup>[220]</sup>

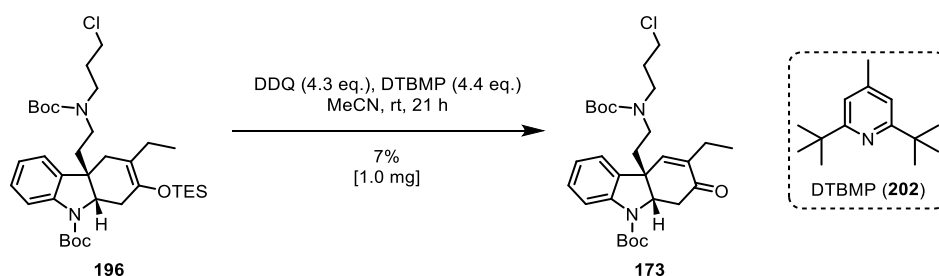
The formation of the TIPS silyl enol ether **201** via the 1,4-hydrosilylation method from *N*-Boc *exo*-enone **170** was unsuccessful, presumably due to too much steric hinderance in the triisopropylsilane (Scheme 79a). Therefore, the *N*-Boc triethylsilyl enol ether **196** was submitted to the Pd<sup>(II)</sup>-catalysed oxidation method (Scheme 79b). Since this reaction was performed on a small scale, 1,2-dichloroethane was used as the solvent in place of CH<sub>2</sub>Cl<sub>2</sub>, as the CH<sub>2</sub>Cl<sub>2</sub> quickly evaporated. A new product with a lower R<sub>f</sub> value was observed, that was presumed to be the *N*-Boc *endo*-enone **173**, however incomplete conversion of the *N*-Boc silyl enol ether **196** was observed, even upon prolonged reaction time and further addition of *tert*-butyl hydroperoxide (TBHP).

## Results and Discussion



Scheme 79. a) Unsuccessful 1,4-hydrosilylation of *N*-Boc *exo*-enone **170** with triisopropylsilane; b) Attempted Pd<sup>(II)</sup>-catalysed oxidation of *N*-Boc triethylsilyl enol ether **196**.

Alternative conditions for the oxidation of the silyl enol ether **196** to the desired *endo*-enone **173** were therefore sought. A method employing DDQ as a hydride abstracting reagent with 2,6-di-*tert*-butyl-4-methylpyridine (DTBMP) (**202**) was of interest, as it had been reported for the oxidation of TES<sup>[212]</sup> and TBS<sup>[221]</sup> enol ethers of cyclohexanone substrates. This oxidation was proposed to occur via allylic hydride abstraction by DDQ to give an allylic cation, which upon aqueous workup provides the enone.<sup>[222,223]</sup> Under these conditions, the *endo*-enone **173** was obtained, albeit in trace amounts (Scheme 80). However, due to excessive side product formation, alternative oxidation methods were sought.

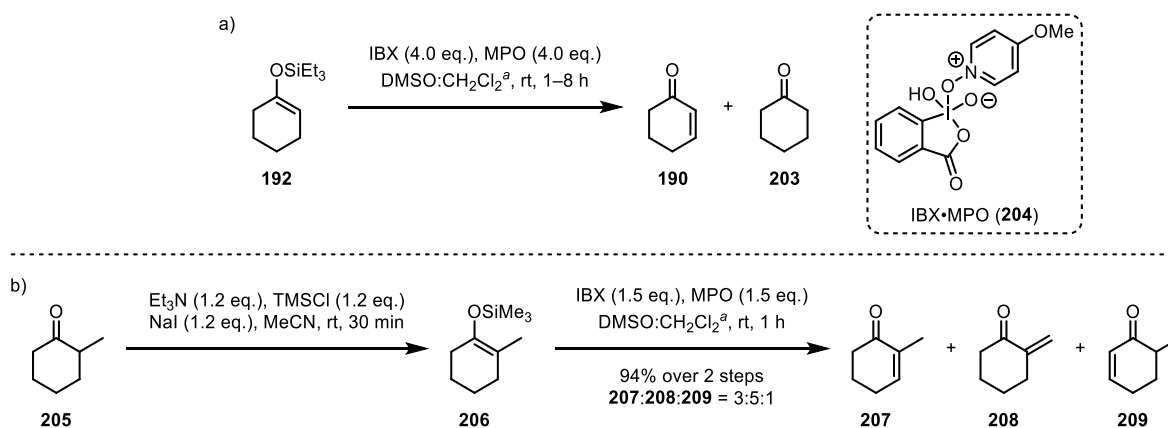


Scheme 80. DDQ-mediated oxidation of silyl enol ether **196** to *endo*-enone **173**.

Nicolaou and co-workers had extended their IBX-mediated oxidation to silyl enol ethers substrates, to afford the corresponding enones. In this modified method either IBX (**183**) or the IBX•MPO complex (**204**) (MPO = 4-methoxypyridine *N*-oxide) could be applied as the oxidant, with a faster oxidation reported for the latter (Scheme 81). Furthermore, the triethylsilyl enol

## Results and Discussion

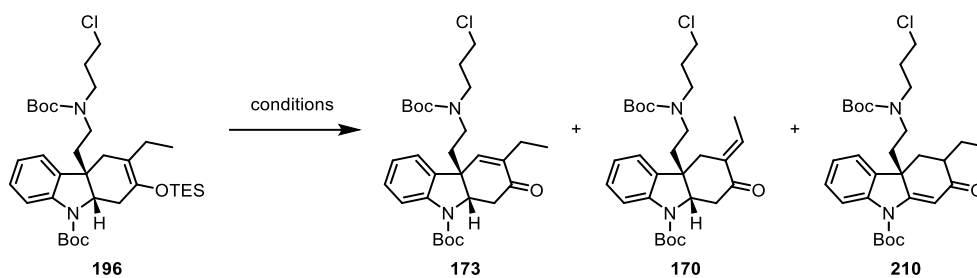
ether **192** was reported as a substrate (Scheme 81a). Notably, when the  $\alpha$ -substituted thermodynamic silyl enol ether **206** was submitted to this protocol a mixture of the enones **207:208:209** was obtained, with a higher selectivity for the *exo*-enone **208** (Scheme 81b).<sup>[224]</sup> This was interesting as *exo*-enone **208** was selectively formed over the thermodynamically favoured *endo*-enone **207**. This preference for the *exo*-enone **208** was thought to be under statistical control due to the availability of three  $\beta$ -protons at the methyl group to afford the *exo*-enone **208**, compared to only two available  $\beta$ -protons to afford the *endo*-enones **207** and **209**. The mechanism of this transformation with the silyl enol ether was proposed to be analogous to that with the enol generated from the carbonyl compound (Scheme 72). However, based on this proposed mechanism it is unclear how the undesired *endo*-enone **209** was formed.



Scheme 81. IBX-mediated Nicolaou oxidation with silyl enol ether substrates: a) with TES enol ether **192**; b) with  $\alpha$ -substituted thermodynamic silyl enol ether **206**. <sup>a</sup>When the substrate was not fully soluble in DMSO, CH<sub>2</sub>Cl<sub>2</sub> was added dropwise until a clear solution was obtained.

Crucially, when substrates containing heteroatoms such as nitrogen were used, the corresponding saturated ketones were reportedly obtained as major inseparable side products. This was proposed to be due to coordination of the heteroatoms to the IBX (**183**), therefore additional equivalents of IBX (**183**) were required. This unproductive coordination was proposed to result in a slower rate of the desired oxidation reaction relative to the competing hydrolysis of the silyl enol ether, thus giving the saturated ketones in a higher yield.<sup>[224]</sup> This highlights the importance of the *N*-Boc-protection in silyl enol ether **196**.

Silyl enol ether **196** was submitted under the conditions reported by Nicolaou and co-workers using IBX•MPO (**204**) (Table 15, entry 1) and IBX (**183**) (Table 15, entry 2) as the oxidants.

Table 15. Optimisation of reaction conditions for the IBX-mediated Nicolaou oxidation of silyl enol ether **196**.

Entry	Reagents (eq.)	Solvent	<i>T</i> (°C)	Time (h)	Scale (μmol)	Result (%)
<b>1</b>	IBX (4.2) MPO (4.5)	DMSO	rt	94	42	<b>173</b> (5)
<b>2</b>	IBX (4.3)	DMSO	rt	67	42	<b>173</b> (9)
<b>3</b>	IBX (2.1)	DMSO:CH <sub>2</sub> Cl <sub>2</sub> (3:1)	55	22	89	<b>173:170:210</b> (30:20:6)
<b>4<sup>a</sup></b>	IBX (1.5)	DMSO:CH <sub>2</sub> Cl <sub>2</sub> (3:1)	rt	44	89	<b>173:170</b> (41:17)
<b>5</b>	IBX (2.0)	DMSO:CH <sub>2</sub> Cl <sub>2</sub> (3:1)	55	21	660	<b>173:170</b> (32:13)

<sup>a</sup>With freshly prepared IBX.

Gratifyingly, both of these reaction conditions gave the desired *endo*-enone **173** as the major product. As these test reactions were performed on a small scale, the minor side products were not isolated at this stage. Since using IBX (**183**) as the oxidant afforded the desired product **173** in a higher yield and with a shorter reaction time, IBX (**183**) was taken forward in the optimisation studies. When performing the reaction on a larger scale, CH<sub>2</sub>Cl<sub>2</sub> was added to the reaction mixture for full dissolution of the substrate **196** (Table 15, entry 3). Since the addition of CH<sub>2</sub>Cl<sub>2</sub> was reported to slow the reaction rate,<sup>[224]</sup> the reaction was heated to 55 °C, as in the Nicolaou oxidation with carbonyl substrates.<sup>[193]</sup> Under these conditions, the desired *endo*-enone **173** was obtained in a higher yield of 30%. Additionally, the *exo*-enone **170** and the undesired regioisomeric *endo*-enone **210** were determined to be the minor products. The *exo*-enone **170** could be resubmitted to the 1,4-hydrosilylation reaction. When freshly prepared IBX (**183**) was applied the reaction could be performed at room temperature and the desired

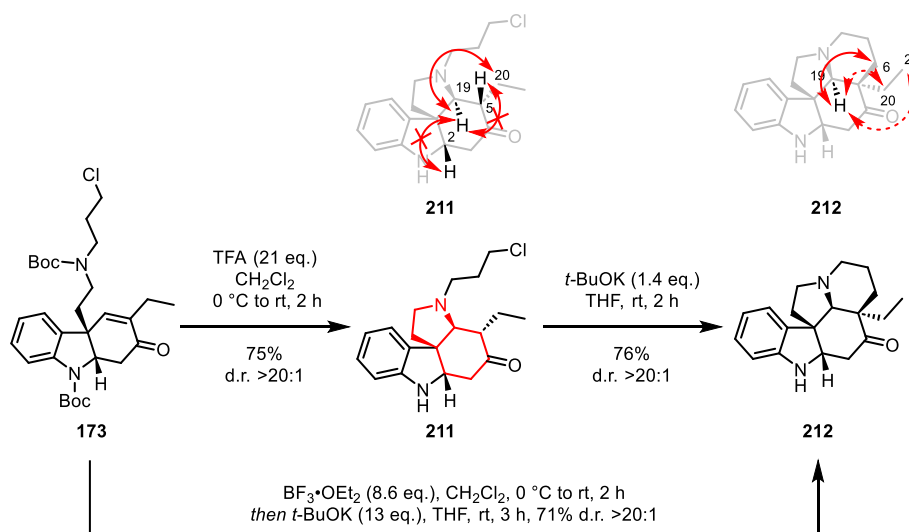
## Results and Discussion

*endo*-enone **173** was obtained in a yield of 41% (Table 15, entry 4). When the IBX (**183**) was not freshly prepared and the reaction was performed on a larger scale (Table 15, entry 5), heating of the reaction to 55 °C and 2.0 equivalents of IBX (**183**) were required; the *endo*-enone **173** was then obtained in a slightly lower yield of 32%. Although these oxidation reactions were also performed in DMSO, the saturated ketone **172** was not obtained under any of these conditions compared to when DMSO was used as the solvent for the Saegusa–Ito oxidation (Table 14, entries 5 and 6). It was thought that in the Nicolaou oxidation the oxidation of the silyl enol ether **196** was faster than the competing hydrolysis.

After investigating multiple approaches for the *exo*-to-*endo* double bond migration, it was eventually found that a multi-step redox strategy via a 1,4-hydrosilylation of the *N*-Boc *exo*-enone **170** followed by an IBX-mediated Nicolaou oxidation of the silyl enol ether **196** afforded the desired *N*-Boc *endo*-enone **173**.

### 3.7 Ring-Closing Sequence

With the desired *endo*-enone **173** in hand, we turned our efforts to the ring-closing sequence for the construction of the D and E rings of aspidospermidine (**1**). *N*-deprotection and concomitant *aza*-Michael addition proceeded smoothly in the presence of trifluoroacetic acid, furnishing the tetracyclic product **211** in 75% yield with high diastereoselectivity (Scheme 82). Upon construction of the D ring a [4.3.0] fused bicyclic system in tetracycle **211** was formed (shown in red in Scheme 82), for which *cis* stereochemistry is more stable.<sup>[167]</sup> From analysis of the NOESY spectrum of tetracycle **211**, NOE correlations were not observed between H19 and H2 nor between H19 and H5, which indicates *trans* stereochemistry between H19 and H2 and between H19 and H5 (Scheme 82). Furthermore, NOE correlations were observed between H19 and one H20 in the ethyl group at C5, thus indicating *cis* stereochemistry between H19 and the ethyl group at C5. The ethyl substituent at C5 occupies the thermodynamically favoured pseudoequatorial position in the cyclohexanone C ring of tetracycle **211**.



Scheme 82. Ring-closing sequence from *endo*-enone **173** over one- or two-pot transformations with [4.3.0] *cis*-fused bicyclic system in tetracycle **211** shown in red and observed NOE correlations for tetracycle **211** and pentacycle **212** shown.

The final E ring in pentacycle **212** was established by an intramolecular enolate alkylation using *t*-BuOK as the base (Scheme 82). Again, high stereocontrol over the newly formed quaternary carbon stereocentre was achieved; thus, completing the assembly of the pentacyclic framework. From analysis of the NOESY spectrum of **212**, the strongest NOE correlation was observed between H19 and to one H6, which suggested *cis* stereochemistry between them.

However, weaker NOE correlations were also observed between H19 and one H20 and between H19 and H21.

Conformational analysis of pentacycle **212** with *cis*- and *trans*-fused E rings was performed in Chem3D with MM2 energy minimisation (Figure 9). In both isomers the E ring was calculated to have a twist-boat conformation (Figure 9 middle). However, in the *trans*-fused pentacycle **213** destabilising *syn*-pentane interactions between H20 and H10 and H11 were present (hydrogens involved are shown in yellow in Figure 9 lower right). Crucially, these *syn*-pentane interactions were absent in the *cis*-fused pentacycle **212** (Figure 9 upper right). It was proposed that the destabilising *syn*-pentane interactions would already emerge during bond formation en route to the *trans*-fused isomer **213**, but not to the *cis*-fused isomer **212**, which could account for the high diastereoselectivity of the intramolecular enolate alkylation reaction for the *cis*-fused product **212**. Furthermore, in the *cis*-fused pentacycle **212** the calculated distance of 4.0 Å between H19 and one H6 means that although these hydrogens have *trans* stereochemistry it is still expected that a NOE correlation would be observed between them (Figure 9 upper right).

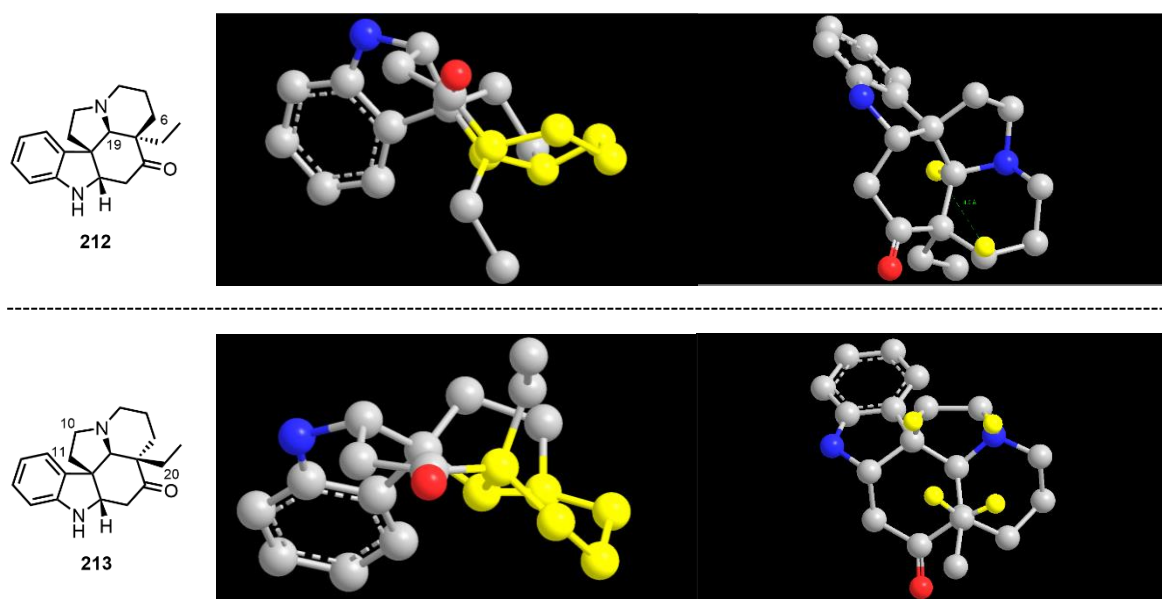


Figure 9. Conformational analysis of *cis*- and *trans*-fused pentacycles **212** and **213** (upper and lower, respectively) in Chem3D with MM2 energy minimisation: calculated conformation of the piperidine E ring for both isomers (middle); calculated bond distance of 4.0 Å between H19 and one H6 in the *cis*-fused isomer **212** (upper right); hydrogen atoms involved in the *syn*-pentane interactions in the *trans*-fused isomer **213** shown in yellow (lower right).

## Results and Discussion

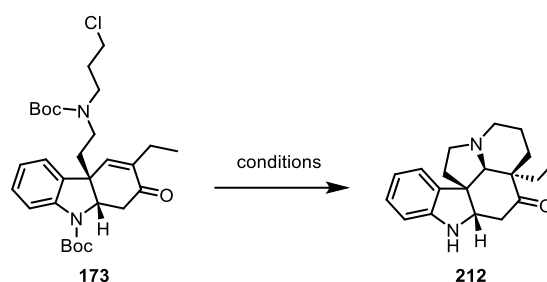
We were intrigued to see if the D/E ring closures could be performed as a one-pot transformation. In which the enolate, formed upon the *aza*-Michael addition, is not protonated and can therefore undergo the subsequent intramolecular enolate alkylation. To this end, neutral or non-Brønsted acidic conditions for the *N*-deprotection of *endo*-enone **173** were sought (Table 16). Ceric ammonium nitrate (CAN) was employed for *N*-Boc deprotection under neutral conditions.<sup>[225]</sup> In this method, CAN was proposed to act as a one-electron oxidant for the formation of radical cations from *t*-butoxycarbonyl groups.<sup>[225,226]</sup> A stoichiometric quantity of CAN was required for complete conversion of the *endo*-enone **173** (Table 16, entry 1). *t*-BuOK was then added to the reaction mixture. Formation of neither the tetracycle **211** nor the pentacycle **212** was observed. It was then proposed that after complete conversion of the *endo*-enone **173**, the reaction solvent could be exchanged from MeCN to THF to increase the solubility of the *t*-BuOK. Again, formation of neither the tetracycle **211** nor the pentacycle **212** was observed (Table 16, entry 2).

Boc-deprotection methods employing Lewis acid catalysts were then looked to. In which coordination of the Lewis acid to the carbonyl group in the carbamate induces fragmentation.<sup>[227]</sup> Zinc bromide was first applied (Table 16, entry 3), as it was reported as a mild Lewis acid for the selective Boc-deprotection of secondary amines.<sup>[228,229]</sup> However, no conversion of the *endo*-enone **173** was observed. Trimethylsilyl iodide, which had also been reported as a Lewis acid for the deprotection of carbamates, was then employed (Table 16, entry 4).<sup>[230,231]</sup> While complete conversion of the *N*-Boc *endo* enone **173** was observed under these conditions, formation of neither the tetracycle **211** nor pentacycle **212** was observed.

BF<sub>3</sub>•OEt<sub>2</sub> had also been reported as a Lewis acid for the Boc-deprotection of amines.<sup>[232,233]</sup> In these reported conditions, BF<sub>3</sub>•OEt<sub>2</sub> was used in excess. Therefore, if *t*-BuOK would be added directly to the reaction mixture after Boc-deprotection, then *t*-BuOK would also be required in excess as the Lewis acid-base complex between BF<sub>3</sub>•OEt<sub>2</sub> and *t*-BuOK would initially form. Consequently, THF was chosen as the reaction solvent due to the high solubility of *t*-BuOK therein.<sup>[234]</sup> Conversion of the *N*-Boc *endo* enone **173** was only observed upon heating under reflux (Table 16, entry 5). This was believed to be due to competing coordination of the THF to the BF<sub>3</sub>•OEt<sub>2</sub>. Upon complete conversion of *N*-Boc *endo*-enone **173**, excess *t*-BuOK was added to the reaction mixture. The desired pentacycle **212** was obtained with minor impurities. Due to the small quantity of material isolated, further purification was not performed.

Results and Discussion

Table 16. Screening of reaction conditions for the one-pot ring-closing sequence.



Entry	Reagents (eq.)	Solvent	$T$ (°C)	Time (h)	Scale ( $\mu\text{mol}$ )	Result (%)
1	i) CAN (3.3)	MeCN	i) reflux	i) 19	6.0	decomposition
	ii) <i>t</i> -BuOK (5.1)		ii) rt to reflux	ii) 3		
2	i) CAN (4.4)	i) MeCN	i) reflux	i) 2	3.9	decomposition
	ii) <i>t</i> -BuOK (14)	ii) THF	ii) rt	ii) 3		
3	ZnBr <sub>2</sub> (7.6)	CH <sub>2</sub> Cl <sub>2</sub>	rt	21	21	no reaction
4	TMSI (9.8)	MeCN	0	1	10	decomposition
5	i) BF <sub>3</sub> •OEt <sub>2</sub> (24)	THF	i) 0 to reflux	i) 2	10	<b>212</b> (<71%) <sup>a</sup>
	ii) <i>t</i> -BuOK (120)		ii) reflux	ii) 0.5		
6	i) BF <sub>3</sub> •OEt <sub>2</sub> (6.0)	PhMe	i) 0 to rt	i) 2	5.3	presumed <b>211</b> and <b>212</b> <sup>b</sup>
	ii) <i>t</i> -BuOK (53)		ii) rt to reflux	ii) 62		
7	i) BF <sub>3</sub> •OEt <sub>2</sub> (8.6)	i) CH <sub>2</sub> Cl <sub>2</sub>	i) 0 to rt	i) 2	9.4	<b>212</b> (71%)
	ii) <i>t</i> -BuOK (120)	ii) THF	ii) rt	iii) 3		

<sup>a</sup>With minor impurities. <sup>b</sup>Observed by TLC analysis

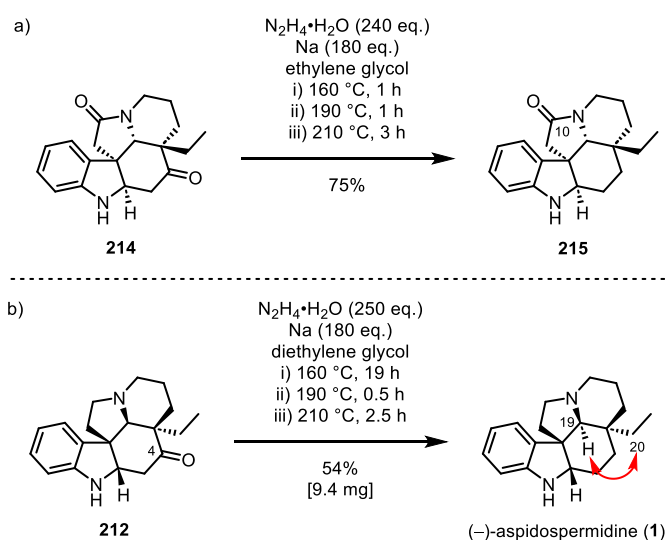
To circumvent the presumed competing coordination of the THF to the BF<sub>3</sub>•OEt<sub>2</sub>, the reaction solvent was changed to PhMe as a non-coordinating solvent in which *t*-BuOK is soluble (Table 16, entry 6).<sup>[234]</sup> Notably, the complete conversion of *N*-Boc *endo*-enone **173** occurred at room temperature. Upon addition of *t*-BuOK, a product with the same R<sub>f</sub> value as tetracycle **211** was

## Results and Discussion

observed. However, complete conversion of the presumed tetracycle **211** to pentacycle **212** was not observed upon addition of excess base, which eventually resulted in solubility issues, nor upon prolonged heating under reflux. Finally, the Boc-deprotection with  $\text{BF}_3 \cdot \text{OEt}_2$  was performed in  $\text{CH}_2\text{Cl}_2$ , as a non-coordinating solvent. The solvent was then to be exchanged for THF, due to the high solubility of *t*-BuOK therein, which was crucial due to the use of excess base. Complete conversion of the *N*-Boc *endo*-enone **173** was observed under these conditions (Table 16, entry 7). The  $\text{CH}_2\text{Cl}_2$  solvent was removed under reduced pressure. The residue was then dissolved in THF and excess *t*-BuOK was added to the reaction mixture. Pleasingly, the desired pentacycle **212** was obtained in a yield of 71%—which was higher than the yield of 56% over two steps when the ring-closures were performed separately. Gratifyingly, both the *aza*-Michael addition and intramolecular enolate alkylation reactions proceeded with high diastereoselectivity, when performed over one- or two-steps, due to the high substrate-induced stereocontrol.

### 3.8 Deoxygenation

For the final step in the synthesis to aspidospermidine (**1**)—the deoxygenation—a Wolff–Kishner reduction was envisaged. The Huang–Minlon modification of the Wolff–Kishner reduction was applied for deoxygenation of the ketone **214** to give 10-oxo-aspidospermidine (**215**) in the penultimate step of the synthesis of (+)-aspidospermidine (**1**) by Marino and co-workers (Scheme 83a).<sup>[86,104]</sup> Based on these conditions, the deoxygenation of 4-oxo-aspidospermidine (**212**) was performed to yield (–)-aspidospermidine (**1**) in a yield of 54% (Scheme 83b). In our reaction, diethylene glycol was used as the reaction solvent in place of ethylene glycol, as the boiling point of ethylene glycol of 197 °C<sup>[235]</sup> is lower than the temperature of 210 °C that was used in the N<sub>2</sub> liberation step in the method reported by Marino and co-workers.<sup>[236]</sup> Whereas the boiling point of diethylene glycol is 245 °C.<sup>[237]</sup>



Scheme 83. Wolff–Kishner reduction: a) of ketone **214** as reported by Marino and co-workers in the synthesis of (+)-aspidospermidine (**1**);<sup>[86]</sup> b) of 4-oxo-aspidospermidine (**212**) to furnish (–)-aspidospermidine (**1**).

The spectroscopic data of the obtained aspidospermidine (**1**) were in accordance with reported values (Table 17 and Table 18).<sup>[86]</sup> Furthermore, from analysis of the NOESY spectrum of the final product (**1**), the strongest NOE correlation was observed between H19 and to one H20, which suggested *cis* stereochemistry between H19 and the ethyl group (Scheme 83). Interestingly, from measurement of the optical rotation value ( $[\alpha]_D^{20} -17$  (*c* 0.065, CHCl<sub>3</sub>), lit.<sup>[86]</sup>  $[\alpha]_D^{20} +20.5$  (*c* 0.6, CHCl<sub>3</sub>)) it was determined that the unnatural enantiomer of aspidospermidine (**1**) had been synthesised. Therefore, as discussed in section 3.4.2, it was not

## Results and Discussion

possible to extrapolate the stereochemical results from the related Pd-catalysed allylic substitution method reported by Trost and co-workers to our system.<sup>[96]</sup>

In conclusion, (–)-aspidospermidine (**1**) was synthesised in seven linear steps from commercially available starting materials; this represents the shortest enantioselective synthesis of aspidospermidine (**1**) reported to date. Moreover, this synthesis has a high efficiency with three construction steps (one-pot alkylation and Boc-protection of tryptamine (**8**); one-pot allylic substitution and cyclisation with tryptamine derivative **94**; and one-pot ring-closing sequence of *endo*-enone **173**), two strategic redox reactions (1,4-hydrosilylation of **170** and Wolff–Kishner reduction of pentacycle **212**) and only two concession steps (*N*-Boc protection of indoline **166** and Nicolaou oxidation of **196**). This resulted in an overall ideality of 71% for our synthetic route to aspidospermidine (**1**).<sup>[238]</sup> In this synthesis, the herein developed enantioselective Pd-catalysed allylic substitution reaction acted as the key stereo defining step. The remaining three stereocentres of the natural product were then established under substrate-induced stereocontrol. This work represents not only the first application of a Pd-catalysed allylic substitution reaction with a 3-substituted indole derivative in the synthesis of aspidospermidine (**1**) but more broadly of *Aspidosperma* alkaloids.

Table 17. Comparison of synthetic aspidospermidine (**1**) <sup>1</sup>H NMR data

Entry	Marino's Synthetic (+)- <b>1</b> [ppm] (500 MHz) <sup>[86]</sup>	Our Synthetic (-)- <b>1</b> [ppm] (600 MHz)	$\Delta\delta$ ( $\delta_{\text{ours}} - \delta_{\text{Marino's}}$ ) [ppm] <sup>1</sup>
<b>1</b>	7.09 (d, $J = 7.5$ Hz, 1H)	7.08 (dd, $J = 7.4, 1.3$ Hz, 1H)	-0.01
<b>2</b>	7.03 (t, $J = 7.5$ Hz, 1H)	7.01 (ddd, $J = 7.6, 7.6, 1.3$ Hz, 1H)	-0.02
<b>3</b>	6.74 (t, $J = 7.2$ Hz, 1H)	6.73 (ddd, $J = 7.4, 7.4, 1.0$ Hz, 1H)	-0.01
<b>4</b>	6.65 (d, $J = 7.5$ Hz, 1H)	6.64 (d, $J = 7.7$ Hz, 1H)	-0.01
<b>5</b>	3.52 (dd, $J = 11, 7.0$ Hz, 1H)	3.51 (dd, $J = 11.1, 6.2$ Hz, 1H)	-0.01
<b>6</b>	3.15 – 3.12 (m, 1 H)	3.16 – 3.09 (m, 1H)	—
<b>7</b>	3.08 (br d $J = 10.5$ Hz, 1H)	3.08 – 3.02 (m, 1H)	—
<b>8</b>	2.35 – 2.22 (m, 2H)	2.34 – 2.23 (m, 2H)	—
<b>9</b>	2.24 (s, 1H)	2.22 (s, 1H)	-0.02
<b>10</b>	1.99 – 1.92 (m, 2H)	2.00 – 1.90 (m, 2H)	—
<b>11</b>	1.81 – 1.71 (m, 1H)	1.79 – 1.68 (m, 1H)	—
<b>12</b>	1.68 – 1.62 (m, 2H)	1.67 – 1.59 (m, 2H)	—
<b>13</b>	1.54 – 1.47 (m, 2H)	1.55 – 1.43 (m, 3H)	—
<b>14</b>	1.42 – 1.36 (m, 1H)	1.39 (dddd, $J = 14.4, 13.2, 11.1, 3.6$ Hz, 1H)	—
<b>15</b>	1.26 (m, 1 H)	1.11 (td, $J = 13.6, 13.6, 4.7$ Hz, 1H)	—
<b>16</b>	1.16 – 1.05 (m, 1H)	1.06 (ddd, $J = 13.5, 3.7$ Hz, 1H)	—
<b>17</b>	0.92 – 0.84 (m, 1H)	0.92 – 0.82 (m, 1H)	—
<b>18</b>	0.64 (t, $J = 6.6$ Hz, 3H)	0.64 (dd, $J = 7.5, 7.5$ Hz, 3H)	0

<sup>1</sup> A systematic shift is present. Our spectra were referenced using the residual solvent peak of CDCl<sub>3</sub> at 7.26 ppm.

Table 18. Comparison of natural and synthetic aspidospermidine (**1**) <sup>13</sup>C NMR data

<b>Entry</b>	<b>He's Natural (+)-1 [ppm] (125 MHz)<sup>[239]</sup></b>	<b>Marino's Synthetic (+)-1 [ppm] (125 MHz)<sup>[86]</sup></b>	<b>Our Synthetic (-)-1 [ppm] (151 MHz)</b>	<b><math>\Delta\delta</math> (<math>\delta_{\text{ours}} - \delta_{\text{natural}}</math>)<sup>2</sup> [ppm]</b>	<b><math>\Delta\delta</math> (<math>\delta_{\text{ours}} - \delta_{\text{Marino's}}</math>) [ppm]</b>
<b>1</b>	149.3	149.6	149.6	0.3	0
<b>2</b>	135.6	135.9	135.9	0.3	0
<b>3</b>	127.0	127.3	127.2	0.2	-0.1
<b>4</b>	122.7	123.0	123.0	0.3	0
<b>5</b>	118.8	119.2	119.1	0.3	-0.1
<b>6</b>	110.1	110.6	110.5	0.4	-0.1
<b>7</b>	71.1	71.5	71.4	0.3	-0.1
<b>8</b>	65.4	65.9	65.8	0.4	-0.1
<b>9</b>	53.7	54.1	54.0	0.3	-0.1
<b>10</b>	52.9	53.9	53.5	0.6	-0.4
<b>11</b>	52.9	53.2	53.2	0.3	0
<b>12</b>	38.7	39.0	39.0	0.3	0
<b>13</b>	35.5	35.8	35.8	0.3	0
<b>14</b>	34.3	34.7	34.6	0.3	-0.1
<b>15</b>	29.8	30.2	30.1	0.3	-0.1
<b>16</b>	28.1	28.3	28.3	0.2	0
<b>17</b>	23.0	23.2	23.2	0.2	0
<b>18</b>	21.6	22.0	21.9	0.3	-0.1
<b>19</b>	6.6	7.0	7.0	0.4	0

<sup>2</sup> A systematic shift is present. Our spectra were referenced using the solvent peak of CDCl<sub>3</sub> at 77.16 ppm.

## 4 Summary and Outlook

### 4.1 Summary

The aim of this work was to apply an enantioselective Pd-catalysed allylic substitution reaction with a 3-substituted indole derivative—for the first time—in the total synthesis of aspidospermidine (**1**).

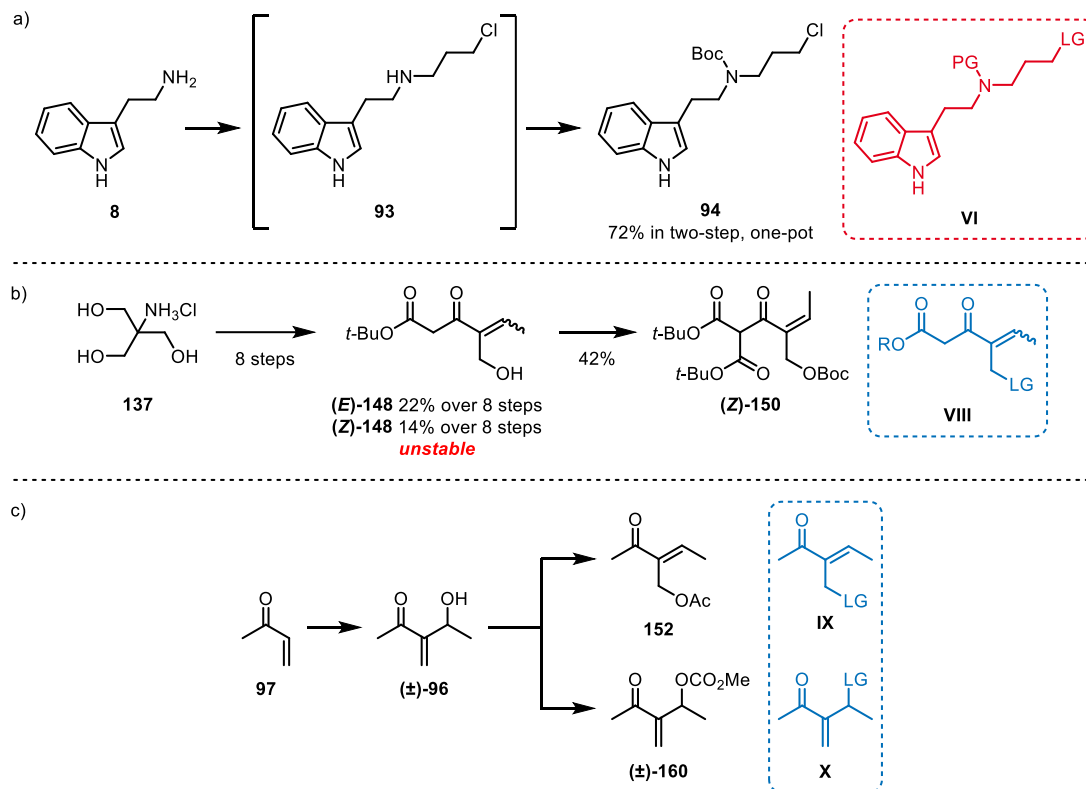
This work commenced with preparation of the substrates for the allylic substitution reaction. The tryptamine derivative **94** was prepared in a modified one-pot procedure by a mono-alkylation and *N*-Boc protection of tryptamine (**8**) (Scheme 84a). The  $\beta$ -keto esters **148**, which were the proposed allylic alkylation substrates in strategy 1, were finally obtained over 8 steps, featuring a Wittig olefination and aldol addition reactions (Scheme 84b). Although the  $\beta$ -keto esters **148** could have been used as unactivated allylic alkylation substrates, the carbonate derivative **150** was also prepared as an activated allylic alkylation substrate. Unfortunately, the  $\beta$ -keto esters **148** were unstable. Due to the instability and long syntheses of the  $\beta$ -keto esters **148**, an alternative strategy was sought. In strategy 2, the  $\alpha,\beta$ -unsaturated ketones **96**, **152** and **160** were prepared as the allylic alkylation substrates using Morita–Baylis–Hillman and  $S_N2'$  Mitsunobu reactions (Scheme 84c).

From screening of the allylic substitution reaction with the tryptamine derivative **94** and the allylic alkylation substrates **96**, **152** and **160** under non-stereoselective conditions, both the allylic alcohol **96** and allylic acetate **152** were shown to afford the (*E*)-indolenine product **164** (Scheme 85a). The allylic alcohol **96** was determined to be the allylic alkylation substrate best suited for our strategy, due to the ease of its preparation and delivering the indolenine **164** in the highest yield.

From screening studies of the allylic substitution reaction with chiral ligands, it was found that the Trost ligands DACH-phenyl **L3** and DACH-naphthyl **L4** both afforded the enantioenriched indolenine **164**, with the DACH-phenyl **L3** ligand giving the indolenine **164** in the highest yield (Scheme 85b). From optimisation studies, the enantioselectivity of the transformation was shown to increase upon increasing the steric bulk of the borane additive from  $\text{Et}_3\text{B}$  to 9-BBN-octyl (**165**) and by lowering the reaction temperature from 50 °C to room temperature. Interestingly, formation of the indolenine product **164** was only observed when the reaction was performed in THF. The indolenine **164** was finally obtained with high enantioselectivity (e.r. 91:9) and in a reasonable yield of 42%. Furthermore, the allylic substitution reaction was shown to proceed with excellent chemo- and regioselectivity. It is worth noting that this key

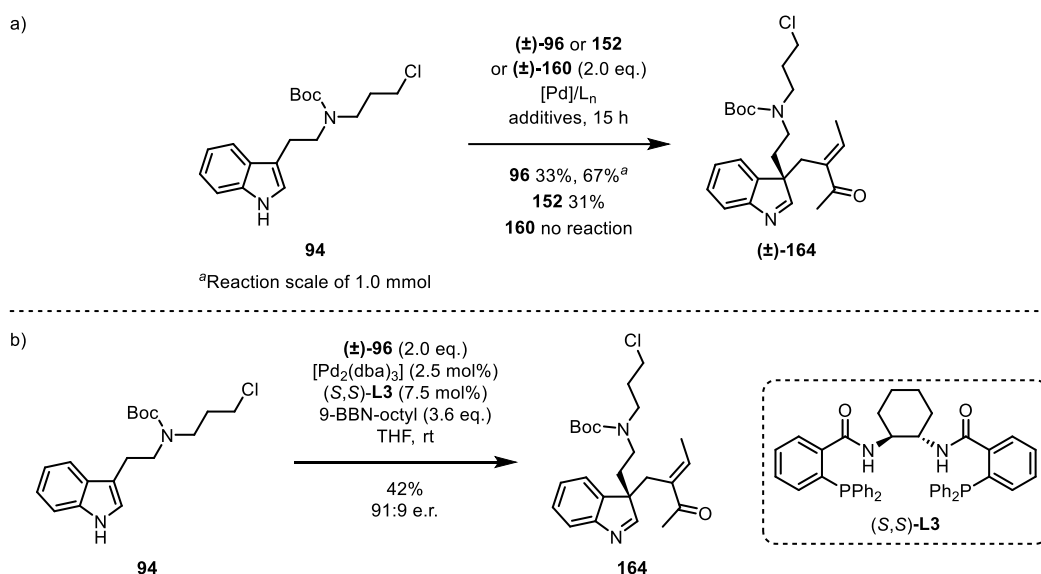
## Summary and Outlook

step of the synthesis not only constructed the stereo dictating quaternary carbon stereocentre, but also assembled the entire framework of aspidospermidine (**1**).



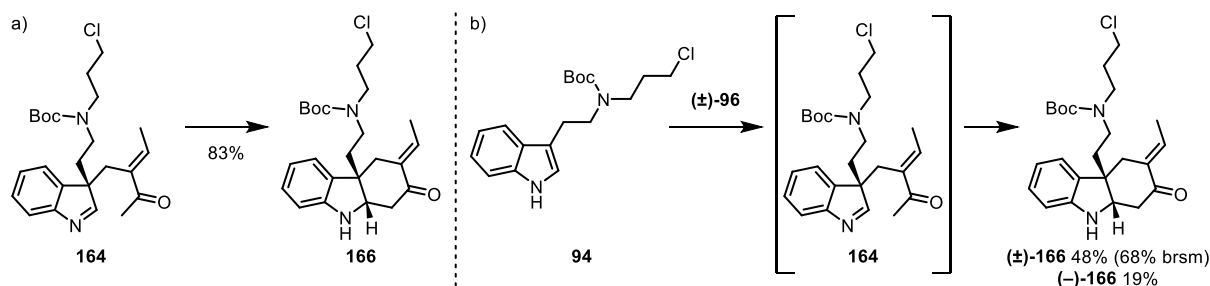
Scheme 84. Preparation of substrates for the allylic substitution reaction: a) tryptamine derivative **94**; b)  $\beta$ -keto esters **148** and **150**; c)  $\alpha,\beta$ -unsaturated ketones **96**, **152** and **160**.

## Summary and Outlook



Scheme 85. Pd-catalysed allylic substitution reaction with tryptamine derivative **94**: a) screening of allylic alkylation substrates **96**, **152** and **160** under non-stereoselective conditions; b) optimised enantioselective reaction conditions with allylic alkylation substrate **96**.

A highly diastereoselective intramolecular Mannich reaction of indolenine **164** afforded the *cis*-fused tricycle **166** (Scheme 86a). The allylic substitution and Mannich reaction could also be performed as a one-pot process (Scheme 86b), albeit with diminished yield.

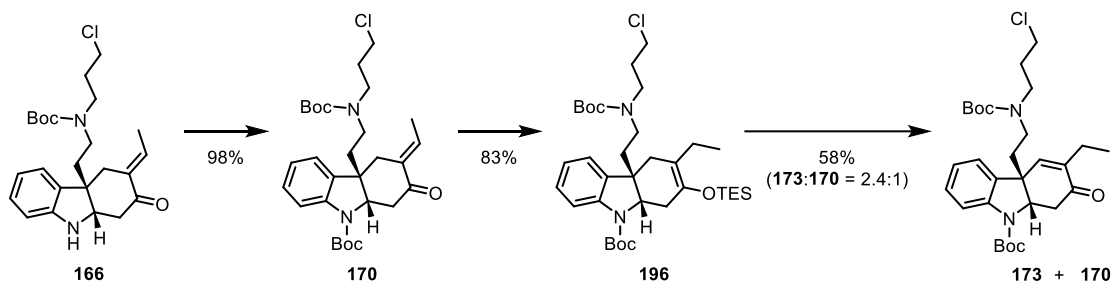


Scheme 86. Intramolecular Mannich reaction to afford the *cis*-fused tricycle **166**: a) from indolenine **164**; b) from tryptamine derivative **94** in a one-pot allylic substitution cyclisation sequence.

The ensuing *exo*-to-*endo* double bond migration presented a significant challenge. Direct double bond migration methods from the *exo*-enone **166** and *N*-Boc *exo*-enone **170** were unsuccessful. An IBX-mediated Nicolaou oxidation and an  $\alpha$ -substitution- $\beta$ -elimination strategy from the saturated ketone **169** both afforded the undesired *endo*-enone **171**. A Saegusa–Ito oxidation from the thermodynamic silyl enol ether was then envisioned. The

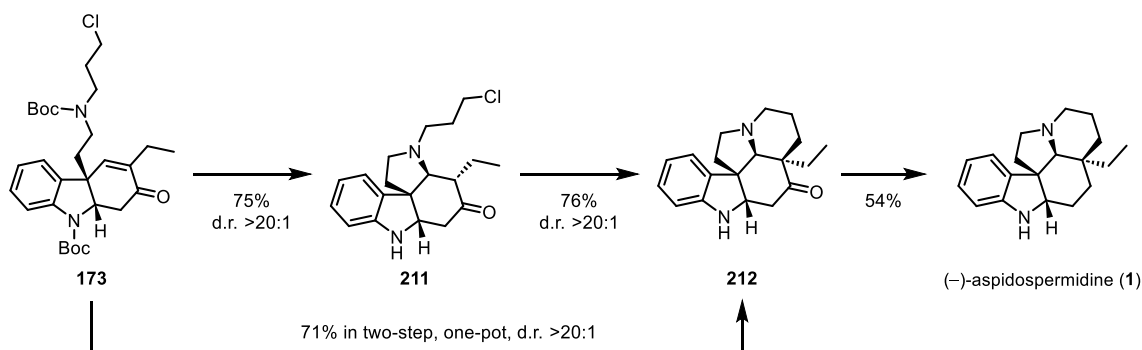
## Summary and Outlook

thermodynamic silyl enol ether could not be obtained from the saturated ketone **169**, but rather from a 1,4-hydrosilylation of the *N*-Boc *exo*-enone **170** (Scheme 87). Unfortunately, none of the Saegusa–Ito oxidation protocols applied with the silyl enol ether **196** afforded the desired *endo*-enone **173**. Finally, a Nicolaou oxidation with the silyl enol ether **196** gave the desired *N*-Boc *endo*-enone **173**.



Scheme 87. *Exo*-to-*endo* double bond migration sequence, via a 1,4-hydrosilylation and Nicolaou oxidation.

*N*-deprotection and concomitant *aza*-Michael addition proceeded in the presence of trifluoroacetic acid, furnishing the *cis*-fused tetracyclic product **211** (Scheme 88). The *cis*-fused E ring in pentacycle **212** was installed by an intramolecular enolate alkylation using *t*-BuOK. The *D/E* ring closures could also be performed as a one-pot transformation. In which, the deprotection was performed with  $\text{BF}_3 \cdot \text{OEt}_2$  and subsequent addition of *t*-BuOK induced the ring-closing sequence, affording pentacycle **212** in a yield of 71% from *endo*-enone **173**—which was higher than the yield of 56% over the two separate steps. Gratifyingly, both the *aza*-Michael addition and intramolecular enolate alkylation reactions proceeded with high diastereoselectivity, when performed over one- or two-steps, due to the high substrate-induced stereocontrol. A final Wolff–Kishner reduction yielded (–)-aspidospermidine (**1**).



Scheme 88. Ring-closing sequence and Wolff–Kishner reduction to yield (–)-aspidospermidine (**1**).

## Summary and Outlook

In conclusion, this work herein represents the first application of a Pd-catalysed allylic substitution reaction with a 3-substituted indole derivative in the synthesis of aspidospermidine (**1**) and more broadly of *Aspidosperma* alkaloids. From investigation into the key Pd-catalysed allylic substitution reaction, a new class of allylic alkylation substrates for use with 3-substituted indole derivatives was uncovered, namely the Morita–Baylis–Hillman adducts and derivatives thereof. Although the use of allylic carbonates and acetates derived from Morita–Baylis–Hillman adducts have been reported as allylic alkylation substrates with other nucleophiles; they have not been reported in Pd-catalysed allylic substitution reactions with 3-substituted indole derivatives. Thus, this work expands the scope of the Pd-catalysed allylic substitution methodology. The allylic substitution reaction was initially developed in a racemic manner and then rendered enantioselective (e.r. of 91:9). In our pathway to (–)-aspidospermidine (**1**), the allylic substitution acted as the key stereo defining step. The remaining stereocenters of the natural product were then established under substrate control. This culminated in the shortest enantioselective synthesis of aspidospermidine (**1**) reported to date, over seven linear steps from commercially available starting materials. It is envisioned that this novel strategy could be employed for efficient enantioselective syntheses of other members of the *Aspidosperma* alkaloid family and related polycyclic natural products.

## 4.2 Outlook

Since the enantioselective synthesis of aspidospermidine (**1**) by the proposed Pd-catalysed allylic substitution strategy with a 3-substituted indole derivative was accomplished, the aim of this work achieved. However, there remains areas for future work.

Further optimisation of the allylic substitution reaction, in terms of the yield and enantioselectivity, could be performed. In the allylic substitution reaction, the stereocentre is created on the nucleophile, therefore methods to increase the enantioselectivity of this transformation would have to address the facial selectivity of the prochiral nucleophile. Methods to increase the stereoselectivity of the allylic substitution when the stereocentre is generated on the electrophilic allylic alkylation substrate, such as the addition of halide ions,<sup>[106,113,114]</sup> would not be expected to influence the enantioselectivity of our system. Nonetheless, other chiral ligands could be explored, for example phosphoramidite ligands **L7**–**9** and **L11**, which have been reported with activated allylic alkylation substrates with 3-substituted indole derivatives (Figure 10).<sup>[97,98,149,150]</sup> Notably, Wang and co-workers had recently reported the use of phosphoramidite ligand (*S,R,R*)-**L11** with unactivated allylic alcohols.<sup>[150]</sup> Since, applying the hemilabile Carreira phosphoramidite olefin ligand (*R*)-**L2** in our system did not afford the indolenine product **164**, phosphoramidite ligands **L8** and **L11** may be a more suitable option for our system rather than hemilabile phosphoramidite olefin ligands **L2**, **L7** and **L9**. Furthermore, PHOX-based ligands such as (*S,S<sub>p</sub>*)-**L10**, as reported by You and co-workers, could also be investigated.

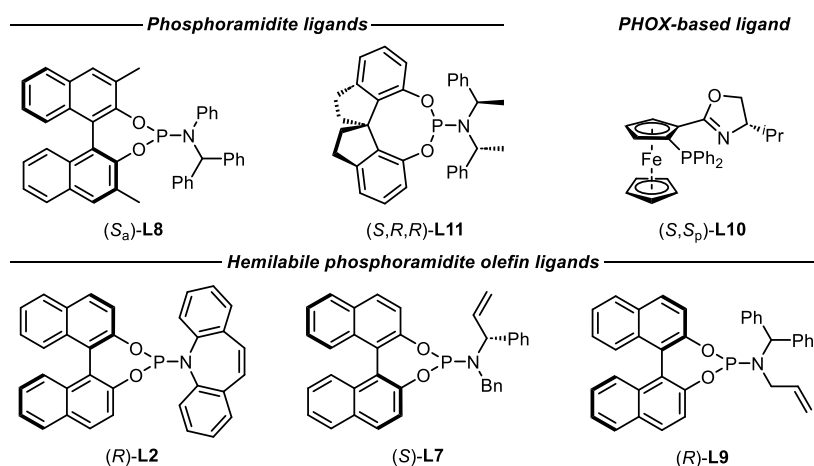


Figure 10. Chiral ligands that could be tested in the enantioselective allylic substitution reaction.

## Summary and Outlook

The use of chiral boranes, such as Alpine-borane<sup>®</sup> (**216**) or diisopinocampheylborane (**217**) (Figure 11), could also be considered. Notably, the use of chiral boranes in Pd-catalysed allylic substitution reactions with 3-substituted indole derivatives has not been reported. This may be due to steric bulk limitations of the borane. As Trost and co-workers had reported that increasing the steric bulk of the borane additive from Et<sub>3</sub>B to 9-BBN-hexyl (**89**) was beneficial in terms of the yield and enantioselectivity of their Pd-catalysed allylic substitution reaction; however, further increasing the steric bulk of the borane additive to dicyclohexylborane-hexyl (**90**) was shown to be detrimental with respect to the yield and enantioselectivity while applying disiamylborane-hexyl (**91**) was found to inhibit the reaction altogether.<sup>[96]</sup>

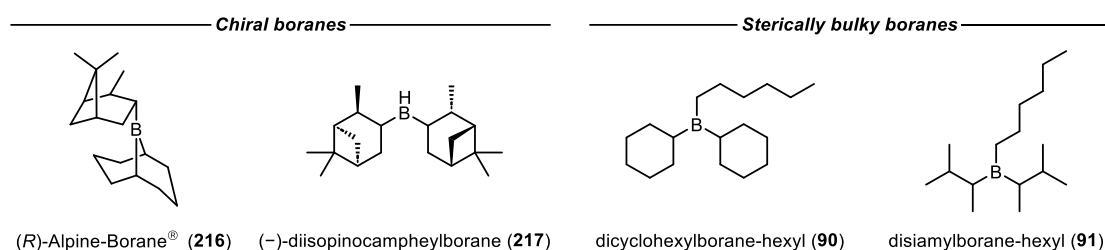
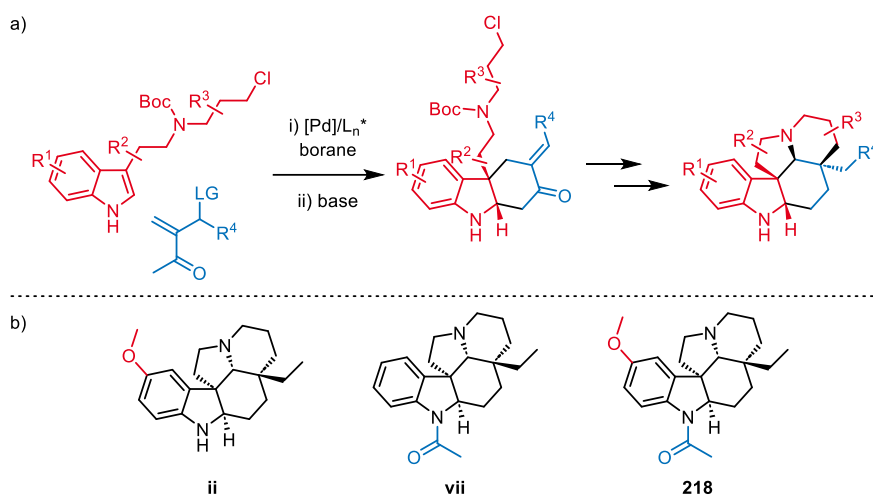


Figure 11. Chiral boranes that could be applied in the allylic substitution reaction and sterically bulky boranes employed by Trost and co-workers in their related system.<sup>[96]</sup>

The substrate scope of the allylic substitution reaction could be investigated in terms of tryptamine derivatives as well as Morita–Baylis–Hillman adducts (Scheme 89a). This could result in the efficient syntheses of aspidospermidine derivatives, whose biological activities could be evaluated. In the study by Zèches-Hanrot and co-workers investigating the antiplasmodial activity of (+)-aspidospermidine (**1**) and derivatives thereof against two strains of *Plasmodium falciparum*, compounds **vii** and **ii** were found to have the lowest IC<sub>50</sub> values and hence higher antiplasmodial activities against a chloroquine-resistant strain of *P. falciparum* after 24 and 72 hours, respectively (Scheme 89b). Therefore, derivative **218**, which combines the 5-methoxy substituent of compound **ii** with the *N*-acetyl substituent of compound **vii**, could be synthesised to determine whether these substituents have additive effects with respect to their antiplasmodial activities against the chloroquine-resistant strain of *P. falciparum*. Furthermore, derivative **218** is a novel compound. Notably the (*S,S*)-configured Trost ligands would be required in the allylic substitution reaction to establish the correct absolute stereochemistry of derivative **218**.

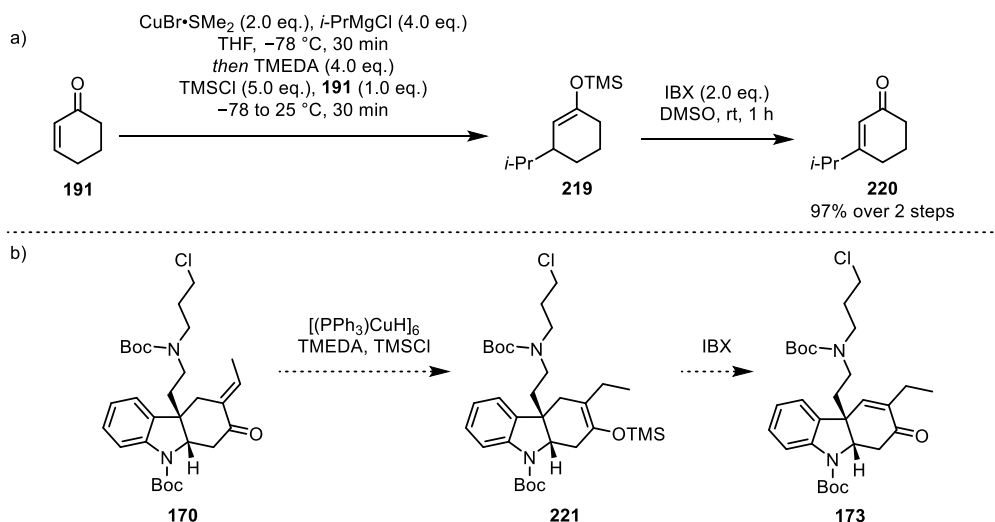
## Summary and Outlook



Scheme 89. a) Tryptamine derivatives and Morita–Baylis–Hillman adducts for the synthesis of aspidospermidine derivatives. b) Aspidospermidine derivatives **ii** and **vii** with antiparasitic activity against a chloroquine-resistant strain of *P. falciparum* and potential target compound **218** for evaluation of its antiparasitic activity.

Finally, an alternative method for the *exo*-to-*endo* double bond migration based upon a cascade reaction reported by Nicolaou and co-workers could be attempted. Nicolaou and co-workers reported that the conjugate addition of cuprate reagents to enones followed by trapping of the *in situ* generated copper enolate with TMSCl gave the trimethylsilyl enol ethers (Scheme 90a). The isolated trimethylsilyl enol ethers were then oxidised to the 4-substituted enones by the IBX-mediated Nicolaou oxidation.<sup>[224]</sup> It is proposed that Stryker's reagent, [(PPh<sub>3</sub>)CuH]<sub>6</sub>, could be used for hydride addition at the 4-position of *exo*-enone **170**, followed by trapping of the thermodynamic enolate with TMSCl, to afford the trimethylsilyl enol ether **221** (Scheme 90b). A Nicolaou oxidation is then proposed to furnish the *endo*-enone **173**. It is expected that prior *N*-Boc protection would still be required, otherwise coordination of the indoline nitrogen atom to the IBX (**183**) could result in a slower oxidation rate relative to the competing hydrolysis of the silyl enol ether.<sup>[224]</sup> The thermodynamic trimethylsilyl enol ether **221** generated by this method could also be submitted to Saegusa–Ito protocols, to determine whether the unreactivity of the triethylsilyl enol ether **196** under the applied Saegusa–Ito protocols was due to the difference between the triethyl and trimethyl substituents. As trimethylsilyl enol ethers are far more commonly employed in Saegusa–Ito reactions.<sup>[214]</sup>

## Summary and Outlook



Scheme 90. Alternative *exo*-to-*endo* double bond migration strategy via conjugate addition of cuprate reagents to enones, followed by trapping of the *in situ* generated enolate as a silyl enol ether and a subsequent Nicolaou oxidation: a) as reported by Nicolaou and co-workers with 2-cyclohexen-1-one (**191**);<sup>[224]</sup> b) as proposed for the double bond migration from *exo*-enone **170** to *endo*-enone **173**.

## 5 Experimental

### 5.1 General Experimental Conditions

#### Experimental Procedures, Glassware and Reagents

Unless otherwise stated, non-aqueous reactions were performed under anhydrous conditions, under a positive pressure of dry nitrogen and the glassware was dried with a heat gun. All reagents and solvents were purchased from commercially available sources and were used without further purification unless stated otherwise. The solvents that were used for flash chromatography were purified by distillation under reduced pressure prior to use, with the exception of PhMe and Et<sub>3</sub>N, which were directly used.

#### Chromatography

Reactions were monitored by thin-layer chromatography (TLC), using preconditioned plates (Macherey–Nagel ALUGRAM<sup>®</sup> Xtra SIL G UV254 or Merck Supelco TLC Aluminium oxide 60 F<sub>254</sub>, neutral). Visualisation was affected by quenching of UV fluorescence ( $\lambda_{254}$  nm) and by staining with standard solutions of KMnO<sub>4</sub> and cerium molybdate followed by heating. Flash chromatography was performed using SiliaFlash<sup>®</sup> Silica Gel (particle size 40–63  $\mu$ m) or Merck Millipore Aluminium oxide 90 active neutral (particle size 63–200  $\mu$ m).

#### Nuclear Magnetic Resonance (NMR)

<sup>1</sup>H NMR spectra were recorded at 300 MHz, 400 MHz, 500 MHz or 600 MHz using a Bruker AVANCE I 400, Bruker AVANCE II 400, Bruker AVANCE III HD 400, Bruker AVANCE I 500 or Bruker AVANCE III HD 600 spectrometer, respectively. Spectra were referenced using residual solvent peaks (CDCl<sub>3</sub> = 7.26 ppm, CD<sub>3</sub>OD = 3.31 ppm and DMSO-d<sub>6</sub> = 2.50 ppm). Coupling constants (*J*) are quoted to the nearest 0.1 Hz. Assignment of proton signals was assisted by <sup>1</sup>H-<sup>1</sup>H COSY, HSQC and HMBC experiments. Assignment of stereochemistry was assisted by NOESY experiments. <sup>13</sup>C NMR spectra were recorded at 101 MHz or 151 MHz using a Bruker AVANCE I 400, Bruker AVANCE II 400, Bruker AVANCE III HD 400 or Bruker AVANCE III HD 600 spectrometer, respectively. Spectra were referenced using solvent peaks (CDCl<sub>3</sub> = 77.16 ppm, CD<sub>3</sub>OD = 49.00 ppm and DMSO-d<sub>6</sub> = 39.52 ppm). Peaks are generally reported to one decimal place. Assignment of carbon signals was assisted by HSQC and HMBC experiments.

### **Infrared Spectra (IR)**

Infrared spectra were recorded using a Bruker ALPHA-P FT-IR spectrometer as thin film samples, with Diamant-ATR. Absorption maxima ( $\nu_{\max}$ ) are quoted in wavenumbers ( $\text{cm}^{-1}$ ).

### **Mass Spectrometry**

Mass spectra were recorded on a Thermo ISQ LT EI instrument using Electron Ionisation Gas Chromatography Mass Spectrometry (EI-GCMS) and Electron Ionisation Direct Insertion Probe (EI-DIP). High resolution mass spectra were recorded on an Agilent 6224 ESI-TOF instrument using Electrospray Ionisation (ESI<sup>+</sup>).

### **Melting Point**

Melting points were measured on a Büchi Melting Point M-565 instrument.

### **Chiral HPLC**

Analytical chiral HPLC was conducted using an Agilent 1260 Infinity II system with a Chiralpak AD-H column.

### **Optical Rotation**

Optical rotations were measured using an A. Krüss GmbH P8000 Polarimeter, at 589 nm (sodium D line) and 20 °C with a cell path length of 1 dm and concentrations ( $c$ ) reported in g/100 mL. Specific rotations are denoted as: ( $c$  in g/100 mL, solvent)  $[\alpha]_{\text{D}}^{20}$ .

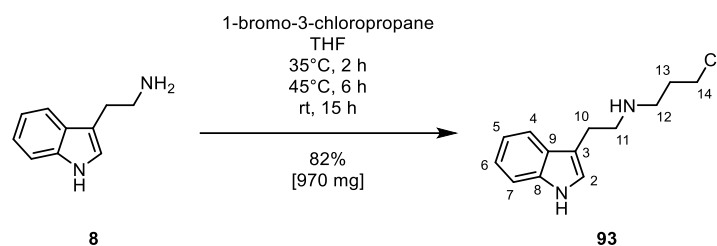
## Experimental

### 5.2 Synthetic Procedures

The numbering of carbon atoms shown in the schemes in the experimental section is not necessarily according to IUPAC nomenclature but instead for assignment purposes.

#### Preparation of Compound **93**

Compound **93** was prepared according to a literature procedure.<sup>[152]</sup>



Tryptamine (**8**) (1.7 g, 11 mmol) was added to a flask, followed by THF (20 mL) and 1-bromo-3-chloropropane (0.50 mL, 5.0 mmol). The resulting mixture was stirred at 35 °C for 2 h, followed by stirring at 45 °C for 6 h and then at room temperature for 15 h. The reaction mixture was quenched with water and concentrated under reduced pressure. The residue was taken up in EtOAc and the resulting mixture was acidified to *ca* pH 2 with aq. HCl (6.0 M) at 0 °C. The aqueous layer was washed with Et<sub>2</sub>O to remove unreacted 1-bromo-3-chloropropane. The aqueous layer was then basified to *ca* pH 12 with aq. NaOH (2.0 M) at 0 °C. The aqueous layer was extracted with EtOAc. The combined organic extracts were dried over brine, MgSO<sub>4</sub>, filtered and concentrated under reduced pressure. The crude material was purified by flash chromatography (EtOAc/MeOH/Et<sub>3</sub>N, 100:3:1) to afford *N*-(2-(1*H*-indol-3-yl)ethyl)-3-chloropropan-1-amine (**93**) as a pale brown oil (970 mg, 4.1 mmol, 82%).

The obtained spectroscopic data matched literature values.<sup>[152]</sup>

**R<sub>f</sub>** = 0.53 (EtOAc/MeOH/Et<sub>3</sub>N, 100:3:1);

**<sup>1</sup>H NMR** (500 MHz, CDCl<sub>3</sub>) δ 8.10 (s, 1H, N–H<sub>1</sub>), 7.63 (dd, <sup>3</sup>*J*<sub>4,5</sub> = 7.7 Hz, <sup>4</sup>*J*<sub>4,6</sub> = 1.1 Hz, 1H, H<sub>4</sub>), 7.37 (dd, <sup>3</sup>*J*<sub>6,7</sub> = 8.1 Hz, <sup>4</sup>*J*<sub>5,7</sub> = 0.9 Hz, 1H, H<sub>7</sub>), 7.20 (ddd, <sup>3</sup>*J*<sub>6,7</sub> = 8.1 Hz, <sup>3</sup>*J*<sub>5,6</sub> = 7.0 Hz, <sup>4</sup>*J*<sub>4,6</sub> = 1.2 Hz, 1H, H<sub>6</sub>), 7.12 (ddd, <sup>3</sup>*J*<sub>4,5</sub> = 8.0 Hz, <sup>3</sup>*J*<sub>5,6</sub> = 7.0 Hz, <sup>4</sup>*J*<sub>5,7</sub> = 1.1 Hz, 1H, H<sub>5</sub>), 7.06 (d,

## Experimental

$^3J_{N-H_{1,2}} = 2.3$  Hz, 1H, H<sub>2</sub>), 3.58 (t,  $^3J_{13,14} = 6.5$  Hz, 2H, H<sub>14</sub>), 3.03 – 2.99 (m, 4H, H<sub>10,11</sub>)<sup>3</sup>, 2.82 (t,  $^3J_{12,13} = 6.9$  Hz, 2H, H<sub>12</sub>), 1.96 (p,  $^3J_{12,13} = 6.7$  Hz,  $^3J_{13,14} = 6.7$  Hz, 2H, H<sub>13</sub>) ppm;

**$^{13}C$  NMR** (126 MHz, CDCl<sub>3</sub>)  $\delta$  136.6 (C, C<sub>8</sub>), 127.5 (C, C<sub>9</sub>), 122.3 (CH, C<sub>6</sub>), 122.2 (CH, C<sub>2</sub>), 119.5 (CH, C<sub>5</sub>), 119.0 (CH, C<sub>4</sub>), 113.7 (C, C<sub>3</sub>), 111.3 (CH, C<sub>7</sub>), 49.9 (CH<sub>2</sub>, C<sub>11</sub>), 46.8 (CH<sub>2</sub>, C<sub>12</sub>), 43.1 (CH<sub>2</sub>, C<sub>14</sub>), 32.6 (CH<sub>2</sub>, C<sub>13</sub>), 25.6 (CH<sub>2</sub>, C<sub>10</sub>) ppm;

**HRMS** (ESI<sup>+</sup>) C<sub>13</sub>H<sub>17</sub>ClN<sub>2</sub>: 237.108 [M+H]<sup>+</sup> (calcd 237.12);

**IR** (thin film) 3307 (N–H), 2954, 2923, 2869, 2853, 1459, 1377, 740 (C–Cl) cm<sup>-1</sup>.

---

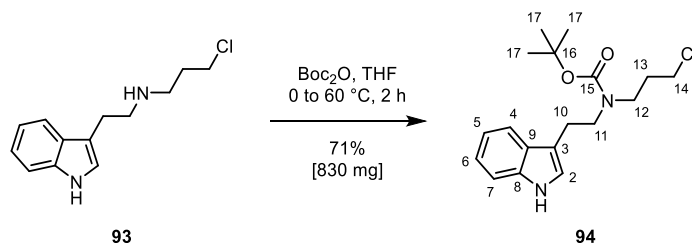
<sup>3</sup> Overlapping signals therefore not possible to accurately integrate, integrals shown are corrected.

## Experimental

### Preparation of Compound 94

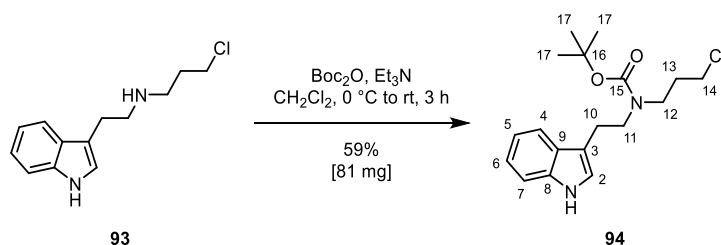
#### Method A

Compound **94** was prepared according to a literature procedure.<sup>[152]</sup>



Compound **93** (840 mg, 3.5 mmol) in THF (25 mL) was added to a flask. The resulting mixture was cooled to 0 °C and di-*tert*-butyl dicarbonate ( $\text{Boc}_2\text{O}$ ) (1.0 mL, 4.5 mol) in THF (10 mL) was added. The resulting mixture was stirred at 60 °C for 2 h. The reaction mixture was then concentrated under reduced pressure. The crude material was purified by flash chromatography (petroleum ether 40–65/ $\text{Et}_2\text{O}$ , 7:3) to afford *tert*-butyl (2-(1*H*-indol-3-yl)ethyl)(3-chloropropyl)carbamate (**94**) as a colourless, viscous oil (830 mg, 2.5 mmol, 71%).

#### Method B

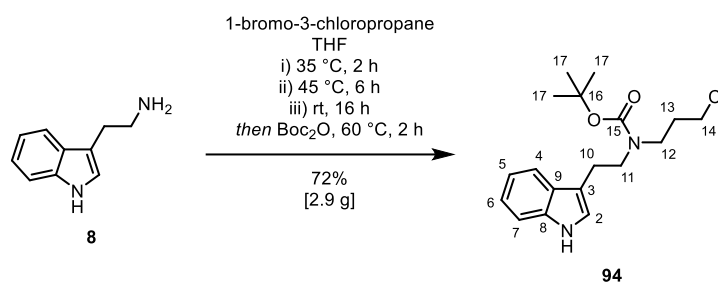


Compound **93** (97 mg, 0.41 mmol) in  $\text{CH}_2\text{Cl}_2$  (4.0 mL) was added to a flask. The resulting mixture was cooled to 0 °C and di-*tert*-butyl dicarbonate ( $\text{Boc}_2\text{O}$ ) (110 mg, 0.50 mmol) and  $\text{Et}_3\text{N}$  (0.1 mL, 0.72 mmol) were added to the flask. The resulting mixture was stirred at room temperature for 3 h. The reaction mixture was then concentrated under reduced pressure. The crude material was purified by flash chromatography (petroleum ether 40–65/ $\text{Et}_2\text{O}$ , 7:3) to afford *tert*-butyl (2-(1*H*-indol-3-yl)ethyl)(3-chloropropyl)carbamate (**94**) as a colourless, viscous oil (81 mg, 0.24 mmol, 59%).

## Experimental

### Method C

Compound **94** was prepared according to a modified literature procedure.<sup>[152]</sup>



Tryptamine (**8**) (4.4 g, 28 mmol) was added to a flask, followed by THF (50 mL) and 1-bromo-3-chloropropane (1.2 mL, 12 mmol). The resulting mixture was stirred at 35 °C for 2 h, then at 45 °C for 6 h and at room temperature for a further 16 h. The reaction mixture was diluted with THF (55 mL) and a solution of di-*tert*-butyl dicarbonate (Boc<sub>2</sub>O) (7.6 mL, 34 mol) in THF (10 mL) was added. The resulting mixture was stirred at 60 °C for 2 h. The reaction mixture was then concentrated under reduced pressure. The residue was taken up in EtOAc and washed with water. The aqueous layer was then extracted with EtOAc. The combined organic extracts were dried over brine, MgSO<sub>4</sub>, filtered and concentrated under reduced pressure. The crude material was purified by flash chromatography (petroleum ether 40–65/Et<sub>2</sub>O, 7:3) to afford *tert*-butyl (2-(1*H*-indol-3-yl)ethyl)(3-chloropropyl)carbamate (**94**) as a colourless oil (2.9 g, 8.6 mmol, 72%).

The obtained spectroscopic data matched literature values.<sup>[152]</sup>

**R<sub>f</sub>** = 0.32 (petroleum ether 40–65/Et<sub>2</sub>O, 7:3);

**<sup>1</sup>H NMR** (600 MHz, CDCl<sub>3</sub>) δ = δ 8.32 (s, 1H, N–H<sub>1</sub>), 7.66 (d, <sup>3</sup>J<sub>4,5</sub> = 7.0 Hz, 1H, H<sub>4</sub>), 7.36 (d, <sup>3</sup>J<sub>6,7</sub> = 7.1 Hz, 1H, H<sub>7</sub>), 7.21 (dd, <sup>3</sup>J<sub>5,6</sub> = 6.9 Hz, <sup>3</sup>J<sub>6,7</sub> = 6.9 Hz, 1H, H<sub>6</sub>), 7.17 – 7.11 (m, 1H, H<sub>5</sub>), 6.98 (s, 1H, H<sub>2</sub>), 3.53 (app. s, 4H, H<sub>11</sub>, H<sub>14</sub>), 3.42 – 3.26 (m, 2H, H<sub>12</sub>), 3.09 – 2.96 (m, 2H, H<sub>10</sub>), 2.07 – 1.91 (m, 2H, H<sub>13</sub>), 1.48 (app. d, 9H, H<sub>17</sub>)<sup>4</sup> ppm;

**<sup>13</sup>C NMR** (151 MHz, CDCl<sub>3</sub>) δ = 155.8 (C=O, C<sub>15</sub>)<sup>5</sup>, 155.7 (C=O, C<sub>15</sub>)<sup>5</sup>, 136.4 (C, C<sub>8</sub>), 127.5 (C, C<sub>9</sub>), 122.1 (CH, C<sub>6</sub>), 122.0 (CH, C<sub>2</sub>), 119.3 (CH, C<sub>5</sub>), 118.8 (CH, C<sub>4</sub>), 113.1 (C, C<sub>3</sub>), 111.3 (CH, C<sub>7</sub>), 79.8 (C–O, C<sub>16</sub>)<sup>5</sup>, 79.7 (C–O, C<sub>16</sub>)<sup>5</sup>, 48.7 (CH<sub>2</sub>, C<sub>11</sub>), 45.2 (CH<sub>2</sub>, C<sub>12</sub>)<sup>5</sup>, 45.1 (CH<sub>2</sub>,

<sup>4</sup> Peak in <sup>1</sup>H NMR spectrum is split in a 4:5 ratio due to the presence of *N*-Boc rotamers.

<sup>5</sup> Peaks in <sup>13</sup>C NMR spectrum are split due to the presence of *N*-Boc rotamers.

### *Experimental*

$C_{12})^5$ , 42.8 ( $CH_2, C_{14})^5$ , 42.5 ( $CH_2, C_{14})^5$ , 31.9 ( $CH_2, C_{13})^5$ , 31.5 ( $CH_2, C_{13})^5$ , 28.6 ( $CH_3, C_{17})^5$ , 28.5 ( $CH_3, C_{17})^5$ , 24.8 ( $CH_2, C_{10})^5$ , 24.1 ( $CH_2, C_{10})^5$  ppm;

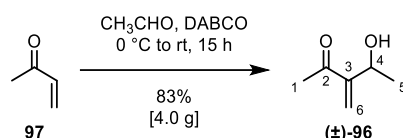
**HRMS** (ESI<sup>+</sup>)  $C_{18}H_{25}ClN_2O_2$ : 359.1493 [M+Na]<sup>+</sup> (calcd 359.1493);

**IR** (thin film) 3414, 3319 (N–H), 2974, 2929, 1666 (C=O), 1158 (C–O), 738 (C–Cl)  $cm^{-1}$ .

## Experimental

### Preparation of Compound **96**

Compound **96** was prepared according to a modified literature procedure.<sup>[153]</sup>



1,4-Diazabicyclo[2.2.2]octane (DABCO) (480 mg, 4.3 mmol) and freshly distilled acetaldehyde (**98**) (2.9 mL, 51 mmol) were added to a flask. The resulting mixture was cooled to  $0^\circ\text{C}$  and freshly distilled methyl vinyl ketone (**97**) (3.5 mL, 42 mmol) was added dropwise. The resulting mixture was stirred at room temperature for 15 h. The reaction mixture was then diluted with EtOAc and quenched with 1.0 M aq. HCl. The aqueous layer was extracted with EtOAc. The combined organic extracts were dried over brine,  $\text{MgSO}_4$ , filtered and concentrated under reduced pressure. The crude material was purified by Kugelrohr distillation (8 mbar,  $80^\circ\text{C}$  to 0.6 mbar,  $190^\circ\text{C}$ ) to afford 4-hydroxy-3-methylenepentan-2-one (**96**) as a colourless oil (4.0 g, 35 mmol, 83%).

The obtained spectroscopic data matched literature values.<sup>[153]</sup>

$R_f = 0.27$  (petroleum ether 40–65/ $\text{Et}_2\text{O}$ , 8:2);

$^1\text{H NMR}$  (400 MHz,  $\text{CDCl}_3$ )  $\delta = 6.08$  (s, 1H,  $\text{H}_6$ ), 6.03 (d,  $^4J_{4,6} = 1.2$  Hz, 1H,  $\text{H}_6$ ), 4.64 (q,  $^3J_{4,5} = 6.5$  Hz, 1H,  $\text{H}_4$ ), 2.78 (s, 1H, OH), 2.35 (s, 3H,  $\text{H}_1$ ), 1.33 (d,  $^3J_{4,5} = 6.5$  Hz, 3H,  $\text{H}_5$ ) ppm;

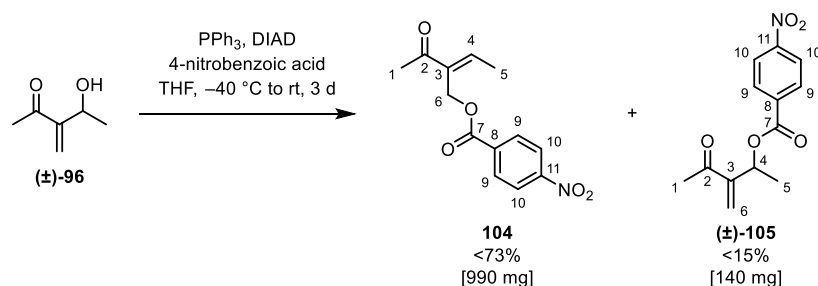
$^{13}\text{C NMR}$  (126 MHz,  $\text{CDCl}_3$ )  $\delta = 200.9$  (C=O,  $\text{C}_2$ ), 151.5 (C=C,  $\text{C}_3$ ), 125.0 ( $\text{CH}_2$ ,  $\text{C}_6$ ), 66.9 (CH,  $\text{C}_4$ ), 26.5 ( $\text{CH}_3$ ,  $\text{C}_1$ ), 22.2 ( $\text{CH}_3$ ,  $\text{C}_5$ ) ppm;

$\text{MS}$  (EI-GCMS)  $m/z$  (%) = 100 (6), 99 (100), 71 (8), 69 (3), 45 (9), 43 (85);

$\text{IR}$  (neat) 3430 (O–H), 2975, 2931, 1664 (C=O), 1365, 1287, 1084 (C–O), 951, 588  $\text{cm}^{-1}$ .

## Experimental

### Preparation of Compounds **104** and **105**



Triphenylphosphine (1.3 g, 5.0 mmol) and 4-nitrobenzoic acid (**101**) (0.80 g, 4.8 mmol) were added to a flask, followed compound **96** (410 mg, 3.6 mmol) in THF (30 mL). The resulting mixture was cooled to  $-40\text{ }^\circ\text{C}$  and diisopropyl azodicarboxylate (DIAD) (0.95 mL, 4.8 mmol) was slowly added. The resulting mixture was stirred at  $-30\text{ }^\circ\text{C}$  for 3 h, followed by stirring at room temperature for 3 d. The reaction mixture was then concentrated under reduced pressure. The residue was taken up in  $\text{Et}_2\text{O}$  and washed with water and aq. NaOH (2.0 M). The aqueous layer was extracted with  $\text{Et}_2\text{O}$ . The combined organic extracts were washed with sat. aq.  $\text{NaHCO}_3$ , dried over brine,  $\text{MgSO}_4$ , filtered and concentrated under reduced pressure. The crude material was purified by repeated flash chromatography (petroleum ether 40–65/ $\text{EtOAc}$ , 8:2) to afford, (*E*)-2-acetylbut-2-en-1-yl 4-nitrobenzoate (**104**) as a pale yellow solid (990 mg, 3.8 mmol, <73%) with inseparable impurities, and 3-methylene-4-oxopent-2-en-1-yl 4-nitrobenzoate (**105**), which was further purified by recrystallisation (petroleum ether 40–65/ $\text{EtOAc}$ , 1:1) as a pale yellow solid (140 mg, 0.53 mmol, <15%) with inseparable impurities.

(*E*)-2-Acetylbut-2-en-1-yl 4-nitrobenzoate (**104**):

$R_f = 0.24$  (petroleum ether 40–65/ $\text{EtOAc}$ , 8:2);

$^1\text{H NMR}$  (500 MHz,  $\text{CDCl}_3$ )  $\delta$  8.28 – 8.24 (m, 2H,  $\text{H}_{10}$ ), 8.19 – 8.14 (m, 2H,  $\text{H}_9$ ), 7.10 (q,  $^3J_{4,5} = 7.1$  Hz, 1H,  $\text{H}_4$ ), 5.16 (s, 2H,  $\text{H}_6$ ), 2.38 (s, 3H,  $\text{H}_1$ ), 2.08 (d,  $^3J_{4,5} = 7.1$  Hz, 3H,  $\text{H}_5$ ) ppm;

$^{13}\text{C NMR}$  (126 MHz,  $\text{CDCl}_3$ )  $\delta$  197.7 (C=O,  $\text{C}_2$ ), 164.7 (C=O,  $\text{C}_7$ ), 150.7 (C,  $\text{C}_8$ ), 145.4 (CH,  $\text{C}_4$ ), 137.0 (C=C,  $\text{C}_3$ ), 135.6 (C,  $\text{C}_{11}$ ), 130.9 (CH,  $\text{C}_9$ ), 123.7 (CH,  $\text{C}_{10}$ ), 58.2 ( $\text{CH}_2$ ,  $\text{C}_6$ ), 25.7 ( $\text{CH}_3$ ,  $\text{C}_1$ ), 15.3 ( $\text{CH}_3$ ,  $\text{C}_5$ ) ppm;

$\text{MS}$  (EI-DIP)  $m/z$  (%) 220 (18), 150 (100), 113 (75), 97 (6);

Further analytical data (IR and m.p.) were not collected due to the presence of inseparable impurities.

## Experimental

3-Methylene-4-oxopentan-2-yl 4-nitrobenzoate (**105**):

$R_f = 0.45$  (petroleum ether 40–65/EtOAc, 8:2);

$^1\text{H NMR}$  (500 MHz,  $\text{CDCl}_3$ )  $\delta$  8.31 – 8.27 (m, 2H,  $\text{H}_{10}$ ), 8.23 – 8.20 (m, 2H,  $\text{H}_9$ ), 6.18 (s, 1H,  $\text{H}_6$ ), 6.09 (d,  $^4J_{4,6} = 1.1$  Hz, 1H,  $\text{H}_6$ ), 6.02 (qd,  $^3J_{4,5} = 6.5$  Hz,  $^4J_{4,6} = 1.1$  Hz, 1H,  $\text{H}_4$ ), 2.39 (s, 3H,  $\text{H}_1$ ), 1.52 (d,  $^3J_{4,5} = 6.5$  Hz, 3H,  $\text{H}_5$ ) ppm;

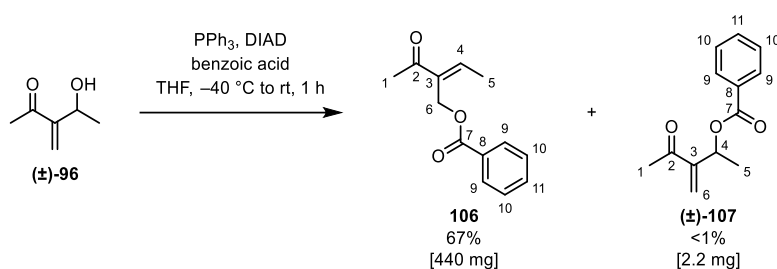
$^{13}\text{C NMR}$  (126 MHz,  $\text{CDCl}_3$ )  $\delta$  197.8 (C=O,  $\text{C}_2$ ), 163.6 (C=O,  $\text{C}_7$ ) 151.0 (C,  $\text{C}_{11}$ ), 149.0 (C=C,  $\text{C}_3$ ), 130.9 (CH,  $\text{C}_9$ ), 130.9 (C,  $\text{C}_8$ ), 124.9 ( $\text{CH}_2$ ,  $\text{C}_6$ ), 123.7 (CH,  $\text{C}_{10}$ ), 69.7 (CH,  $\text{C}_4$ ), 26.2 ( $\text{CH}_3$ ,  $\text{C}_1$ ), 20.7 ( $\text{CH}_3$ ,  $\text{C}_5$ ) ppm,

$\text{MS}$  (EI-DIP)  $m/z$  (%) 220 (23), 150 (92), 113 (61);

Further analytical data (IR and m.p.) were not collected due to the presence of inseparable impurities.

## Experimental

### Preparation of Compounds **106** and **107**



Triphenylphosphine (1.1 g, 4.2 mmol) and benzoic acid (**102**) (480 mg, 3.9 mmol) were added to a flask, followed by compound **96** (350 mg, 3.1 mmol) in THF (30 mL). The resulting mixture was cooled to  $-40\text{ }^\circ\text{C}$  and diisopropyl azodicarboxylate (DIAD) (0.80 mL, 4.0 mmol) was slowly added. The resulting mixture was stirred at  $-30\text{ }^\circ\text{C}$  for 1 h. The reaction mixture was then concentrated under reduced pressure. The residue was taken up in  $\text{Et}_2\text{O}$  and washed with sat. aq.  $\text{NaHCO}_3$ . The aqueous layer was extracted with  $\text{Et}_2\text{O}$ . The combined organic extracts were dried over brine,  $\text{MgSO}_4$ , filtered and concentrated under reduced pressure. The residue was triturated (petroleum ether 40–65/ $\text{Et}_2\text{O}$ , 95:5), filtered and concentrated under reduced pressure. The crude material was purified by flash chromatography (petroleum ether 40–65/ $\text{Et}_2\text{O}$ , 7:3) to afford (*E*)-2-acetylbut-2-en-1-yl benzoate (**106**) as a colourless oil (440 mg, 2.0 mmol, 67%) and 3-methylene-4-oxopent-2-en-1-yl benzoate (**107**) as a colourless oil (2.2 mg, 1.0  $\mu\text{mol}$ , <1%).

(*E*)-2-Acetylbut-2-en-1-yl benzoate (**106**):

$R_f$  = 0.36 (petroleum ether 40–65/ $\text{Et}_2\text{O}$ , 7:3);

$^1\text{H NMR}$  (500 MHz,  $\text{CDCl}_3$ )  $\delta$  = 8.01 – 7.96 (m, 2H,  $\text{H}_9$ ), 7.53 (tt,  $^3J_{10,11}$  = 7.4 Hz,  $^4J_{9,11}$  = 1.2 Hz, 1H,  $\text{H}_{11}$ ), 7.41 (dd,  $^3J_{9,10}$  = 7.6 Hz,  $^3J_{10,11}$  = 7.6 Hz, 2H,  $\text{H}_{10}$ ), 7.06 (q,  $^3J_{4,5}$  = 7.1 Hz, 1H,  $\text{H}_4$ ), 5.12 (s, 2H,  $\text{H}_6$ ), 2.36 (s, 3H,  $\text{H}_1$ ), 2.05 (d,  $^3J_{4,5}$  = 7.1 Hz, 3H,  $\text{H}_5$ ) ppm;

$^{13}\text{C NMR}$  (126 MHz,  $\text{CDCl}_3$ )  $\delta$  = 197.8 (C=O,  $\text{C}_2$ ), 166.6 (C=O,  $\text{C}_7$ ), 144.7 (CH,  $\text{C}_4$ ), 137.6 (C,  $\text{C}_8$ ), 133.1 (CH,  $\text{C}_{11}$ ), 130.2 (C=C,  $\text{C}_3$ ), 129.8 (CH,  $\text{C}_9$ ), 128.5 (CH,  $\text{C}_{10}$ ), 57.4 ( $\text{CH}_2$ ,  $\text{C}_6$ ), 25.8 ( $\text{CH}_3$ ,  $\text{C}_1$ ), 15.2 ( $\text{CH}_3$ ,  $\text{C}_5$ ) ppm;

$\text{MS}$  (EI-GCMS)  $m/z$  (%) 175 (24), 113 (17), 105 (100), 77 (42), 43 (31);

$\text{IR}$  (thin film) 2956, 2924, 2854, 1717 (C=O), 1672 (C=O), 1269 (C–O), 1109 (C–O), 711 (C=C)  $\text{cm}^{-1}$ .

## Experimental

3-Methylene-4-oxopentan-2-yl benzoate (**107**):

$R_f = 0.55$  (petroleum ether 40–65/Et<sub>2</sub>O, 7:3);

**<sup>1</sup>H NMR** (600 MHz, CDCl<sub>3</sub>)  $\delta = 8.07$  (dd,  $^3J_{9,10} = 8.4$  Hz,  $^4J_{9,11} = 1.2$  Hz, 2H, H<sub>9</sub>), 7.57 (dd,  $^3J_{10,11} = 7.5$  Hz,  $^4J_{9,11} = 1.0$  Hz, 1H, H<sub>11</sub>), 7.45 (t,  $^3J_{10,11} = 7.9$  Hz, 3H, H<sub>10</sub>), 6.13 (s, 1H, H<sub>6</sub>), 6.09 (d,  $^4J_{4,6} = 1.2$  Hz, 1H, H<sub>6</sub>), 5.98 (qd,  $^3J_{4,5} = 6.5$  Hz,  $^4J_{4,6} = 1.2$  Hz, 1H, H<sub>4</sub>), 2.38 (s, 3H, H<sub>1</sub>), 1.49 (d,  $^3J_{4,5} = 6.5$  Hz, 3H, H<sub>5</sub>) ppm;

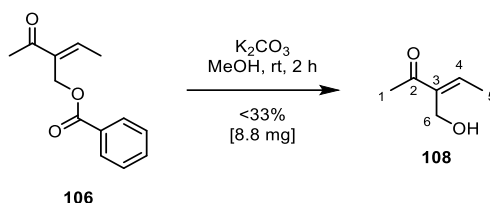
**<sup>13</sup>C NMR** (151 MHz, CDCl<sub>3</sub>)  $\delta = 198.0$  (C=O, C<sub>2</sub>), 165.5 (C=O, C<sub>7</sub>), 149.7 (C=C, C<sub>3</sub>), 133.3 (C, C<sub>8</sub>), 133.2 (CH, C<sub>11</sub>), 129.7 (CH, C<sub>9</sub>), 128.6 (CH, C<sub>10</sub>), 124.4 (CH<sub>2</sub>, C<sub>6</sub>), 68.7 (CH, C<sub>4</sub>), 26.3 (CH<sub>3</sub>, C<sub>1</sub>), 21.0 (CH<sub>3</sub>, C<sub>5</sub>) ppm;

**MS** (EI-GCMS)  $m/z$  (%) 175 (34), 113 (14), 105 (100), 77 (42), 43 (33);

**IR** (thin film) 2954, 2924, 2854, 1720 (C=O), 1677 (C=O), 1269 (C–O), 1112 (C–O), 1079, 1070, 711 (C=C) cm<sup>-1</sup>.

## Experimental

### Preparation of Compound 108



Compound **106** (51 mg, 0.23 mmol) and  $\text{K}_2\text{CO}_3$  (70 mg, 0.51 mmol) were added to a flask, followed by MeOH (2.5 mL). The resulting mixture was stirred at room temperature for 2 h. The reaction mixture was then quenched with  $\text{H}_2\text{O}$  and the aqueous layer was extracted with EtOAc. The combined organic extracts were dried over brine,  $\text{MgSO}_4$ , filtered and concentrated under reduced pressure. The crude material was purified by flash chromatography (petroleum ether 40–65/ $\text{Et}_2\text{O}$ , 4:6) to afford (E)-3-(hydroxymethyl)pent-3-en-2-one (**108**) as a colourless oil (8.8 mg, 77  $\mu\text{mol}$ ,  $<33\%$ ).

$R_f$  = 0.34 (petroleum ether 40–65/ $\text{Et}_2\text{O}$ , 4:6);

$^1\text{H NMR}$  (400 MHz,  $\text{CDCl}_3$ )  $\delta$  = 6.97 (q,  $^3J_{4,5}$  = 7.1 Hz, 1H,  $\text{H}_4$ ), 4.18 (s, 2H,  $\text{H}_6$ ), 2.32 (s, 3H,  $\text{H}_1$ ), 1.98 (d,  $^3J_{4,5}$  = 7.1 Hz, 3H,  $\text{H}_5$ ) ppm;

$^{13}\text{C NMR}$  (101 MHz,  $\text{CDCl}_3$ )  $\delta$  = 143.5 (C=C,  $\text{C}_4$ ), 64.6 ( $\text{CH}_2$ ,  $\text{C}_6$ ), 25.9 ( $\text{CH}_3$ ,  $\text{C}_1$ ), 15.0 ( $\text{CH}_3$ ,  $\text{C}_5$ ) ppm;

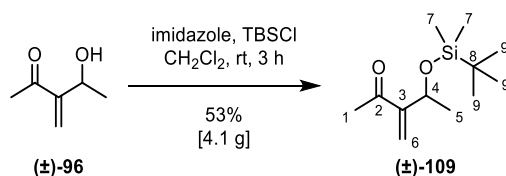
$\text{MS}$  (EI-GCMS)  $m/z$  (%) 114 [ $\text{M}$ ] $^+$  (2), 86 (10), 71 (66);

$\text{IR}$  (thin film) 3348 (O–H), 2957, 2924, 2854, 1722 (C=O), 1462, 1377, 1269, 1250, 1105 (C–O)  $\text{cm}^{-1}$ .

## Experimental

### Preparation of Compound 109

Compound **109** was prepared according to a modified literature procedure.<sup>[153]</sup>



Imidazole (14 g, 200 mmol) and *tert*-butyldimethylsilyl chloride (TBSCl) (12 g, 80 mmol) were added to a flask, followed by compound **96** (3.9 g, 34 mmol) in  $\text{CH}_2\text{Cl}_2$  (200 mL). The resulting mixture was stirred at room temperature for 3 h. The reaction mixture was then quenched with sat. aq.  $\text{NH}_4\text{Cl}$ . The aqueous layer was extracted with  $\text{CH}_2\text{Cl}_2$ . The combined organic extracts were dried over brine,  $\text{MgSO}_4$ , filtered and concentrated under reduced pressure. The crude material was purified by repeated flash chromatography (petroleum ether 40–65/ $\text{Et}_2\text{O}$ , 100:1) to afford 4-((*tert*-butyldimethylsilyl)oxy)-3-methylenepentan-2-one (**109**) as a colourless oil (4.1 g, 18 mmol, 53%).

The obtained spectroscopic data matched literature values.<sup>[153]</sup>

$R_f = 0.43$  (petroleum ether 40–65/ $\text{Et}_2\text{O}$ , 39:1);

$^1\text{H NMR}$  (500 MHz,  $\text{CDCl}_3$ )  $\delta$  6.17 (dd,  $4J_{4,6} = 1.1$  Hz,  $^2J_{6,6} = 1.0$  Hz, 1H,  $\text{H}_6$ ), 6.06 (dd,  $^2J_{6,6} = 0.9$  Hz,  $^4J_{4,6} = 0.9$  Hz, 1H,  $\text{H}_6$ ), 4.76 (qt,  $^3J_{4,5} = 6.2$  Hz,  $^4J_{4,6} = 1.1$  Hz,  $^4J_{4,6} = 1.0$  Hz, 1H,  $\text{H}_4$ ), 2.34 (s, 3H,  $\text{H}_1$ ), 1.21 (d,  $^3J_{4,5} = 6.2$  Hz, 3H,  $\text{H}_5$ ), 0.89 (s, 9H,  $\text{H}_9$ ), 0.05 (s, 3H,  $\text{H}_7$ ), 0.01 (s, 3H,  $\text{H}_7$ ) ppm;

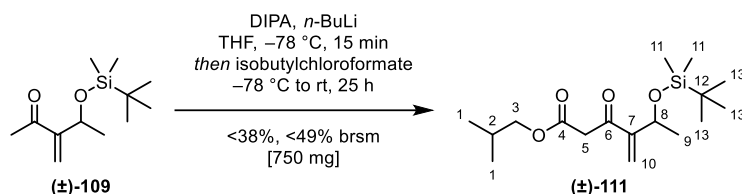
$^{13}\text{C NMR}$  (126 MHz,  $\text{CDCl}_3$ )  $\delta$  199.4 (C=O,  $\text{C}_2$ ), 153.8 (C=C,  $\text{C}_3$ ), 124.3 (C=C,  $\text{C}_6$ ), 66.1 (C–O,  $\text{C}_4$ ), 26.6 ( $\text{CH}_3$ ,  $\text{C}_1$ ), 26.0 ( $\text{CH}_3$ ,  $\text{C}_9$ ), 25.0 ( $\text{CH}_3$ ,  $\text{C}_5$ ), 18.3 (C,  $\text{C}_8$ ), –4.8 (Si– $\text{CH}_3$ ,  $\text{C}_7$ ), –4.9 (Si– $\text{CH}_3$ ,  $\text{C}_7$ ) ppm;

$\text{MS}$  (EI-GCMS)  $m/z$  (%) 43 (12), 97 (8), 113 (3), 127 (87), 171 (100), 213 (3);

$\text{IR}$  (neat) 2956, 2930, 2887, 2858, 1677 (C=O), 1363, 1253, 1086 (C–O), 978 (C=C), 826, 774  $\text{cm}^{-1}$ .

## Experimental

### Preparation of Compound 111



Diisopropylamine (DIPA) (1.1 mL, 7.8 mmol) and THF (18 mL) were added to a flask. The resulting mixture was cooled to  $-78\text{ }^{\circ}\text{C}$  and *n*-BuLi (1.6 M in hexanes, 4.7 mL, 7.5 mmol) was slowly added. The resulting mixture was stirred at  $-78\text{ }^{\circ}\text{C}$  for 15 min. Compound **109** (1.4 g, 6.1 mmol) in THF (12 mL) was then slowly added. The resulting mixture was stirred at  $-78\text{ }^{\circ}\text{C}$  for 15 min. Isobutyl chloroformate (**110**) (1.0 mL, 7.6 mmol) in THF (12 mL) was then slowly added. The resulting mixture was stirred at  $-78\text{ }^{\circ}\text{C}$  for 15 min, followed by stirring at  $0\text{ }^{\circ}\text{C}$  for 1 h and then at room temperature for 24 h. The reaction mixture was then quenched with sat. aq.  $\text{NH}_4\text{Cl}$ . The aqueous layer was extracted with EtOAc. The combined organic extracts were dried over brine,  $\text{MgSO}_4$ , filtered and concentrated under reduced pressure. The crude material was purified by repeated flash chromatography (petroleum ether 40–65/ $\text{Et}_2\text{O}$ , 39:1) to afford isobutyl 5-((*tert*-butyldimethylsilyl)oxy)-4-methylene-3-oxohexanoate (**111**) as a colourless oil (750 mg, 2.3 mmol,  $<38\%, <49\% \text{ brsm}$ ) with small amounts of inseparable impurities.

**R<sub>f</sub>** = 0.33 (petroleum ether 40–65/ $\text{Et}_2\text{O}$ , 39:1);

**$^1\text{H}$  NMR** (500 MHz,  $\text{CDCl}_3$ )  $\delta$  6.27 (d,  $^4J_{8,10} = 1.4\text{ Hz}$ , 1H,  $\text{H}_{10}$ ), 6.07 (app. s, 1H,  $\text{H}_{10}$ ), 4.76 (qdd,  $^3J_{8,9} = 6.3\text{ Hz}$ ,  $^4J_{8,10} = 1.2\text{ Hz}$ ,  $^4J_{8,10} = 1.1\text{ Hz}$ , 1H,  $\text{H}_8$ ), 3.92 (d,  $^3J_{2,3} = 6.7\text{ Hz}$ , 2H,  $\text{H}_3$ ), 3.74 (app. d, 2H,  $\text{H}_5$ )<sup>6</sup>, 1.93 (hept,  $^3J_{1,2} = 6.7\text{ Hz}$  1H,  $\text{H}_2$ ), 1.22 (d,  $^3J_{8,9} = 6.3\text{ Hz}$ , 3H,  $\text{H}_9$ ), 0.92 (d,  $^3J_{1,2} = 6.7\text{ Hz}$ , 6H,  $\text{H}_1$ ), 0.89 (s, 9H,  $\text{H}_{13}$ ), 0.06 (s, 3H,  $\text{H}_{11}$ ), 0.01 (s, 3H,  $\text{H}_{11}$ ) ppm;

**$^{13}\text{C}$  NMR** (126 MHz,  $\text{CDCl}_3$ )  $\delta$  193.4 (C=O,  $\text{C}_6$ ), 167.7 (C=O,  $\text{C}_4$ ), 153.1 (C=C,  $\text{C}_7$ ), 125.5 (C=C,  $\text{C}_{10}$ ), 71.6 ( $\text{CH}_2$ ,  $\text{C}_3$ ), 66.1 (CH,  $\text{C}_8$ ), 46.0 ( $\text{CH}_2$ ,  $\text{C}_5$ )<sup>6</sup>, 27.8 (CH,  $\text{C}_2$ ), 26.0 ( $\text{CH}_3$ ,  $\text{C}_{13}$ ), 24.8 ( $\text{CH}_3$ ,  $\text{C}_9$ ), 19.2 ( $\text{CH}_3$ ,  $\text{C}_1$ ), 18.3 (Si–C,  $\text{C}_{12}$ ),  $-4.8$  (Si– $\text{CH}_3$ ,  $\text{C}_{11}$ ),  $-4.9$  (Si– $\text{CH}_3$ ,  $\text{C}_{11}$ ) ppm;

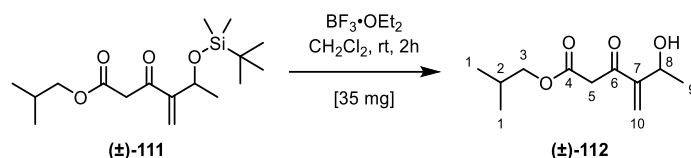
**HRMS** (ESI<sup>+</sup>)  $\text{C}_{17}\text{H}_{32}\text{O}_4\text{Si}$ : 351.20 [ $\text{M}+\text{Na}$ ]<sup>+</sup> (calcd 351.20);

**IR** (thin film) 2957, 2930, 2857, 1742 (C=O), 1679 (C=O), 1253, 1004, 974, 834, 777  $\text{cm}^{-1}$ .

<sup>6</sup> Signal appeared as an apparent doublet in the  $^1\text{H}$  NMR spectrum with  $J = 7.2\text{ Hz}$ , which is unexpected. The corresponding signal in the  $^{13}\text{C}$  NMR spectrum at 46.0 ppm is suggestive of the keto tautomer. In the HSQC spectrum the peak appears as a methylene carbon ( $\text{CH}_2$ ), which is also suggestive of the keto tautomer.

## Experimental

### Preparation of Compound 112



Compound **111** (50 mg, 0.15 mmol) and  $\text{CH}_2\text{Cl}_2$  (1.5 mL) were added to a flask, followed by  $\text{BF}_3 \cdot \text{OEt}_2$  (40  $\mu\text{L}$ ). The resulting mixture was stirred at room temperature for 2 h. The reaction mixture was then quenched with sat. aq.  $\text{NaHCO}_3$ . The aqueous layer was extracted with  $\text{Et}_2\text{O}$ . The combined organic extracts were dried over brine,  $\text{MgSO}_4$ , filtered and concentrated under reduced pressure to afford a crude mixture of isobutyl 5-hydroxy-4-methylene-3-oxohexanoate (**112**), with impurities present<sup>7</sup>, as a colourless oil (35 mg).

$R_f = 0.47$  (petroleum ether 40–65/ $\text{Et}_2\text{O}$ , 1:1);

$^1\text{H NMR}$  (600 MHz,  $\text{CDCl}_3$ )  $\delta = 6.15$  (d,  $^4J_{8,10} = 1.2$  Hz, 1H,  $\text{H}_{10}$ ), 6.08 (s, 1H,  $\text{H}_{10}$ ), 4.68 (q,  $^3J_{8,9} = 6.5$  Hz, 1H,  $\text{H}_8$ ), 3.90 (d,  $^3J_{2,3} = 6.7$  Hz, 2H,  $\text{H}_3$ ), 3.74 (app. d, 2H,  $\text{H}_5$ )<sup>8</sup>, 2.03 – 1.96 (m, 1H,  $\text{H}_2$ ), 1.33 (d,  $^3J_{8,9} = 6.8$  Hz, 3H,  $\text{H}_9$ ), 0.90 (d,  $^3J_{1,2} = 6.7$  Hz, 6H,  $\text{H}_1$ )<sup>9</sup> ppm;

$^{13}\text{C NMR}$  (151 MHz,  $\text{CDCl}_3$ )  $\delta = 194.6$  (C=O,  $\text{C}_6$ ), 167.5 (C=O,  $\text{C}_4$ ), 151.2 (C=C,  $\text{C}_7$ ), 125.7 (C=C,  $\text{C}_{10}$ ), 71.5 ( $\text{CH}_2$ ,  $\text{C}_3$ ), 66.5 (CH,  $\text{C}_8$ ), 45.9 ( $\text{CH}_2$ ,  $\text{C}_5$ )<sup>8</sup>, 28.1 (CH,  $\text{C}_2$ ), 22.4 ( $\text{CH}_3$ ,  $\text{C}_9$ ) ppm;

Further analytical data (HRMS and IR) were not collected due to the presence as a crude mixture.

<sup>7</sup> The product decomposed during chromatography, therefore it was not possible to purify the crude product by chromatography.

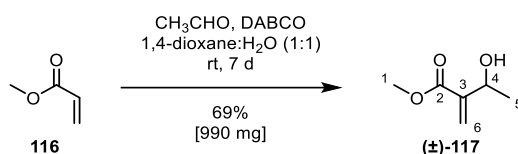
<sup>8</sup> Signal appeared as an apparent doublet in the  $^1\text{H NMR}$  spectrum with  $J = 3.9$  Hz, which is unexpected. The corresponding signal in the  $^{13}\text{C NMR}$  spectrum at 45.9 ppm is suggestive of the keto tautomer. In the HSQC spectrum the peak appears as a methylene carbon ( $\text{CH}_2$ ), which is also suggestive of the keto tautomer.

<sup>9</sup> Overlapping signals therefore not possible to accurately integrate, integrals shown are corrected.

## Experimental

### Preparation of Compound **117**

Compound **117** was prepared according to a literature procedure.<sup>[164]</sup>



1,4-Diazabicyclo[2.2.2]octane (DABCO) (1.1 g, 9.8 mmol) was added to a flask, followed by 1,4-dioxane (0.5 mL), water (0.5 mL), methyl acrylate (**116**) (2.7 mL, 30 mmol) and acetaldehyde (**98**) (0.6 mL, 11 mmol). The resulting mixture was stirred at room temperature for 7 d. The reaction mixture was then diluted with water. The aqueous layer was extracted with Et<sub>2</sub>O. The combined organic extracts were washed with aq. HCl (1.0 M) and dried over brine, MgSO<sub>4</sub>, filtered and concentrated under reduced pressure. The crude material was purified by flash chromatography (petroleum ether 40–65/Et<sub>2</sub>O, 6:4) to afford methyl 3-hydroxy-2-methylenebutanoate (**117**) as a colourless oil (990 mg, 7.6 mmol, 69%).

The obtained spectroscopic data matched literature values.<sup>[164]</sup>

**R<sub>f</sub>** = 0.32 (petroleum ether 40–65/Et<sub>2</sub>O, 6:4);

**<sup>1</sup>H NMR** (300 MHz, CDCl<sub>3</sub>)  $\delta$  = 6.22 (dd, <sup>2</sup>*J*<sub>6,6</sub> = 0.8 Hz, <sup>4</sup>*J*<sub>4,6</sub> = 0.6 Hz, 1H, H<sub>6</sub>), 5.83 (dd, <sup>4</sup>*J*<sub>4,6</sub> = 1.1 Hz, <sup>2</sup>*J*<sub>6,6</sub> = 1.0 Hz, 1H, H<sub>6</sub>), 4.62 (qd, <sup>3</sup>*J*<sub>4,OH</sub> = 6.2 Hz, <sup>3</sup>*J*<sub>4,5</sub> = 6.2 Hz, 1H, H<sub>4</sub>), 3.79 (s, 3H, H<sub>1</sub>), 2.65 (d, <sup>3</sup>*J*<sub>4,OH</sub> = 5.4 Hz, 1H, OH), 1.39 (d, <sup>3</sup>*J*<sub>4,5</sub> = 6.5 Hz, 3H, H<sub>5</sub>) ppm;

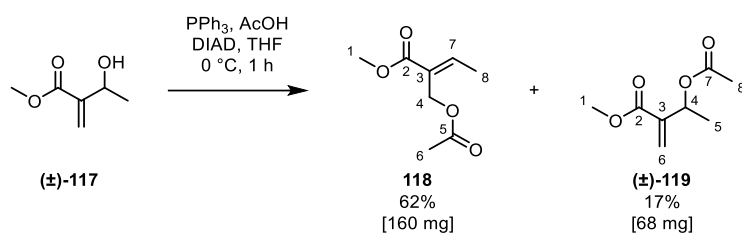
**<sup>13</sup>C NMR** (75 MHz, CDCl<sub>3</sub>)  $\delta$  = 167.2 (C=O, C<sub>2</sub>), 143.5 (C=C, C<sub>3</sub>), 124.4 (C=C, C<sub>6</sub>), 67.3 (CH, C<sub>4</sub>), 52.1 (CH<sub>3</sub>, C<sub>1</sub>), 22.2 (CH<sub>3</sub>, C<sub>5</sub>) ppm;

**MS** (EI-GCMS) *m/z* (%) 115 (60), 99 (18), 98 (24), 70 (15), 45 (17);

**IR** (thin film) 2953, 2922, 2869, 2853, 1721 (C=O), 1460, 1377 cm<sup>-1</sup>.

## Experimental

### Preparation of Compounds **118** and **119**



Triphenylphosphine (600 mg, 2.3 mmol) was added to a flask, followed by compound **117** (190 mg, 1.5 mmol), THF (13 mL) and acetic acid (AcOH) (0.30 mL, 5.2 mmol). The resulting mixture was cooled to 0 °C and diisopropyl azodicarboxylate (DIAD) (0.45 mL, 2.3 mmol) was added dropwise. The resulting mixture was stirred for 1 h at 0 °C. The reaction mixture was then concentrated under reduced pressure. The residue was diluted with sat. aq. NaHCO<sub>3</sub> and the aqueous layer was extracted with Et<sub>2</sub>O. The combined organic extracts were dried over brine, MgSO<sub>4</sub>, filtered and concentrated under reduced pressure. The crude material was purified by flash chromatography (petroleum ether 40–65/Et<sub>2</sub>O, 8:2) to afford methyl (*E*)-2-(acetoxymethyl)but-2-enoate (**118**) as a colourless oil (160 mg, 0.93 mmol, 62%) and methyl 3-acetoxy-2-methylenebutanoate (**119**) as a colourless oil (68 mg, 0.39 mmol, 17%).

Methyl (*E*)-2-(acetoxymethyl)but-2-enoate (**118**):

**R<sub>f</sub>** = 0.32 (petroleum ether 40–65/Et<sub>2</sub>O, 8:2);

**<sup>1</sup>H NMR** (400 MHz, CDCl<sub>3</sub>) δ = 7.15 (q, <sup>3</sup>J<sub>7,8</sub> = 7.3 Hz, 1H, H<sub>7</sub>), 4.86 (s, 2H, H<sub>4</sub>), 3.77 (s, 3H, H<sub>1</sub>), 2.05 (s, 3H, H<sub>6</sub>), 1.93 (d, <sup>3</sup>J<sub>7,8</sub> = 7.3 Hz, 3H, H<sub>8</sub>) ppm;

**<sup>13</sup>C NMR** (101 MHz, CDCl<sub>3</sub>) δ = 171.0 (C=O, C<sub>5</sub>), 167.0 (C=O, C<sub>2</sub>), 144.8 (C=C, C<sub>7</sub>), 128.1 (C=C, C<sub>3</sub>), 57.9 (CH<sub>2</sub>, C<sub>4</sub>), 52.1 (CH<sub>3</sub>, C<sub>1</sub>), 21.0 (CH<sub>3</sub>, C<sub>6</sub>), 14.7 (CH<sub>3</sub>, C<sub>8</sub>) ppm;

**MS** (EI-GCMS) *m/z* (%) 141 (8), 129 (100), 113 (5), 98 (18), 59 (18), 43 (76);

**IR** (thin film) 2953, 2922, 2869, 2853, 1744 (C=O), 1726 (C=O), 1460, 1377, 1249 (C–O), 1231 (C–O) cm<sup>-1</sup>.

Methyl 3-acetoxy-2-methylenebutanoate (**119**):

**R<sub>f</sub>** = 0.42 (petroleum ether 40–65/Et<sub>2</sub>O, 8:2);

**<sup>1</sup>H NMR** (400 MHz, CDCl<sub>3</sub>) δ = 6.28 (dd, <sup>2</sup>J<sub>6,6</sub> = 0.8 Hz, <sup>4</sup>J<sub>4,6</sub> = 0.7 Hz, 1H, H<sub>6</sub>), 5.81 (dd, <sup>2</sup>J<sub>6,6</sub> = 1.1 Hz, <sup>4</sup>J<sub>4,6</sub> = 1.1 Hz, 1H, H<sub>6</sub>), 5.69 (qdd, <sup>3</sup>J<sub>4,5</sub> = 6.5 Hz, <sup>4</sup>J<sub>4,6</sub> = 1.2 Hz, <sup>4</sup>J<sub>4,6</sub> = 0.5 Hz, 1H, H<sub>4</sub>), 3.77 (s, 3H, H<sub>1</sub>), 2.07 (s, 3H, H<sub>8</sub>), 1.39 (d, <sup>3</sup>J<sub>4,5</sub> = 6.5 Hz, 3H, H<sub>5</sub>) ppm;

## *Experimental*

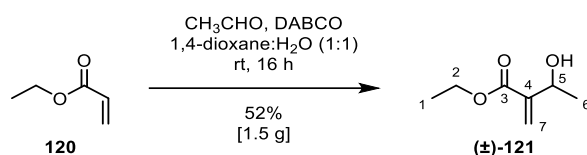
**<sup>13</sup>C NMR** (101 MHz, CDCl<sub>3</sub>)  $\delta$  = 170.0 (C=O, C<sub>7</sub>), 165.9 (C=O, C<sub>2</sub>), 141.2 (C=C, C<sub>3</sub>), 124.9 (C=C, C<sub>6</sub>), 68.3 (CH, C<sub>4</sub>), 52.1 (CH<sub>3</sub>, C<sub>1</sub>), 21.3 (CH<sub>3</sub>, C<sub>8</sub>), 20.3 (CH<sub>3</sub>, C<sub>5</sub>) ppm;

**MS** (EI-GCMS)  $m/z$  (%) 141 (7), 129 (97), 113 (6), 98 (18), 82 (6), 59 (18), 43 (100);

**IR** (thin film) 2954, 2922, 2869, 2852, 1735 (C=O), 1459, 1377, 1261 (C–O), 1083 (C–O), 1021 (C–O), 802 cm<sup>-1</sup>.

## Experimental

### Preparation of Compound **121**



1,4-Diazabicyclo[2.2.2]octane (DABCO) (2.2 g, 20 mmol) was added to a flask, followed by 1,4-dioxane (5.0 mL), water (5.0 mL), ethyl acrylate (**120**) (6.8 mL, 62 mmol) and acetaldehyde (**98**) (1.1 mL, 20 mmol). The resulting mixture was stirred at room temperature for 16 h. The reaction mixture was diluted with water. The aqueous layer was extracted with Et<sub>2</sub>O. The combined organic extracts were washed with aq. HCl (1.0 M) and dried over brine, MgSO<sub>4</sub>, filtered and concentrated under reduced pressure to afford ethyl 3-hydroxy-2-methylenebutanoate (**121**) as a colourless oil (1.5 g, 10 mmol, 52%). This material was deemed sufficiently pure to be used without further purification.

The obtained spectroscopic data matched literature values.<sup>[177]</sup>

**R<sub>f</sub>** = 0.41 (petroleum ether 40–65/EtOAc, 9:1);

**<sup>1</sup>H NMR** (500 MHz, CDCl<sub>3</sub>)  $\delta$  6.21 (app. s, 1H, H<sub>7</sub>), 5.80 (app. t, <sup>2</sup>J<sub>7,7</sub> = 1.0 Hz, 1H, H<sub>7</sub>), 4.61 (q, <sup>3</sup>J<sub>5,6</sub> = 6.5 Hz, 1H, H<sub>5</sub>), 4.24 (q, <sup>3</sup>J<sub>1,2</sub> = 7.1 Hz, 2H, H<sub>2</sub>), 2.72 (s, 1H, OH), 1.39 (d, <sup>3</sup>J<sub>5,6</sub> = 6.5 Hz, 3H, H<sub>6</sub>), 1.32 (t, <sup>3</sup>J<sub>1,2</sub> = 7.1 Hz, 3H, H<sub>1</sub>) ppm;

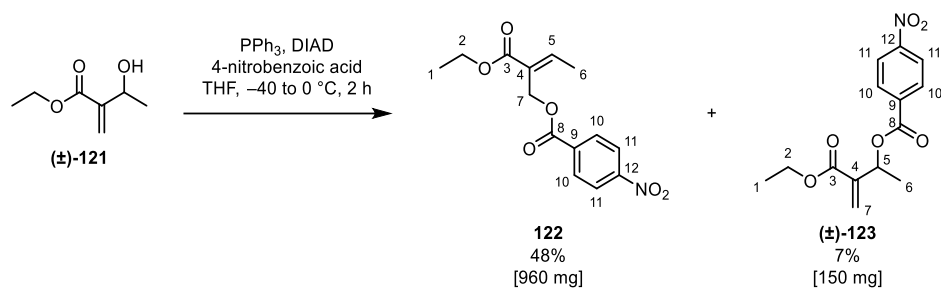
**<sup>13</sup>C NMR** (126 MHz, CDCl<sub>3</sub>)  $\delta$  166.8 (C=O, C<sub>3</sub>), 143.8 (C=C, C<sub>4</sub>), 124.1 (CH<sub>2</sub>, C<sub>7</sub>), 67.4 (CH, C<sub>5</sub>), 61.0 (CH<sub>2</sub>, C<sub>2</sub>), 22.2 (CH<sub>3</sub>, C<sub>6</sub>), 14.3 (CH<sub>3</sub>, C<sub>1</sub>) ppm;

**MS** (EI-GCMS) *m/z* (%) 73 (30), 71 (24), 45 (24), 43 (42);

**IR** (neat) 3428 (O–H), 2979, 2933, 1710 (C=O), 1629 (C=C), 1450, 1402, 1089 (C–O) cm<sup>-1</sup>.

## Experimental

### Preparation of Compounds **122** and **123**



Triphenylphosphine (2.4 g, 9.3 mmol) and 4-nitrobenzoic acid (**101**) (1.6 g, 9.4 mmol) were added to a flask, followed by THF (60 mL) and compound **121** (1.0 g, 6.9 mmol). The resulting mixture was cooled to  $-40$  °C and diisopropyl azodicarboxylate (DIAD) (1.9 mL, 9.6 mmol) was slowly added. The resulting mixture was stirred at  $-40$  °C for 2 h, followed by stirring at  $0$  °C for 15 min. The reaction mixture was then concentrated under reduced pressure. The residue was taken up in  $\text{Et}_2\text{O}$  and washed with water and aq. NaOH (2.0 M). The aqueous layer was extracted with  $\text{Et}_2\text{O}$ . The combined organic layers were washed with sat. aq.  $\text{NaHCO}_3$  and dried over brine,  $\text{MgSO}_4$ , filtered and concentrated under reduced pressure. The crude material was purified by flash chromatography (petroleum ether 40–65/ $\text{EtOAc}$ , 9:1) to afford (*E*)-2-(ethoxycarbonyl)but-2-en-1-yl 4-nitrobenzoate (**122**) as a yellow solid (960 mg, 3.3 mmol, 48%) and 3-(ethoxycarbonyl)but-3-en-2-yl 4-nitrobenzoate (**123**) as a yellow solid (150 mg, 0.51 mmol, 7%).

(*E*)-2-(Ethoxycarbonyl)but-2-en-1-yl 4-nitrobenzoate (**122**):

$R_f$  = 0.30 (petroleum ether 40–65/ $\text{EtOAc}$ , 9:1);

$^1\text{H NMR}$  (400 MHz,  $\text{CD}_3\text{OD}$ )  $\delta$  8.35 – 8.30 (m, 2H,  $\text{H}_{11}$ ), 8.23 – 8.16 (m, 2H,  $\text{H}_{10}$ ), 7.25 (q,  $^3J_{5,6} = 7.3$  Hz, 1H,  $\text{H}_5$ ), 5.18 (s, 2H,  $\text{H}_7$ ), 4.22 (q,  $^3J_{1,2} = 7.1$  Hz, 2H,  $\text{H}_2$ ), 2.02 (d,  $^3J_{5,6} = 7.3$  Hz, 3H,  $\text{H}_6$ ), 1.27 (t,  $^3J_{1,2} = 7.1$  Hz, 3H,  $\text{H}_1$ ) ppm;

$^{13}\text{C NMR}$  (101 MHz,  $\text{CD}_3\text{OD}$ )  $\delta$  167.7 (C=O,  $\text{C}_3$ ), 165.8 (C=O,  $\text{C}_8$ ), 152.1 (C,  $\text{C}_9$ ), 146.4 (CH,  $\text{C}_5$ ), 136.7 (C,  $\text{C}_{12}$ ), 131.8 (C,  $\text{C}_{10}$ ), 129.2 (C=C,  $\text{C}_4$ ), 124.7 (C,  $\text{C}_{11}$ ), 62.0 ( $\text{CH}_2$ ,  $\text{C}_2$ ), 60.0 ( $\text{CH}_2$ ,  $\text{C}_7$ ), 14.8 ( $\text{CH}_3$ ,  $\text{C}_6$ ), 14.5 ( $\text{CH}_3$ ,  $\text{C}_1$ ) ppm;

$\text{MS}$  (EI-DIP)  $m/z$  (%) 248 (11), 150 (80), 143 (100), 45 (4);

$\text{IR}$  (neat) 2984, 1719 (C=O), 1703 (C=O), 1607 (C=C), 1526 (N–O), 1259 (C–O), 1098 (C–O), 717 (C=C)  $\text{cm}^{-1}$ ;

**m.p.** 55–56 °C.

## Experimental

3-(Ethoxycarbonyl)but-3-en-2-yl 4-nitrobenzoate (**123**):

**R<sub>f</sub>** = 0.41 (petroleum ether 40–65/EtOAc, 9:1);

**<sup>1</sup>H NMR** (400 MHz, CDCl<sub>3</sub>) δ 8.32 – 8.27 (m, 2H, H<sub>11</sub>), 8.25 – 8.19 (m, 2H, H<sub>10</sub>), 6.37 (s, 1H, H<sub>7</sub>), 6.00 (qd, <sup>3</sup>J<sub>5,6</sub> = 6.5 Hz, <sup>4</sup>J<sub>5,7</sub> = 1.2 Hz, 1H, H<sub>5</sub>), 5.90 (t, <sup>4</sup>J<sub>5,7</sub> = 1.0 Hz, 1H, H<sub>7</sub>), 4.25 (q, <sup>3</sup>J<sub>1,2</sub> = 7.2 Hz, 2H, H<sub>2</sub>), 1.58 (d, <sup>3</sup>J<sub>5,6</sub> = 6.5 Hz, 3H, H<sub>6</sub>), 1.30 (t, <sup>3</sup>J<sub>1,2</sub> = 7.1 Hz, 3H, H<sub>1</sub>) ppm;

**<sup>13</sup>C NMR** (101 MHz, CDCl<sub>3</sub>) δ 165.2 (C=O, C<sub>3</sub>), 163.7 (C=O, C<sub>8</sub>), 150.7 (C, C<sub>12</sub>), 140.9 (C=C, C<sub>4</sub>), 135.8 (C, C<sub>9</sub>), 130.9 (C, C<sub>10</sub>), 125.3 (CH<sub>2</sub>, C<sub>7</sub>), 123.7 (C, C<sub>11</sub>), 70.2 (CH, C<sub>5</sub>), 61.2 (CH<sub>2</sub>, C<sub>2</sub>), 20.2 (CH<sub>3</sub>, C<sub>6</sub>), 14.3 (CH<sub>3</sub>, C<sub>1</sub>) ppm;

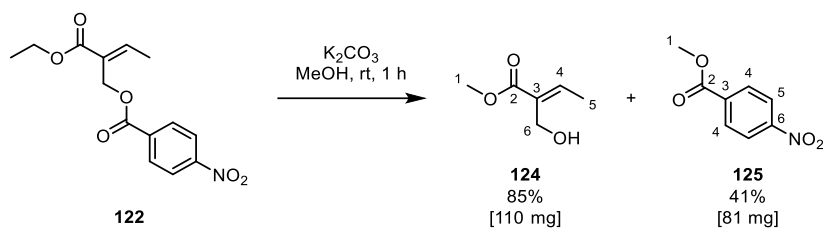
**MS** (EI-DIP) *m/z* (%) 248 (9), 150 (99), 143 (100), 45 (3);

**IR** (neat) 2983, 1720 (C=O), 1634 (C=O), 1605 (C=C), 1525 (N–O), 1267 (C–O), 1174 (C–O), 1098 (C–O), 1077, 719 (C=C) cm<sup>-1</sup>;

**m.p.** 34–35 °C.

## Experimental

### Preparation of Compounds **124** and **125**



Compound **122** (300 mg, 1.0 mmol) and  $K_2CO_3$  (160 mg, 1.2 mmol) were added to a flask, followed by methanol (10 mL). The resulting mixture was stirred at room temperature for 1 h. The reaction mixture was then quenched with water. The aqueous layer was extracted with EtOAc. The combined organic extracts were dried over brine,  $MgSO_4$ , filtered and concentrated under reduced pressure. The crude material was purified by flash chromatography (petroleum ether 40–65/Et<sub>2</sub>O, 7:3 → 3:7) to afford methyl (*E*)-2-(hydroxymethyl)but-2-enoate (**124**) as a colourless oil (110 mg, 0.85 mmol, 85%) and methyl 4-nitrobenzoate (**125**) as a white crystalline solid (81 mg, 0.45 mmol, 41%).

Methyl (*E*)-2-(hydroxymethyl)but-2-enoate (**124**):

The obtained spectroscopic data matched literature values.<sup>[240]</sup>

$R_f$  = 0.11 (petroleum ether 40–65/Et<sub>2</sub>O, 7:3)/0.23 (petroleum ether 40–65/Et<sub>2</sub>O, 7:1);

<sup>1</sup>H NMR (600 MHz, CDCl<sub>3</sub>)  $\delta$  = 6.98 (q, <sup>3</sup>*J*<sub>4,5</sub> = 7.2 Hz, 1H, H<sub>4</sub>), 4.36 (s, 2H, H<sub>6</sub>), 3.78 (s, 3H, H<sub>1</sub>), 1.90 (d, <sup>3</sup>*J*<sub>4,5</sub> = 7.2 Hz, 3H, H<sub>5</sub>) ppm;

<sup>13</sup>C NMR (151 MHz, CDCl<sub>3</sub>)  $\delta$  = 168.1 (C=O, C<sub>2</sub>), 140.9 (CH, C<sub>4</sub>), 131.9 (C=C, C<sub>3</sub>), 57.1 (CH<sub>2</sub>, C<sub>6</sub>), 52.0 (CH<sub>3</sub>, C<sub>1</sub>), 14.3 (CH<sub>3</sub>, C<sub>5</sub>) ppm;

MS (EI-GCMS) *m/z* (%) 130 [M]<sup>+</sup> (3), 115 (89), 102 (5), 99 (47), 71 (31);

IR (thin film) 3433 (O–H), 2924 (O–H), 1711 (C=O), 1651 (C=C), 1437, 1379 (O–H), 1279, 1217 (C–O), 1006, 760 cm<sup>-1</sup>.

Methyl 4-nitrobenzoate (**125**):

The obtained spectroscopic data matched literature values.<sup>[241]</sup>

$R_f$  = 0.77 (petroleum ether 40–65/EtOAc, 7:1);

<sup>1</sup>H NMR (500 MHz, CDCl<sub>3</sub>)  $\delta$  8.32 – 8.27 (2H, m, H<sub>4</sub>), 8.25 – 8.19 (2H, m, H<sub>5</sub>), 3.98 (3H, s, H<sub>1</sub>) ppm;

## *Experimental*

**<sup>13</sup>C NMR** (151 MHz, CDCl<sub>3</sub>) δ 165.3 (C=O, C<sub>2</sub>), 150.7 (C, C<sub>6</sub>), 135.6 (C, C<sub>3</sub>), 130.9 (CH, C<sub>5</sub>), 123.7 (CH, C<sub>4</sub>), 53.0 (CH<sub>3</sub>, C<sub>1</sub>) ppm;

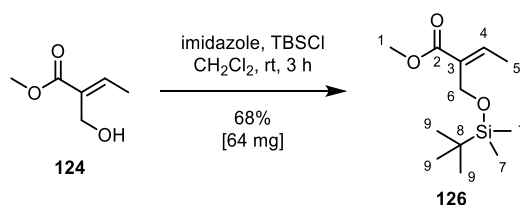
**MS** (EI-DIP) *m/z* (%) 181 [M]<sup>+</sup> (33), 150 (100), 122 (1);

**IR** (neat) 3112, 3078, 1715 (C=O), 1607, 1596, 1519 (N–O), 716 cm<sup>-1</sup>;

**m.p.** 95–96 °C, lit.<sup>[241]</sup> 94–96 °C.

## Experimental

### Preparation of Compound 126



Imidazole (130 mg, 1.9 mmol) and *tert*-butyldimethylsilyl chloride (TBSCl) (230 mg, 1.5 mmol) were added to a flask, followed by methyl (*E*)-2-(hydroxymethyl)but-2-enoate (**124**) (49 mg, 0.38 mmol) in CH<sub>2</sub>Cl<sub>2</sub> (1.9 mL). The resulting mixture was stirred at room temperature for 3 h. The reaction mixture was then quenched with sat. aq. NH<sub>4</sub>Cl. The aqueous layer was extracted with CH<sub>2</sub>Cl<sub>2</sub>. The combined organic extracts were dried over brine MgSO<sub>4</sub>, filtered and concentrated under reduced pressure. The crude material was purified by flash chromatography (petroleum ether 40–65/Et<sub>2</sub>O, 40:1) to afford methyl (*E*)-2-(((*tert*-butyldimethylsilyl)oxy)methyl)but-2-enoate (**126**) as a colourless oil (64 mg, 0.26 mmol, 68%).

The obtained spectroscopic data matched literature values.<sup>[242]</sup>

**R<sub>f</sub>** = 0.48 (petroleum ether 40–65/Et<sub>2</sub>O, 39:1);

**<sup>1</sup>H NMR** (600 MHz, CDCl<sub>3</sub>) δ 6.97 (q, <sup>3</sup>J<sub>4,5</sub> = 7.2 Hz, 1H, H<sub>4</sub>), 4.41 (s, 2H, H<sub>6</sub>), 3.74 (s, 2H, H<sub>1</sub>), 1.91 (d, <sup>3</sup>J<sub>4,5</sub> = 7.2 Hz, 3H, H<sub>5</sub>), 0.89 (s, 9H, H<sub>9</sub>)<sup>10</sup>, 0.08 (s, 6H, H<sub>7</sub>)<sup>10</sup> ppm;

**<sup>13</sup>C NMR** (151 MHz, CDCl<sub>3</sub>) δ 167.8 (C=O, C<sub>2</sub>), 141.5 (C=C, C<sub>4</sub>), 132.6 (C=C, C<sub>3</sub>), 57.1 (CH<sub>2</sub>, C<sub>6</sub>), 51.8 (CH<sub>3</sub>, C<sub>1</sub>), 26.0 (CH<sub>3</sub>, C<sub>9</sub>), 18.5 (Si–C, C<sub>8</sub>), 14.6 (CH<sub>3</sub>, C<sub>5</sub>), –5.2 (Si–CH<sub>3</sub>, C<sub>7</sub>) ppm;

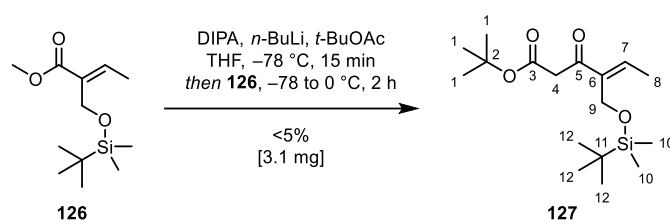
**MS** (EI-DIP) *m/z* (%) 187 (21), 99 (11), 59 (100), 57 (49);

**IR** (thin film) 2954, 2927, 2854, 1719 (C=O), 1251 (C–O), 1083 (C–O), 839 (C=C), 778, 739 cm<sup>–1</sup>.

<sup>10</sup> Corrected integral.

## Experimental

### Preparation of Compound 127



Diisopropylamine (DIPA) (0.20 mL, 1.4 mmol) and THF (3.0 mL) were added to a flask. The resulting mixture was cooled to  $-78\text{ }^{\circ}\text{C}$  and *n*-BuLi (1.6 M in hexanes, 0.70 mL, 1.1 mmol) was slowly added. The resulting mixture was stirred at  $-78\text{ }^{\circ}\text{C}$  for 1 min and *tert*-butyl acetate (0.10 mL, 0.75 mmol) in THF (2.0 mL) was then added dropwise. The resulting mixture was stirred at  $-78\text{ }^{\circ}\text{C}$  for 15 min. Compound **126** (50 mg, 0.20 mmol) in THF (2.0 mL) was added to the mixture at  $-78\text{ }^{\circ}\text{C}$ . The resulting mixture was stirred at  $-78\text{ }^{\circ}\text{C}$  for 15 min, followed by stirring at  $0\text{ }^{\circ}\text{C}$  for 2 h. The reaction mixture was then quenched with sat. aq.  $\text{NH}_4\text{Cl}$ . The aqueous layer was extracted with EtOAc. The combined organic extracts were dried over brine,  $\text{MgSO}_4$ , filtered and concentrated under reduced pressure. The crude material was purified by repeated flash chromatography (petroleum ether 40–65/ $\text{Et}_2\text{O}$ , 9:1; petroleum ether 40–65/ $\text{Et}_2\text{O}$ , 17:3) to afford *tert*-butyl (*E*)-4-(((*tert*-butyldimethylsilyl)oxy)methyl)-3-oxohex-4-enoate (**127**) as a colourless oil (3.1 mg,  $9.4\text{ }\mu\text{mol}$ ,  $<5\%$ ), with inseparable impurities.

$R_f = 0.48$  (petroleum ether 40–65/ $\text{Et}_2\text{O}$ , 9:1);

$^1\text{H NMR}$  (600 MHz,  $\text{CDCl}_3$ )  $\delta$  6.84 (q,  $^3J_{7,8} = 7.1\text{ Hz}$ , 1H,  $\text{H}_7$ ), 4.43 (s, 2H,  $\text{H}_9$ ), 3.61 (s, 2H,  $\text{H}_4$ ), 1.98 (d,  $^3J_{7,8} = 7.1\text{ Hz}$ , 3H,  $\text{H}_8$ ), 1.45 (s,  $\text{H}_1$ , 9H), 0.88 (s, 9H,  $\text{H}_{12}$ )<sup>11</sup>, 0.07 (s, 6H,  $\text{H}_{10}$ ) ppm;

$^{13}\text{C NMR}$  (151 MHz,  $\text{CDCl}_3$ )  $\delta$  193.5 (C=O,  $\text{C}_5$ ), 167.3 (C=O,  $\text{C}_3$ ), 142.6 (C=C,  $\text{C}_7$ ), 140.9 (C=C,  $\text{C}_6$ ), 81.7 (C,  $\text{C}_2$ ), 56.1 ( $\text{CH}_2$ ,  $\text{C}_9$ ), 47.0 ( $\text{CH}_2$ ,  $\text{C}_4$ ), 28.1 ( $\text{CH}_3$ ,  $\text{C}_1$ ), 26.0 ( $\text{CH}_3$ ,  $\text{C}_{12}$ ), 18.4 (Si–C,  $\text{C}_{11}$ ), 15.0 ( $\text{CH}_3$ ,  $\text{C}_8$ ),  $-5.2$  (Si– $\text{CH}_3$ ,  $\text{C}_{10}$ ) ppm;

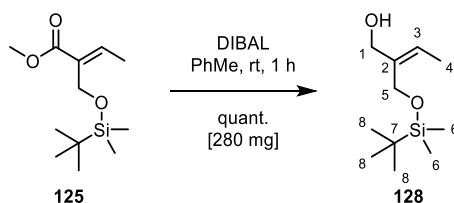
**HRMS** (ESI<sup>+</sup>)  $\text{C}_{17}\text{H}_{32}\text{O}_4\text{Si}$ : 351.195 [ $\text{M}+\text{Na}$ ]<sup>+</sup> (calcd 351.20);

**IR** (thin film) 2954, 2924, 2869, 2854, 1737 (C=O), 1460, 1377, 1368, 1255, 1152 (C–O), 1080 (C–O), 837 (C=C)  $\text{cm}^{-1}$ .

<sup>11</sup> Corrected integral.

## Experimental

### Preparation of Compound 128



Methyl (*E*)-2-(((*tert*-butyldimethylsilyl)oxy)methyl)but-2-enoate (**125**) (320 mg, 1.3 mmol) and PhMe (13 mL) were added to a flask, followed by diisobutylaluminium hydride (DIBAL) (1.2 M in PhMe, 2.2 mL, 2.6 mmol). The resulting mixture was stirred at room temperature for 1 h. The reaction mixture was then quenched with MeOH. Sat. aq. Rochelle salt solution was added to the reaction mixture and the resulting mixture was stirred for 15 h at room temperature until two clear layers had formed. The aqueous layer was extracted with Et<sub>2</sub>O. The combined organic extracts were dried over brine, MgSO<sub>4</sub>, filtered and concentrated under reduced pressure. The crude material was purified by flash chromatography (petroleum ether 40–65/Et<sub>2</sub>O, 9:1) to afford (*Z*)-2-(((*tert*-butyldimethylsilyl)oxy)methyl)but-2-en-1-ol (**128**) as a colourless oil (280 mg, 1.3 mmol, quant.).

**R<sub>f</sub>** = 0.34 (petroleum ether 40–65/Et<sub>2</sub>O, 9:1);

**<sup>1</sup>H NMR** (600 MHz, CDCl<sub>3</sub>) δ 5.57 (qt, <sup>3</sup>*J*<sub>3,4</sub> = 7.0 Hz, <sup>4</sup>*J*<sub>3,5</sub> = 1.1 Hz, 1H, H<sub>3</sub>), 4.37 (d, <sup>4</sup>*J*<sub>3,5</sub> = 1.3 Hz, 2H, H<sub>5</sub>), 4.14 (d, <sup>3</sup>*J*<sub>1,OH</sub> = 6.0 Hz, 2H, H<sub>1</sub>), 2.48 (t, <sup>3</sup>*J*<sub>1,OH</sub> = 6.0 Hz, 1H, OH), 1.64 (d, <sup>3</sup>*J*<sub>3,4</sub> = 7.0 Hz, 3H, H<sub>4</sub>), 0.91 (s, 9H, H<sub>8</sub>), 0.11 (s, 6H, H<sub>6</sub>) ppm;

**<sup>13</sup>C NMR** (151 MHz, CDCl<sub>3</sub>) δ 137.9 (C=C, C<sub>2</sub>), 123.7 (C=C, C<sub>3</sub>), 67.5 (CH<sub>2</sub>, C<sub>1</sub>), 61.0 (CH<sub>2</sub>, C<sub>5</sub>), 26.2 (CH<sub>3</sub>, C<sub>8</sub>), 18.4 (Si–C, C<sub>7</sub>), 13.1 (CH<sub>3</sub>, C<sub>4</sub>), –5.3 (Si–CH<sub>3</sub>, C<sub>6</sub>) ppm;

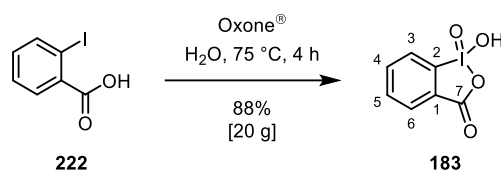
**MS** (EI-DIP) *m/z* (%) 185 (4), 159 (2), 145 (1), 131 (2), 85 (18), 71 (25), 57 (43);

**IR** (thin film) 2955, 2924, 2853, 1465, 1256, 1075 (C–O), 837 (C=C), 776, 740 cm<sup>–1</sup>.

## Experimental

### Preparation of Compound 183

2-Iodoxybenzoic acid (IBX) (**183**) was prepared according to a literature procedure.<sup>[243]</sup>



Oxone<sup>®</sup> (110 g, 180 mmol) was added to a flask, followed by 2-iodobenzoic acid (**222**) (20 g, 81 mmol) and water (400 mL). The resulting mixture was vigorously stirred at 75 °C for 4 h. The reaction mixture was then cooled to 0 °C and filtered. The crude product was washed with water (100 mL) and acetone (2 × 10 mL) to afford 2-iodoxybenzoic acid (IBX) (**183**) as a white solid (20 g, 71 mmol, 88%).

The obtained spectroscopic data matched literature values.<sup>[244]</sup>

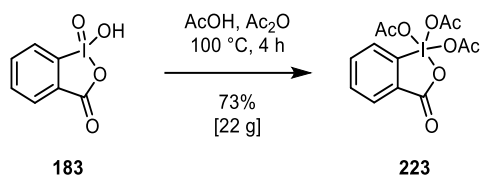
<sup>1</sup>H NMR (400 MHz, DMSO-d<sub>6</sub>) δ = 8.14 (dd, <sup>3</sup>J<sub>3,4</sub> = 8.0 Hz, <sup>4</sup>J<sub>3,5</sub> = 1.0 Hz, 1H, H<sub>3</sub>), 8.05 – 7.97 (m, 2H, H<sub>4,6</sub>), 7.84 (ddd, <sup>3</sup>J<sub>4,5</sub> = 7.4 Hz, <sup>3</sup>J<sub>5,6</sub> = 7.4 Hz, <sup>4</sup>J<sub>3,5</sub> = 1.1 Hz, 1H, H<sub>5</sub>) ppm;

<sup>13</sup>C NMR (101 MHz, DMSO-d<sub>6</sub>) δ = 167.5 (C=O, C<sub>7</sub>), 146.6 (C, C<sub>1</sub>), 133.4 (CH, C<sub>4</sub>), 132.9 (CH, C<sub>5</sub>), 131.5 (C, C<sub>2</sub>), 130.1 (CH, C<sub>6</sub>), 125.0 (CH, C<sub>3</sub>) ppm.

## Experimental

### Preparation of Compound 223

Dess–Martin periodinane (DMP) (**223**) was prepared according to a modified literature procedure.<sup>[245]</sup>

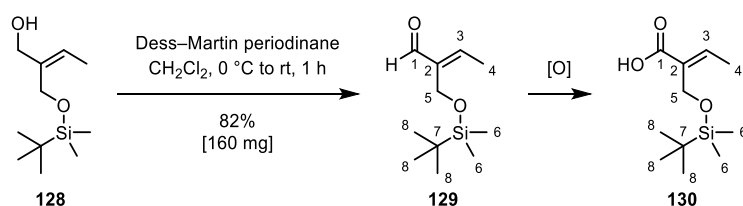


2-Iodoxybenzoic acid (IBX) (**183**) (20 g, 71 mmol) was added to a flask, followed by acetic acid (AcOH) (44 mL, 770 mmol) and acetic anhydride (Ac<sub>2</sub>O) (91 mL, 960 mmol). The resulting mixture was stirred at 100 °C for 4 h. The reaction mixture was then concentrated under reduced pressure. The crude product was co-evaporated with PhMe and then washed with Et<sub>2</sub>O (3 × 30 mL) to afford Dess–Martin periodinane (DMP) (**223**) as white solid (22 g, 52 mmol, 73%).

Due to the instability of the product **223**, characterisation was not performed. The formation of DMP (**223**) was confirmed by its use as the oxidising agent in the test oxidation reaction of 1-octanol to 1-octanal, which was observed to be complete within 2 h by TLC analysis.

## Experimental

### Preparation of Compounds **129** and **130**



Dess–Martin periodinane (**223**) (790 mg, 1.9 mmol) was added to a flask. The flask was cooled to 0 °C and compound **128** (200 mg, 0.92 mmol) in CH<sub>2</sub>Cl<sub>2</sub> (4.6 mL) was added to the flask. The resulting mixture was stirred at 0 °C for 30 min, followed by stirring at room temperature for 30 min. The reaction mixture was then quenched with sat. aq. NaHCO<sub>3</sub>. The aqueous layer was extracted with CH<sub>2</sub>Cl<sub>2</sub>. The combined organic extracts were dried over brine, MgSO<sub>4</sub>, filtered and concentrated under reduced pressure. The crude material was purified by flash chromatography (petroleum ether 40–65/Et<sub>2</sub>O, 19:1) to afford (*E*)-2-(((*tert*-butyldimethylsilyl)oxy)methyl)but-2-enal (**129**) as a colourless oil (160 mg, 0.75 mmol, 82%).

Autoxidation of the aldehyde, (*E*)-2-(((*tert*-butyldimethylsilyl)oxy)methyl)but-2-enal (**129**), to the corresponding carboxylic acid, (*E*)-2-(((*tert*-butyldimethylsilyl)oxy)methyl)but-2-enoic acid (**130**), a pale yellow solid, was observed.

(*E*)-2-(((*tert*-Butyldimethylsilyl)oxy)methyl)but-2-enal (**129**):

**R<sub>f</sub>** = 0.25 (petroleum ether 40–65/Et<sub>2</sub>O, 19:1), 0.65 (petroleum ether 40–65/Et<sub>2</sub>O, 3:1);

**<sup>1</sup>H NMR** (600 MHz, CDCl<sub>3</sub>) δ 9.38 (s, 1H, H<sub>1</sub>), 6.73 (q, <sup>3</sup>J<sub>3,4</sub> = 7.1 Hz, 1H, H<sub>3</sub>), 4.39 (s, 2H, H<sub>5</sub>), 2.11 (d, <sup>3</sup>J<sub>3,4</sub> = 7.1 Hz, 3H, H<sub>4</sub>), 0.88 (s, 9H, H<sub>8</sub>), 0.07 (s, 6H, H<sub>6</sub>) ppm;

**<sup>13</sup>C NMR** (151 MHz, CDCl<sub>3</sub>) δ 193.8 (C=O, C<sub>1</sub>), 153.6 (C=C, C<sub>3</sub>), 143.0 (C=C, C<sub>2</sub>), 54.8 (CH<sub>2</sub>, C<sub>5</sub>), 26.0 (CH<sub>3</sub>, C<sub>8</sub>), 18.5 (Si–C, C<sub>7</sub>), 15.4 (CH<sub>3</sub>, C<sub>4</sub>), –5.3 (Si–CH<sub>3</sub>, C<sub>6</sub>) ppm;

**MS** (EI-GCMS) *m/z* (%) 157 (100), 57 (3);

**IR** (thin film) 2955, 2927, 2855, 1692 (C=O), 1469, 1253, 1079 (C–O), 838 (C=C), 777, 739 cm<sup>–1</sup>.

## Experimental

(*E*)-2-(((*tert*-Butyldimethylsilyl)oxy)methyl)but-2-enoic acid (**130**):

**R<sub>f</sub>** = 0.44 (petroleum ether 40–65/Et<sub>2</sub>O, 3:1);

**<sup>1</sup>H NMR** (400 MHz, CDCl<sub>3</sub>) δ 7.10 (q, <sup>3</sup>J<sub>3,4</sub> = 7.3 Hz, 1H, H<sub>3</sub>), 4.45 (s, 2H, H<sub>5</sub>), 1.91 (d, <sup>3</sup>J<sub>3,4</sub> = 7.2 Hz, 3H, H<sub>4</sub>), 0.91 (s, 9H, H<sub>8</sub>)<sup>12</sup>, 0.12 (s, 6H, H<sub>6</sub>) ppm;

**<sup>13</sup>C NMR** (101 MHz, CDCl<sub>3</sub>) δ 170.6 (C=O, C<sub>1</sub>), 143.0 (C=C, C<sub>3</sub>), 130.9 (C=C, C<sub>2</sub>), 57.5 (CH<sub>2</sub>, C<sub>5</sub>), 26.0 (CH<sub>3</sub>, C<sub>8</sub>), 18.4 (Si–C, C<sub>7</sub>), 14.6 (CH<sub>3</sub>, C<sub>4</sub>), –5.2 (Si–CH<sub>3</sub>, C<sub>6</sub>) ppm;

**HRMS** (ESI<sup>+</sup>) C<sub>11</sub>H<sub>22</sub>O<sub>3</sub>Si: 253.12 [M+Na]<sup>+</sup> (calcd 253.13);

**IR** (thin film) 2955, 2922, 2852, 1692 (C=O), 1648, 1463, 1255, 1082 (C–O), 837 (C=C), 777, 741 cm<sup>–1</sup>;

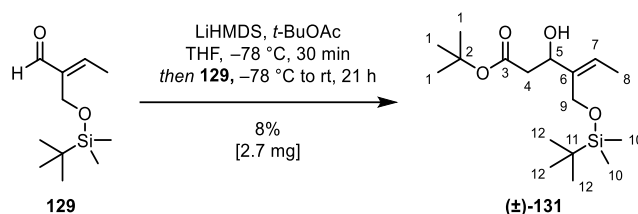
**m.p.** 40–41 °C.

---

<sup>12</sup> Corrected integral.

## Experimental

### Preparation of Compound 131



LiHMDS (1.0 M in THF, 0.60 mL, 0.60 mmol) and THF (0.65 ml) were added to a flask. The resulting mixture was cooled to  $-78\text{ }^{\circ}\text{C}$  and *tert*-butyl acetate (50  $\mu\text{L}$ , 0.37 mmol) was slowly added. The resulting mixture was stirred at  $-78\text{ }^{\circ}\text{C}$  for 30 min. Compound **129** (24 mg, 0.11 mmol) in THF (0.25 ml) was then slowly added. The resulting mixture was stirred at  $-78\text{ }^{\circ}\text{C}$  for 15 min, followed by stirring at  $0\text{ }^{\circ}\text{C}$  for 1 h and then at room temperature for 20 h. The reaction mixture was then quenched with sat. aq.  $\text{NH}_4\text{Cl}$ . The aqueous layer was extracted with  $\text{Et}_2\text{O}$ . The combined organic extracts were dried over brine,  $\text{MgSO}_4$ , filtered and concentrated under reduced pressure. The crude material was purified by flash chromatography (petroleum ether 40–65/ $\text{Et}_2\text{O}$ , 3:1) to afford *tert*-butyl (*E*)-4-(((*tert*-butyldimethylsilyl)oxy)methyl)-3-hydroxyhex-4-enoate (**131**) as a colourless oil (2.7 mg, 8.2  $\mu\text{mol}$ , 8%).

$R_f = 0.48$  (petroleum ether 40–65/ $\text{Et}_2\text{O}$ , 3:1);

$^1\text{H NMR}$  (600 MHz,  $\text{CDCl}_3$ )  $\delta$  5.63 (q,  $^3J_{7,8} = 7.0$  Hz, 1H,  $\text{H}_7$ ), 4.52 (t,  $^3J_{4,5} = 6.9$  Hz, 1H,  $\text{H}_5$ ), 4.36 (d,  $^4J_{5,9} = 6.5$  Hz, 2H,  $\text{H}_9$ ), 3.53 (s, 1H, OH), 2.59 (d,  $^3J_{4,5} = 7.7$  Hz, 1H,  $\text{H}_4$ ), 2.59 (d,  $^3J_{4,5} = 6.0$  Hz, 1H,  $\text{H}_4$ ), 1.65 (d,  $^3J_{7,8} = 6.9$  Hz, 3H,  $\text{H}_8$ ), 1.43 (s, 9H,  $\text{H}_1$ ), 0.91 (s, 9H,  $\text{H}_{12}$ ), 0.11 (s, 3H,  $\text{H}_{10}$ ), 0.10 (s, 3H,  $\text{H}_{10}$ ) ppm;

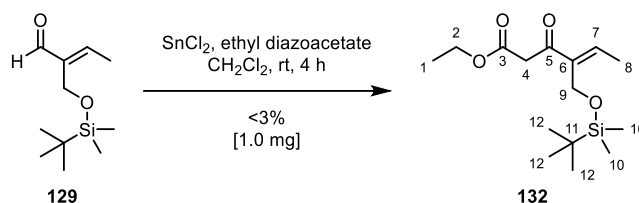
$^{13}\text{C NMR}$  (151 MHz,  $\text{CDCl}_3$ )  $\delta$  171.7 (C=O,  $\text{C}_3$ ), 138.3 (C=C,  $\text{C}_6$ ), 123.4 (C=C,  $\text{C}_7$ ), 80.8 (C,  $\text{C}_2$ ), 72.8 (C–O,  $\text{C}_5$ ), 59.5 ( $\text{CH}_2$ ,  $\text{C}_9$ ), 42.6 ( $\text{CH}_2$ ,  $\text{C}_4$ ), 28.2 ( $\text{CH}_3$ ,  $\text{C}_1$ ), 26.0 ( $\text{CH}_3$ ,  $\text{C}_{12}$ ), 18.3 (Si–C,  $\text{C}_{11}$ ), 13.1 ( $\text{CH}_3$ ,  $\text{C}_8$ ),  $-5.4$  (Si– $\text{CH}_3$ ,  $\text{C}_{10}$ ) ppm;

**HRMS** ( $\text{ESI}^+$ )  $\text{C}_{17}\text{H}_{34}\text{O}_4\text{Si}$ : 353.21 [ $\text{M}+\text{Na}$ ] $^+$  (calcd 353.21);

**IR** (thin film) 2954, 2924, 2854, 1733 (C=O), 1460, 1377 (O–H), 1258, 1153 (C–O), 1080 (C–O), 837 (C=C), 777, 740  $\text{cm}^{-1}$ .

## Experimental

### Preparation of Compound 132



$\text{SnCl}_2$  (24.1 mg, 0.13 mmol) was added to a flask, followed by  $\text{CH}_2\text{Cl}_2$  (0.2 mL), ethyl diazoacetate (15  $\mu\text{L}$ , 0.14 mmol) and compound **129** (21 mg, 98  $\mu\text{mol}$ ) in  $\text{CH}_2\text{Cl}_2$  (0.3 mL). The resulting mixture was stirred at room temperature for 4 h. The reaction mixture was then quenched with sat. aq.  $\text{NH}_4\text{Cl}$ . The aqueous layer was extracted with  $\text{Et}_2\text{O}$ . The combined organic extracts were dried over brine,  $\text{MgSO}_4$ , filtered and concentrated under reduced pressure. The crude material was purified by flash chromatography (petroleum ether 40–65/ $\text{Et}_2\text{O}$ , 3:1) to afford ethyl (*E*)-4-(((*tert*-butyldimethylsilyl)oxy)methyl)-3-oxohex-4-enoate (**132**) as a colourless oil (1.0 mg, 3.3  $\mu\text{mol}$ ,  $<3\%$ ) with solvent impurities.

$R_f$  = 0.48 (petroleum ether 40–65/ $\text{Et}_2\text{O}$ , 3:1);

$^1\text{H NMR}$  (300 MHz,  $\text{CDCl}_3$ )  $\delta$  6.85 (q,  $^3J_{7,8} = 7.1$  Hz, 1H,  $\text{H}_7$ ), 4.43 (s, 2H,  $\text{H}_9$ ), 4.18 (q,  $^3J_{1,2} = 7.1$  Hz, 2H,  $\text{H}_2$ ), 3.71 (s, 2H,  $\text{H}_4$ ), 1.98 (d,  $^3J_{7,8} = 7.1$  Hz, 3H,  $\text{H}_8$ ), 1.27 (t,  $^3J_{1,2} = 7.0$  Hz, 3H,  $\text{H}_1$ )<sup>13</sup>, 0.88 (s, 9H,  $\text{H}_{12}$ )<sup>13</sup>, 0.07 (s, 6H,  $\text{H}_{10}$ )<sup>13</sup> ppm.

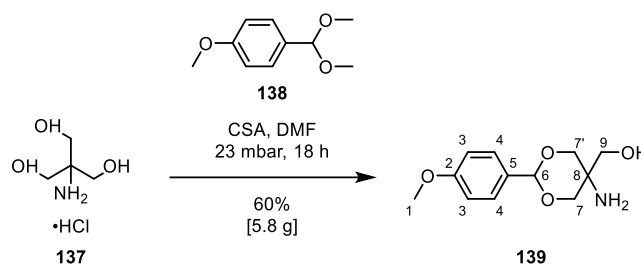
Upon removal of the solvent impurities under oil pump vacuum, decomposition of compound **132** was observed, therefore it was not possible to collect further analytical data ( $^{13}\text{C NMR}$ , HRMS, IR).

<sup>13</sup> Overlapping signals therefore not possible to accurately integrate, integrals shown are corrected.

## Experimental

### Preparation of Compound 139

Compound **139** was prepared according to a literature procedure.<sup>[171]</sup>



TRIS hydrochloride (**137**) (6.4 g, 41 mmol) was added to a flask, followed by DMF (50 mL), *p*-anisaldehyde dimethyl acetate (**138**) (6.8 mL, 40 mmol) and camphorsulfonic acid (CSA) (480 mg, 2.1 mmol). The resulting mixture was stirred on a rotary evaporator at 23 mbar at room temperature for 18 h. The reaction mixture was then quenched with Et<sub>3</sub>N (0.33 mL, 2.4 mmol) and concentrated under reduced pressure. The residue was taken up in EtOAc and washed with aq. NaOH (30%) and ice-water. The aqueous layer was extracted with EtOAc. The combined organic extracts were dried over brine, MgSO<sub>4</sub>, filtered and concentrated under reduced pressure. The crude material was purified by recrystallisation (EtOAc) to afford (5-amino-2-(4-methoxyphenyl)-1,3-dioxan-5-yl)methanol (**139**) as white crystals (5.8 g, 24 mmol, 60%).

The obtained spectroscopic data matched literature values.<sup>[171]</sup>

**<sup>1</sup>H NMR** (300 MHz, CD<sub>3</sub>OD)  $\delta$  = 7.50 – 7.42 (m, 2H, H<sub>4</sub>), 6.99 – 6.90 (m, 2H, H<sub>3</sub>), 5.46 (s, 1H, H<sub>6</sub>), 4.03 (dt, <sup>2</sup>*J*<sub>7,7'</sub> = 11.7 Hz, <sup>4</sup>*J*<sub>7,7'</sub> = 1.6 Hz, 2H, H<sub>7</sub>), 3.87 (dt, <sup>2</sup>*J*<sub>7,7'</sub> = 11.7 Hz, <sup>4</sup>*J*<sub>7,7'</sub> = 1.7 Hz, 2H, H<sub>7'</sub>), 3.83 (s, 3H, H<sub>1</sub>), 3.44 (s, 2H, H<sub>9</sub>) ppm;

**<sup>13</sup>C NMR** (75 MHz, CD<sub>3</sub>OD)  $\delta$  = 161.6 (C, C<sub>2</sub>), 132.1 (C, C<sub>5</sub>), 128.6 (CH, C<sub>4</sub>), 114.4 (CH, C<sub>3</sub>), 103.0 (CH, C<sub>6</sub>), 74.9 (CH<sub>2</sub>, C<sub>7</sub>), 65.2 (CH<sub>2</sub>, C<sub>9</sub>), 55.7 (CH<sub>3</sub>, C<sub>1</sub>), 51.60 (C, C<sub>8</sub>) ppm;

**<sup>1</sup>H NMR** (300 MHz, CDCl<sub>3</sub>)  $\delta$  = 7.48 – 7.39 (m, 2H, H<sub>4</sub>), 6.95 – 6.87 (m, 2H, H<sub>3</sub>), 5.41 (s, 1H, H<sub>6</sub>), 3.95 – 3.82 (m, 4H, H<sub>7</sub>), 3.81 (s, 3H, H<sub>1</sub>), 3.37 (s, 2H, H<sub>9</sub>), 2.14 (s, 4H, NH<sub>2</sub>, OH) ppm;

**<sup>13</sup>C NMR** (75 MHz, CDCl<sub>3</sub>)  $\delta$  = 160.3 (C, C<sub>2</sub>), 130.5 (C, C<sub>5</sub>), 127.4 (CH, C<sub>4</sub>), 113.9 (CH, C<sub>3</sub>), 102.1 (CH, C<sub>6</sub>), 74.7 (CH<sub>2</sub>, C<sub>7</sub>), 65.0 (CH<sub>2</sub>, C<sub>9</sub>), 55.5 (CH<sub>3</sub>, C<sub>1</sub>), 50.8 (C, C<sub>8</sub>) ppm;

**HRMS** (ESI<sup>+</sup>) C<sub>12</sub>H<sub>17</sub>NO<sub>4</sub>: 240.1086 (found *m/z*) [M+H]<sup>+</sup> (calcd 240.1230), 262.0905 (found *m/z*) [M+Na]<sup>+</sup> (calcd 262.1050);

## *Experimental*

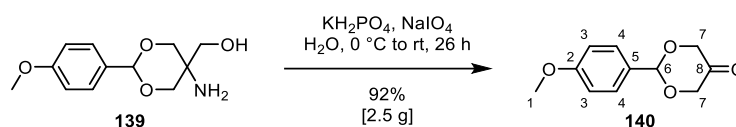
**IR** (neat) 3343 (N–H), 3285 (N–H), 2967, 2936, 2861, 1614 (C=C), 1519, 1252 (C–O), 1029 (C–O), 830  $\text{cm}^{-1}$ ;

**m.p.** 139–141 °C, lit.<sup>[171]</sup> 142 °C.

## Experimental

### Preparation of Compound 140

Compound **140** was prepared according to a literature procedure.<sup>[171]</sup>



Compound **139** (5.8 g, 24 mmol) was added to a flask, followed by water (240 mL) and  $\text{KH}_2\text{PO}_4$  (7.3 g, 53 mmol). The resulting mixture was cooled to  $0\text{ }^\circ\text{C}$  and  $\text{NaIO}_4$  (12 g, 56 mmol) was added over 5 min. The resulting mixture was stirred at room temperature for 26 h. The reaction mixture was then diluted with EtOAc. The aqueous layer was extracted with EtOAc. The combined organic extracts were washed over sat. aq.  $\text{NaHCO}_3$ , dried over brine,  $\text{MgSO}_4$ , filtered and concentrated under reduced pressure. The crude material was purified by flash chromatography (petroleum ether 40–65/EtOAc, 7:3) to afford 2-(4-methoxyphenyl)-1,3-dioxan-5-one (**140**) as a white solid (4.5 g, 22 mmol, 92%).

$R_f = 0.26$  (petroleum ether 40–65/EtOAc, 7:3);

$^1\text{H NMR}$  (400 MHz,  $\text{CDCl}_3$ )  $\delta = 7.49 - 7.43$  (m, 2H,  $\text{H}_4$ ),  $6.96 - 6.89$  (m, 2H,  $\text{H}_3$ ),  $5.86$  (s, 1H,  $\text{H}_6$ ),  $4.55 - 4.42$  (m, 4H,  $\text{H}_7$ ),  $3.82$  (s, 3H,  $\text{H}_1$ ) ppm;

$^{13}\text{C NMR}$  (101 MHz,  $\text{CDCl}_3$ )  $\delta = 204.5$  (C=O,  $\text{C}_8$ ),  $160.5$  (C,  $\text{C}_2$ ),  $129.3$  (C,  $\text{C}_5$ ),  $127.6$  (CH,  $\text{C}_4$ ),  $114.0$  (CH,  $\text{C}_3$ ),  $99.1$  (CH,  $\text{C}_6$ ),  $72.6$  ( $\text{CH}_2$ ,  $\text{C}_7$ ),  $55.5$  ( $\text{CH}_3$ ,  $\text{C}_1$ ) ppm;

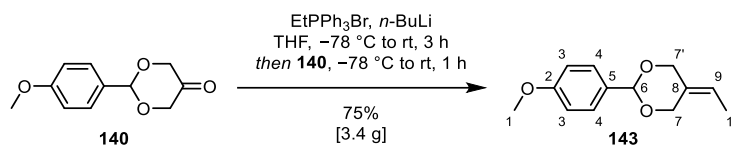
$\text{HRMS}$  ( $\text{ESI}^+$ )  $\text{C}_{11}\text{H}_{12}\text{O}_4$ : 209.0806 (found  $m/z$ ) [ $\text{M}+\text{H}$ ] $^+$  (calcd 209.0808);

$\text{IR}$  (thin film) 2840, 1742 (C=O), 1613 (C=C), 1587 (C=C), 1516, 1387, 1246 (C–O), 1172, 1123 (C–O), 1027, 970, 825, 735,  $424\text{ cm}^{-1}$ ;

**m.p.** 71–73  $^\circ\text{C}$ .

## Experimental

### Preparation of Compound 143



Ethyltriphenylphosphonium bromide (11 g, 53 mmol) was added to a flask, followed by THF (100 mL). The resulting mixture was cooled to  $-78\text{ }^{\circ}\text{C}$  and *n*-BuLi (1.6 M in hexanes, 16 mL) was slowly added. The resulting mixture was stirred at room temperature for 3 h. The resulting mixture was then cooled to  $-78\text{ }^{\circ}\text{C}$  and compound **140** (4.1 g, 20 mmol) in THF (100 mL) was slowly added. The resulting mixture was stirred at room temperature for 1 h. The reaction mixture was then quenched with acetone and Et<sub>2</sub>O, filtered through Celite and concentrated under reduced pressure. The crude material was purified by flash chromatography (petroleum ether 40–65/Et<sub>2</sub>O, 8:2) to afford 5-ethylidene-2-(4-methoxyphenyl)-1,3-dioxane (**143**) as a yellow solid (3.4 g, 15 mmol, 75%).

**R<sub>f</sub>** = 0.51 (petroleum ether 40–65/Et<sub>2</sub>O, 8:2);

**<sup>1</sup>H NMR** (500 MHz, CDCl<sub>3</sub>)  $\delta$  = 7.44 – 7.38 (m, 2H, H<sub>4</sub>), 6.92 – 6.86 (m, 2H, H<sub>3</sub>), 5.59 (s, 1H, H<sub>6</sub>), 5.48 (qdd, <sup>3</sup>*J*<sub>9,10</sub> = 6.9 Hz, <sup>4</sup>*J*<sub>7,9</sub> = 0.8 Hz, 1H, H<sub>9</sub>), 4.87 (ddd, <sup>2</sup>*J*<sub>7,7'</sub> = 13.0 Hz, <sup>4</sup>*J*<sub>7,7'</sub> = 0.8 Hz, <sup>4</sup>*J*<sub>7,7'</sub> = 0.8 Hz 1H, H<sub>7</sub>), 4.54 – 4.47 (m, 1H, H<sub>7'</sub>), 4.38 (dd, <sup>2</sup>*J*<sub>7,7'</sub> = 12.5 Hz, <sup>4</sup>*J*<sub>7,9</sub> = 1.6 Hz, 1H, H<sub>7'</sub>), 4.35 (d, <sup>2</sup>*J*<sub>7,7'</sub> = 13.1 Hz, 1H, H<sub>7</sub>), 3.80 (s, 3H, H<sub>1</sub>), 1.67 (dt, <sup>3</sup>*J*<sub>9,10</sub> = 6.9 Hz, <sup>5</sup>*J*<sub>7,10</sub> = 1.6 Hz, 3H, H<sub>10</sub>) ppm;

**<sup>13</sup>C NMR** (126 MHz, CDCl<sub>3</sub>)  $\delta$  = 160.1 (C, C<sub>2</sub>), 131.0 (C, C<sub>5</sub>), 130.0 (C=C, C<sub>8</sub>), 127.5 (CH, C<sub>4</sub>), 120.9 (C=C, C<sub>9</sub>), 113.8 (CH, C<sub>3</sub>), 101.7 (CH, C<sub>6</sub>), 72.6 (CH<sub>2</sub>, C<sub>7'</sub>), 66.1 (CH<sub>2</sub>, C<sub>7</sub>), 55.4 (CH<sub>3</sub>, C<sub>1</sub>), 12.4 (CH<sub>3</sub>, C<sub>10</sub>) ppm;

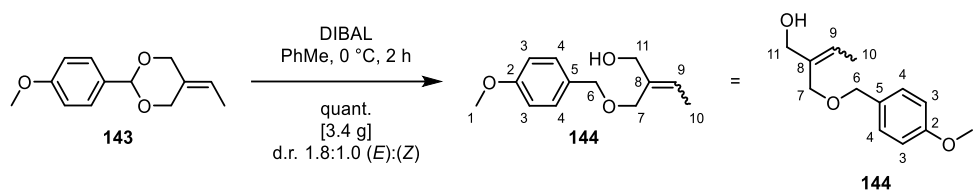
**HRMS** (ESI<sup>+</sup>) C<sub>13</sub>H<sub>16</sub>O<sub>3</sub>: 243.0872 (found *m/z*) [M+Na]<sup>+</sup> (calcd 243.0992);

**IR** (thin film) 2967, 2834, 1614 (C=C), 1517, 1386, 1246 (C–O), 1171, 1115 (C–O), 1073, 1031, 1011, 822 cm<sup>-1</sup>;

**m.p.** 44–46 °C.

## Experimental

### Preparation of Compounds (*Z*)-**144** and (*E*)-**144**



Compound **143** (3.4 g, 15 mmol) was added to a flask, followed by PhMe (150 mL). The resulting mixture was cooled to 0 °C and diisobutylaluminium hydride (DIBAL) (1.2 M in PhMe, 23 mL) was slowly added. The resulting mixture was stirred at 0 °C for 2 h. The reaction mixture was then quenched with MeOH. Sat. aq. Rochelle salt solution was added to the reaction mixture and the resulting mixture was stirred for 16 h at room temperature until two clear layers had formed. The aqueous layer was extracted with EtOAc. The combined organic extracts were dried over brine, MgSO<sub>4</sub>, filtered and concentrated under reduced pressure. The crude material was purified by flash chromatography (petroleum ether 40–65/Et<sub>2</sub>O, 8:2) to afford an inseparable diastereomeric mixture of 2-(((4-methoxybenzyl)oxy)methyl)but-2-en-1-ol (**144**) as a pale yellow oil (3.4 g, 15 mmol, quant., d.r. 1.8:1.0 (*E*):(*Z*)).

**R<sub>f</sub>** = 0.28 (petroleum ether 40–65/Et<sub>2</sub>O, 8:2);

(*Z*)-2-(((4-methoxybenzyl)oxy)methyl)but-2-en-1-ol ((*Z*)-**144**):

**<sup>1</sup>H NMR** (400 MHz, CDCl<sub>3</sub>) δ = 7.30 – 7.22 (m, 2H, H<sub>4</sub>)<sup>14</sup>, 6.91 – 6.85 (m, 2H, H<sub>3</sub>)<sup>14</sup>, 5.71 (q, <sup>3</sup>J<sub>9,10</sub> = 6.9 Hz, <sup>4</sup>J<sub>7,9</sub> = 1.0 Hz, <sup>4</sup>J<sub>9,11</sub> = 1.0 Hz, 1H, H<sub>9</sub>), 4.46 (s, 2H, H<sub>6</sub>), 4.16 (t, <sup>4</sup>J<sub>7,9</sub> = 0.8 Hz, 2H, H<sub>7</sub>), 4.13 (q, <sup>4</sup>J<sub>9,11</sub> = 1.1 Hz, 2H, H<sub>11</sub>), 3.81 (s, 3H, H<sub>1</sub>), 1.66 (d, <sup>3</sup>J<sub>9,10</sub> = 7.0 Hz, 3H, H<sub>10</sub>) ppm;

**<sup>13</sup>C NMR** (101 MHz, CDCl<sub>3</sub>) δ = 159.4 (C, C<sub>2</sub>), 136.0 (C=C, C<sub>8</sub>), 130.3 (C, C<sub>5</sub>), 129.5 (CH, C<sub>4</sub>), 127.0 (CH, C<sub>9</sub>), 114.0 (CH, C<sub>3</sub>), 72.4 (CH<sub>2</sub>, C<sub>6</sub>), 67.4 (CH<sub>2</sub>, C<sub>11</sub>), 66.6 (CH<sub>2</sub>, C<sub>7</sub>), 55.4 (CH<sub>3</sub>, C<sub>1</sub>), 13.2 (CH<sub>3</sub>, C<sub>10</sub>) ppm;

(*E*)-2-(((4-methoxybenzyl)oxy)methyl)but-2-en-1-ol ((*E*)-**144**):

**<sup>1</sup>H NMR** (400 MHz, CDCl<sub>3</sub>) δ = 7.30 – 7.22 (m, 2H, H<sub>4</sub>)<sup>14</sup>, 6.91 – 6.85 (m, 2H, H<sub>3</sub>)<sup>14</sup>, 5.64 (qt, <sup>3</sup>J<sub>9,10</sub> = 6.9 Hz, <sup>4</sup>J<sub>7,9</sub> = 0.8 Hz, 1H, H<sub>9</sub>), 4.45 (s, 2H, H<sub>6</sub>), 4.26 (s, 2H, H<sub>11</sub>), 4.06 (t, <sup>4</sup>J<sub>7,9</sub> = 1.0 Hz, 2H, H<sub>7</sub>), 3.80 (s, 3H, H<sub>1</sub>), 1.72 (d, <sup>3</sup>J<sub>9,10</sub> = 7.0 Hz, 3H, H<sub>10</sub>) ppm;

<sup>14</sup> Overlapping signals therefore not possible to accurately integrate, integrals shown are corrected.

## *Experimental*

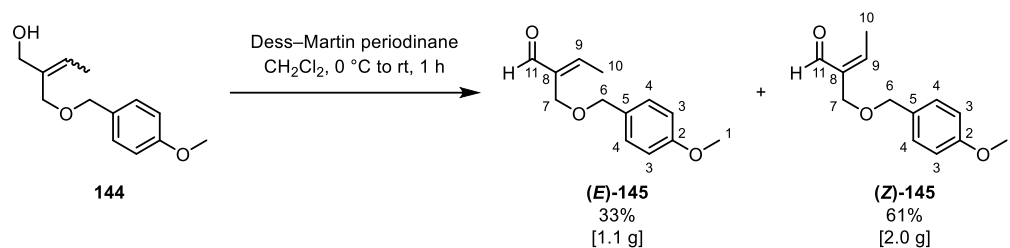
**<sup>13</sup>C NMR** (101 MHz, CDCl<sub>3</sub>)  $\delta$  = 159.4 (C, C<sub>2</sub>), 135.7 (C=C, C<sub>8</sub>), 130.2 (C, C<sub>5</sub>), 129.6 (CH, C<sub>4</sub>), 126.3 (CH, C<sub>9</sub>), 114.0 (CH, C<sub>3</sub>), 74.8 (CH<sub>2</sub>, C<sub>7</sub>), 72.1 (CH<sub>2</sub>, C<sub>6</sub>), 59.9 (CH<sub>2</sub>, C<sub>11</sub>), 55.4 (CH<sub>3</sub>, C<sub>1</sub>), 13.3 (CH<sub>3</sub>, C<sub>10</sub>) ppm;

**HRMS** (ESI<sup>+</sup>) C<sub>13</sub>H<sub>18</sub>O<sub>3</sub>: 245.1155 [M+Na]<sup>+</sup> (calcd 245.1148);

**IR** (thin film) 3402 (O–H), 2932, 2859, 1612 (C=C), 1586, 1512, 1244 (C–O), 1173 (C–O), 1063 (C–O), 1032, 1007, 818 cm<sup>-1</sup>.

## Experimental

### Preparation of Compounds (*E*)-145 and (*Z*)-145



Dess–Martin periodinane (**223**) (13 g, 31 mmol) was added to a flask, followed by CH<sub>2</sub>Cl<sub>2</sub> (60 mL). The resulting mixture was cooled to 0 °C and compound **144** (3.3 g, 15 mmol, d.r. 1.8:1.0 (*E*):(*Z*)) in CH<sub>2</sub>Cl<sub>2</sub> (15 mL) was added to the flask. The resulting mixture was stirred at 0 °C for 30 min, followed by stirring at room temperature for 30 min. The reaction mixture was then quenched with sat. aq. NaHCO<sub>3</sub>. Sat. aq. Na<sub>2</sub>S<sub>2</sub>O<sub>3</sub> was added to the flask and the resulting mixture was stirred until two clear layers had formed. The aqueous layer was extracted with CH<sub>2</sub>Cl<sub>2</sub>. The combined organic extracts were dried over brine, MgSO<sub>4</sub>, filtered and concentrated under reduced pressure. The crude material was purified by flash chromatography (petroleum ether 40–65/Et<sub>2</sub>O, 8:2) to afford (*E*)-2-(((4-methoxybenzyl)oxy)methyl)but-2-enal ((*E*)-**145**) as a pale yellow oil (1.1 g, 5.0 mmol, 33%) and (*Z*)-2-(((4-methoxybenzyl)oxy)methyl)but-2-enal ((*Z*)-**145**) as a pale yellow oil (2.0 g, 9.1 mmol, 61%).

(*E*)-2-(((4-methoxybenzyl)oxy)methyl)but-2-enal ((*E*)-**145**):

**R<sub>f</sub>** = 0.16 (petroleum ether 40–65/Et<sub>2</sub>O, 8:2);

**<sup>1</sup>H NMR** (500 MHz, CDCl<sub>3</sub>) δ = 9.44 (s, 1H, H<sub>11</sub>), 7.31 – 7.22 (m, 2H, H<sub>4</sub>), 6.92 – 6.86 (m, 2H, H<sub>3</sub>), 6.82 (q, <sup>3</sup>J<sub>9,10</sub> = 7.1 Hz, 1H, H<sub>9</sub>), 4.44 (s, 2H, H<sub>6</sub>), 4.21 (s, 2H, H<sub>7</sub>), 3.80 (s, 3H, H<sub>1</sub>), 2.07 (d, <sup>3</sup>J<sub>9,10</sub> = 7.1 Hz, 3H, H<sub>10</sub>) ppm;

**<sup>13</sup>C NMR** (126 MHz, CDCl<sub>3</sub>) δ = 193.8 (C=O, C<sub>1</sub>), 159.4 (C, C<sub>2</sub>), 154.7 (CH, C<sub>9</sub>), 140.9 (C=C, C<sub>8</sub>), 130.4 (C, C<sub>5</sub>), 129.6 (CH, C<sub>4</sub>), 113.9 (CH, C<sub>3</sub>), 72.7 (CH<sub>2</sub>, C<sub>6</sub>), 60.6 (CH<sub>2</sub>, C<sub>7</sub>), 55.4 (CH<sub>3</sub>, C<sub>1</sub>), 15.4 (CH<sub>3</sub>, C<sub>10</sub>) ppm;

**HRMS** (ESI<sup>+</sup>) C<sub>13</sub>H<sub>16</sub>O<sub>3</sub>: 243.1003 (found *m/z*) [M+Na]<sup>+</sup> (calcd 243.0992);

**IR** (thin film) 2953, 2923, 2853, 1685 (C=O), 1648 (C=C), 1612 (C=C), 1513, 1461, 1246 (C–O), 1078 (C–O), 1034, 819 cm<sup>-1</sup>.

## Experimental

(*Z*)-2-(((4-methoxybenzyl)oxy)methyl)but-2-enal ((*Z*)-**145**):

**R<sub>f</sub>** = 0.23 (petroleum ether 40–65/Et<sub>2</sub>O, 8:2);

**<sup>1</sup>H NMR** (500 MHz, CDCl<sub>3</sub>) δ = 10.16 (s, 1H, H<sub>11</sub>), 7.29 – 7.24 (m, 2H, H<sub>4</sub>), 6.90 – 6.82 (m, 3H, H<sub>3,9</sub>), 4.48 (s, 2H, H<sub>6</sub>), 4.12 (t, <sup>4</sup>*J*<sub>7,10</sub> = 1.4 Hz, 2H, H<sub>7</sub>), 3.80 (s, 3H, H<sub>1</sub>), 2.17 (dt, <sup>3</sup>*J*<sub>9,10</sub> = 7.7 Hz, <sup>4</sup>*J*<sub>7,10</sub> = 1.4 Hz, 3H, H<sub>10</sub>) ppm;

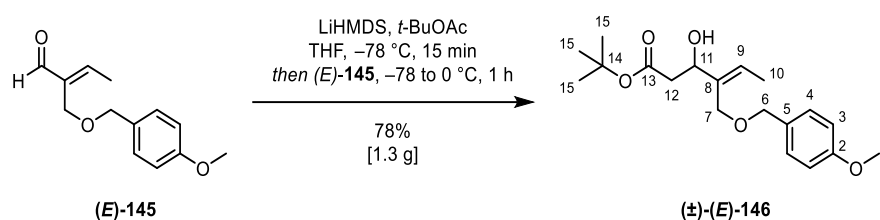
**<sup>13</sup>C NMR** (126 MHz, CDCl<sub>3</sub>) δ = 190.0 (C=O, C<sub>11</sub>), 159.4 (C, C<sub>2</sub>), 145.4 (C=C, C<sub>9</sub>), 137.4 (C=C, C<sub>8</sub>), 130.3 (C, C<sub>5</sub>), 129.5 (CH, C<sub>4</sub>), 113.9 (CH, C<sub>3</sub>), 72.8 (CH<sub>2</sub>, C<sub>6</sub>), 67.2 (CH<sub>2</sub>, C<sub>7</sub>), 55.4 (CH<sub>3</sub>, C<sub>1</sub>), 13.1 (CH<sub>3</sub>, C<sub>10</sub>) ppm;

**HRMS** (ESI<sup>+</sup>) C<sub>13</sub>H<sub>16</sub>O<sub>3</sub>: 243.0995 (found *m/z*) [M+Na]<sup>+</sup> (calcd 243.0992);

**IR** (thin film) 2953, 2922, 2853, 1673 (C=O), 1612 (C=C), 1513, 1460, 1246 (C–O), 1098 (C–O), 1034, 821 cm<sup>-1</sup>.

## Experimental

### Preparation of Compound (*E*)-146



LiHMDS (1.0 M in THF, 7.5 mL, 7.5 mmol) and THF (30 mL) were added to a flask. The resulting mixture was cooled to  $-78 \text{ } ^\circ\text{C}$  and *tert*-butyl acetate (0.80 mL, 6.0 mmol) was slowly added. The resulting mixture was stirred at  $-78 \text{ } ^\circ\text{C}$  for 15 min. Compound (*E*)-145 (1.1 g, 5.0 mmol) in THF (20 mL) was then slowly added to the flask. The resulting mixture was stirred at  $-78 \text{ } ^\circ\text{C}$  for 15 min, followed by stirring at  $0 \text{ } ^\circ\text{C}$  for 45 min. The reaction mixture was then quenched with sat. aq.  $\text{NH}_4\text{Cl}$ . The aqueous layer was extracted with  $\text{Et}_2\text{O}$ . The combined organic extracts were dried over brine,  $\text{MgSO}_4$ , filtered and concentrated under reduced pressure. The crude material was purified by flash chromatography (petroleum ether 40–65/ $\text{Et}_2\text{O}$ , 6:4) to afford *tert*-butyl (*E*)-3-hydroxy-4-(((4-methoxybenzyl)oxy)methyl)hex-4-enoate ((*E*)-146) as a colourless oil (1.3 g, 3.9 mmol, 78%).

$R_f = 0.36$  (petroleum ether 40–65/ $\text{Et}_2\text{O}$ , 6:4);

$^1\text{H NMR}$  (400 MHz,  $\text{CDCl}_3$ )  $\delta = 7.33 - 7.23$  (m, 2H,  $\text{H}_4$ ), 6.93 – 6.84 (m, 2H,  $\text{H}_3$ ), 5.79 (q,  $^3J_{9,10} = 6.9$  Hz, 1H,  $\text{H}_9$ ), 4.58 – 4.47 (m, 1H,  $\text{H}_{11}$ ), 4.45 (s, 2H,  $\text{H}_6$ ), 4.16 – 4.07 (m, 2H,  $\text{H}_7$ ), 3.81 (s, 3H,  $\text{H}_1$ ), 3.33 (d,  $^3J_{11,\text{OH}} = 5.0$  Hz, 1H, OH), 2.55 (d,  $^3J_{11,12} = 8.0$  Hz, 1H,  $\text{H}_{12}$ ), 2.54 (d,  $^3J_{11,12} = 5.3$  Hz, 1H,  $\text{H}_{12}$ ), 1.66 (d,  $^3J_{9,10} = 7.0$ , 3H,  $\text{H}_{10}$ ), 1.44 (s, 9H,  $\text{H}_{15}$ ) ppm;

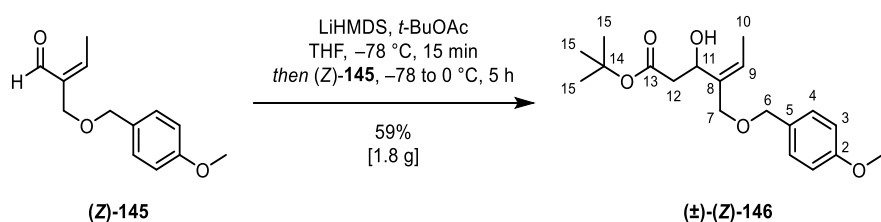
$^{13}\text{C NMR}$  (101 MHz,  $\text{CDCl}_3$ )  $\delta = 171.9$  (C=O,  $\text{C}_{13}$ ), 159.5 (C,  $\text{C}_2$ ), 136.7 (C=C,  $\text{C}_8$ ), 130.3 (C,  $\text{C}_5$ ), 129.6 (CH,  $\text{C}_4$ ), 126.4 (CH,  $\text{C}_9$ ), 114.0 (CH,  $\text{C}_3$ ), 81.1 (C,  $\text{C}_{14}$ ), 72.4 ( $\text{CH}_2$ ,  $\text{C}_6$ ), 72.3 (CH,  $\text{C}_{11}$ ), 65.1 ( $\text{CH}_2$ ,  $\text{C}_7$ ), 55.4 ( $\text{CH}_3$ ,  $\text{C}_1$ ), 42.2 ( $\text{CH}_2$ ,  $\text{C}_{12}$ ), 28.3 ( $\text{CH}_3$ ,  $\text{C}_{15}$ ), 13.3 ( $\text{CH}_3$ ,  $\text{C}_{10}$ ) ppm;

**HRMS** ( $\text{ESI}^+$ )  $\text{C}_{19}\text{H}_{28}\text{O}_5$ : 359.1827 [ $\text{M}+\text{Na}$ ] $^+$  (calcd 359.1829);

**IR** (thin film) 3480 (O–H), 2956, 2923, 2852, 1730 (C=O), 1613 (C=C), 1514, 1265 (C–O), 1249 (C–O), 1173 (C–O), 1152 (C–O), 738  $\text{cm}^{-1}$ .

## Experimental

### Preparation of Compound (Z)-146



LiHMDS (1.0 M in THF, 28 mL, 28 mmol) and THF (75 mL) were added to a flask. The resulting mixture was cooled to  $-78\text{ }^{\circ}\text{C}$  and *tert*-butyl acetate (3.0 mL, 22 mmol) was slowly added. The resulting mixture was stirred at  $-78\text{ }^{\circ}\text{C}$  for 15 min. Compound (Z)-145 (2.0 g, 9.1 mmol) in THF (15 mL) was then slowly added to the flask. The resulting mixture was stirred at  $-78\text{ }^{\circ}\text{C}$  for 15 min, followed by stirring at  $0\text{ }^{\circ}\text{C}$  for 5 h. The reaction mixture was then quenched with sat. aq.  $\text{NH}_4\text{Cl}$ . The aqueous layer was extracted with  $\text{Et}_2\text{O}$ . The combined organic extracts were dried over brine,  $\text{MgSO}_4$ , filtered and concentrated under reduced pressure. The crude material was purified by flash chromatography (petroleum ether 40–65/ $\text{Et}_2\text{O}$ , 6:4) to afford *tert*-butyl (Z)-3-hydroxy-4-(((4-methoxybenzyl)oxy)methyl)hex-4-enoate ((Z)-146) as a colourless oil (1.8 g, 5.4 mmol, 59%).

$R_f = 0.43$  (petroleum ether 40–65/ $\text{Et}_2\text{O}$ , 6:4);

$^1\text{H NMR}$  (400 MHz,  $\text{CDCl}_3$ )  $\delta = 7.32 - 7.21$  (m, 2H,  $\text{H}_4$ ), 6.92 – 6.84 (m, 2H,  $\text{H}_3$ ), 5.63 (dt,  $^3J_{9,10} = 7.0$  Hz,  $^4J_{7,9} = 1.2$  Hz,  $^4J_{7,9} = 0.6$  Hz, 1H,  $\text{H}_9$ ), 5.01 (ddd,  $^3J_{11,12} = 9.0$  Hz,  $^3J_{11,12} = 5.3$  Hz,  $^3J_{11,\text{OH}} = 5.2$  Hz, 1H,  $\text{H}_{11}$ ), 4.44 (s, 2H,  $\text{H}_6$ ), 4.12 (ddt,  $^2J_{7,7} = 11.3$  Hz,  $^4J_{6,7} = 1.1$  Hz,  $^4J_{7,9} = 1.1$  Hz, 1H,  $\text{H}_7$ ), 4.02 (dt,  $^2J_{7,7} = 11.2$  Hz,  $^4J_{6,7} = 0.9$  Hz, 1H,  $\text{H}_7$ ), 3.80 (s, 3H,  $\text{H}_1$ ), 3.34 (d,  $^3J_{11,\text{OH}} = 5.6$  Hz, 1H, OH), 2.70 (dd,  $^2J_{12,12} = 15.3$  Hz,  $^3J_{11,12} = 9.1$  Hz, 1H,  $\text{H}_{12}$ ), 2.41 (dd,  $^2J_{12,12} = 15.3$  Hz,  $^3J_{11,12} = 5.0$ , 1H,  $\text{H}_{12}$ ), 1.73 (ddd,  $^3J_{9,10} = 7.0$  Hz,  $^5J_{7,10} = 1.0$  Hz,  $^5J_{7,10} = 1.0$  Hz, 3H,  $\text{H}_{10}$ ), 1.45 (s, 9H,  $\text{H}_{15}$ ) ppm;

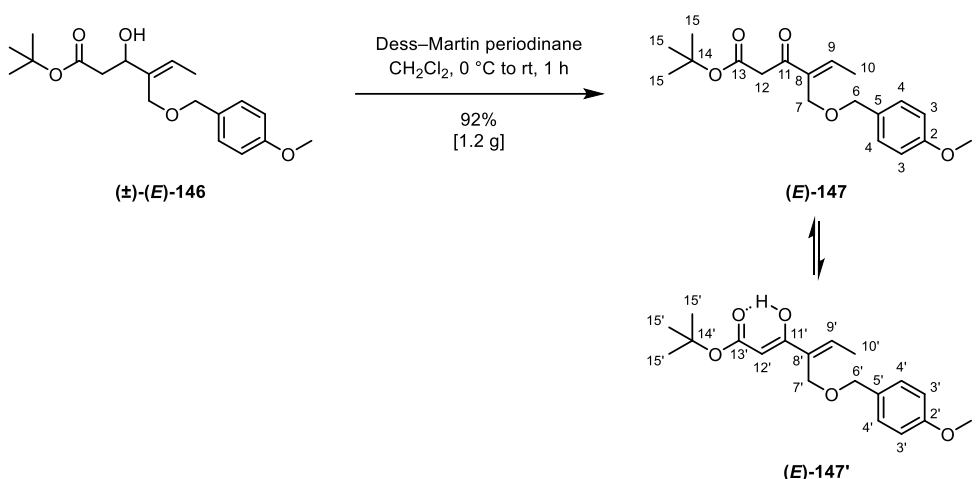
$^{13}\text{C NMR}$  (101 MHz,  $\text{CDCl}_3$ )  $\delta = 171.5$  (C=O,  $\text{C}_{13}$ ), 159.5 (C,  $\text{C}_2$ ), 136.3 (C=C,  $\text{C}_8$ ), 130.2 (C,  $\text{C}_5$ ), 129.6 (CH,  $\text{C}_4$ ), 127.2 (CH,  $\text{C}_9$ ), 114.0 (CH,  $\text{C}_3$ ), 81.0 (C,  $\text{C}_{14}$ ), 72.5 ( $\text{CH}_2$ ,  $\text{C}_7$ ), 72.1 ( $\text{CH}_2$ ,  $\text{C}_6$ ), 66.5 (CH,  $\text{C}_{11}$ ), 55.4 ( $\text{CH}_3$ ,  $\text{C}_1$ ), 42.3 ( $\text{CH}_2$ ,  $\text{C}_{12}$ ), 28.3 ( $\text{CH}_3$ ,  $\text{C}_{15}$ ), 13.3 ( $\text{CH}_3$ ,  $\text{C}_{10}$ ) ppm;

$\text{HRMS}$  ( $\text{ESI}^+$ )  $\text{C}_{19}\text{H}_{28}\text{O}_5$ : 359.1833 [ $\text{M}+\text{Na}$ ] $^+$  (calcd 359.1829);

$\text{IR}$  (thin film) 3486 (O–H), 2925, 2854, 1726 (C=O), 1613 (C=C), 1264 (C–O), 1248 (C–O), 1173 (C–O), 1151 (C–O), 1036, 735  $\text{cm}^{-1}$ .

## Experimental

### Preparation of Compound (E)-147



Dess–Martin periodinane (**223**) (3.2 g, 7.1 mmol) was added to a flask, followed by CH<sub>2</sub>Cl<sub>2</sub> (20 mL). The resulting mixture was cooled to 0 °C and compound (E)-**146** (1.3 g, 3.9 mmol) in CH<sub>2</sub>Cl<sub>2</sub> (20 mL) was added to the flask. The resulting mixture was stirred at 0 °C for 30 min, followed by stirring at room temperature for 1 h. The reaction mixture was then quenched with sat. aq. NaHCO<sub>3</sub>. Sat. aq. Na<sub>2</sub>S<sub>2</sub>O<sub>3</sub> was added to the flask and the resulting mixture was stirred until two clear layers had formed. The aqueous layer was extracted with CH<sub>2</sub>Cl<sub>2</sub>. The combined organic extracts were dried over brine, MgSO<sub>4</sub>, filtered and concentrated under reduced pressure. The crude material was purified by flash chromatography (petroleum ether 40–65/Et<sub>2</sub>O, 8:2) to afford keto and enol tautomers *tert*-butyl (E)-4-(((4-methoxybenzyl)oxy)methyl)-3-oxohex-4-enoate ((E)-**147**) and *tert*-butyl (2Z,4E)-3-hydroxy-4-(((4-methoxybenzyl)oxy)methyl)hexa-2,4-dienoate ((E)-**147'**) as a colourless oil (1.2 g, 3.6 mmol, 92%).

R<sub>f</sub> = 0.31 (petroleum ether 40–65/Et<sub>2</sub>O, 8:2);

<sup>1</sup>H NMR (600 MHz, CDCl<sub>3</sub>) δ = 12.41 (s, 1H, O–H)<sup>15</sup>, 7.29 – 7.23 (m, 2H, H<sub>4,4'</sub>)<sup>15</sup>, 6.94 (q, <sup>3</sup>J<sub>9,10</sub> = 7.1 Hz, 1H, H<sub>9</sub>), 6.90 – 6.85 (m, 2H, H<sub>3,3'</sub>)<sup>15</sup>, 6.79 (q, <sup>3</sup>J<sub>9',10'</sub> = 7.2 Hz, 1H, H<sub>9'</sub>)<sup>15</sup>, 5.22 (s, 1H, H<sub>12</sub>)<sup>15</sup>, 4.45 (s, 2H, H<sub>6</sub>)<sup>15</sup>, 4.44 (s, 2H, H<sub>6</sub>), 4.25 (s, 2H, H<sub>7</sub>), 4.12 (s, 2H, H<sub>7</sub>)<sup>15</sup>, 3.81 (s, 3H, H<sub>1'</sub>)<sup>15</sup>, 3.80 (s, 3H, H<sub>1</sub>), 3.61 (s, 2H, H<sub>12</sub>), 1.95 (d, <sup>3</sup>J<sub>9,10</sub> = 7.1 Hz, 3H, H<sub>10</sub>), 1.82 (d, <sup>3</sup>J<sub>9',10'</sub> = 7.3 Hz, 3H, H<sub>10'</sub>)<sup>15</sup>, 1.50 (s, 9H, H<sub>15</sub>)<sup>15</sup>, 1.44 (s, 9H, H<sub>15</sub>) ppm;

<sup>15</sup> Integral corrected for enol tautomer, keto:enol tautomer ratio 14:1 in CDCl<sub>3</sub>.

## Experimental

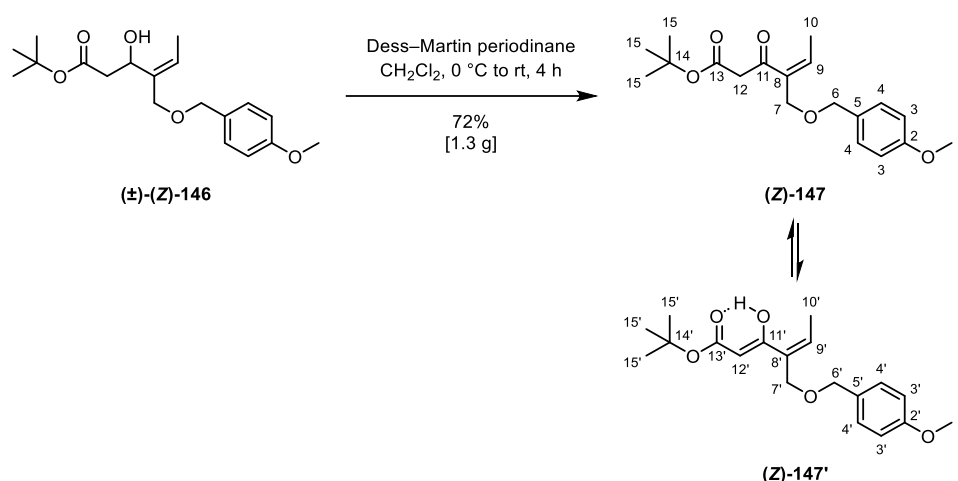
**<sup>13</sup>C NMR** (151 MHz, CDCl<sub>3</sub>)  $\delta$  = 193.4 (C=O, C<sub>11</sub>), 170.4 (C=O, C<sub>11'</sub>), 167.2 (C=O, C<sub>13,13'</sub>), 159.4 (C, C<sub>2,2'</sub>), 144.7 (CH, C<sub>9</sub>), 138.7 (C=C, C<sub>8</sub>), 135.6 (CH, C<sub>9'</sub>), 131.3 (C=C, C<sub>8'</sub>), 130.4 (C, C<sub>5,5'</sub>), 129.7 (CH, C<sub>4,4'</sub>), 113.94 (CH, C<sub>3'</sub>), 113.91 (CH, C<sub>3</sub>), 89.6 (CH, C<sub>12'</sub>), 81.8 (C, C<sub>14,14'</sub>), 72.5 (CH<sub>2</sub>, C<sub>6</sub>), 71.9 (CH<sub>2</sub>, C<sub>6'</sub>), 62.7 (CH<sub>2</sub>, C<sub>7'</sub>), 62.1 (CH<sub>2</sub>, C<sub>7</sub>), 55.4 (CH<sub>3</sub>, C<sub>1,1'</sub>), 46.7 (CH<sub>2</sub>, C<sub>12</sub>), 28.5 (CH<sub>3</sub>, C<sub>15'</sub>), 28.1 (CH<sub>3</sub>, C<sub>15</sub>), 15.2 (CH<sub>3</sub>, C<sub>10</sub>), 14.4 (CH<sub>3</sub>, C<sub>10'</sub>) ppm;

**HRMS** (ESI<sup>+</sup>) C<sub>19</sub>H<sub>26</sub>O<sub>5</sub>: 359.1670 [M+Na]<sup>+</sup> (calcd 357.1672);

**IR** (thin film) 2977, 2931, 2865, 1731 (C=O), 1672 (C=O), 1612 (C=C), 1513, 1368, 1247 (C–O), 1147 (C–O), 1077, 1034, 821 cm<sup>-1</sup>.

## Experimental

### Preparation of Compound (Z)-147



Dess–Martin periodinane (5.0 g, 12 mmol) was added to a flask, followed by CH<sub>2</sub>Cl<sub>2</sub> (30 mL). The resulting mixture was cooled to 0 °C and compound (Z)-146 (1.8 g, 5.4 mmol) in CH<sub>2</sub>Cl<sub>2</sub> (20 mL) was added to the flask. The resulting mixture was stirred at 0 °C for 30 min, followed by stirring at room temperature for 4 h. The reaction mixture was then quenched with sat. aq. NaHCO<sub>3</sub>. Sat. aq. Na<sub>2</sub>S<sub>2</sub>O<sub>3</sub> was added to the flask and the resulting mixture was stirred until two clear layers had formed. The aqueous layer was extracted with CH<sub>2</sub>Cl<sub>2</sub>. The combined organic extracts were dried over brine, MgSO<sub>4</sub>, filtered and concentrated under reduced pressure. The crude material was purified by flash chromatography (petroleum ether 40–65/Et<sub>2</sub>O, 9:1) to afford keto and enol tautomers *tert*-butyl (Z)-4-(((4-methoxybenzyl)oxy)methyl)-3-oxohex-4-enoate ((Z)-147) and *tert*-butyl (2Z,4Z)-3-hydroxy-4-(((4-methoxybenzyl)oxy)methyl)hexa-2,4-dienoate ((Z)-147') as a colourless oil (1.3 g, 3.9 mmol, 72%).

R<sub>f</sub> = 0.31 (petroleum ether 40–65/Et<sub>2</sub>O, 9:1);

<sup>1</sup>H NMR (500 MHz, CDCl<sub>3</sub>) δ = 12.41 (s, 1H, O–H)<sup>16</sup>, 7.26 – 7.21 (m, 2H, H<sub>4,4'</sub>), 6.90 – 6.84 (m, 2H, H<sub>3,3'</sub>), 6.14 (q, <sup>3</sup>J<sub>9,10</sub> = 7.2 Hz, 1H, H<sub>9</sub>), 6.00 (q, <sup>3</sup>J<sub>9',10'</sub> = 7.2 Hz, 1H, H<sub>9'</sub>)<sup>16</sup>, 5.09 (s, 1H, H<sub>12'</sub>)<sup>16</sup>, 4.44 (s, 2H, H<sub>6'</sub>)<sup>16</sup>, 4.41 (s, 2H, H<sub>6</sub>), 4.15 (s, 2H, H<sub>7</sub>), 4.06 (s, 2H, H<sub>7'</sub>)<sup>16</sup>, 3.80 (s, 3H, H<sub>1,1'</sub>), 3.56 (s, 2H, H<sub>12</sub>), 1.99 (d, <sup>3</sup>J<sub>7,8</sub> = 7.2 Hz, 3H, H<sub>10</sub>), 1.95 (d, <sup>3</sup>J<sub>7',8'</sub> = 7.2 Hz, 3H, H<sub>10'</sub>)<sup>16</sup>, 1.50 (s, 9H, H<sub>15'</sub>)<sup>16</sup>, 1.44 (s, 9H, H<sub>15</sub>) ppm;

<sup>16</sup> Integral corrected for enol tautomer, keto:enol tautomer ratio 4:1 in CDCl<sub>3</sub>.

## Experimental

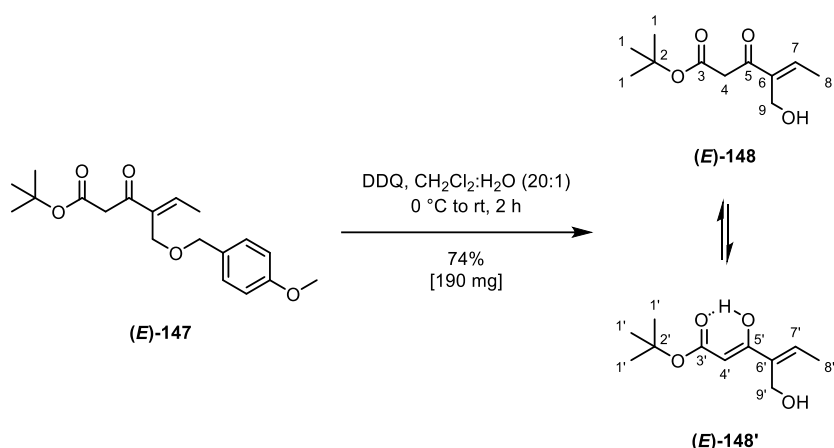
**<sup>13</sup>C NMR** (126 MHz, CDCl<sub>3</sub>)  $\delta$  = 196.2 (C=O, C<sub>11</sub>), 171.1 (C=O, C<sub>11'</sub>), 166.9 (C=O, C<sub>13,13'</sub>), 159.5 (C, C<sub>2,2'</sub>), 140.0 (CH, C<sub>9</sub>), 137.0 (C=C, C<sub>8</sub>), 134.0 (CH, C<sub>9'</sub>), 132.4 (C=C, C<sub>8'</sub>), 129.9 (C, C<sub>5,5'</sub>), 129.7 (CH, C<sub>4</sub>), 129.6 (CH, C<sub>4'</sub>), 114.0 (CH, C<sub>3</sub>), 113.9 (CH, C<sub>3'</sub>), 93.2 (CH, C<sub>12</sub>), 81.8 (C, C<sub>14,14'</sub>), 71.83 (CH<sub>2</sub>, C<sub>7</sub>), 71.80 (CH<sub>2</sub>, C<sub>6,6'</sub>), 71.7 (CH<sub>2</sub>, C<sub>7'</sub>), 55.4 (CH<sub>3</sub>, C<sub>1,1'</sub>), 49.8 (CH<sub>2</sub>, C<sub>12</sub>), 28.5 (CH<sub>3</sub>, C<sub>15'</sub>), 28.1 (CH<sub>3</sub>, C<sub>15</sub>), 15.8 (CH<sub>3</sub>, C<sub>10</sub>), 15.7 (CH<sub>3</sub>, C<sub>10'</sub>) ppm;

**HRMS** (ESI<sup>+</sup>) C<sub>19</sub>H<sub>26</sub>O<sub>5</sub>: 359.1670 [M+Na]<sup>+</sup> (calcd 357.1672);

**IR** (thin film) 2978, 2934, 2858, 1732 (C=O), 1693 (C=O), 1613 (C=C), 1513, 1367, 1247 (C–O), 1153 (C–O), 1063, 1035, 821 cm<sup>-1</sup>.

## Experimental

### Preparation of Compound (*E*)-148



Compound (*E*)-**147** (400 mg, 1.2 mmol) in CH<sub>2</sub>Cl<sub>2</sub> (11 mL) was added to a flask, followed by water (0.60 mL). The resulting mixture was cooled to 0 °C and 2,3-dichloro-5,6-dicyano-1,4-benzoquinone (DDQ) (410 mg, 1.8 mmol) was added. The resulting mixture was stirred at room temperature for 2 h. The reaction mixture was then quenched with sat. aq. NaHCO<sub>3</sub>. The aqueous layer was extracted with CH<sub>2</sub>Cl<sub>2</sub>. The combined organic extracts were dried over brine, MgSO<sub>4</sub>, filtered and concentrated under reduced pressure. The crude material was purified by flash chromatography (petroleum ether 40–65/Et<sub>2</sub>O, 4:6) to afford keto and enol tautomers *tert*-butyl (*E*)-4-(hydroxymethyl)-3-oxohex-4-enoate ((*E*)-**148**) and *tert*-butyl (2*Z*,4*E*)-3-hydroxy-4-(hydroxymethyl)hexa-2,4-dienoate ((*E*)-**148'**) as a colourless oil (190 mg, 0.89 mmol, 74%).

*R*<sub>f</sub> = 0.43 (petroleum ether 40–65/Et<sub>2</sub>O, 4:6);

<sup>1</sup>H NMR (400 MHz, CDCl<sub>3</sub>) δ = 12.52 (s, 1H, O–H)<sup>17</sup>, 6.83 (q, <sup>3</sup>*J*<sub>7,8</sub> = 7.1 Hz, 1H, H<sub>7</sub>), 6.65 (q, <sup>3</sup>*J*<sub>7',8'</sub> = 7.3 Hz, 1H, H<sub>7'</sub>)<sup>17</sup>, 5.28 (s, 1H, H<sub>4</sub>)<sup>17</sup>, 4.36 (s, 2H, H<sub>9</sub>), 4.34 (s, 2H, H<sub>9'</sub>)<sup>17</sup>, 3.62 (s, 2H, H<sub>4</sub>), 2.52 (s, 1H, O–H), 1.99 (d, <sup>3</sup>*J*<sub>7,8</sub> = 7.1 Hz, 3H, H<sub>8</sub>), 1.90 (d, <sup>3</sup>*J*<sub>7',8'</sub> = 7.3 Hz, 3H, H<sub>8'</sub>)<sup>17</sup>, 1.50 (s, 9H, H<sub>1</sub>)<sup>17</sup>, 1.45 (s, 9H, H<sub>1</sub>) ppm;

<sup>13</sup>C NMR<sup>18</sup> (101 MHz, CDCl<sub>3</sub>) δ = 195.7 (C=O, C<sub>5</sub>), 166.9 (C=O, C<sub>3</sub>), 142.7 (C=C, C<sub>7</sub>), 140.9 (CH, C<sub>6</sub>), 82.2 (C, C<sub>2</sub>), 56.8 (CH<sub>2</sub>, C<sub>9</sub>), 46.4 (CH<sub>2</sub>, C<sub>4</sub>), 28.1 (CH<sub>3</sub>, C<sub>1</sub>), 14.8 (CH<sub>3</sub>, C<sub>8</sub>) ppm;

<sup>17</sup> Integral corrected for enol tautomer, keto:enol tautomer ratio 30:1 in CDCl<sub>3</sub>.

<sup>18</sup> Due to the low ratio of the enol tautomer (keto:enol 30:1 in CDCl<sub>3</sub>), only the signals of the keto tautomer are described.

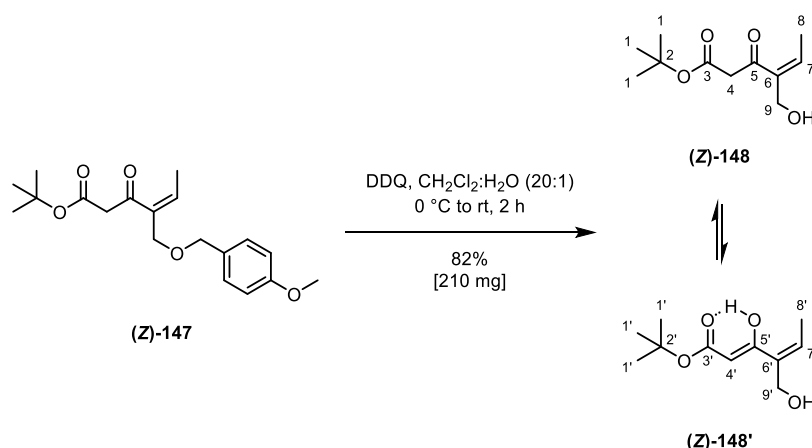
## *Experimental*

**HRMS** (ESI<sup>+</sup>) C<sub>11</sub>H<sub>18</sub>O<sub>4</sub>: 237.1084 [M+Na]<sup>+</sup> (calcd 237.1097);

**IR** (thin film) 3441 (O–H), 2977, 2933, 1729 (C=O), 1393, 1254, 1151 (C–O), 1026, 843 cm<sup>-1</sup>.

## Experimental

### Preparation of Compound (Z)-148



Compound (Z)-147 (410 mg, 1.2 mmol) in CH<sub>2</sub>Cl<sub>2</sub> (11 mL) was added to a flask, followed by water (0.60 mL). The resulting mixture was cooled to 0 °C and 2,3-dichloro-5,6-dicyano-1,4-benzoquinone (DDQ) (420 mg, 1.9 mmol) was added. The resulting mixture was stirred at room temperature for 2 h. The reaction mixture was then quenched with sat. aq. NaHCO<sub>3</sub>. The aqueous layer was extracted with CH<sub>2</sub>Cl<sub>2</sub>. The combined organic extracts were dried over brine, MgSO<sub>4</sub>, filtered and concentrated under reduced pressure. The crude material was purified by flash chromatography (petroleum ether 40–65/Et<sub>2</sub>O, 6:4) to afford keto and enol tautomers *tert*-butyl (Z)-4-(hydroxymethyl)-3-oxohex-4-enoate ((Z)-148) and *tert*-butyl (2Z,4Z)-3-hydroxy-4-(hydroxymethyl)hexa-2,4-dienoate ((Z)-148') as a colourless oil (210 mg, 0.98 mmol, 82%).

R<sub>f</sub> = 0.28 (petroleum ether 40–65/Et<sub>2</sub>O, 6:4);

<sup>1</sup>H NMR (400 MHz, CDCl<sub>3</sub>) δ = 12.51 (s, 1H, O–H)<sup>19</sup>, 6.21 (q, <sup>3</sup>J<sub>7,8</sub> = 7.3 Hz, 1H, H<sub>7</sub>), 6.00 (q, <sup>3</sup>J<sub>7',8'</sub> = 7.2 Hz, 1H, H<sub>7'</sub>)<sup>19</sup>, 5.08 (s, 1H, H<sub>4</sub>)<sup>19</sup>, 4.29 (s, 2H, H<sub>9</sub>), 4.22 (s, 2H, H<sub>9'</sub>)<sup>19</sup>, 3.62 (s, 2H, H<sub>4</sub>), 1.97 (d, <sup>3</sup>J<sub>7,8</sub> = 7.4 Hz, 3H, H<sub>8</sub>), 1.92 (d, <sup>3</sup>J<sub>7',8'</sub> = 7.2 Hz, 3H, H<sub>8'</sub>)<sup>19</sup>, 1.51 (s, 9H, H<sub>1</sub>)<sup>19</sup>, 1.46 (s, 9H, H<sub>1</sub>) ppm;

<sup>13</sup>C NMR (101 MHz, CDCl<sub>3</sub>) δ = 196.9 (C=O, C<sub>5</sub>), 172.9 (C=O, C<sub>3</sub>), 170.7 (C=O, C<sub>5'</sub>), 167.0 (C=O, C<sub>3</sub>), 140.0 (C=C, C<sub>6</sub>), 138.6 (CH, C<sub>7</sub>), 135.1 (C=C, C<sub>6'</sub>), 132.8 (CH, C<sub>7'</sub>), 93.7 (CH, C<sub>4</sub>), 82.3 (C, C<sub>2</sub>), 81.4 (C, C<sub>2'</sub>), 65.9 (CH<sub>2</sub>, C<sub>9</sub>), 65.7 (CH<sub>2</sub>, C<sub>9'</sub>), 50.3 (CH<sub>2</sub>, C<sub>4</sub>), 28.5 (CH<sub>3</sub>, C<sub>1</sub>), 28.1 (CH<sub>3</sub>, C<sub>1</sub>), 15.9 (CH<sub>3</sub>, C<sub>8</sub>), 15.7 (CH<sub>3</sub>, C<sub>8'</sub>) ppm;

<sup>19</sup> Integral corrected for enol tautomer, keto:enol tautomer ratio 3:1 in CDCl<sub>3</sub>.

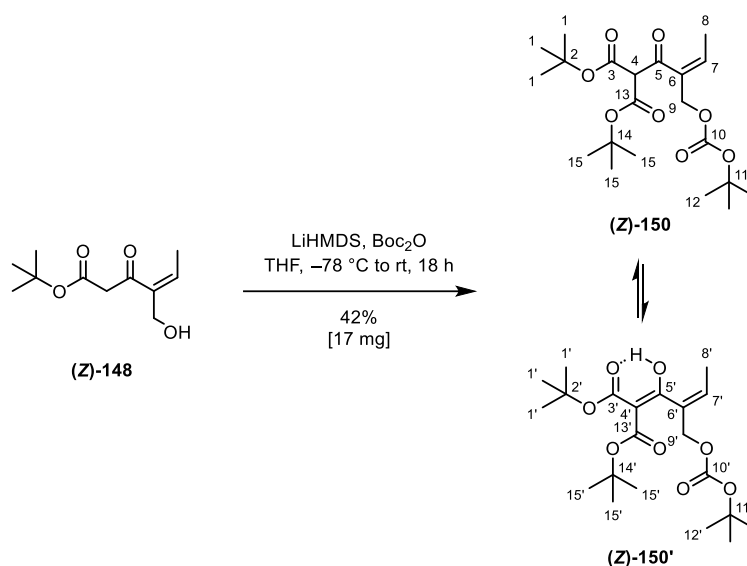
## *Experimental*

**HRMS** (ESI<sup>+</sup>) C<sub>11</sub>H<sub>18</sub>O<sub>4</sub>: 237.1075 [M+Na]<sup>+</sup> (calcd 237.1097);

**IR** (thin film) 3433 (O–H), 2978, 2931, 1729 (C=O), 1689 (C=O), 1624 (C=C), 1393, 1317, 1249, 1149 (C–O), 1001, 838 cm<sup>-1</sup>.

## Experimental

### Preparation of Compound (Z)-150



Compound (Z)-148 (21 mg, 98  $\mu$ mol) in THF (1.0 mL) was added to a flask. The resulting mixture was cooled to  $-78$  °C and LiHMDS (1.0 M in THF, 0.20 mL, 0.20 mmol) was slowly added. The resulting mixture was stirred for 15 min. Di-*tert*-butyl dicarbonate (Boc<sub>2</sub>O) (60  $\mu$ L, 0.26 mmol) was then added and the resulting mixture was stirred at  $-78$  °C for 15 min, followed by at 0 °C for 1 h and at room temperature for 18 h. The reaction mixture was then quenched with sat. aq. NH<sub>4</sub>Cl. The aqueous layer was extracted with Et<sub>2</sub>O. The combined organic extracts were dried over brine, MgSO<sub>4</sub>, filtered and concentrated under reduced pressure. The crude material was purified by flash chromatography (petroleum ether 40–65/Et<sub>2</sub>O, 19:1) to afford keto and enol tautomers di-*tert*-butyl (Z)-2-(2-(((*tert*-butoxycarbonyl)oxy)methyl)but-2-enoyl)malonate ((Z)-150) and di-*tert*-butyl (Z)-2-(2-(((*tert*-butoxycarbonyl)oxy)methyl)-1-hydroxybut-2-en-1-ylidene)malonate ((Z)-150') as a colourless oil (17 mg, 41  $\mu$ mol, 42%).

R<sub>f</sub> = 0.56 (petroleum ether 40–65/Et<sub>2</sub>O, 19:1);

<sup>1</sup>H NMR<sup>20</sup> (600 MHz, CDCl<sub>3</sub>)  $\delta$  = 6.11 (q, <sup>3</sup>J<sub>7,8</sub> = 7.2 Hz, 1H, H<sub>7</sub>), 5.60 (s, 1H, H<sub>4</sub>), 4.59 (s, 2H, H<sub>9</sub>), 1.92 (d, <sup>3</sup>J<sub>7,8</sub> = 7.2 Hz, 3H), 1.52 (s, 9H, H<sub>12</sub>), 1.47 (s, 18H, H<sub>1,15</sub>) ppm;

<sup>13</sup>C NMR<sup>20</sup> (151 MHz, CDCl<sub>3</sub>)  $\delta$  = 163.3 (C=O, C<sub>5</sub>), 154.1 (C=O, C<sub>3/13</sub>)<sup>21</sup>, 153.3 (C=O, C<sub>10</sub>), 149.8 (C=O, C<sub>3/13</sub>)<sup>21</sup>, 136.4 (C=C, C<sub>7</sub>), 130.3 (C=C, C<sub>6</sub>), 112.9 (CH, C<sub>4</sub>), 83.8 (CH<sub>3</sub>, C<sub>11</sub>), 82.4

<sup>20</sup> Due to the low ratio of the enol tautomer (keto:enol 25:1 in CDCl<sub>3</sub>), only the signals of the keto tautomer are described.

<sup>21</sup> Not possible to differentiate between the two C atoms.

## *Experimental*

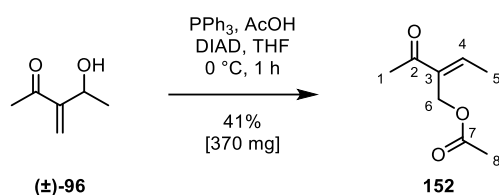
(CH<sub>3</sub>, C<sub>2/14</sub>)<sup>21</sup>, 80.9 (CH<sub>3</sub>, C<sub>2/14</sub>)<sup>21</sup>, 68.5 (CH<sub>2</sub>, C<sub>9</sub>), 28.3 (CH<sub>3</sub>, C<sub>1/15</sub>)<sup>21</sup>, 27.9 (CH<sub>3</sub>, C<sub>1/15</sub>)<sup>21</sup>, 27.8 (CH<sub>3</sub>, C<sub>12</sub>), 15.5 (CH<sub>3</sub>, C<sub>8</sub>) ppm;

**HRMS** (ESI<sup>+</sup>) C<sub>21</sub>H<sub>34</sub>O<sub>8</sub>: 437.2171 [M+Na]<sup>+</sup> (calcd 437.2146);

**IR** (thin film) 2980, 2934, 1762 (C=O), 1742 (C=O), 1718 (C=O), 1649 (C=C), 1275, 1254, 1160 (C–O), 1138 (C–O), 1109, 860 cm<sup>-1</sup>.

## Experimental

### Preparation of Compound 152



Triphenylphosphine (1.8 g, 6.9 mmol) was added to a flask, followed by compound **96** (660 mg, 5.8 mmol), THF (47 mL) and acetic acid (AcOH) (0.93 mL, 16 mmol). The resulting mixture was cooled to  $0\text{ }^\circ\text{C}$  and diisopropyl azodicarboxylate (DIAD) (1.4 mL, 7.0 mmol) was added dropwise. The resulting mixture was stirred for 1 h at  $0\text{ }^\circ\text{C}$ . The reaction mixture was then concentrated under reduced pressure. The residue was diluted with sat. aq.  $\text{NaHCO}_3$  and the aqueous layer was extracted with  $\text{Et}_2\text{O}$ . The combined organic extracts were dried over brine,  $\text{MgSO}_4$ , filtered and concentrated under reduced pressure. The residue was triturated (petroleum ether 40–65/ $\text{Et}_2\text{O}$ , 95:5), filtered and concentrated under reduced pressure. The crude material was purified by flash chromatography (petroleum ether 40–65/ $\text{EtOAc}$ , 7:3) followed by Kugelrohr distillation ( $7 \times 10^{-2}$  mbar,  $160\text{ }^\circ\text{C}$  to  $6 \times 10^{-2}$  mbar,  $200\text{ }^\circ\text{C}$ ) to afford (*E*)-2-acetylbut-2-en-1-yl acetate (**152**) as a colourless oil (370 mg, 2.4 mmol, 41%).

$R_f = 0.35$  (petroleum ether 40–65/ $\text{EtOAc}$ , 7:3);

$^1\text{H NMR}$  (400 MHz,  $\text{CDCl}_3$ )  $\delta = 7.00$  (q,  $^3J_{4,5} = 7.1$ , 1H, H<sub>4</sub>), 4.85 (s, 2H, H<sub>6</sub>), 2.33 (s, 3H, H<sub>1</sub>), 2.02 (s, 3H, H<sub>8</sub>), 1.99 (d,  $^3J_{4,5} = 7.1$ , 3H, H<sub>5</sub>) ppm;

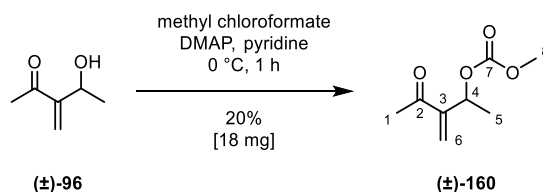
$^{13}\text{C NMR}$  (101 MHz,  $\text{CDCl}_3$ )  $\delta = 197.9$  (C=O, C<sub>2</sub>), 171.0 (C=O, C<sub>7</sub>), 144.6 (C=C, C<sub>4</sub>), 137.6 (C=C, C<sub>3</sub>), 56.9 (CH<sub>2</sub>, C<sub>6</sub>), 25.7 (CH<sub>3</sub>, C<sub>1</sub>), 21.0 (CH<sub>3</sub>, C<sub>8</sub>), 15.1 (CH<sub>3</sub>, C<sub>5</sub>) ppm;

$\text{MS}$  (EI-GCMS)  $m/z$  (%) = 141 (1), 113 (100), 97 (8);

$\text{IR}$  (thin film) 2954, 2923, 1738 (C=O), 1673 (C=O), 1369, 1231 (C–O),  $1026\text{ cm}^{-1}$ .

## Experimental

### Preparation of Compound 160



Compound **96** (54  $\mu$ L, 0.50 mmol) was added to a flask, followed by  $\text{CH}_2\text{Cl}_2$  (0.42 mL). The resulting mixture was cooled to 0 °C and methyl chloroformate (60  $\mu$ L, 0.78 mmol), 4-dimethylaminopyridine (DMAP) (6.1 mg, 0.050 mmol) and pyridine (50  $\mu$ L, 0.62 mmol) were added. The resulting mixture was stirred for 1 h at 0 °C. The reaction mixture was then quenched with 1.0 M aq. HCl. The aqueous layer was extracted with  $\text{Et}_2\text{O}$ . The combined organic extracts were dried over brine,  $\text{MgSO}_4$ , filtered and concentrated under reduced pressure. The crude material was purified by flash chromatography (petroleum ether 40–65/ $\text{Et}_2\text{O}$ , 8:2) to afford methyl (3-methylene-4-oxopentan-2-yl) carbonate (**160**) as a colourless oil (18 mg, 0.10 mmol, 20%).

$R_f$  = 0.33 (petroleum ether 40–65/ $\text{Et}_2\text{O}$ , 8:2);

$^1\text{H NMR}$  (600 MHz,  $\text{CDCl}_3$ )  $\delta$  = 6.13 (s, 1H,  $\text{H}_6$ ), 6.07 (d,  $^4J_{4,6}$  = 1.2 Hz, 1H,  $\text{H}_6$ ), 5.63 (qd,  $^3J_{4,5}$  = 6.5 Hz,  $^4J_{4,6}$  = 1.2 Hz, 1H,  $\text{H}_4$ ), 3.76 (s, 3H,  $\text{H}_8$ ), 2.35 (s, 3H,  $\text{H}_1$ ), 1.38 (d,  $^3J_{4,5}$  = 6.5 Hz, 3H,  $\text{H}_5$ ) ppm;

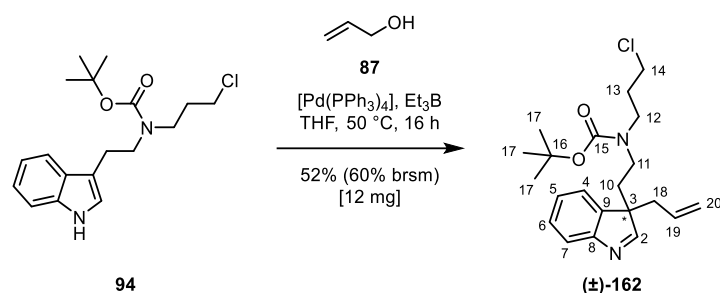
$^{13}\text{C NMR}$  (151 MHz,  $\text{CDCl}_3$ )  $\delta$  = 197.9 (C=O,  $\text{C}_2$ ), 154.9 (C=O,  $\text{C}_7$ ), 149.1 (C=C,  $\text{C}_3$ ), 124.7 (C=C,  $\text{C}_6$ ), 71.6 (CH,  $\text{C}_4$ ), 54.9 ( $\text{CH}_3$ ,  $\text{C}_8$ ), 26.1 ( $\text{CH}_3$ ,  $\text{C}_1$ ), 20.8 ( $\text{CH}_3$ ,  $\text{C}_5$ ) ppm;

$\text{HRMS}$  ( $\text{ESI}^+$ )  $\text{C}_8\text{H}_{12}\text{O}_4$ : 195.0654 (found  $m/z$ ) [ $\text{M}+\text{Na}$ ] $^+$  (calcd 195.0646);

$\text{IR}$  (thin film) 2959, 2920, 2851, 1747 (C=O), 1677 (C=O), 1262 (C–O), 1076  $\text{cm}^{-1}$ .

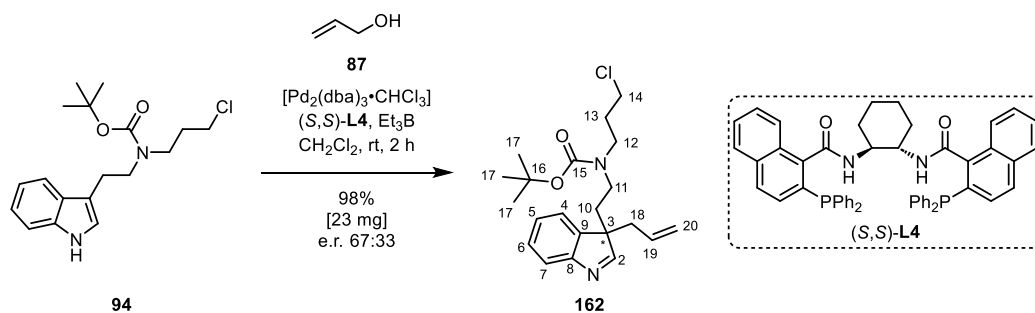
## Preparation of Compound 162

### Non-stereoselective method:



$[\text{Pd}(\text{PPh}_3)_4]$  (4.7 mg, 4.1  $\mu\text{mol}$ ) was added to a flask, followed by compound **94** (21 mg, 62  $\mu\text{mol}$ ) in THF (1.0 mL),  $\text{Et}_3\text{B}$  (1.0 M in hexanes, 70  $\mu\text{L}$ , 70  $\mu\text{mol}$ ) and allyl alcohol (**87**) (12  $\mu\text{L}$ , 180  $\mu\text{mol}$ ). The resulting mixture was stirred at 50 °C for 16 h. The reaction mixture was then diluted with EtOAc and washed with sat. aq.  $\text{NaHCO}_3$ . The organic layer was dried over brine,  $\text{MgSO}_4$ , filtered and concentrated under reduced pressure. The crude material was purified by flash chromatography (petroleum ether 40–65/ $\text{Et}_2\text{O}$ , 6:4) to afford *tert*-butyl (2-(3-allyl-3*H*-indol-3-yl)ethyl)(3-chloropropyl)carbamate (**162**) as a colourless oil (12 mg, 32  $\mu\text{mol}$ , 52%, 60% brsm).

### Enantioselective method:



$[\text{Pd}_2(\text{dba})_3 \cdot \text{CHCl}_3]$  (2.4 mg, 2.3  $\mu\text{mol}$ ) and (*S,S*)-DACH-naphthyl Trost Ligand **L4** (4.5 mg, 6.5  $\mu\text{mol}$ ) were added to a flask, followed by compound **94** (21 mg, 62  $\mu\text{mol}$ ) in  $\text{CH}_2\text{Cl}_2$  (0.6 mL). The resulting mixture was stirred at room temperature for 15 min.  $\text{Et}_3\text{B}$  (1.0 M in hexanes, 80  $\mu\text{L}$ , 80  $\mu\text{mol}$ ) was then added to the flask and the resulting mixture was stirred for a further 5 min. Allyl alcohol (**87**) (12  $\mu\text{L}$ , 180  $\mu\text{mol}$ ) was then added to the flask and the resulting mixture was stirred for 2 h. The reaction mixture was then quenched with EtOAc and aq.  $\text{NaOH}$  (2.0 M). The resulting mixture was stirred for 2 h. The organic layer was separated and washed with sat. aq.  $\text{Na}_2\text{CO}_3$ , dried over brine,  $\text{MgSO}_4$ , filtered and concentrated under reduced pressure. The crude material was purified by flash chromatography

## Experimental

(petroleum ether 40–65/Et<sub>2</sub>O, 6:4) to afford *tert*-butyl (*R*)-(2-(3-allyl-3*H*-indol-3-yl)ethyl)(3-chloropropyl)carbamate (**162**) as a colourless oil (23 mg, 61 μmol, 98%, e.r. 67:33).

**R<sub>f</sub>** = 0.23 (petroleum ether 40–65/Et<sub>2</sub>O, 6:4);

**<sup>1</sup>H NMR** (400 MHz, CDCl<sub>3</sub>) δ 8.04 (s, 1H, H<sub>2</sub>), 7.63 (d, <sup>3</sup>J<sub>4,5</sub> = 7.7 Hz, 1H, H<sub>4</sub>), 7.44 – 7.22 (m, 3H, H<sub>5,6,7</sub>), 5.56 – 5.35 (m, 1H, H<sub>19</sub>), 5.12 – 4.90 (m, 2H, H<sub>20</sub>), 3.43 (s, 2H, H<sub>14</sub>), 3.28 – 2.90 (m, 2H, H<sub>12</sub>)<sup>22</sup>, 2.89 – 2.55 (m, 2H, H<sub>11</sub>)<sup>23</sup>, 2.51 (d, <sup>3</sup>J<sub>18,19</sub> = 7.7 Hz, 2H, H<sub>18</sub>), 2.36 – 2.14 (m, 1H, H<sub>10</sub>), 2.14 – 2.02 (m, 1H, H<sub>10</sub>), 1.82 (s, 2H, H<sub>13</sub>), 1.42 (s, 9H, H<sub>17</sub>)<sup>22</sup> ppm;

**<sup>13</sup>C NMR** (101 MHz, CDCl<sub>3</sub>) δ 177.4 (C=O, C<sub>15</sub>), 155.5 (C, C<sub>8</sub>), 140.8 (C, C<sub>9</sub>), 132.2 (C=C, C<sub>19</sub>), 128.3 (CH, C<sub>6</sub>), 126.5 (CH, C<sub>5</sub>), 122.1 (CH, C<sub>7</sub>), 121.6 (CH, C<sub>4</sub>), 119.1 (CH<sub>2</sub>, C=C), 80.0 (C–O, C<sub>16</sub>), 60.1 (C, C<sub>3</sub>), 45.1 (CH<sub>2</sub>, C<sub>12</sub>), 43.6 (CH<sub>2</sub>, C<sub>11</sub>), 42.5 (CH<sub>2</sub>, C<sub>14</sub>), 32.7 (CH<sub>2</sub>, C<sub>10</sub>), 31.6 (CH<sub>2</sub>, C<sub>13</sub>), 28.6 (CH<sub>3</sub>, C<sub>17</sub>) ppm;

**HRMS** (ESI<sup>+</sup>) C<sub>21</sub>H<sub>29</sub>ClN<sub>2</sub>O<sub>2</sub>: 377.2005 [M+H]<sup>+</sup> (calcd 377.1990);

**IR** (thin film) 2956, 2924, 2854, 1690 (C=O), 1455, 1415, 1366, 1159 (C–O), 770 (C–Cl), 754 (C–Cl), 535 cm<sup>-1</sup>;

**[α]<sub>D</sub><sup>20</sup>** +2.1 (*c* 0.9, CHCl<sub>3</sub>);

**HPLC** (Chiralpak AD-H, *n*-hexane/*i*-PrOH (10:1), 1.0 mL·min<sup>-1</sup>, λ 254 nm):  
t<sub>Rmajor</sub> = 6.671 min, t<sub>Rminor</sub> = 7.336 min.

---

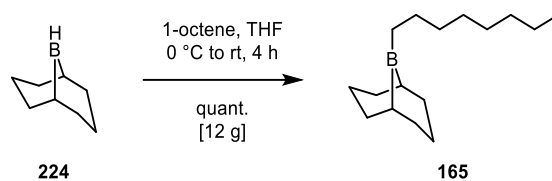
<sup>22</sup> Corrected integral.

<sup>23</sup> Overlapping signals therefore not possible to accurately integrate, integrals shown are corrected.

## Experimental

### Preparation of Compound 165

Compound **165** was prepared according to a literature procedure.<sup>[246]</sup>



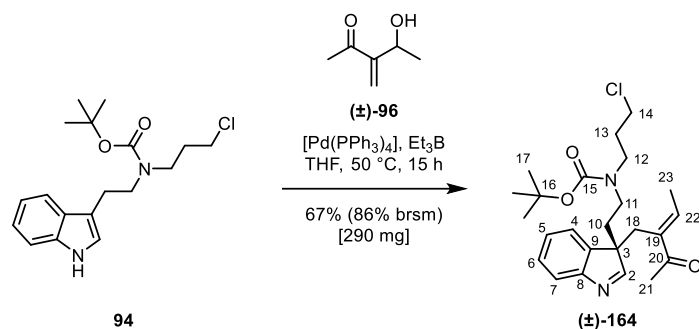
1-Octene (10 mL, 64 mmol) was added to a flask. The solution was cooled to 0 °C and 9-borabicyclo[3.3.1]nonane (9-BBN) (**224**) (0.50 M in THF, 100 mL, 50 mmol) was added. The resulting mixture was stirred at room temperature for 4 h. The reaction was then concentrated under reduced pressure under inert conditions to give crude 9-octyl-9-borabicyclo[3.3.1]nonane (9-BBN-octyl) (**165**) as a colourless oil (12 g) which was directly used without purification.

As compound **165** is pyrophoric, analytical data were not collected.

## Experimental

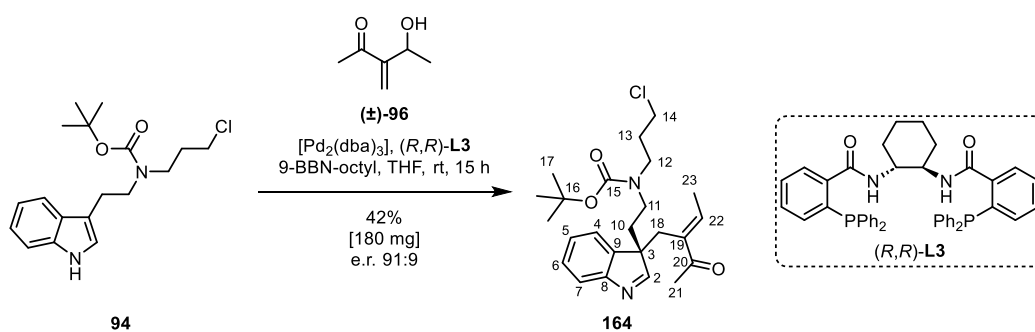
### Preparation of Compound 164

#### Non-enantioselective method:



[Pd(PPh<sub>3</sub>)<sub>4</sub>] (60 mg, 0.052 mmol) was added to a flask at room temperature, followed by compound **94** (340 mg, 1.0 mmol) in THF (1.3 mL) and Et<sub>3</sub>B (1.0 M in THF, 3.6 mL, 3.6 mmol). The resulting mixture was stirred at 50 °C. Compound **96** (0.22 mL, 2.0 mmol) in THF (1.3 mL) was then added dropwise over 2.5 h. The resulting mixture was stirred at 50 °C for 15 h. The reaction mixture was then diluted with EtOAc and washed with sat. aq. NaHCO<sub>3</sub>. The aqueous layer was extracted with EtOAc. The combined organic extracts were dried over brine, MgSO<sub>4</sub>, filtered and concentrated under reduced pressure. The crude material was purified by flash chromatography (petroleum ether 40–65/Et<sub>2</sub>O, 2:8) to afford *tert*-butyl (*E*)-2-(3-(2-(3-chloropropyl)but-2-en-1-yl)-3*H*-indol-3-yl)ethyl carbamate (**164**) as a colourless oil (290 mg, 0.67 mmol, 67%, 86% brsm).

#### Enantioselective method:



[Pd<sub>2</sub>(dba)<sub>3</sub>] (24 mg, 0.025 mmol), (*R,R*)-DACH phenyl Trost ligand **L3** (53 mg, 0.077 mmol) and compound **94** (340 mg, 1.0 mmol) were added to a flask at room temperature, followed by THF (4.8 mL). The resulting mixture was stirred for 15 min. 9-BBN-octyl (**165**) (840 mg, 3.6 mmol) was added and the resulting mixture was stirred for a further 5 min. Compound **96** (0.22 mL, 2.0 mmol) in THF (1.3 mL) was then added dropwise over 2.5 h. The resulting mixture was stirred at room temperature for 15 h. The reaction mixture was then diluted with

## Experimental

EtOAc and washed with sat. aq. NaHCO<sub>3</sub>. The aqueous layer was extracted with EtOAc. The combined organic extracts were dried over brine, MgSO<sub>4</sub>, filtered and concentrated under reduced pressure. The crude material was purified by flash chromatography (petroleum ether 40–65/Et<sub>2</sub>O, 2:8) to afford *tert*-butyl (*R,E*)-(2-(3-(2-acetylbut-2-en-1-yl)-3*H*-indol-3-yl)ethyl)(3-chloropropyl)carbamate (**164**) as a colourless oil (180 mg, 0.42 mmol, 42%, e.r. 91:9).

**R<sub>f</sub>** = 0.35 (petroleum ether 40–65/Et<sub>2</sub>O, 2:8);

**<sup>1</sup>H NMR** (600 MHz, CDCl<sub>3</sub>) δ = 7.96 – 7.82 (m, 1H, H<sub>2</sub>), 7.49 (d, <sup>3</sup>J<sub>4,5</sub> = 5.7 Hz, 1H, H<sub>4</sub>), 7.33 – 7.26 (m, 2H, H<sub>6+7</sub>), 7.19 (dd, <sup>3</sup>J<sub>5,6</sub> = 7.5 Hz, <sup>3</sup>J<sub>4,5</sub> = 7.5 Hz, 1H, H<sub>5</sub>), 6.44 (app. s, 1H, H<sub>22</sub>), 3.38 (app. s, 2H, H<sub>14</sub>), 3.19 – 2.94 (m, 2H, H<sub>12</sub>)<sup>24</sup>, 3.06 (d, <sup>2</sup>J<sub>18,18</sub> = 13.2 Hz, 1H, H<sub>18</sub>), 2.94 – 2.84 (m, 1H, H<sub>18</sub>), 2.81 – 2.45 (m, 2H, H<sub>11</sub>), 2.34 – 2.17 (m, 1H, H<sub>10</sub>), 2.17 – 2.07 (m, 1H, H<sub>10</sub>), 2.00 – 1.84 (m, 3H, H<sub>21</sub>), 1.86 – 1.68 (m, 2H, H<sub>13</sub>), 1.49 (d, <sup>3</sup>J<sub>22,23</sub> = 7.1 Hz, 3H, H<sub>23</sub>), 1.38 (s, 9H, H<sub>17</sub>)<sup>25</sup> ppm;

**<sup>13</sup>C NMR** (151 MHz, CDCl<sub>3</sub>) δ = 200.1 (C=O, C<sub>20</sub>), 177.7 (C=C, C<sub>2</sub>), 155.5 (C, C<sub>8</sub>), 155.2 (C=O, C<sub>15</sub>), 140.5 (C=C, C<sub>22</sub>)<sup>26</sup>, 140.2 (C=C, C<sub>22</sub>)<sup>26</sup>, 139.8 (C, C<sub>9</sub>), 138.3 (C=C, C<sub>19</sub>), 128.2 (CH, C<sub>6</sub>), 126.0 (CH, C<sub>5</sub>), 123.2 (CH, C<sub>7</sub>)<sup>26</sup>, 123.0 (CH, C<sub>7</sub>)<sup>26</sup>, 121.1 (CH, C<sub>4</sub>), 79.8 (C–O, C<sub>16</sub>), 61.4 (C, C<sub>3</sub>)<sup>26</sup>, 61.2 (C, C<sub>3</sub>)<sup>26</sup>, 44.9 (CH<sub>2</sub>, C<sub>12</sub>), 43.5 (CH<sub>2</sub>, C<sub>11</sub>), 42.4 (CH<sub>2</sub>, C<sub>14</sub>)<sup>26</sup>, 42.2 (CH<sub>2</sub>, C<sub>14</sub>)<sup>26</sup>, 33.9 (CH<sub>2</sub>, C<sub>10</sub>)<sup>26</sup>, 33.4 (CH<sub>2</sub>, C<sub>10</sub>)<sup>26</sup>, 31.6 (CH<sub>2</sub>, C<sub>13</sub>)<sup>26</sup>, 31.3 (CH<sub>2</sub>, C<sub>13</sub>)<sup>26</sup>, 30.4 (CH<sub>2</sub>, C<sub>18</sub>), 28.5 (CH<sub>3</sub>, C<sub>17</sub>), 25.5 (CH<sub>3</sub>, C<sub>21</sub>), 15.6 (CH<sub>3</sub>, C<sub>23</sub>) ppm;

**HRMS** (ESI<sup>+</sup>) C<sub>24</sub>H<sub>34</sub>ClN<sub>2</sub>O<sub>3</sub>: 433.2263 [M+H]<sup>+</sup> (calcd 433.2252), 455.2088 [M+Na]<sup>+</sup> (calcd 455.2072);

**IR** (thin film) 2954, 2922, 2869, 2853, 1691 (C=O), 1670 (C=O), 1458, 1161 (C–O), 737 (C–Cl) cm<sup>-1</sup>;

[α]<sub>D</sub><sup>20</sup> –37 (c 0.50, CHCl<sub>3</sub>);

**HPLC** (Chiralpak AD-H, *n*-hexane/*i*-PrOH (9:1), 0.5 mL·min<sup>-1</sup>, λ 254 nm): t<sub>Rminor</sub> = 36.016 min, t<sub>Rmajor</sub> = 38.059 min.

<sup>24</sup> Overlapping signals therefore not possible to accurately integrate, integrals shown are corrected.

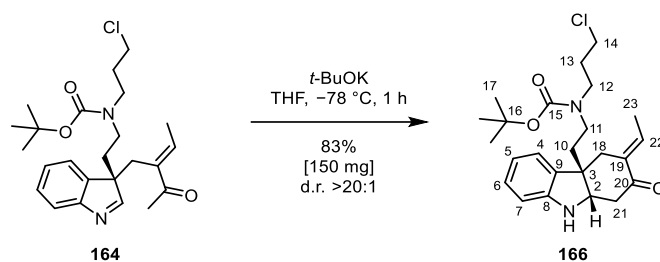
<sup>25</sup> Corrected integral.

<sup>26</sup> Peaks in <sup>13</sup>C NMR spectrum are split due to the presence of *N*-Boc rotamers.

## Experimental

### Preparation of Compound 166

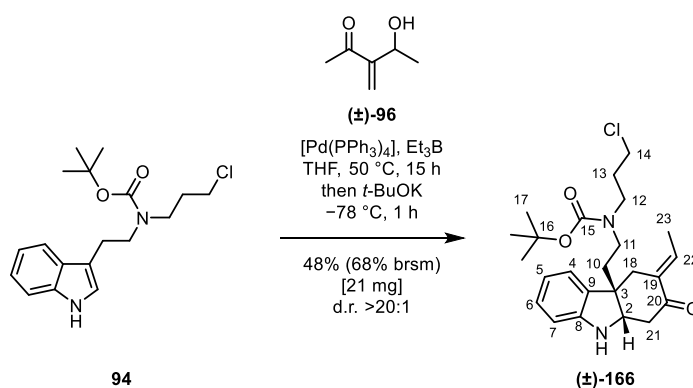
#### Method A



$t\text{-BuOK}$  (79 mg, 0.71 mmol) was added to a flask, followed by THF (4.4 mL). The resulting mixture was cooled to  $-78\text{ }^\circ\text{C}$  and compound **164** (180 mg, 0.42 mmol) was added dropwise in THF (4.0 mL). The solution was stirred at  $-78\text{ }^\circ\text{C}$  for 1 h. The reaction mixture was allowed to warm to room temperature and then quenched with sat. aq.  $\text{NH}_4\text{Cl}$ . The aqueous layer was extracted with EtOAc. The combined organic extracts were dried over brine,  $\text{MgSO}_4$ , filtered and concentrated under reduced pressure. The crude product was purified by flash chromatography (6:4 petroleum ether:  $\text{Et}_2\text{O}$ ) to afford *tert*-butyl (3-chloropropyl)(2-((4a*R*,9a*S*,*E*)-3-ethylidene-2-oxo-1,2,3,4,9,9a-hexahydro-4a*H*-carbazol-4a-yl)ethyl)carbamate (**166**) as a viscous colourless oil (150 mg, 0.35 mmol, 83%, d.r.  $>20:1$ ).

#### Method B

##### Non-enantioselective method:

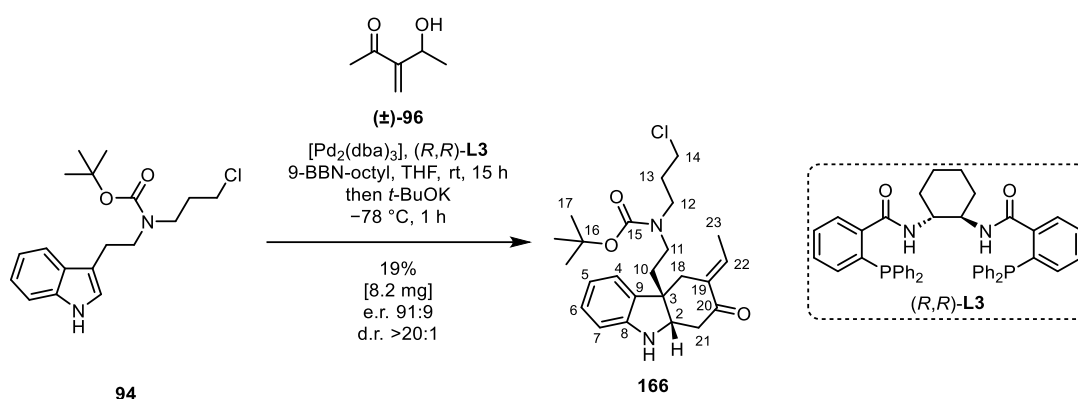


$[\text{Pd}(\text{PPh}_3)_4]$  (7.2 mg, 6.2  $\mu\text{mol}$ ) was added to a flask, followed by compound **94** (35 mg, 0.10 mmol) in THF (0.25 mL) and  $\text{Et}_3\text{B}$  (1.0 M in THF, 0.36 mL, 0.36 mmol). The resulting mixture was stirred at  $50\text{ }^\circ\text{C}$ . Compound **96** (22  $\mu\text{L}$ , 0.20 mmol) in THF (0.25 mL) was then added dropwise over 2.5 h. The resulting mixture was stirred at  $50\text{ }^\circ\text{C}$  for 15 h. The resulting mixture was cooled to  $-78\text{ }^\circ\text{C}$  and  $t\text{-BuOK}$  (65 mg, 0.58 mmol) was added to the flask. The solution

## Experimental

was stirred at  $-78\text{ }^{\circ}\text{C}$  for 1 h. The reaction mixture was allowed to warm to room temperature and then quenched with sat. aq.  $\text{NH}_4\text{Cl}$ . The reaction mixture was washed with sat. aq.  $\text{NaHCO}_3$ . The aqueous layer was extracted with  $\text{EtOAc}$ . The combined organic extracts were dried over brine,  $\text{MgSO}_4$ , filtered and concentrated under reduced pressure. The crude product was purified by flash chromatography (petroleum ether 40–65/ $\text{Et}_2\text{O}$ , 4:6) to afford *tert*-butyl (*E*)-(3-chloropropyl)(2-(3-ethylidene-2-oxo-1,2,3,4,9,9a-hexahydro-4a*H*-carbazol-4a-yl)ethyl)carbamate (**166**) as a colourless oil (21 mg, 0.48 mmol, 48%, 68% brsm, d.r. >20:1).

### Enantioselective method:



$[\text{Pd}_2(\text{dba})_3]$  (2.8 mg,  $3.1\text{ }\mu\text{mol}$ ), (*R,R*)-DACH phenyl Trost ligand **L3** (5.9 mg,  $8.5\text{ }\mu\text{mol}$ ) and compound **94** (34 mg, 0.10 mmol) were added to a flask, followed by THF (0.48 mL). The resulting mixture was stirred for 15 min. 9-BBN-octyl (**165**) (88 mg, 0.38 mmol) was added and the resulting mixture was stirred for a further 5 min. Compound **96** (22  $\mu\text{L}$ , 0.20 mmol) in THF (0.13 mL) was then added dropwise over 2.5 h. The resulting mixture was stirred at room temperature for 15 h. The resulting mixture was cooled to  $-78\text{ }^{\circ}\text{C}$  and *t*-BuOK (71 mg, 0.63 mmol) was added to the flask. The solution was stirred at  $-78\text{ }^{\circ}\text{C}$  for 1 h. The reaction mixture was allowed to warm to room temperature and then quenched with sat. aq.  $\text{NH}_4\text{Cl}$ . The reaction mixture was washed with sat. aq.  $\text{NaHCO}_3$ . The aqueous layer was extracted with  $\text{EtOAc}$ . The combined organic extracts were dried over brine,  $\text{MgSO}_4$ , filtered and concentrated under reduced pressure. The crude product was purified by flash chromatography (petroleum ether 40–65/ $\text{Et}_2\text{O}$ , 4:6) to afford *tert*-butyl (3-chloropropyl)(2-((4*R*,9*aS*,*E*)-3-ethylidene-2-oxo-1,2,3,4,9,9a-hexahydro-4a*H*-carbazol-4a-yl)ethyl)carbamate (**166**) as a colourless oil (8.2 mg, 0.19 mmol, 19%, e.r. 91:9, d.r. >20:1).

## Experimental

**R<sub>f</sub>** = 0.39 (petroleum ether 40–65/Et<sub>2</sub>O, 4:6);

**<sup>1</sup>H NMR** (600 MHz, CDCl<sub>3</sub>) δ = 6.97 (d, <sup>3</sup>J<sub>4,5</sub> = 7.4 Hz, 1H, H<sub>4</sub>), 6.94 (app. s, 1H, H<sub>6</sub>), 6.64 (dd, <sup>3</sup>J<sub>4,5</sub> = 6.9 Hz, <sup>3</sup>J<sub>5,6</sub> = 6.9 Hz, 1H, H<sub>5</sub>), 6.59 (app. s, 1H, H<sub>22</sub>), 6.43 (app. s, 1H, H<sub>7</sub>), 4.13 (app. d, 1H, H<sub>2</sub>)<sup>27</sup>, 3.86 (s, 1H, N–H<sub>1</sub>), 3.47 (t, <sup>3</sup>J<sub>13,14</sub> = 6.1 Hz, 2H, H<sub>14</sub>), 3.42 – 3.32 (m, 1H, H<sub>18</sub>), 3.23 (app. s, 3H, H<sub>11</sub>, H<sub>12</sub>), 2.97 – 2.86 (m, 1H, H<sub>18</sub>), 2.83 (d, <sup>3</sup>J<sub>2,21</sub> = 14.5 Hz, 1H, H<sub>21</sub>), 2.76 (dd, <sup>2</sup>J<sub>11,11</sub> = 15.3 Hz, J<sub>10,11</sub> = 4.1 Hz, 1H, H<sub>11</sub>), 2.63 – 2.50 (m, 2H, H<sub>11</sub>, H<sub>21</sub>), 2.08 – 1.98 (m, 1H, H<sub>10</sub>), 1.90 (app. s, 3H, H<sub>10</sub>, H<sub>13</sub>), 1.54 (app. s, 3H, H<sub>23</sub>), 1.42 (s, 9H, H<sub>17</sub>) ppm;

**<sup>13</sup>C NMR** (151 MHz, CDCl<sub>3</sub>) δ = 199.1 (C=O, C<sub>20</sub>)<sup>28</sup>, 198.8 (C=O, C<sub>20</sub>)<sup>28</sup>, 155.4 (C=O, C<sub>15</sub>), 150.0 (C, C<sub>8</sub>), 134.0 (C=C, C<sub>22</sub>), 132.3 (C, C<sub>9</sub>), 132.0 (C=C, C<sub>19</sub>), 128.3 (CH, C<sub>6</sub>), 122.7 (CH, C<sub>4</sub>), 118.6 (CH, C<sub>5</sub>), 108.9 (CH, C<sub>7</sub>), 79.8 (C–O, C<sub>16</sub>), 60.4 (CH, C<sub>2</sub>), 48.3 (C, C<sub>3</sub>), 44.9 (CH<sub>2</sub>, C<sub>12</sub>)<sup>28</sup>, 44.3 (CH<sub>2</sub>, C<sub>12</sub>)<sup>28</sup>, 44.2 (CH<sub>2</sub>, C<sub>11</sub>), 43.7 (CH<sub>2</sub>, C<sub>18</sub>), 42.6 (CH<sub>2</sub>, C<sub>14</sub>)<sup>28</sup>, 42.4 (CH<sub>2</sub>, C<sub>14</sub>)<sup>28</sup>, 39.6 (CH<sub>2</sub>, C<sub>10</sub>)<sup>28</sup>, 39.2 (CH<sub>2</sub>, C<sub>10</sub>)<sup>28</sup>, 35.8 (CH<sub>2</sub>, C<sub>21</sub>)<sup>28</sup>, 35.5 (CH<sub>2</sub>, C<sub>21</sub>)<sup>28</sup>, 31.8 (CH<sub>2</sub>, C<sub>13</sub>)<sup>28</sup>, 31.5 (CH<sub>2</sub>, C<sub>13</sub>)<sup>28</sup>, 28.5 (CH<sub>3</sub>, C<sub>17</sub>), 13.4 (CH<sub>2</sub>, C<sub>23</sub>) ppm;

**HRMS** (ESI<sup>+</sup>) C<sub>24</sub>H<sub>33</sub>ClN<sub>2</sub>O<sub>3</sub>: 433.2244 [M+H]<sup>+</sup> (calcd 433.2252), 455.2076 [M+Na]<sup>+</sup> (calcd 455.2072);

**IR** (thin film) 3367 (N–H), 2954, 2923, 2869, 2853, 1691 (C=O), 1634, 1607 (C=C), 1463, 1377, 1366, 1162 (C–O), 741 (C–Cl) cm<sup>-1</sup>;

[α]<sub>D</sub><sup>20</sup> –60 (c 0.50, CHCl<sub>3</sub>).

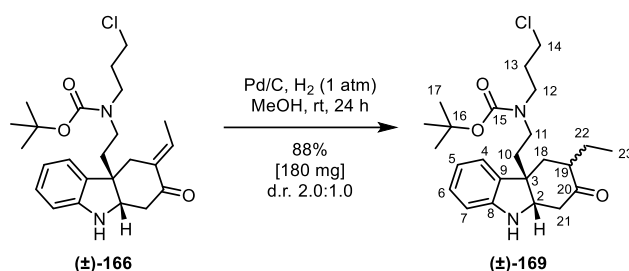
---

<sup>27</sup> Peak in <sup>1</sup>H NMR spectrum is split in a 1:1 ratio due to the presence of *N*-Boc rotamers.

<sup>28</sup> Peaks in <sup>13</sup>C NMR spectrum are split due to the presence of *N*-Boc rotamers.

## Experimental

### Preparation of Compound 169



Palladium 10 wt.% on activated carbon (17 mg) was added to a flask, followed by compound **166** (210 mg, 0.48 mmol) in MeOH (4.8 mL). The flask was evacuated and flushed with hydrogen. The resulting mixture was vigorously stirred under a hydrogen atmosphere (1 atm) at room temperature for 24 h. The reaction mixture was filtered through Celite and concentrated under reduced pressure. The crude product was purified by flash chromatography (petroleum ether 40–65/Et<sub>2</sub>O, 4:6) to afford an inseparable diastereomeric mixture of *tert*-butyl (3-chloropropyl)(2-(3-ethyl-2-oxo-1,2,3,4,9,9a-hexahydro-4*H*-carbazol-4a-yl)ethyl)carbamate (**169**) as a colourless oil (180 mg, 0.42 mmol, 88%, d.r. 2.0:1.0)<sup>29</sup>.

$R_f = 0.33$  (petroleum ether 40–65/Et<sub>2</sub>O, 4:6);

Major diastereomer:

<sup>1</sup>H NMR (400 MHz, CDCl<sub>3</sub>, 50 °C)  $\delta = 7.09 - 6.98$  (m, 3H, H<sub>4,6</sub>)<sup>30</sup>,  $6.77 - 6.69$  (m, 1H, H<sub>5</sub>)<sup>30</sup>,  $6.59$  (d, <sup>3</sup>J<sub>6,7</sub> = 7.6 Hz, 1H, H<sub>7</sub>),  $3.99$  (app. s, 1H, H<sub>2</sub>),  $3.85$  (s, 1H, N–H<sub>1</sub>)<sup>30</sup>,  $3.49$  (t, <sup>3</sup>J<sub>13,14</sub> = 6.4 Hz, 3H, H<sub>14</sub>)<sup>30</sup>,  $3.30 - 3.22$  (m, 3H, H<sub>12</sub>)<sup>30</sup>,  $3.42 - 3.19$  (m, 1H, H<sub>11</sub>)<sup>30</sup>,  $3.11 - 2.89$  (m, 1H, H<sub>11</sub>)<sup>30</sup>,  $2.57$  (dd, <sup>3</sup>J<sub>2,21</sub> = 5.9 Hz, <sup>3</sup>J<sub>2,21</sub> = 2.1 Hz, 2H, H<sub>21,21</sub>),  $2.35 - 2.20$  (m, 1H, H<sub>19</sub>),  $2.17 - 1.83$  (m, 7H, H<sub>10,18</sub>)<sup>30</sup>,  $1.79 - 1.69$  (m, 1H, H<sub>22</sub>),  $1.44$  (s, 9H, H<sub>17</sub>)<sup>30</sup>,  $1.31 - 1.21$  (m, 1H, H<sub>22</sub>),  $0.88$  (dd, <sup>3</sup>J<sub>22,23</sub> = 7.4 Hz, <sup>3</sup>J<sub>22,23</sub> = 7.4 Hz, 3H, H<sub>23</sub>) ppm;

<sup>13</sup>C NMR (101 MHz, CDCl<sub>3</sub>, 50 °C)  $\delta = 211.3$  (C=O, C<sub>20</sub>),  $155.4$  (C=O, C<sub>15</sub>),  $148.9$  (C, C<sub>8</sub>),  $134.6$  (C, C<sub>9</sub>),  $128.2$  (CH, C<sub>6</sub>),  $122.9$  (CH, C<sub>4</sub>),  $119.3$  (CH, C<sub>5</sub>),  $109.9$  (CH, C<sub>7</sub>),  $79.8$  (C–O, C<sub>16</sub>),  $63.5$  (CH, C<sub>2</sub>),  $47.3$  (CH, C<sub>19</sub>),  $46.3$  (C, C<sub>3</sub>),  $45.05$  (CH<sub>2</sub>, C<sub>12</sub>),  $44.2$  (CH<sub>2</sub>, C<sub>11</sub>),  $44.0$  (CH<sub>2</sub>, C<sub>21</sub>),  $42.5$  (CH<sub>2</sub>, C<sub>14</sub>),  $39.2$  (CH<sub>2</sub>, C<sub>10</sub>),  $36.1$  (CH<sub>2</sub>, C<sub>18</sub>),  $31.8$  (CH<sub>2</sub>, C<sub>13</sub>),  $28.6$  (CH<sub>3</sub>, C<sub>17</sub>),  $22.6$  (CH<sub>2</sub>, C<sub>22</sub>),  $11.5$  (CH<sub>3</sub>, C<sub>23</sub>) ppm;

<sup>29</sup> Diastereomeric ratio was determined from the <sup>1</sup>H spectrum of the crude product.

<sup>30</sup> Overlapping signals of major and minor diastereomer therefore not possible to accurately integrate, integrals shown are corrected.

## Experimental

Minor diastereomer:

**<sup>1</sup>H NMR** (400 MHz, CDCl<sub>3</sub>, 50 °C)  $\delta$  = 7.09 – 6.98 (m, 6H, H<sub>4,6</sub>)<sup>30</sup>, 6.77 – 6.69 (m, 3H, H<sub>5</sub>)<sup>30</sup>, 6.51 (d, <sup>3</sup>J<sub>6,7</sub> = 7.8 Hz, 1H, H<sub>7</sub>), 4.17 (app. s, 1H, H<sub>2</sub>), 3.85 (s, 3H, N–H<sub>1</sub>)<sup>30</sup>, 3.49 (t, <sup>3</sup>J<sub>13,14</sub> = 6.4 Hz, 5H, H<sub>14</sub>)<sup>30</sup>, 3.30 – 3.22 (m, 3H, H<sub>12</sub>)<sup>30</sup>, 3.42 – 3.19 (m, 1H, H<sub>11</sub>)<sup>30</sup>, 3.11 – 2.89 (m, 3H, H<sub>11</sub>)<sup>30</sup>, 2.63 (dd, <sup>3</sup>J<sub>21,21</sub> = 15.9 Hz, <sup>3</sup>J<sub>2,21</sub> = 3.9 Hz, 1H, H<sub>21</sub>), 2.47 (dd, <sup>3</sup>J<sub>21,21</sub> = 15.9 Hz, <sup>3</sup>J<sub>2,21</sub> = 3.2 Hz, 1H, H<sub>21</sub>), 2.17 – 1.83 (m, 13H, H<sub>10,18</sub>)<sup>30</sup>, 1.68 – 1.57 (m, 1H, H<sub>22</sub>), 1.44 (s, 9H, H<sub>17</sub>)<sup>30</sup>, 1.42 – 1.33 (m, 1H, H<sub>22</sub>), 0.78 (dd, <sup>3</sup>J<sub>22,23</sub> = 7.5 Hz, <sup>3</sup>J<sub>22,23</sub> = 7.5 Hz, 3H, H<sub>23</sub>) ppm;

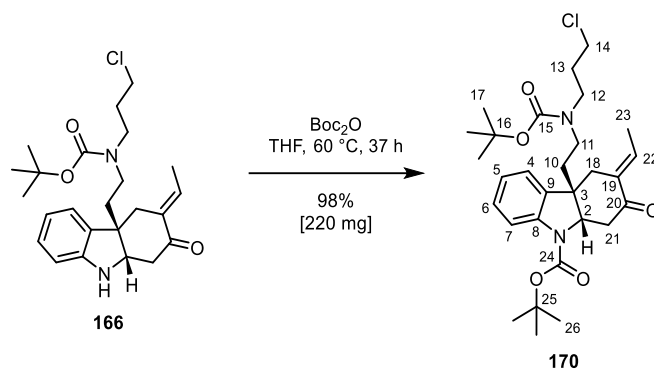
**<sup>13</sup>C NMR** (101 MHz, CDCl<sub>3</sub>, 50 °C)  $\delta$  = 212.8 (C=O, C<sub>20</sub>), 155.4 (C=O, C<sub>15</sub>), 150.4 (C, C<sub>8</sub>), 132.5 (C, C<sub>9</sub>), 128.5 (CH, C<sub>6</sub>), 123.3 (CH, C<sub>4</sub>), 119.1 (CH, C<sub>5</sub>), 109.2 (CH, C<sub>7</sub>), 79.8 (C–O, C<sub>16</sub>), 60.9 (CH, C<sub>2</sub>), 47.2 (C, C<sub>3</sub>), 45.9 (CH, C<sub>19</sub>), 45.1 (CH<sub>2</sub>, C<sub>12</sub>), 44.2 (CH<sub>2</sub>, C<sub>11</sub>), 43.6 (CH<sub>2</sub>, C<sub>21</sub>), 42.5 (CH<sub>2</sub>, C<sub>14</sub>), 39.4 (CH<sub>2</sub>, C<sub>10</sub>), 36.1 (CH<sub>2</sub>, C<sub>18</sub>), 31.8 (CH<sub>2</sub>, C<sub>13</sub>), 28.6 (CH<sub>3</sub>, C<sub>17</sub>), 22.9 (CH<sub>2</sub>, C<sub>22</sub>), 10.9 (CH<sub>3</sub>, C<sub>23</sub>) ppm;

**HRMS** (ESI<sup>+</sup>) C<sub>24</sub>H<sub>35</sub>ClN<sub>2</sub>O<sub>3</sub>: 435.2387 [M+H]<sup>+</sup> (calcd 435.2409), 457.2216 [M+Na]<sup>+</sup> (calcd 457.2228);

**IR** (thin film) 3354 (N–H), 2958, 2925, 2870, 1688 (C=O), 1608 (C=C), 1481, 1466, 1416, 1366, 1161 (C–O), 744 (C–Cl) cm<sup>-1</sup>.

## Experimental

### Preparation of Compound 170



Compound **166** (180 mg, 0.42 mmol) was added to a flask followed by di-*tert*-butyl dicarbonate ( $\text{Boc}_2\text{O}$ ) (0.24 mL, 1.0 mmol) in THF (4.2 mL). The resulting mixture was stirred at  $60\text{ }^\circ\text{C}$  for 37 h. The reaction mixture was then concentrated under reduced pressure. The crude product was purified by flash chromatography (petroleum ether 40–65/ $\text{Et}_2\text{O}$ , 1:1) to afford *tert*-butyl (4*aR*,9*aS*,*E*)-4*a*-(2-((*tert*-butoxycarbonyl)(3-chloropropyl)amino)ethyl)-3-ethylidene-2-oxo-1,2,3,4,4*a*,9*a*-hexahydro-9*H*-carbazole-9-carboxylate (**170**) as a white foam (220 mg, 0.41 mmol, 98%).

$R_f = 0.36$  (petroleum ether 40–65/ $\text{Et}_2\text{O}$ , 1:1);

$^1\text{H NMR}$  (400 MHz,  $\text{CDCl}_3$ ,  $50\text{ }^\circ\text{C}$ )  $\delta = 7.64$  (app. s, 1H,  $\text{H}_7$ ), 7.15 (ddd,  $^3J_{5,6} = 7.2\text{ Hz}$ ,  $^3J_{6,7} = 7.2\text{ Hz}$ ,  $^4J_{4,6} = 1.1\text{ Hz}$ , 1H,  $\text{H}_6$ ), 7.04 (dd,  $^3J_{4,5} = 7.2\text{ Hz}$ ,  $^3J_{4,6} = 1.0\text{ Hz}$ , 1H,  $\text{H}_4$ ), 6.95 (ddd,  $^3J_{4,5} = 7.4\text{ Hz}$ ,  $^3J_{5,6} = 7.4\text{ Hz}$ ,  $^4J_{5,7} = 0.8\text{ Hz}$ , 1H,  $\text{H}_5$ ), 6.66 (q,  $^3J_{22,23} = 7.2\text{ Hz}$ , 1H,  $\text{H}_{22}$ ), 4.52 (app. s, 1H,  $\text{H}_2$ ), 3.47 (t,  $^3J_{13,14} = 6.3\text{ Hz}$ , 2H,  $\text{H}_{14}$ ), 3.30 – 3.10 (m, 4H,  $\text{H}_{11,12}$ )<sup>31</sup>, 2.97 – 2.70 (m, 4H,  $\text{H}_{18,21}$ ), 1.96 (t,  $^3J_{10,11} = 8.3\text{ Hz}$ , 2H,  $\text{H}_{10}$ )<sup>31</sup>, 1.89 (tt,  $^3J_{13,14} = 6.6\text{ Hz}$ ,  $^3J_{12,13} = 6.6\text{ Hz}$ , 2H,  $\text{H}_{13}$ )<sup>31</sup>, 1.66 (d,  $^3J_{22,23} = 7.2\text{ Hz}$ , 2H,  $\text{H}_{23}$ ), 1.57 (s, 9H,  $\text{H}_{26}$ ), 1.43 (s, 9H,  $\text{H}_{17}$ ) ppm;

$^{13}\text{C NMR}$  (101 MHz,  $\text{CDCl}_3$ ,  $50\text{ }^\circ\text{C}$ )  $\delta = 197.2$  (C=O,  $\text{C}_{20}$ ), 155.4 (C=O,  $\text{C}_{15}$ ), 151.9 (C=O,  $\text{C}_{24}$ ), 142.1 ( $\text{CH}_2$ ,  $\text{C}_{18}$ ), 134.8 (C=C,  $\text{C}_{22}$ ), 134.7 (C=C,  $\text{C}_{19}$ ), 133.9 (C,  $\text{C}_9$ ), 128.7 (CH,  $\text{C}_6$ ), 123.2 (CH,  $\text{C}_5$ ), 122.5 (CH,  $\text{C}_4$ ), 115.7 (CH,  $\text{C}_7$ ), 81.9 (C–O,  $\text{C}_{25}$ ), 80.0 (C–O,  $\text{C}_{16}$ ), 63.1 (CH,  $\text{C}_2$ ), 46.7 (C,  $\text{C}_3$ ), 45.1 ( $\text{C}_{11,12}$ ), 43.8 ( $\text{CH}_2$ ,  $\text{C}_{21}$ ), 42.4 ( $\text{CH}_2$ ,  $\text{C}_{14}$ ), 40.2 ( $\text{CH}_2$ ,  $\text{C}_{10}$ ), 34.3 ( $\text{CH}_2$ ,  $\text{C}_{18}$ ), 31.8 ( $\text{CH}_2$ ,  $\text{C}_{13}$ ), 28.64 ( $\text{CH}_3$ ,  $\text{C}_{17}$ ), 28.60 ( $\text{CH}_3$ ,  $\text{C}_{26}$ ), 13.6 ( $\text{CH}_3$ ,  $\text{C}_{23}$ ) ppm;

**HRMS** ( $\text{ESI}^+$ )  $\text{C}_{29}\text{H}_{41}\text{ClN}_2\text{O}_5$ : 555.2602 [ $\text{M}+\text{Na}$ ]<sup>+</sup> (calcd 55.2596);

<sup>31</sup> Overlapping signals therefore not possible to accurately integrate, integrals shown are corrected.

## *Experimental*

**IR** (thin film) 2954, 2922, 2853, 1696 (C=O), 1635 (C=C), 1482, 1378, 1367, 1166 (C–O), 739 (C–Cl)  $\text{cm}^{-1}$ ;

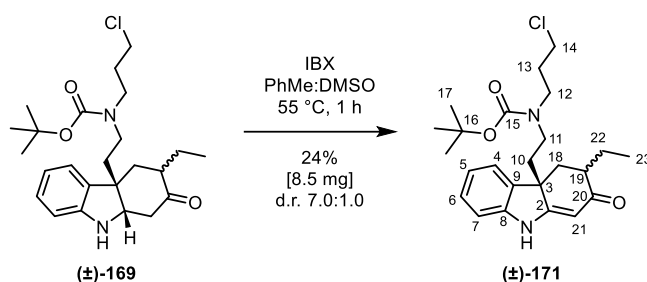
$[\alpha]_D^{20} +16$  (*c* 0.50,  $\text{CHCl}_3$ );

**m.p.** 52–54 °C.

## Experimental

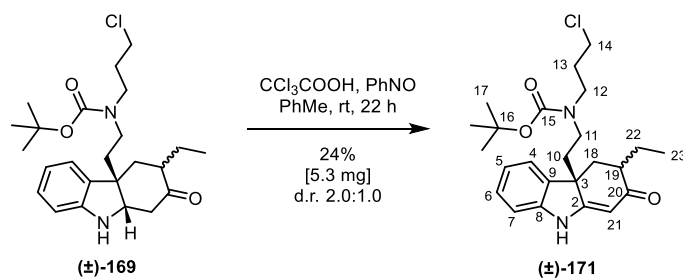
### Preparation of Compound 171

#### Method A



2-Iodoxybenzoic acid (IBX) (**183**) (48 mg, 0.17 mmol, d.r. 2.0:1.0) was added to a flask, followed by compound **169** (37 mg, 0.085 mmol) in PhMe:DMSO (0.57 mL: 0.29 mL). The resulting mixture was heated at 55 °C for 1 h. The reaction mixture was then diluted with aq. NaHCO<sub>3</sub> (5%). The aqueous layer was extracted with Et<sub>2</sub>O. The combined organic extracts were concentrated under reduced pressure. The residue was taken up in Et<sub>2</sub>O and filtered through Celite. The filtrate was then washed with sat. aq. NaHCO<sub>3</sub> and H<sub>2</sub>O, dried over brine, MgSO<sub>4</sub>, filtered and concentrated under reduced pressure. The crude product was purified by flash chromatography (petroleum ether 40–65/EtOAc, 4:6) to afford *tert*-butyl (3-chloropropyl)(2-((4*aR*)-3-ethyl-2-oxo-2,3,4,9-tetrahydro-4*aH*-carbazol-4*a*-yl)ethyl)carbamate (**171**) as a colourless oil (8.5 mg, 0.020 mmol, 24%, d.r. 7.0:1.0)<sup>32</sup>.

#### Method B



Trichloroacetic acid (27 mg, 0.17 mmol, d.r. 2.0:1.0) and nitrosobenzene (PhNO) (17 mg, 0.16 mmol) were added to a flask, followed by compound **169** (22 mg, 0.051 mmol) in PhMe (0.50 mL). The resulting mixture was stirred at room temperature for 5 h. The reaction mixture was then diluted with sat. aq. NaHCO<sub>3</sub> and the aqueous layer was extracted with EtOAc. The combined organic extracts were dried over brine, MgSO<sub>4</sub>, filtered and

<sup>32</sup> Diastereomeric ratio was determined from the <sup>1</sup>H spectrum of the crude product.

## Experimental

concentrated under reduced pressure. The crude product was purified by column chromatography (petroleum ether 40–65/EtOAc, 4:6) to afford *tert*-butyl (3-chloropropyl)(2-((4a*R*)-3-ethyl-2-oxo-2,3,4,9-tetrahydro-4a*H*-carbazol-4a-yl)ethyl)carbamate (**171**) as a colourless oil (5.3 mg, 12  $\mu$ mol, 24%, d.r. 2.0:1.0)<sup>33</sup>.

**R<sub>f</sub>** = major diastereomer 0.39, minor diastereomer 0.25 (petroleum ether 40–65/EtOAc, 4:6);

Major diastereomer<sup>34</sup>:

**<sup>1</sup>H NMR** (400 MHz, CDCl<sub>3</sub>, 50 °C)  $\delta$  = 7.65 (s, 1H, N–H<sub>1</sub>), 7.25 – 7.17 (m, 2H, H<sub>4,6</sub>), 6.99 (ddd, <sup>3</sup>*J*<sub>4,5</sub> = 7.5 Hz, <sup>3</sup>*J*<sub>5,6</sub> = 7.5 Hz, <sup>4</sup>*J*<sub>5,7</sub> = 1.0 Hz, 1H, H<sub>5</sub>), 6.87 (d, *J* = 7.8 Hz, 1H, H<sub>7</sub>), 5.42 (s, 1H, H<sub>21</sub>), 3.43 (t, <sup>3</sup>*J*<sub>13,14</sub> = 6.4 Hz, 2H, H<sub>14</sub>), 3.24 – 3.06 (m, 2H, H<sub>12</sub>), 3.06 – 2.73 (m, 2H, H<sub>11</sub>)<sup>35</sup>, 2.59 – 2.46 (m, 2H, H<sub>18,19</sub>), 2.11 – 1.91 (m, 3H, H<sub>10,22</sub>)<sup>35</sup>, 1.85 (tt, <sup>3</sup>*J*<sub>12,13</sub> = 6.6 Hz, <sup>3</sup>*J*<sub>13,14</sub> = 6.6 Hz, 2H, H<sub>13</sub>), 1.80 – 1.68 (m, 1H, H<sub>18</sub>), 1.66 – 1.48 (m, 1H, H<sub>22</sub>), 1.37 (s, 9H, H<sub>17</sub>), 0.94 (dd, <sup>3</sup>*J*<sub>22,23</sub> = 7.5 Hz, <sup>3</sup>*J*<sub>22,23</sub> = 7.5 Hz, 3H, H<sub>23</sub>) ppm;

**<sup>13</sup>C NMR** (101 MHz, CDCl<sub>3</sub>, 50 °C)  $\delta$  = 198.5 (C=O, C<sub>20</sub>), 173.3 (C=C, C<sub>2</sub>), 155.4 (C=O, C<sub>15</sub>), 143.9 (C, C<sub>8</sub>), 134.5 (C, C<sub>9</sub>), 128.6 (C, C<sub>6</sub>), 123.0 (C, C<sub>4</sub>), 122.1 (C, C<sub>5</sub>), 109.9 (C, C<sub>7</sub>), 97.8 (C=C, C<sub>21</sub>), 80.0 (C–O, C<sub>16</sub>), 48.3 (C, C<sub>3</sub>), 44.9 (CH<sub>2</sub>, C<sub>12</sub>), 44.0 (CH<sub>2</sub>, C<sub>11</sub>) 42.6 (CH, C<sub>19</sub>), 42.4 (CH<sub>2</sub>, C<sub>14</sub>), 38.5 (CH<sub>2</sub>, C<sub>10</sub>), 35.4 (CH<sub>2</sub>, C<sub>18</sub>), 31.7 (CH<sub>2</sub>, C<sub>13</sub>), 28.6 (CH<sub>3</sub>, C<sub>17</sub>), 24.9 (CH<sub>2</sub>, C<sub>22</sub>), 11.1 (CH<sub>3</sub>, C<sub>23</sub>) ppm;

**HRMS** (ESI<sup>+</sup>) C<sub>24</sub>H<sub>33</sub>ClN<sub>2</sub>O<sub>3</sub>: 433.2236 [M+H]<sup>+</sup> (calcd 433.2252), 455.2065 [M+Na]<sup>+</sup> (calcd 455.2072);

**IR** (thin film) 3185 (N–H), 2963, 2927, 2856, 1693 (C=O), 1627 (C=C), 1588 (N–H), 1468, 1366, 1194 (C–O), 1163, 750 (C–Cl) cm<sup>-1</sup>.

---

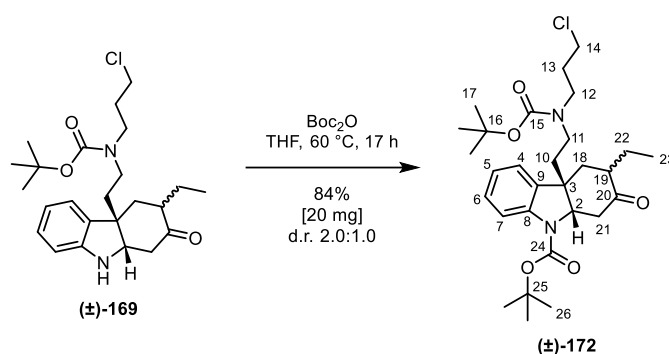
<sup>33</sup> Diastereomeric ratio was determined from the <sup>1</sup>H spectrum of the crude product.

<sup>34</sup> Only the major diastereomer is described, due to small quantity of minor diastereomer obtained.

<sup>35</sup> Overlapping signals therefore not possible to accurately integrate, integrals shown are corrected.

## Experimental

### Preparation of Compound 172



Compound **169** (19 mg, 44  $\mu\text{mol}$ , d.r. 2.0:1.0) was added to a flask followed by di-*tert*-butyl dicarbonate ( $\text{Boc}_2\text{O}$ ) (20  $\mu\text{L}$ , 87  $\mu\text{mol}$ ) in THF (0.50 mL). The resulting mixture was stirred at 60 °C for 17 h. The reaction mixture was then concentrated under reduced pressure. The crude product was purified by flash chromatography (petroleum ether 40–65/ $\text{Et}_2\text{O}$ , 7:3) to afford *tert*-butyl (4*aR*,9*aS*)-4*a*-(2-((*tert*-butoxycarbonyl)(3-chloropropyl)amino)ethyl)-3-ethyl-2-oxo-1,2,3,4,4*a*,9*a*-hexahydro-9*H*-carbazole-9-carboxylate (**172**) as a colourless oil (20 mg, 37  $\mu\text{mol}$ , 84%, d.r. 2.0:1.0)<sup>36</sup>.

$R_f$  = 0.31 major diastereomer, 0.23 minor diastereomer (petroleum ether 40–65/ $\text{Et}_2\text{O}$ , 7:3);

Major diastereomer<sup>37</sup>:

<sup>1</sup>H NMR (400 MHz,  $\text{CDCl}_3$ , 50 °C)  $\delta$  = 7.72 (app. s, 1H, H<sub>7</sub>), 7.22 (ddd, <sup>3</sup> $J_{6,7}$  = 7.6 Hz, <sup>3</sup> $J_{5,6}$  = 7.5 Hz, <sup>4</sup> $J_{4,6}$  = 1.4 Hz, 1H, H<sub>6</sub>), 7.12 (dd, <sup>3</sup> $J_{4,5}$  = 7.5 Hz, <sup>4</sup> $J_{4,6}$  = 1.4 Hz, 1H, H<sub>4</sub>), 7.02 (ddd, <sup>3</sup> $J_{5,6}$  = 7.5 Hz, <sup>3</sup> $J_{4,5}$  = 7.4 Hz, <sup>4</sup> $J_{5,7}$  = 1.0 Hz, 1H, H<sub>5</sub>), 4.33 (dd, <sup>3</sup> $J_{2,21}$  = 11.3 Hz, <sup>3</sup> $J_{2,21}$  = 4.9 Hz, 1H, H<sub>2</sub>), 3.45 (t, <sup>3</sup> $J_{13,14}$  = 6.4 Hz, 2H, H<sub>14</sub>), 3.27 – 3.04 (m, 4H, H<sub>11,12</sub>)<sup>38</sup>, 2.91 (dd, <sup>3</sup> $J_{21,21}$  = 15.6 Hz, <sup>3</sup> $J_{2,21}$  = 4.9 Hz, 1H, H<sub>21</sub>), 2.44 (dd, <sup>3</sup> $J_{21,21}$  = 15.6 Hz, <sup>3</sup> $J_{2,21}$  = 11.2 Hz, 1H, H<sub>21</sub>), 2.33 – 2.15 (m, 2H, H<sub>18,19</sub>), 2.08 – 1.91 (m, 2H, H<sub>10,18</sub>), 1.91 – 1.75 (m, 5H, H<sub>10,13,22</sub>)<sup>38</sup>, 1.57 (s, 9H, H<sub>26</sub>), 1.40 (s, 9H, H<sub>17</sub>)<sup>39</sup>, 0.94 (dd, <sup>3</sup> $J_{22,23}$  = 7.4 Hz, <sup>3</sup> $J_{22,23}$  = 7.4 Hz, 3H, H<sub>23</sub>) ppm;

<sup>13</sup>C NMR (101 MHz,  $\text{CDCl}_3$ , 50 °C)  $\delta$  = 210.9 (C=O, C<sub>20</sub>), 155.4 (C=O, C<sub>15</sub>), 151.8 (C=O, C<sub>24</sub>), 140.9 (C, C<sub>8</sub>), 136.6 (C, C<sub>9</sub>), 128.7 (CH, C<sub>6</sub>), 123.4 (CH, C<sub>5</sub>), 123.3 (CH, C<sub>4</sub>), 115.9 (CH, C<sub>7</sub>), 81.9 (C, C<sub>25</sub>), 79.9 (C, C<sub>16</sub>), 63.2 (CH, C<sub>2</sub>), 47.1 (CH, C<sub>19</sub>), 45.1 (C, C<sub>3</sub>), 45.0 (CH<sub>2</sub>, C<sub>12</sub>),

<sup>36</sup> Diastereomeric ratio was determined from the <sup>1</sup>H spectrum of the crude product.

<sup>37</sup> Only major diastereomer is described, due to small quantity of minor diastereomer obtained. It was not possible to differentiate the diastereomers from the NOESY NMR spectrum.

<sup>38</sup> Overlapping signals therefore not possible to accurately integrate, integrals shown are corrected.

<sup>39</sup> Corrected integral.

### *Experimental*

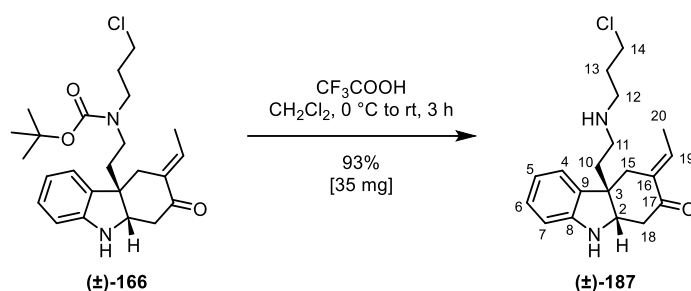
43.6 (CH<sub>2</sub>, C<sub>11</sub>), 42.4 (CH<sub>2</sub>, C<sub>21</sub>), 42.2 (CH<sub>2</sub>, C<sub>14</sub>), 39.7 (CH<sub>2</sub>, C<sub>10</sub>), 36.2 (CH<sub>2</sub>, C<sub>18</sub>), 31.8 (CH<sub>2</sub>, C<sub>13</sub>), 28.63 (CH<sub>3</sub>, C<sub>17</sub>), 28.61 (CH<sub>3</sub>, C<sub>26</sub>), 22.8 (CH<sub>2</sub>, C<sub>22</sub>), 11.2 (CH<sub>3</sub>, C<sub>23</sub>) ppm;

**HRMS** (ESI<sup>+</sup>) C<sub>29</sub>H<sub>43</sub>ClN<sub>2</sub>O<sub>5</sub>: 557.2749 [M+Na]<sup>+</sup> (calcd 557.2753);

**IR** (thin film) 2961, 2926, 2870, 1694 (C=O), 1482, 1388, 1366, 1164 (C–O), 752 (C–Cl) cm<sup>-1</sup>.

## Experimental

### Preparation of Compound 187



Compound **166** (51 mg, 0.12 mmol) in  $\text{CH}_2\text{Cl}_2$  (1.2 mL) was added to a flask. The resulting mixture was cooled to  $0^\circ\text{C}$  and trifluoroacetic acid (130  $\mu\text{L}$ , 1.7 mmol) was slowly added. The resulting mixture was stirred at room temperature for 3 h. The reaction mixture was then quenched with sat. aq.  $\text{NaHCO}_3$ . The aqueous layer was extracted with  $\text{CH}_2\text{Cl}_2$ . The combined organic extracts were dried over brine,  $\text{MgSO}_4$ , filtered and concentrated under reduced pressure. The crude product was purified by flash chromatography ( $\text{CH}_2\text{Cl}_2/\text{MeOH}/\text{Et}_3\text{N}$ , 200:1:1) to afford (*E*)-4a-(2-((3-chloropropyl)amino)ethyl)-3-ethylidene-1,3,4,4a,9,9a-hexahydro-2*H*-carbazol-2-one (**187**) as a yellow oil (35 mg, 0.11 mmol, 92%).

$R_f = 0.39$  ( $\text{CH}_2\text{Cl}_2/\text{MeOH}/\text{Et}_3\text{N}$ , 200:1:1);

$^1\text{H NMR}$  (600 MHz,  $\text{CDCl}_3$ )  $\delta$  7.00 – 6.95 (m, 2H,  $\text{H}_{4,6}$ ), 6.67 (ddd,  $^3J_{4,5} = 7.4$  Hz,  $^3J_{5,6} = 7.4$  Hz,  $^4J_{5,7} = 1.0$  Hz, 1H,  $\text{H}_5$ ), 6.62 (app. qd,  $^3J_{19,20} = 7.8$  Hz,  $^4J_{15,19} = 1.6$  Hz, 1H,  $\text{H}_{19}$ ), 6.46 (dd,  $^3J_{6,7} = 7.9$  Hz,  $^4J_{5,7} = 0.7$  Hz, 1H,  $\text{H}_7$ ), 4.12 (dd,  $^3J_{2,18} = 4.3$  Hz,  $^3J_{2,18} = 4.3$  Hz, 1H,  $\text{H}_2$ ), 3.55 (t,  $^3J_{13,14} = 6.4$  Hz, 2H,  $\text{H}_{14}$ ), 2.83 (d,  $^2J_{15,15} = 14.5$  Hz, 1H,  $\text{H}_{15}$ ), 2.77 (dd,  $^2J_{18,18} = 15.2$  Hz,  $^3J_{2,18} = 4.3$  Hz, 1H,  $\text{H}_{18}$ ), 2.71 (t,  $^3J_{12,13} = 7.0$  Hz, 2H,  $\text{H}_{12}$ ), 2.59 (app. dt,  $^2J_{15,15} = 14.5$  Hz,  $^4J_{15,19} = 1.6$  Hz, 1H,  $\text{H}_{15}$ ), 2.58 (dd,  $^2J_{18,18} = 15.2$  Hz,  $^3J_{2,18} = 4.4$  Hz, 1H,  $\text{H}_{18}$ ), 2.56 – 2.51 (m, 2H,  $\text{H}_{11}$ )<sup>40</sup>, 2.08 – 2.00 (m, 1H,  $\text{H}_{10}$ ), 1.97 – 1.91 (m, 1H,  $\text{H}_{10}$ ), 1.89 (p,  $^3J_{12,13} = 6.8$  Hz,  $^3J_{13,14} = 6.8$  Hz, 2H,  $\text{H}_{13}$ ), 1.56 (dd,  $^3J_{19,20} = 7.2$  Hz,  $^4J_{15,20} = 1.4$  Hz, 3H,  $\text{H}_{20}$ ) ppm;

$^{13}\text{C NMR}$  (151 MHz,  $\text{CDCl}_3$ )  $\delta$  199.0 (C=O,  $\text{C}_{17}$ ), 150.0 (C,  $\text{C}_8$ ), 134.3 (C=C,  $\text{C}_{19}$ ), 134.2 (C=C,  $\text{C}_{16}$ ), 132.7 (C,  $\text{C}_9$ ), 128.3 (CH,  $\text{C}_6$ ), 122.9 (CH,  $\text{C}_4$ ), 118.8 (CH,  $\text{C}_5$ ), 109.0 (CH,  $\text{C}_7$ ), 60.8 (CH,  $\text{C}_2$ ), 48.7 (C,  $\text{C}_3$ ), 46.9 ( $\text{CH}_2$ ,  $\text{C}_{12}$ ), 45.6 ( $\text{CH}_2$ ,  $\text{C}_{11}$ ), 44.4 ( $\text{CH}_2$ ,  $\text{C}_{18}$ ), 43.0 ( $\text{CH}_2$ ,  $\text{C}_{14}$ ), 41.2 ( $\text{CH}_2$ ,  $\text{C}_{10}$ ), 35.8 ( $\text{CH}_2$ ,  $\text{C}_{15}$ ), 32.4 ( $\text{CH}_2$ ,  $\text{C}_{13}$ ), 13.5 ( $\text{CH}_3$ ,  $\text{C}_{13}$ ) ppm;

<sup>40</sup> Overlapping signals therefore not possible to accurately integrate, integrals shown are corrected.

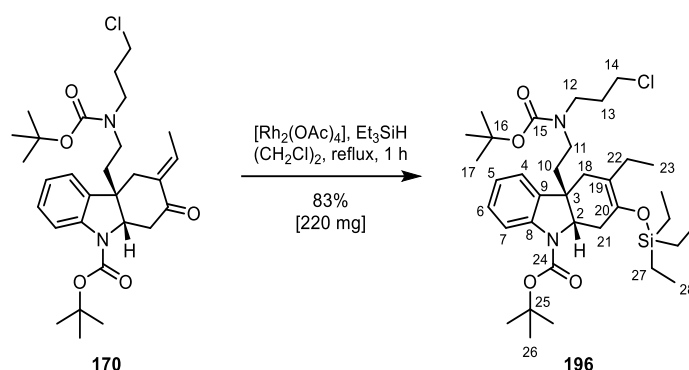
## *Experimental*

**HRMS** (ESI<sup>+</sup>) C<sub>19</sub>H<sub>25</sub>ClN<sub>2</sub>O: 333.1725 [M+H]<sup>+</sup> (calcd 333.1728);

**IR** (thin film) 3328 (N–H), 2954, 2922, 2852, 1698 (C=O), 1631, 1606 (C=C), 1485, 1465, 1262, 741 (C–Cl) cm<sup>-1</sup>.

## Experimental

### Preparation of Compound 196



$[\text{Rh}_2(\text{OAc})_4]$  (10 mg, 0.023 mmol) was added to a flask, followed by 1,2-dichloroethane (2.0 mL) and triethylsilane (0.17 mL, 1.1 mmol). The resulting mixture was stirred at room temperature for 10 min. Compound **170** (220 mg, 0.41 mmol) in 1,2-dichloroethane (2.0 mL) was added to the flask. The resulting mixture was stirred at reflux for 1 h. The reaction mixture was concentrated under reduced pressure. The crude product was purified by flash chromatography (neutral aluminium oxide, petroleum ether 40–65/EtOAc, 8:2) to afford *tert*-butyl (4*aR*,9*aS*)-4*a*-(2-((*tert*-butoxycarbonyl)(3-chloropropyl)amino)ethyl)-3-ethyl-2-((triethylsilyl)oxy)-1,4,4*a*,9*a*-tetrahydro-9*H*-carbazole-9-carboxylate (**196**) as a colourless oil (220 mg, 0.34 mmol, 83%).

$R_f$  = 0.52 (neutral aluminium oxide, petroleum ether 40–65/EtOAc, 8:2);

$^1\text{H NMR}$  (400 MHz,  $\text{CDCl}_3$ , 50 °C)  $\delta$  = 7.64 (app. s, 1H, H<sub>7</sub>), 7.12 (dd,  $^3J_{5,6}$  = 7.6 Hz,  $^3J_{6,7}$  = 7.6 Hz, 1H, H<sub>6</sub>), 7.04 (d,  $^3J_{4,5}$  = 7.5 Hz, 1H, H<sub>4</sub>), 6.94 (dd,  $^3J_{4,5}$  = 7.3,  $^3J_{5,6}$  = 7.3 Hz, 1H, H<sub>5</sub>), 4.29 (app. s, 1H, H<sub>2</sub>), 3.46 (t,  $^3J_{13,14}$  = 6.4 Hz, 2H, H<sub>14</sub>), 3.30 – 3.11 (m, 2H, H<sub>12</sub>)<sup>41</sup>, 3.11 – 2.77 (m, 2H, H<sub>11</sub>)<sup>41</sup>, 2.56 (dd,  $^2J_{21,21}$  = 15.6 Hz,  $^3J_{2,21}$  = 5.7 Hz, 1H, H<sub>21</sub>), 2.43 – 2.33 (m, 1H, H<sub>21</sub>)<sup>41</sup>, 2.33 (d,  $^2J_{18,18}$  = 14.9 Hz, 1H, H<sub>18</sub>), 2.26 (d,  $^3J_{18,18}$  = 14.9 Hz, 1H, H<sub>18</sub>), 2.07 – 1.94 (m, 1H, H<sub>22</sub>), 1.94 – 1.78 (m, 5H, H<sub>10,13,22</sub>), 1.58 (s, 9H, H<sub>26</sub>), 1.42 (s, 9H, H<sub>17</sub>)<sup>41</sup>, 0.92 (t,  $^3J_{27,28}$  = 7.8 Hz, 9H, H<sub>28</sub>), 0.79 (dd,  $^3J_{22,23}$  = 7.2 Hz,  $^3J_{22,23}$  = 7.2 Hz, 3H, H<sub>23</sub>), 0.58 (q,  $^3J_{27,28}$  = 7.9 Hz, 6H, H<sub>27</sub>) ppm;

$^{13}\text{C NMR}$  (101 MHz,  $\text{CDCl}_3$ , 50 °C)  $\delta$  = 155.5 (C=O, C<sub>15</sub>), 152.3 (C=O, C<sub>24</sub>), 142.9 (C, C<sub>8</sub>), 142.1 (C=C, C<sub>20</sub>), 136.9 (C, C<sub>9</sub>), 127.9 (CH, C<sub>6</sub>), 122.8 (CH, C<sub>5</sub>), 122.7 (CH, C<sub>4</sub>), 116.0 (C=C, C<sub>19</sub>), 115.3 (CH, C<sub>7</sub>), 81.2 (C–O, C<sub>25</sub>), 79.8 (C–O, C<sub>16</sub>), 65.7 (CH, C<sub>2</sub>), 47.2 (C, C<sub>3</sub>), 45.0 (CH<sub>2</sub>,

<sup>41</sup> Overlapping signals therefore not possible to accurately integrate, integrals shown are corrected.

### *Experimental*

C<sub>12</sub>), 44.1 (CH<sub>2</sub>, C<sub>11</sub>), 42.5 (CH<sub>2</sub>, C<sub>14</sub>), 40.8 (CH<sub>2</sub>, C<sub>10</sub>), 37.7 (CH<sub>2</sub>, C<sub>18</sub>), 34.7 (CH<sub>2</sub>, C<sub>21</sub>), 31.8 (CH<sub>2</sub>, C<sub>13</sub>), 28.70 (CH<sub>3</sub>, C<sub>17</sub>), 28.66 (CH<sub>3</sub>, C<sub>26</sub>), 22.7 (CH<sub>2</sub>, C<sub>22</sub>), 12.2 (CH<sub>3</sub>, C<sub>23</sub>), 6.8 (CH<sub>3</sub>, C<sub>28</sub>), 5.6 (Si-CH<sub>2</sub>, C<sub>27</sub>) ppm;

**HRMS** (ESI<sup>+</sup>) C<sub>35</sub>H<sub>57</sub>ClN<sub>2</sub>O<sub>5</sub>Si: 671.3612 [M+Na]<sup>+</sup> (calcd 671.3617);

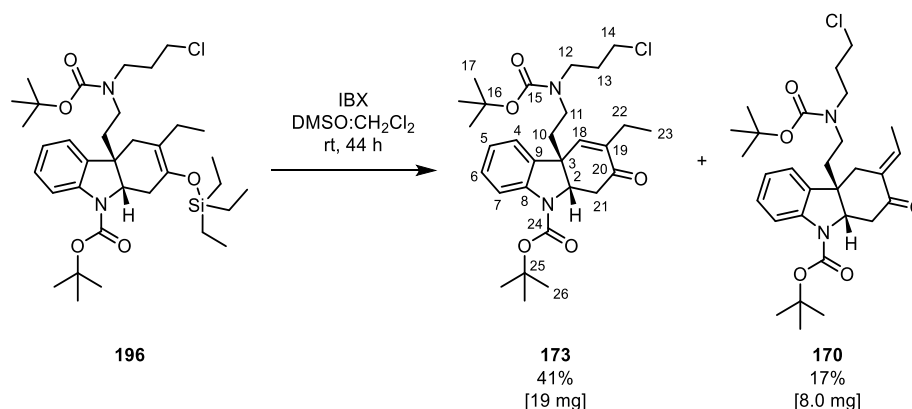
**IR** (thin film) 2954, 2922, 2872, 2853, 1697 (C=O), 1378, 1167 (C-O), 747 (C-Cl) cm<sup>-1</sup>;

**[α]<sub>D</sub><sup>20</sup>** +16 (c 0.50, CHCl<sub>3</sub>).

## Experimental

### Preparation of Compound 173

#### Method A

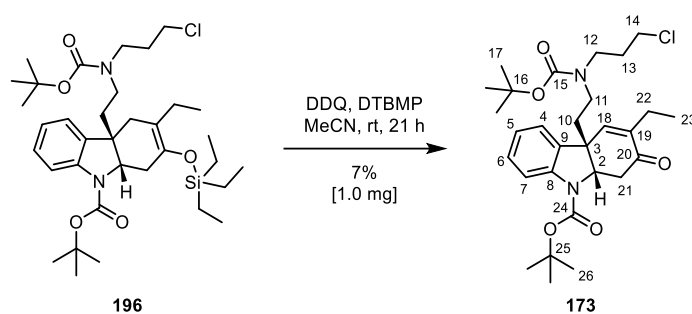


2-Iodoxybenzoic acid (IBX) (**183**) (39 mg, 0.014 mmol) was added to a flask, followed by compound **196** (57 mg, 0.088 mmol) in DMSO:CH<sub>2</sub>Cl<sub>2</sub> (0.68:0.23 mL). The resulting mixture was stirred vigorously at room temperature for 44 h. The reaction mixture was then diluted with aq. NaHCO<sub>3</sub> (5%). The aqueous layer was extracted with Et<sub>2</sub>O. The combined organic extracts were concentrated under reduced pressure. The residue was taken up in Et<sub>2</sub>O and filtered through Celite. The filtrate was then washed with sat. aq. NaHCO<sub>3</sub> and H<sub>2</sub>O, dried over brine, MgSO<sub>4</sub>, filtered and concentrated under reduced pressure. The crude product was purified by flash chromatography (petroleum ether 40–65/Et<sub>2</sub>O, 7:3) to afford *tert*-butyl (4a*S*,9a*S*)-4a-(2-((*tert*-butoxycarbonyl)(3-chloropropyl)amino)ethyl)-3-ethyl-2-oxo-1,2,4a,9a-tetrahydro-9*H*-carbazole-9-carboxylate (**173**) as a colourless oil (19 mg, 0.036 mmol, 41%) and *tert*-butyl (4a*R*,9a*S*,*E*)-4a-(2-((*tert*-butoxycarbonyl)(3-chloropropyl)amino)ethyl)-3-ethylidene-2-oxo-1,2,3,4,4a,9a-hexahydro-9*H*-carbazole-9-carboxylate (**170**) as a white foam (8.0 mg, 0.015 mmol, 17%)<sup>42</sup>.

<sup>42</sup> The highest yield of compound **173** was obtained when the oxidation was performed with freshly prepared IBX (**183**) on the scale as reported above; however, when the IBX (**183**) was not freshly prepared and the reaction was performed on a larger scale 2.0 eq. of IBX (**183**) were required and the reaction was performed at 55 °C with a slightly lower yield of compound **173** of 32%.

## Experimental

### Method B



2,3-Dichloro-5,6-dicyano-*p*-benzoquinone (DDQ) (27 mg, 0.12 mmol) and 2,6-di-*tert*-butyl-4-methylpyridine (DTBMP) (**202**) (24 mg, 0.12 mmol) were added to a flask, followed by compound **196** (18 mg, 0.028 mmol) in MeCN (0.60 mL). The resulting mixture was stirred at room temperature for 21 h. The reaction mixture was then quenched with sat. aq. Na<sub>2</sub>S<sub>2</sub>O<sub>3</sub>. The aqueous layer was extracted with EtOAc. The combined organic extracts were dried over brine, MgSO<sub>4</sub>, filtered and concentrated under reduced pressure. The residue was taken up in Et<sub>2</sub>O and filtered through a pad of silica gel. The filtrate was concentrated under reduced pressure. The crude product was purified by flash chromatography (petroleum ether 40–65/Et<sub>2</sub>O, 7:3) to afford *tert*-butyl (4*aS*,9*aS*)-4*a*-(2-((*tert*-butoxycarbonyl)(3-chloropropyl)amino)ethyl)-3-ethyl-2-oxo-1,2,4*a*,9*a*-tetrahydro-9*H*-carbazole-9-carboxylate (**173**) as a colourless oil (1.0 mg, 1.9 μmol, 7%).

**R<sub>f</sub>** = 0.34 (petroleum ether 40–65/Et<sub>2</sub>O, 7:3);

**<sup>1</sup>H NMR** (400 MHz, CDCl<sub>3</sub>, 50 °C) δ = 7.75 (d, <sup>3</sup>*J*<sub>6,7</sub> = 8.0 Hz, 1H, H<sub>7</sub>), 7.23 (ddd, <sup>3</sup>*J*<sub>6,7</sub> = 8.1 Hz, <sup>3</sup>*J*<sub>5,6</sub> = 7.5 Hz, <sup>4</sup>*J*<sub>4,6</sub> = 1.3 Hz, 1H, H<sub>6</sub>), 7.15 (dd, <sup>3</sup>*J*<sub>4,5</sub> = 7.5 Hz, <sup>4</sup>*J*<sub>4,6</sub> = 1.4 Hz, 1H, H<sub>4</sub>), 7.04 (ddd, <sup>3</sup>*J*<sub>4,5</sub> = 7.5 Hz, <sup>3</sup>*J*<sub>5,6</sub> = 7.5 Hz, <sup>4</sup>*J*<sub>5,7</sub> = 1.1 Hz, 1H, H<sub>5</sub>), 6.58 (s, 1H, H<sub>18</sub>), 4.63 (dd, <sup>3</sup>*J*<sub>2,21</sub> = 8.8 Hz, <sup>3</sup>*J*<sub>2,21</sub> = 6.0 Hz, 1H, H<sub>2</sub>), 3.49 (t, <sup>3</sup>*J*<sub>13,14</sub> = 6.3 Hz, 2H, H<sub>14</sub>), 3.30 – 3.20 (m, 2H, H<sub>12</sub>), 3.20 – 3.04 (m, 2H, H<sub>11</sub>)<sup>43</sup>, 2.95 (dd, <sup>2</sup>*J*<sub>21,21</sub> = 15.5 Hz, <sup>3</sup>*J*<sub>2,21</sub> = 6.0 Hz, 1H, H<sub>21</sub>), 2.54 (dd, <sup>2</sup>*J*<sub>21,21</sub> = 15.5 Hz, <sup>3</sup>*J*<sub>2,21</sub> = 9.9 Hz, 1H, H<sub>21</sub>), 2.36 – 2.16 (m, 2H, H<sub>22</sub>), 1.98 – 1.83 (m, 4H, H<sub>10,13</sub>), 1.58 (s, 9H, H<sub>26</sub>)<sup>44</sup>, 1.42 (s, 9H, H<sub>17</sub>), 1.05 (t, <sup>3</sup>*J*<sub>22,23</sub> = 7.4 Hz, 3H, H<sub>23</sub>) ppm;

**<sup>13</sup>C NMR** (101 MHz, CDCl<sub>3</sub>, 50 °C) δ = 196.8 (C=O, C<sub>20</sub>), 155.3 (C=O, C<sub>15</sub>), 152.0 (C=O, C<sub>24</sub>), 141.8 (C=C, C<sub>18</sub>), 140.6 (C, C<sub>8</sub>, C=C, C<sub>19</sub>), 133.7 (C, C<sub>9</sub>), 128.9 (CH, C<sub>6</sub>), 123.4 (CH, C<sub>5</sub>), 123.0 (CH, C<sub>4</sub>), 116.2 (CH, C<sub>7</sub>), 82.0 (C, C<sub>25</sub>), 80.1 (C, C<sub>16</sub>), 63.1 (CH, C<sub>2</sub>), 47.0 (C, C<sub>3</sub>),

<sup>43</sup> Overlapping signals therefore not possible to accurately integrate, integrals shown are corrected.

<sup>44</sup> Corrected integral.

## *Experimental*

45.1 (CH<sub>2</sub>, C<sub>12</sub>), 43.9 (CH<sub>2</sub>, C<sub>11</sub>), 42.5 (CH<sub>2</sub>, C<sub>14</sub>), 40.6 (CH<sub>2</sub>, C<sub>21</sub>), 39.7 (CH<sub>2</sub>, C<sub>10</sub>), 31.8 (CH<sub>2</sub>, C<sub>13</sub>), 28.62 (CH<sub>2</sub>, C<sub>17</sub>), 28.60 (CH<sub>2</sub>, C<sub>26</sub>), 22.6 (CH<sub>2</sub>, C<sub>22</sub>), 12.8 (CH<sub>2</sub>, C<sub>23</sub>) ppm;

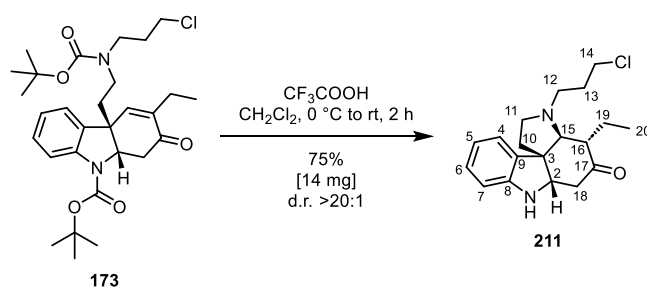
**HRMS** (ESI<sup>+</sup>) C<sub>29</sub>H<sub>41</sub>ClN<sub>2</sub>O<sub>5</sub>: 555.2634 [M+Na]<sup>+</sup> (calcd 55.2596);

**IR** (thin film) 2956, 2923, 2869, 2853, 1686 (C=O), 1479, 1389, 1367, 1163 (C–O), 753 (C–Cl) cm<sup>-1</sup>;

**[α]<sub>D</sub><sup>20</sup>** +55 (*c* 0.50, CHCl<sub>3</sub>).

## Experimental

### Preparation of Compound 211



Compound **173** (30 mg, 0.056 mmol) in  $\text{CH}_2\text{Cl}_2$  (0.57 mL) was added to a flask. The solution was cooled to  $0\text{ }^\circ\text{C}$  and trifluoroacetic acid (90  $\mu\text{L}$ , 1.2 mmol) was added dropwise. The resulting mixture was stirred at room temperature for 2 h. The reaction mixture was then quenched with sat. aq.  $\text{NH}_4\text{Cl}$ . The aqueous layer was extracted with  $\text{CH}_2\text{Cl}_2$ . The combined organic extracts were dried over brine,  $\text{MgSO}_4$ , filtered and concentrated under reduced pressure. The crude product was purified by flash chromatography (petroleum ether 40–65/ $\text{Et}_2\text{O}$ / $\text{Et}_3\text{N}$ , 3:7:0.1) to afford (3a*S*,4*S*,6a*S*,11*bS*)-3-(3-chloropropyl)-4-ethyl-2,3,3a,4,6a,7-hexahydro-1*H*-pyrrolo[2,3-*d*]carbazol-5(6*H*)-one (**211**) as a white solid (14 mg, 0.042 mmol, 75%, d.r. >20:1).

$R_f = 0.47$  (petroleum ether 40–65/ $\text{Et}_2\text{O}$ / $\text{Et}_3\text{N}$ , 3:7:0.1);

$^1\text{H NMR}$  (600 MHz,  $\text{CDCl}_3$ )  $\delta = 7.13$  (dd,  $^3J_{4,5} = 7.4$  Hz,  $^4J_{4,6} = 0.7$  Hz, 1H,  $\text{H}_4$ ), 7.06 (ddd,  $^3J_{5,6} = 7.7$  Hz,  $^3J_{6,7} = 7.7$  Hz,  $^4J_{4,6} = 1.2$  Hz, 1H,  $\text{H}_6$ ), 6.77 (ddd,  $^3J_{4,5} = 7.4$  Hz,  $^3J_{5,6} = 7.4$  Hz,  $^4J_{5,7} = 0.9$  Hz, 1H,  $\text{H}_5$ ), 6.57 (ddd,  $^3J_{6,7} = 7.8$  Hz,  $^4J_{5,7} = 0.7$  Hz, 1H,  $\text{H}_7$ ), 4.00 (dd,  $^3J_{2,18} = 3.9$  Hz,  $^3J_{2,18} = 3.9$  Hz, 1H,  $\text{H}_2$ ), 3.90 (s, 1H,  $\text{N-H}_1$ ), 3.61 – 3.49 (m, 2H,  $\text{H}_{14}$ ), 3.34 – 3.25 (m, 1H,  $\text{H}_{11}$ ), 2.98 (dd,  $^2J_{18,18} = 16.0$  Hz,  $^3J_{2,18} = 3.8$  Hz, 1H,  $\text{H}_{18}$ ), 2.92 (ddd,  $^2J_{12,12} = 12.4$  Hz,  $^3J_{12,13} = 8.7$  Hz,  $^3J_{12,13} = 7.3$  Hz, 1H,  $\text{H}_{12}$ ), 2.67 (d,  $^3J_{15,16} = 1.7$  Hz, 1H,  $\text{H}_{15}$ ), 2.54 (dd,  $^2J_{18,18} = 16.0$ ,  $^3J_{2,18} = 4.1$  Hz, 1H,  $\text{H}_{18}$ ), 2.45 – 2.34 (m, 2H,  $\text{H}_{10,11}$ ), 2.30 (ddd,  $^3J_{16,19} = 8.3$  Hz,  $^3J_{16,19} = 6.5$  Hz,  $^3J_{15,16} = 1.8$  Hz, 1H,  $\text{H}_{16}$ ), 2.23 (ddd,  $^2J_{12,12} = 11.0$  Hz,  $^3J_{12,13} = 6.6$  Hz,  $^3J_{12,13} = 4.2$  Hz, 1H,  $\text{H}_{12}$ ), 2.03 – 1.86 (m, 3H,  $\text{H}_{10,13}$ ), 1.65 – 1.56 (m, 1H,  $\text{H}_{19}$ ), 1.19 – 1.11 (m, 1H,  $\text{H}_{19}$ ), 0.73 (dd,  $^3J_{19,20} = 7.4$  Hz,  $^3J_{19,20} = 7.4$  Hz, 3H,  $\text{H}_{20}$ ) ppm;

$^{13}\text{C NMR}$  (151 MHz,  $\text{CDCl}_3$ )  $\delta = 212.8$  (C=O,  $\text{C}_{17}$ ), 149.8 (C,  $\text{C}_8$ ), 135.6 (C,  $\text{C}_9$ ), 128.3 (CH,  $\text{C}_6$ ), 123.3 (CH,  $\text{C}_4$ ), 119.5 (CH,  $\text{C}_5$ ), 109.6 (CH,  $\text{C}_7$ ), 73.5 (CH,  $\text{C}_{15}$ ), 66.2 (CH,  $\text{C}_2$ ), 52.8 ( $\text{CH}_2$ ,  $\text{C}_{11}$ ), 52.0 (C,  $\text{C}_3$ ), 51.4 (CH,  $\text{C}_{16}$ ), 50.5 ( $\text{CH}_2$ ,  $\text{C}_{12}$ ), 43.0 ( $\text{CH}_2$ ,  $\text{C}_{14}$ ), 41.5 ( $\text{CH}_2$ ,  $\text{C}_{18}$ ), 40.5 ( $\text{CH}_2$ ,  $\text{C}_{10}$ ), 31.5 ( $\text{CH}_2$ ,  $\text{C}_{13}$ ), 22.4 ( $\text{CH}_2$ ,  $\text{C}_{19}$ ), 12.9 ( $\text{CH}_3$ ,  $\text{C}_{20}$ ) ppm;

**HRMS** (ESI<sup>+</sup>)  $\text{C}_{19}\text{H}_{25}\text{ClN}_2\text{O}$ : 333.1732 [ $\text{M}+\text{H}$ ]<sup>+</sup> (calcd 333.1728);

## *Experimental*

**IR** (thin film) 3363 (N–H), 2956, 2924, 2870, 2854, 1706 (C=O), 1609 (N–H), 1485, 1464, 744 (C–Cl)  $\text{cm}^{-1}$ ;

$[\alpha]_D^{20} +24$  ( $c$  0.42,  $\text{CHCl}_3$ );

**m.p.** 93–95  $^{\circ}\text{C}$ <sup>45</sup>.

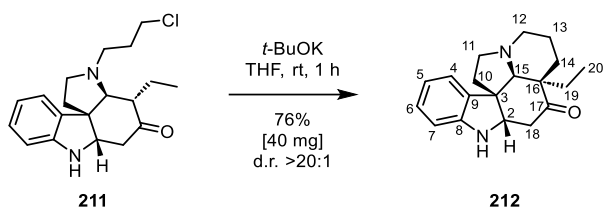
---

<sup>45</sup> Measured from racemic material, due to small quantity of enantioenriched material obtained.

## Experimental

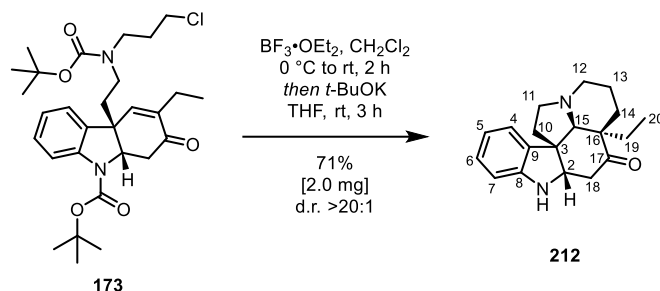
### Preparation of Compound 212

#### Method A



*t*-BuOK (29 mg, 0.24 mmol) was added to a flask, followed by compound **211** (58 mg, 0.17 mmol) in THF (3.5 mL). The resulting mixture was stirred at room temperature for 1 h. The reaction mixture was then quenched with sat. aq. NH<sub>4</sub>Cl. The aqueous layer was extracted with EtOAc. The combined organic extracts were dried over brine, MgSO<sub>4</sub>, filtered and concentrated under reduced pressure. The crude product was purified by flash chromatography (petroleum ether 40–65/Et<sub>2</sub>O/Et<sub>3</sub>N, 6:4:0.1) to afford 4-oxo-aspidospermidine (**212**) as a white solid (40 mg, 0.013 mmol, 76%, d.r. >20:1).

#### Method B



Compound **173** (5.0 mg, 9.4 μmol) in CH<sub>2</sub>Cl<sub>2</sub> (0.50 mL) was added to a flask. The solution was cooled to 0 °C and BF<sub>3</sub>·OEt<sub>2</sub> (10 μL, 81 μmol) was added dropwise. The resulting mixture was stirred at room temperature for 2 h. The reaction mixture was then concentrated under reduced pressure under inert conditions. The residue was dissolved in THF (0.20 mL) and *t*-BuOK (13 mg, 0.12 mmol) was added. The resulting mixture was stirred at room temperature for 3 h. The reaction mixture was then quenched with sat. aq. NH<sub>4</sub>Cl. The aqueous layer was extracted with EtOAc. The combined organic extracts were dried over brine, MgSO<sub>4</sub>, filtered and concentrated under reduced pressure. The crude product was purified by flash chromatography (petroleum ether 40–65/Et<sub>2</sub>O/Et<sub>3</sub>N, 6:4:0.1) 4-oxo-aspidospermidine (**212**) as a white solid (2.0 mg, 6.7 μmol, 71%, d.r. >20:1).

## Experimental

**R<sub>f</sub>** = 0.28 (petroleum ether 40–65/Et<sub>2</sub>O/Et<sub>3</sub>N, 6:4:0.1);

**<sup>1</sup>H NMR** (600 MHz, CDCl<sub>3</sub>) δ = 7.15 (dd, <sup>3</sup>J<sub>4,5</sub> = 7.4 Hz, <sup>4</sup>J<sub>4,6</sub> = 0.7 Hz, 1H, H<sub>4</sub>), 7.05 (ddd, <sup>3</sup>J<sub>5,6</sub> = 7.6 Hz, <sup>3</sup>J<sub>6,7</sub> = 7.6 Hz, <sup>4</sup>J<sub>4,6</sub> = 1.3 Hz, 1H, H<sub>6</sub>), 6.77 (dd, <sup>3</sup>J<sub>4,5</sub> = 7.4, <sup>3</sup>J<sub>5,6</sub> = 7.4 Hz, <sup>4</sup>J<sub>5,7</sub> = 1.0 Hz, 1H, H<sub>5</sub>), 6.58 (d, <sup>3</sup>J<sub>6,7</sub> = 7.8 Hz, 1H, H<sub>7</sub>), 4.00 (dd, <sup>3</sup>J<sub>2,21</sub> = 4.4 Hz, <sup>3</sup>J<sub>2,21</sub> = 4.4 Hz, 1H, H<sub>2</sub>), 3.94 (s, 1H, N–H<sub>1</sub>), 3.13 (td, <sup>2</sup>J<sub>11,11</sub> = 8.7 Hz, <sup>3</sup>J<sub>10,11</sub> = 2.1 Hz, 1H, H<sub>11</sub>), 3.06 (dd, <sup>2</sup>J<sub>18,18</sub> = 16.6 Hz, <sup>3</sup>J<sub>2,18</sub> = 4.8 Hz, 1H, H<sub>18</sub>), 3.03 – 2.98 (m, 1H, H<sub>12</sub>), 2.56 (dd, <sup>2</sup>J<sub>18,18</sub> = 16.7 Hz, <sup>3</sup>J<sub>2,18</sub> = 3.9 Hz, 1H, H<sub>18</sub>), 2.32 (app. q, <sup>3</sup>J<sub>10,11</sub> = 9.0 Hz, 1H, H<sub>11</sub>), 2.27 (s, 1H, H<sub>15</sub>)<sup>46</sup>, 2.31 – 2.20 (m, 1H, H<sub>10</sub>), 2.02 (ddd, <sup>2</sup>J<sub>10,10</sub> = 13.4 Hz, <sup>3</sup>J<sub>10,11</sub> = 8.9 Hz, <sup>3</sup>J<sub>10,11</sub> = 8.9 Hz, 1H, H<sub>10</sub>), 1.92 (ddd, <sup>3</sup>J<sub>12,13</sub> = 11.5 Hz, <sup>3</sup>J<sub>12,13</sub> = 11.1 Hz, <sup>4</sup>J<sub>12,14</sub> = 3.2 Hz, 1H, H<sub>12</sub>), 1.55 – 1.49 (m, 1H, H<sub>19</sub>), 1.49 – 1.38 (m, 2H, H<sub>13</sub>), 1.36 – 1.27 (m, 1H, H<sub>19</sub>), 0.94 (td, <sup>2</sup>J<sub>14,14</sub> = 13.3 Hz, <sup>3</sup>J<sub>13,14</sub> = 4.9 Hz, 1H, H<sub>14</sub>), 0.48 (dd, <sup>3</sup>J<sub>19,20</sub> = 7.5, <sup>3</sup>J<sub>19,20</sub> = 7.5 Hz, 3H, H<sub>20</sub>) ppm;

**<sup>13</sup>C NMR** (151 MHz, CDCl<sub>3</sub>) δ = 213.5 (C=O, C<sub>17</sub>), 150.0 (C, C<sub>8</sub>), 135.9 (C, C<sub>9</sub>), 128.1 (CH, C<sub>6</sub>), 123.8 (CH, C<sub>4</sub>), 119.4 (CH, C<sub>5</sub>), 109.7 (CH, C<sub>7</sub>), 76.2 (CH, C<sub>15</sub>), 67.2 (CH, C<sub>2</sub>), 53.8 (CH<sub>2</sub>, C<sub>11</sub>), 53.1 (CH<sub>2</sub>, C<sub>12</sub>), 52.2 (C, C<sub>3</sub>), 51.0 (C, C<sub>16</sub>), 42.2 (CH<sub>2</sub>, C<sub>18</sub>), 42.1 (CH<sub>2</sub>, C<sub>10</sub>), 30.9 (CH<sub>2</sub>, C<sub>14</sub>), 27.8 (CH<sub>2</sub>, C<sub>19</sub>), 22.8 (CH<sub>2</sub>, C<sub>13</sub>), 7.8 (CH<sub>3</sub>, C<sub>20</sub>) ppm;

**HRMS** (ESI<sup>+</sup>) C<sub>19</sub>H<sub>24</sub>N<sub>2</sub>O: 297.1948 [M+H]<sup>+</sup> (calcd 297.1961);

**IR** (thin film) 3361 (N–H), 2953, 2922, 2868, 2853, 1734, 1704 (C=O), 1486, 1377 cm<sup>-1</sup>;

**[α]<sub>D</sub><sup>20</sup>** –2.8 (c 0.36, CHCl<sub>3</sub>).

**m.p.** 139–141 °C<sup>47</sup>.

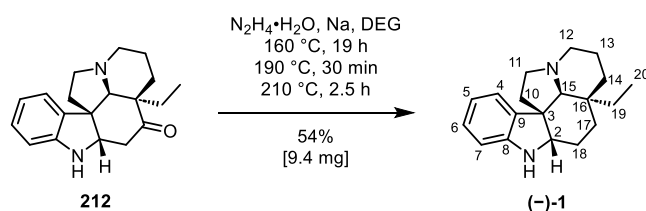
---

<sup>46</sup> Overlapping signals therefore not possible to accurately integrate, integrals shown are corrected.

<sup>47</sup> Measured from racemic material, due to small quantity of enantioenriched material obtained.

## Experimental

### Preparation of Compound (-)-1



Compound **212** (18 mg, 0.061 mmol) was added to a flask, followed by diethylene glycol (DEG) (0.61 mL) and Na (260 mg, 11 mmol). Hydrazine monohydrate (0.75 mL, 15 mmol) was then added dropwise. The resulting mixture was stirred at 160 °C for 19 h, 190 °C for 30 min and 210 °C for 2.5 h. The reaction mixture was allowed to cool to room temperature and then diluted with  $\text{H}_2\text{O}$ . The aqueous layer was extracted with  $\text{CH}_2\text{Cl}_2$ . The combined organic extracts were dried over brine,  $\text{MgSO}_4$ , filtered and concentrated under reduced pressure. The crude product was purified by repeated flash chromatography (petroleum ether 40–65/ $\text{Et}_2\text{O}$ / $\text{Et}_3\text{N}$ , 6:4:0.1; PhMe/ $\text{EtOAc}$ / $\text{Et}_3\text{N}$ , 9:1:0.1) to afford (-)-aspidospermidine (**1**) as a white solid (9.4 mg, 0.033 mmol, 54%).

The obtained spectroscopic data matched literature values.<sup>[86]</sup>

$R_f$  = 0.31 (petroleum ether 40–65/ $\text{Et}_2\text{O}$ / $\text{Et}_3\text{N}$ , 6:4:0.1), 0.38 (PhMe/ $\text{EtOAc}$ / $\text{Et}_3\text{N}$ , 9:1:0.1);

**$^1\text{H}$  NMR** (600 MHz,  $\text{CDCl}_3$ )  $\delta$  = 7.08 (dd,  $^3J_{4,5}$  = 7.4 Hz,  $^4J_{4,6}$  = 1.3 Hz, 1H,  $\text{H}_4$ ), 7.01 (ddd,  $^3J_{5,6}$  = 7.6 Hz,  $^3J_{6,7}$  = 7.6 Hz,  $^4J_{4,6}$  = 1.3 Hz, 1H,  $\text{H}_6$ ), 6.73 (ddd,  $^3J_{4,5}$  = 7.4 Hz,  $^3J_{5,6}$  = 7.4 Hz,  $^3J_{5,7}$  = 1.0 Hz, 1H,  $\text{H}_5$ ), 6.64 (d,  $^3J_{6,7}$  = 7.7 Hz, 1H,  $\text{H}_7$ ), 3.51 (dd,  $^3J_{2,18}$  = 11.1 Hz,  $^3J_{2,18}$  = 6.2 Hz, 1H,  $\text{H}_2$ ), 3.16 – 3.09 (m, 1H,  $\text{H}_{11}$ ), 3.08 – 3.02 (m, 1H,  $\text{H}_{12}$ ), 2.34 – 2.23 (m, 2H,  $\text{H}_{10,11}$ ), 2.22 (s, 1H,  $\text{H}_{15}$ ), 2.00 – 1.90 (m, 2H,  $\text{H}_{12,17}$ ), 1.79 – 1.68 (m, 1H,  $\text{H}_{13}$ ), 1.67 – 1.59 (m, 2H,  $\text{H}_{14,18}$ ), 1.55 – 1.43 (m, 3H,  $\text{H}_{10,13,19}$ ), 1.39 (dddd,  $^2J_{18,18}$  = 14.4 Hz,  $^3J_{17,18}$  = 13.2 Hz,  $^3J_{2,18}$  = 11.1 Hz,  $^3J_{17,18}$  = 3.6 Hz, 1H,  $\text{H}_{18}$ ), 1.11 (td,  $^2J_{14,14}$  = 13.6 Hz,  $^3J_{13,14}$  = 4.7 Hz, 1H,  $\text{H}_{14}$ ), 1.06 (ddd,  $^2J_{17,17}$  = 13.5 Hz,  $^3J_{17,18}$  = 3.7 Hz, 1H,  $\text{H}_{17}$ ), 0.92 – 0.82 (m, 1H,  $\text{H}_{19}$ ), 0.64 (dd,  $^3J_{19,20}$  = 7.5 Hz,  $^3J_{19,20}$  = 7.5 Hz, 3H,  $\text{H}_{20}$ ) ppm;

**$^{13}\text{C}$  NMR** (151 MHz,  $\text{CDCl}_3$ )  $\delta$  = 149.6 (C,  $\text{C}_8$ ), 135.9 (C,  $\text{C}_9$ ), 127.2 (CH,  $\text{C}_6$ ), 123.0 (CH,  $\text{C}_4$ ), 119.1 (CH,  $\text{C}_5$ ), 110.5 (CH,  $\text{C}_7$ ), 71.4 (CH,  $\text{C}_{15}$ ), 65.8 (CH,  $\text{C}_2$ ), 54.0 ( $\text{CH}_2$ ,  $\text{C}_{12}$ ), 53.5 (C,  $\text{C}_3$ ), 53.2 ( $\text{CH}_2$ ,  $\text{C}_{11}$ ), 39.0 ( $\text{CH}_2$ ,  $\text{C}_{10}$ ), 35.8 (C,  $\text{C}_{16}$ ), 34.6 ( $\text{CH}_2$ ,  $\text{C}_{14}$ ), 30.1 ( $\text{CH}_2$ ,  $\text{C}_{19}$ ), 28.3 ( $\text{CH}_2$ ,  $\text{C}_{18}$ ), 23.2 ( $\text{CH}_2$ ,  $\text{C}_{17}$ ), 21.9 ( $\text{CH}_2$ ,  $\text{C}_{13}$ ), 7.0 ( $\text{CH}_3$ ,  $\text{C}_{20}$ ) ppm;

**HRMS** ( $\text{ESI}^+$ )  $\text{C}_{19}\text{H}_{26}\text{N}_2$ : 283.2186 [ $\text{M}+\text{H}$ ]<sup>+</sup> (calcd 283.2169);

## *Experimental*

**IR** (thin film) 3364 (N–H), 2929, 2860, 2779, 2722, 1607, 1481, 1462, 741  $\text{cm}^{-1}$ ;

$[\alpha]_D^{20}$   $-17$  ( $c$  0.065,  $\text{CHCl}_3$ ), lit.<sup>[86]</sup>  $[\alpha]_D^{20}$   $+20.5$  ( $c$  0.6,  $\text{CHCl}_3$ )

**m.p.** 104–106  $^\circ\text{C}$ <sup>48</sup>, lit.<sup>[72]</sup> 104–106  $^\circ\text{C}$ .

---

<sup>48</sup> Measured from racemic material, due to small quantity of enantioenriched material obtained.

## 6 References

- [1] G. P. Moss, P. A. S. Smith, D. Tavernier, *Pure Appl. Chem.* **1995**, *67*, 1307–1375.
- [2] P. M. Dewick, in *Med. Nat. Prod. A Biosynthetic Approach* (Ed.: P.M. Dewick), John Wiley & Sons, Chichester, **2009**, pp. 311–420.
- [3] D. S. Seigler, in *Plant Second. Metab.*, Kluwer Academic Publishers, Boston, **2002**, pp. 628–654.
- [4] K. Vougiannopoulou, N. Fokialakis, N. Aligiannis, C. Cantrell, A. L. Skaltsounis, *Org. Lett.* **2010**, *12*, 1908–1911.
- [5] M. Frederich, M. Tits, L. Angenot, *Trans. R. Soc. Trop. Med. Hyg.* **2008**, *102*, 11–19.
- [6] M. Giampieri, A. Balbi, M. Mazzei, P. La Colla, C. Ibba, R. Loddo, *Antiviral Res.* **2009**, *83*, 179–185.
- [7] U. Scholz, E. Winterfeldt, *Nat. Prod. Rep.* **2000**, *17*, 349–366.
- [8] C. O'Donnell, Master's Thesis, The University of Edinburgh (UK), **2019**.
- [9] J. E. Saxton, in *Chem. Heterocycl. Compd. Indoles, Part Four, Monoterpenoid Indole Alkaloids* (Ed.: J.E. Saxton), John Wiley & Sons, New York, **1983**, pp. 331–437.
- [10] V. Julien C., I.-L. Albert, W. Allan J.B., in *Stud. Nat. Prod. Chem.* (Ed.: Atta-ur-Rahman), Elsevier, Amsterdam, **2017**, pp. 1–29.
- [11] M. A. Toczko, C. H. Heathcock, *J. Org. Chem.* **2000**, *65*, 2642–2645.
- [12] H. Cho, N. T. Tam, C. Cho, *Bull. Korean Chem. Soc.* **2010**, *31*, 3382–3384.
- [13] K. Biemann, M. Spiteller-Friedmann, G. Spiteller, *J. Am. Chem. Soc.* **1963**, *85*, 631–638.
- [14] L. A. Sharp, S. Z. Zard, *Org. Lett.* **2006**, *8*, 831–834.
- [15] S. Whiting, PhD Thesis, University of Southampton (UK), **2007**.
- [16] K. J. Stenning, PhD Thesis, University of Southampton (UK), **2011**.
- [17] J. M. Lopchuk, in *Prog. Heterocycl. Chem.* (Eds.: G.W. Gribble, J.A. Joule), Elsevier Ltd., Oxford, **2011**, pp. 1–25.
- [18] K. Biemann, M. Friedmann-Spiteller, G. Spiteller, *Tetrahedron Lett.* **1961**, *4*, 485–492.

## References

- [19] S. Lin, G. Bernardello, *Int. J. Plant Sci.* **1999**, *160*, 869–878.
- [20] M. A. Wahid, G. F. Smith, *J. Chem. Soc.* **1963**, 4002–4004.
- [21] D. Schumann, B. W. Bycroft, H. Schmid, *Experientia* **1964**, *20*, 202.
- [22] W. Klyne, R. J. Swan, B. W. Bycroft, D. Schumann, H. Schmid, *Helv. Chim. Acta* **1965**, *48*, 443–452.
- [23] B. M. Craven, D. E. Zacharias, *Experientia* **1968**, *24*, 770–771.
- [24] J. D. Medina, L. Di Genova, *Planta Med.* **1979**, *37*, 165–167.
- [25] M. Urrea, A. Ahond, H. Jacquemin, S. K. Kan, C. Poupat, P. P., M. M. Janot, *C. R. Hebd. Seances Acad. Sci. Ser. C* **1987**, *287*, 63.
- [26] Y.-L. He, W.-M. Chen, X.-Z. Feng, *J. Nat. Prod.* **1994**, *57*, 411–414.
- [27] A. C. Mitaine-Offer, M. Sauvain, A. Valentin, J. Callapa, M. Mallié, M. Zèches-Hanrot, *Phytomedicine* **2002**, *9*, 142–145.
- [28] O. Callaghan, C. Lampard, A. R. Kennedy, J. A. Murphy, *J. Chem. Soc., Perkin Trans. I* **1999**, 995–1001.
- [29] Mylan Pharmaceuticals ULC, “Product Monograph: Vinorelbine Tartrate for Injection,” can be found under [https://www.pfizer.ca/sites/default/files/201710/VINORELBINE\\_TARTRATE\\_FOR\\_INJECTION\\_PM.pdf](https://www.pfizer.ca/sites/default/files/201710/VINORELBINE_TARTRATE_FOR_INJECTION_PM.pdf), **2014** (accessed 6 November 2024).
- [30] A. Contin, R. Van Der Heijden, A. W. M. Lefeber, R. Verpoorte, *FEBS Lett.* **1998**, *434*, 413–416.
- [31] Y. Yamazaki, M. Kitajima, M. Arita, H. Takayama, H. Sudo, M. Yamazaki, N. Aimi, K. Saito, *Plant Physiol.* **2004**, *134*, 161–170.
- [32] K. M. Herrmann, L. M. Weaver, *Annu. Rev. Plant Physiol. Plant Mol. Biol.* **1999**, *50*, 473–503.
- [33] I. A. Scott, S. L. Lee, P. de Capite, M. G. Culver, C. R. Hutchinson, *Heterocycles* **1977**, *7*, 979–984.
- [34] J. Stöckigt, M. H. Zenk, *FEBS Lett.* **1977**, *79*, 233–237.

## References

- [35] J. Stöckigt, M. H. Zenk, *Chem. Commun.* **1977**, 646–648.
- [36] A. R. Lippert, A. Naganawa, V. L. Keleshian, J. W. Bode, *J. Am. Chem. Soc.* **2010**, *132*, 15790–15799.
- [37] R. T. Brown, J. Leonard, S. K. Sleight, *Phytochemistry* **1978**, *17*, 899–900.
- [38] N. Nagakura, M. Rüffer, M. H. Zenk, *Perkin Trans. 1* **1979**, 2308–2312.
- [39] S. E. O'Connor, J. J. Maresh, *Nat. Prod. Rep.* **2006**, *23*, 532–547.
- [40] A. I. Scott, A. A. Qureshi, *J. Am. Chem. Soc.* **1969**, *91*, 5874–5876.
- [41] Y. Qu, M. E. A. M. Easson, R. Simionescu, J. Hajicek, A. M. K. Thamm, V. Salim, V. De Luca, *Proc. Natl. Acad. Sci. U. S. A.* **2018**, *115*, 3180–3185.
- [42] B. P. Pritchett, B. M. Stoltz, *Nat. Prod. Rep.* **2018**, *35*, 559–574.
- [43] G. Stork, J. Dolfini, *J. Am. Chem. Soc.* **1963**, *85*, 2872–2873.
- [44] N. Wang, X. Jiang, *Chem. Rec.* **2021**, *21*, 295–314.
- [45] J. E. Saxton, in *Alkaloids Chem. Biol.* (Ed.: G.A. Cordell), Academic Press, San Diego, **1998**, pp. 343–376.
- [46] J. E. Saxton, in *Alkaloids Chem. Biol.* (Ed.: G.A. Cordell), Academic Press, San Diego, **1998**, pp. 2–197.
- [47] J. M. Saya, E. Ruijter, R. V. A. Orru, *Chem. Eur. J.* **2019**, *25*, 8916–8935.
- [48] N. Wang, X. Xiao, C. X. Liu, H. Yao, N. Huang, K. Zou, *Adv. Synth. Catal.* **2022**, *364*, 2479–2501.
- [49] G. Pandey, S. K. Burugu, P. Singh, *Org. Lett.* **2016**, *18*, 1558–1561.
- [50] N. Wang, S. Du, D. Li, X. Jiang, *Org. Lett.* **2017**, *19*, 3167–3170.
- [51] A. Shemet, E. M. Carreira, *Org. Lett.* **2017**, *19*, 5529–5532.
- [52] H. Nambu, T. Tamura, T. Yakura, *J. Org. Chem.* **2019**, *84*, 15990–15996.
- [53] G. Martin, P. Angyal, O. Egyed, S. Varga, T. Soós, *Org. Lett.* **2020**, *22*, 4675–4679.
- [54] S. Katahara, Y. Sugiyama, M. Yamane, Y. Komiya, T. Sato, N. Chida, *Org. Lett.* **2021**, *23*, 3058–3063.

## References

- [55] R. Iyengar, K. Schildknecht, J. Aubé, *Org. Lett.* **2000**, *2*, 1625–1627.
- [56] D. Gnecco, E. Vázquez, A. Galindo, J. L. Terán, L. Orea, *Org. Chem. Mex.* **2003**, *2003*, 185–192.
- [57] Y. Fukuda, M. Shindo, K. Shishido, *Org. Lett.* **2003**, *5*, 749–751.
- [58] R. Iyengar, K. Schildknecht, M. Morton, J. Aube, *J. Org. Chem.* **2005**, *70*, 10645–10652.
- [59] I. Coldham, A. J. M. Burrell, L. E. White, H. Adams, N. Oram, *Angew. Chem. Int. Ed.* **2007**, *46*, 6159–6162.
- [60] T. Ishikawa, K. Kudo, K. Kuroyabu, S. Uchida, T. Kudoh, S. Saito, *J. Org. Chem.* **2008**, *73*, 7498–7508.
- [61] A.-C. Callier-Dublanchet, J. Cassayre, F. Gagosz, B. Quiclet-Sire, L. A. Sharp, S. Z. Zard, *Tetrahedron* **2008**, *64*, 4803–4816.
- [62] C. Sabot, K. C. Guérard, S. Canesi, *Chem. Commun.* **2009**, 2941–2943.
- [63] J. E. D. Barton, J. Harley-Mason, *Chem. Commun.* **1963**, 298–299.
- [64] J. Harley-Mason, M. Kaplan, *Chem. Commun.* **1967**, 915–916.
- [65] M. Node, H. Nagasawa, K. Fuji, *J. Am. Chem. Soc.* **1987**, *109*, 7901–7903.
- [66] A. G. Schultz, L. Pettus, *J. Org. Chem.* **1997**, *62*, 6855–6861.
- [67] H. Tanino, K. Fukuishi, M. Ushiyama, K. Okada, *Tetrahedron* **2004**, *60*, 3273–3282.
- [68] M. Hayashi, K. Motosawa, A. Satoh, M. Shibuya, K. Ogasawara, Y. Iwabuchi, *Heterocycles* **2009**, *77*, 855–863.
- [69] M. Suzuki, Y. Kawamoto, T. Sakai, Y. Yamamoto, K. Tomioka, *Org. Lett.* **2009**, *11*, 653–655.
- [70] J. E. Nidhiry, K. R. Prasad, *Tetrahedron* **2013**, *69*, 5525–5536.
- [71] T. Gallagher, P. Magnus, J. C. Huffman, Y. Chen, J. E. Ellis, *J. Am. Chem. Soc.* **1982**, *104*, 1140–1141.
- [72] E. Wenkert, T. Hudlicky, *J. Org. Chem.* **1988**, *53*, 1953–1957.
- [73] H. Xu, H. Huang, C. Zhao, C. Song, J. Chang, *Org. Lett.* **2019**, *21*, 6457–6460.

## References

- [74] B. P. Pritchett, J. Kikuchi, Y. Numajiri, B. M. Stoltz, *Angew. Chem. Int. Ed.* **2016**, *55*, 13529–13532.
- [75] M. K. Lakshman, D. Sebastian, P. Pradhan, M. C. Neary, A. M. Piette, S. P. Trzebiatowski, A. E. K. Henriques, P. H. Willoughby, *Chem. - A Eur. J.* **2023**, *29*, 1–8.
- [76] D. Desmaële, J. D'Angelo, *J. Org. Chem* **1994**, *59*, 2292–2303.
- [77] P. Forns, A. Diez, M. Rubiralta, *J. Org. Chem.* **1996**, *61*, 7882–7888.
- [78] S. A. Kozmin, T. Iwama, Y. Huang, V. H. Rawal, *J. Am. Chem. Soc.* **2002**, *124*, 4628–4641.
- [79] M. G. Banwell, D. W. Lupton, *Org. Biomol. Chem.* **2005**, *3*, 213–215.
- [80] L. Jiao, E. Herdtweck, T. Bach, *J. Am. Chem. Soc.* **2012**, *134*, 14563–14572.
- [81] Z. Li, S. Zhang, S. Wu, X. Shen, L. Zou, F. Wang, X. Li, F. Peng, H. Zhang, Z. Shao, *Angew. Chem. Int. Ed.* **2013**, *52*, 4117–4121.
- [82] S. Zhao, R. B. Andrade, *J. Am. Chem. Soc.* **2013**, *135*, 13334–13337.
- [83] G. Xia, X. Han, X. Lu, *Org. Lett.* **2014**, *16*, 2058–2061.
- [84] P. Le Ménez, N. Kunesch, *J. Org. Chem.* **1991**, *56*, 2915–2918.
- [85] B. Patro, J. A. Murphy, *Org. Lett.* **2000**, *2*, 3599–3601.
- [86] J. P. Marino, M. B. Rubio, G. Cao, A. De Dios, *J. Am. Chem. Soc.* **2002**, *124*, 13398–13399.
- [87] F. De Simone, J. Gertsch, J. Waser, *Angew. Chem. Int. Ed.* **2010**, *49*, 5767–5770.
- [88] M. Kawano, T. Kiuchi, S. Negishi, H. Tanaka, T. Hoshikawa, J. Matsuo, H. Ishibashi, *Angew. Chem. Int. Ed.* **2013**, *52*, 906–910.
- [89] S. B. Jones, B. Simmons, A. Mastracchio, D. W. C. Macmillan, *Nature* **2011**, *475*, 183–188.
- [90] K. Du, H. Yang, P. Guo, L. Feng, G. Xu, Q. Zhou, L. W. Chung, W. Tang, *Chem. Sci.* **2017**, *8*, 6247–6256.
- [91] D. Jiang, P. Tang, H. Xiong, S. Lei, Y. Zhang, C. Zhang, L. He, H. Qiu, M. Zhang, *Angew. Chemie. Int. Ed.* **2023**, *62*, e202307286.

## References

- [92] X. Yu, T. Zhang, J. Liu, X. Li, *Synthesis* **2021**, *53*, 4341–4352.
- [93] O. Pàmies, J. Margalef, S. Cañellas, J. James, E. Judge, P. J. Guiry, C. Moberg, J. E. Bäckvall, A. Pfaltz, M. A. Pericàs, M. Diéguez, *Chem. Rev.* **2021**, *121*, 4373–4505.
- [94] D. Jiang, P. Tang, H. Xiong, S. Lei, Y. Zhang, C. Zhang, L. He, H. Qiu, M. Zhang, *Angew. Chem. Int. Ed.* **2023**, *62*, e202307286.
- [95] X. Zhang, L. Han, S. L. You, *Chem. Sci.* **2014**, *5*, 1059–1063.
- [96] B. M. Trost, J. Quancard, *J. Am. Chem. Soc.* **2006**, *128*, 6314–6315.
- [97] Y. Liu, H. Du, *Org. Lett.* **2013**, *15*, 740–743.
- [98] Q. L. Xu, L. X. Dai, S. L. You, *Chem. Sci.* **2013**, *4*, 97–102.
- [99] H. F. Tu, X. Zhang, C. Zheng, M. Zhu, S. L. You, *Nat. Catal.* **2018**, *1*, 601–608.
- [100] J. Ruchti, E. M. Carreira, *J. Am. Chem. Soc.* **2014**, *136*, 16756–16759.
- [101] X. Zhang, W. B. Liu, H. F. Tu, S. L. You, *Chem. Sci.* **2015**, *6*, 4525–4529.
- [102] J. M. Müller, C. B. W. Stark, *Angew. Chem. Int. Ed.* **2016**, *55*, 4798–4802.
- [103] Q. Cheng, H. Tu, C. Zheng, J. Qu, G. Helmchen, S. You, *Chem. Rev.* **2019**, *119*, 1855–1969.
- [104] L. Kürti, B. Czako, *Strategic Application of Named Reactions in Organic Synthesis*, Elsevier, Burlington, **2005**.
- [105] B. M. Trost, *J. Org. Chem.* **2004**, *69*, 5813–5837.
- [106] L. Milhau, P. J. Guiry, in *Transit. Met. Catalyzed Enantioselective Allylic Substit. Org. Synth.* (Ed.: U. Kazmaier), Springer, Berlin, Heidelberg, **2012**, pp. 95–154.
- [107] B. M. Trost, M. L. Crawley, *Chem. Rev.* **2003**, *103*, 2921–2943.
- [108] B. M. Trost, D. L. Van Vranken, *Chem. Rev.* **1996**, *96*, 395–422.
- [109] S. L. Rössler, D. A. Petrone, E. M. Carreira, *Acc. Chem. Res.* **2019**, *52*, 2657–2672.
- [110] S. T. Madrahimov, Q. Li, A. Sharma, J. F. Hartwig, *J. Am. Chem. Soc.* **2015**, *137*, 14968–14981.
- [111] G. Poli, G. Prestat, F. Liron, C. Kammerer-Pentier, in *Transit. Met. Catalyzed*

## References

- Enantioselective Allylic Substit. Org. Synth.* (Ed.: Uli Kazmaier), Springer, Berlin, Heidelberg, **2012**, pp. 1–64.
- [112] B. M. Trost, H. Tsui, F. D. Toste, *J. Am. Chem. Soc.* **2000**, *122*, 3534–3535.
- [113] B. M. Trost, F. D. Toste, *J. Am. Chem. Soc.* **1999**, *121*, 4545–4554.
- [114] B. M. Trost, M. K. Brennan, *Org. Lett.* **2007**, *9*, 3961–3964.
- [115] T. R. Ward, *Organometallics* **1996**, *15*, 2836–2838.
- [116] B. Åkermark, S. Hansson, B. Krakenberger, A. Vitagliano, K. Zetterberg, *Organometallics* **1984**, *3*, 679–682.
- [117] R. Prétôt, A. Pfaltz, *Angew. Chem. Int. Ed.* **1998**, *37*, 323–325.
- [118] J. Sprinz, M. Kiefer, G. Helmchen, *Tetrahedron Lett.* **1994**, *35*, 1523–1526.
- [119] J. M. Brown, D. I. Hulmes, P. J. Guiry, *Tetrahedron* **1994**, *50*, 4493–4506.
- [120] A. Togni, U. Burckhardt, V. Gramlich, P. S. Pregosin, R. Salzmann, *J. Am. Chem. Soc.* **1996**, *118*, 1031–1037.
- [121] O. Pàmies, M. Diéguez, C. Claver, *J. Am. Chem. Soc.* **2005**, *127*, 3646–3647.
- [122] G. Helmchen, A. Pfaltz, *Acc. Chem. Res.* **2000**, *33*, 336–345.
- [123] Y. Mata, O. Pàmies, M. Diéguez, *Adv. Synth. Catal.* **2009**, *351*, 3217–3234.
- [124] I. D. G. Watson, A. K. Yudin, *J. Am. Chem. Soc.* **2005**, *127*, 17516–17529.
- [125] I. Dubovyk, I. D. G. Watson, A. K. Yudin, *J. Am. Chem. Soc.* **2007**, *129*, 14172–14173.
- [126] S. T. Madrahimov, D. Markovic, J. F. Hartwig, *J. Am. Chem. Soc.* **2009**, *131*, 7228–7229.
- [127] R. Takeuchi, M. Kashio, *J. Am. Chem. Soc.* **1998**, *120*, 8647–8655.
- [128] R. Takeuchi, N. Ue, K. Tanabe, K. Yamashita, N. Shiga, *J. Am. Chem. Soc.* **2001**, *123*, 9525–9534.
- [129] J. A. Raskatov, S. Spiess, C. Gnamm, K. Brödner, F. Rominger, G. Helmchen, *Chem. - A Eur. J.* **2010**, *16*, 6601–6615.
- [130] J. A. Raskatov, M. Jäkel, B. F. Straub, F. Rominger, G. Helmchen, *Chem. - A Eur. J.*

## References

- 2012**, *18*, 14314–14328.
- [131] B. M. Trost, J. E. Schultz, *Synthesis* **2019**, *51*, 1–30.
- [132] B. M. Trost, D. L. Van Vranken, *Angew. Chem. Int. Ed.* **1992**, *31*, 228–230.
- [133] G. L. Miessler, D. A. Tarr, in *Inorg. Chem.*, Pearson Prentice Hall, New Jersey, **2004**, pp. 412–450.
- [134] K. L. Granberg, J. E. Baeckvall, *J Neurol Neurosurg Psychiatry* **1992**, *114*, 6858–6863.
- [135] T. Takahashi, Y. Jinbo, K. Kitamura, J. Tsuji, *Tetrahedron Lett.* **1984**, *25*, 5921–5924.
- [136] C. P. Butts, E. Filali, G. C. Lloyd-Jones, P. O. Norrby, D. A. Sale, Y. Schramm, *J. Am. Chem. Soc.* **2009**, *131*, 9945–9957.
- [137] J. M. Camus, J. Andrieu, P. Richard, R. Poli, *Eur. J. Inorg. Chem.* **2004**, 1081–1091.
- [138] B. M. Trost, *Chem. Pharm. Bull.* **2002**, *50*, 1–14.
- [139] B. M. Trost, *Tetrahedron* **2015**, *71*, 5708–5733.
- [140] B. M. Trost, D. L. Van Vranken, C. Bingel, *J. Am. Chem. Soc.* **1992**, *114*, 9327–9343.
- [141] J. Tsuji, H. Takahashi, M. Morikawa, *Tetrahedron Lett.* **1965**, *6*, 4387–4388.
- [142] B. M. Trost, T. J. Fullerton, *J. Am. Chem. Soc.* **1973**, *95*, 292–294.
- [143] K. W. Quasdorf, L. E. Overman, *Nature* **2014**, *516*, 181–191.
- [144] C. Li, S. S. Ragab, G. Liu, W. Tang, *Nat. Prod. Rep.* **2020**, *37*, 276–292.
- [145] A. Lin, J. Yang, M. Hashim, *Org. Lett.* **2013**, *15*, 1950–1953.
- [146] M. Kimura, M. Futamata, R. Mukai, Y. Tamaru, *J. Am. Chem. Soc.* **2005**, *127*, 4592–4593.
- [147] M. Kimura, M. Futamata, K. Shibata, Y. Tamaru, *Chem. Commun.* **2003**, 234–235.
- [148] N. Kagawa, J. P. Malerich, V. H. Rawal, *Org. Lett.* **2008**, *10*, 2381–2384.
- [149] R. D. Gao, L. Ding, C. Zheng, L. X. Dai, S. L. You, *Org. Lett.* **2018**, *20*, 748–751.
- [150] X. Chang, C. Che, Z.-F. Wang, C.-J. Wang, *CCS Chem.* **2022**, *4*, 1414–1428.
- [151] F. Richard, P. Clark, A. Hannam, T. Keenan, A. Jean, S. Arseniyadis, *Chem. Soc. Rev.*

## References

- 2024**, 53, 1936–1983.
- [152] W. Zheng, P. A. Cole, *Bioorg. Chem.* **2003**, 31, 398–411.
- [153] C. M. König, K. Harms, U. Koert, *Org. Lett.* **2007**, 9, 4777–4779.
- [154] A. B. Charette, B. Côté, *Tetrahedron Lett.* **1993**, 34, 6833–6836.
- [155] A. B. Charette, B. Côté, S. Monroe, S. Prescott, *J. Org. Chem.* **1995**, 60, 6888–6894.
- [156] D. L. Hughes, R. A. Reamer, J. J. Bergan, E. J. J. Grabowski, *J. Am. Chem. Soc.* **1988**, 110, 6487–6491.
- [157] A. B. Smith, G. R. Ott, *J. Am. Chem. Soc.* **1996**, 118, 13095–13096.
- [158] K. Sato, M. Bokura, H. Moriyama, T. Igarashi, *Chem. Lett.* **1994**, 23, 37–40.
- [159] K. C. Nicolaou, J. J. Liu, C.-K. Hwang, Dai W.-M., Guy R. K., *J. Chem. Soc.* **1992**, 1118–1120.
- [160] M. Wang, C. Li, D. Yin, X. T. Liang, *Tetrahedron Lett.* **2002**, 43, 8727–8729.
- [161] L. Z. Liu, J. C. Han, G. Z. Yue, C. C. Li, Z. Yang, *J. Am. Chem. Soc.* **2010**, 132, 13608–13609.
- [162] A. S. Kende, K. Liu, I. Kaldor, G. Dorey, K. Koch, *J. Am. Chem. Soc.* **1995**, 117, 8258–8270.
- [163] A. Fürstner, I. Konetzki, *J. Org. Chem.* **1998**, 63, 3072–3080.
- [164] A. Latorre, J. A. Sáez, S. Rodríguez, F. V. González, *Tetrahedron* **2014**, 70, 97–102.
- [165] B. Jiang, F. F. Meng, Q. J. Liang, Y. H. Xu, T.-P. Loh, *Org. Lett.* **2017**, 19, 914–917.
- [166] A. Leesment, S. Selberg, M. Tammiste, A. H. Vu, T. H. Nguyen, L. Taylor-King, I. Leito, *Anal. Chem.* **2022**, 94, 4059–4064.
- [167] J. Clayden, N. Greeves, S. Warren, *Organic Chemistry*, Oxford University Press, Oxford, **2012**.
- [168] S. Kudret, J. D’Haen, L. Lutsen, D. Vanderzande, W. Maes, *Adv. Synth. Catal.* **2013**, 355, 569–575.
- [169] M. W. Rathke, A. Lindebt, M. W. Rathke, *J. Org. Chem.* **1970**, 35, 3966–3967.

## References

- [170] C. R. Holmquist, E. J. Roskamp, *J. Org. Chem.* **1989**, *54*, 3258–3260.
- [171] T. Ritter, PhD Thesis, ETH Zürich (CH), **2004**.
- [172] K. Ishihara, M. Kubota, H. Kurihara, H. Yamamoto, *J. Org. Chem.* **1996**, *61*, 4560–4567.
- [173] B. M. Trost, J. Waser, A. Meyer, *J. Am. Chem. Soc.* **2007**, *129*, 14556–14557.
- [174] M. E. Kuehne, F. Xu, *J. Org. Chem.* **1993**, *58*, 7490–7497.
- [175] S. Roth, PhD Thesis, Freie Universität Berlin (DE), **2007**.
- [176] F. G. Bordwell, G. E. Drucker, H. E. Fried, *J. Org. Chem.* **1981**, *46*, 632–635.
- [177] B. M. Trost, M. R. Machacek, H. C. Tsui, *J. Am. Chem. Soc.* **2005**, *127*, 7014–7024.
- [178] T. Nemoto, T. Fukuyama, E. Yamamoto, S. Tamura, T. Fukuda, T. Matsumoto, Y. Akimoto, Y. Hamada, *Org. Lett.* **2007**, *9*, 927–930.
- [179] S. Ma, S. Yu, *Tetrahedron Lett.* **2004**, *45*, 8419–8422.
- [180] S. Ma, S. Yu, Z. Peng, H. Guo, *J. Org. Chem.* **2006**, *71*, 9865–9868.
- [181] G. Bouhaleb, J. Bouajila, F. Rezgui, *Comptes Rendus Chim.* **2017**, *20*, 484–491.
- [182] S. Kumar, S. L. Jain, *Monatsh Chem* **2014**, *145*, 791–795.
- [183] H. Mutlu, J. Ruiz, S. C. Solleder, M. A. R. Meier, *Green Chem.* **2012**, *14*, 1728–1735.
- [184] B. M. Trost, W. J. Bai, C. Hohn, Y. Bai, J. J. Cregg, *J. Am. Chem. Soc.* **2018**, *140*, 6710–6717.
- [185] G. F. Pan, X. Q. Zhu, R. L. Guo, Y. R. Gao, Y. Q. Wang, *Adv. Synth. Catal.* **2018**, *360*, 4774–4783.
- [186] C. Defieber, M. A. Ariger, P. Moriel, E. M. Carreira, *Angew. Chem. Int. Ed.* **2007**, *46*, 3139–3143.
- [187] M. Bandini, A. Melloni, A. Umani-Ronchi, *Org. Lett.* **2004**, *6*, 3199–3202.
- [188] B. M. Trost, F. D. Toste, *J. Am. Chem. Soc.* **2000**, *122*, 11262–11263.
- [189] B. M. Trost, J. Xu, T. Schmidt, *J. Am. Chem. Soc.* **2009**, *131*, 18343–18357.
- [190] M. Tanaka, H. Mitsuhashi, M. Maruno, T. Wakamatsu, *Chem. Lett.* **1994**, *23*, 1455–

## References

- 1458.
- [191] T. Diao, S. S. Stahl, *J. Am. Chem. Soc.* **2011**, *133*, 14566–14569.
- [192] Y. Xue, G. Dong, *J. Am. Chem. Soc.* **2021**, *143*, 8272–8277.
- [193] K. C. Nicolaou, Y. L. Zhong, P. S. Baran, *J. Am. Chem. Soc.* **2000**, *122*, 7596–7597.
- [194] M. J. Gallen, R. Goumont, T. Clark, F. Terrier, C. M. Williams, *Angew. Chem. Int. Ed.* **2006**, *45*, 2929–2934.
- [195] K. C. Nicolaou, T. Montagnon, P. S. Baran, Y. L. Zhong, *J. Am. Chem. Soc.* **2002**, *124*, 2245–2258.
- [196] G. A. Shevchenko, S. Dehn, B. List, *Synlett* **2018**, *29*, 2298–2300.
- [197] M. Lu, D. Zhu, Y. Lu, X. Zeng, B. Tan, Z. Xu, G. Zhong, *J. Am. Chem. Soc.* **2009**, *131*, 4562–4563.
- [198] D. B. Ramachary, C. F. Barbas, *Org. Lett.* **2005**, *7*, 1577–1580.
- [199] C. Poock, M. Kalesse, *Chem. - A Eur. J.* **2021**, *27*, 1615–1619.
- [200] J. Ashenhurst, “Reagent Friday: NBS (N-Bromo Succinimide).,” can be found under <https://www.masterorganicchemistry.com/2011/06/10/reagent-friday-nbs-n-bromo-succinimide/>, **2024** (accessed 1 October 2024).
- [201] E. Glotter, S. Greenfield, D. Lavie, *Tetrahedron Lett.* **1967**, *8*, 5261–5263.
- [202] J. Totobenazara, H. Haroun, J. Rémond, K. Adil, F. Dénès, J. Lebreton, C. Gaulon-Nourry, P. Gosselin, *Org. Biomol. Chem.* **2012**, *10*, 502–505.
- [203] S. Karella, S. Raghavan, *J. Chem. Sci.* **2020**, *132*, 96.
- [204] P. Cazeau, F. Duboudin, F. Moulines, O. Babot, J. Dunogues, *Tetrahedron* **1987**, *43*, 2075–2088.
- [205] R. Bruckner, in (Ed.: M. Harmata), Springer, Berlin, Heidelberg, **2010**, pp. 531–532.
- [206] M. Anada, M. Tanaka, K. Suzuki, H. Nambu, S. Hashimoto, *Chem. Pharm. Bull.* **2006**, *54*, 1622–1623.
- [207] G. Z. Zheng, T. H. Chan, *Organometallics* **1995**, *14*, 70–79.
- [208] K. Riener, M. P. Högerl, P. Gigler, F. E. Kühn, *ACS Catal.* **2012**, *2*, 613–621.

## References

- [209] Y. K. Mirza, P. S. Bera, S. B. Mohite, A. K. Pandey, M. Bera, *Org. Chem. Front.* **2024**, *11*, 4290–4317.
- [210] Y. Murata, D. Yamashita, K. Kitahara, Y. Minasako, A. Nakazaki, S. Kobayashi, *Angew. Chem. Int. Ed.* **2009**, *48*, 1400–1403.
- [211] F. Hessler, I. Císařová, D. Sedlák, P. Bartůněk, M. Kotora, *Chem. - A Eur. J.* **2012**, *18*, 5515–5518.
- [212] F. Peng, M. Dai, A. R. Angeles, S. J. Danishefsky, *Chem. Sci.* **2012**, *3*, 3076–3080.
- [213] S. Hiraoka, S. Harada, A. Nishida, *J. Org. Chem.* **2010**, *75*, 3871–3874.
- [214] J. Le Bras, J. Muzart, in *Org. React.* (Ed.: S.E. Denmark), John Wiley & Sons, New Jersey, **2019**, pp. 1–172.
- [215] Y. Ito, T. Hirao, T. Saegusa, *J. Org. Chem.* **1978**, *43*, 1011–1013.
- [216] X. Hu, Y. Q. Tu, E. Zhang, S. Gao, S. Wang, A. Wang, C. Fan, M. Wang, *Org. Lett.* **2006**, *8*, 1823–1825.
- [217] Z. Wang, in *Compr. Org. Name React. Reagents*, John Wiley & Sons, New Jersey, **2010**, pp. 2462–2466.
- [218] P. A. Grieco, J. L. Collins, E. D. Moher, T. J. Fleck, R. S. Gross, *J. Am. Chem. Soc.* **1990**, *112*, 9436–9437.
- [219] R. C. Larock, T. R. Hightower, G. A. Kraus, P. Hahn, D. Zheng, *Tetrahedron Lett.* **1995**, *36*, 2423–2426.
- [220] J. Q. Yu, H. C. Wu, E. J. Corey, *Org. Lett.* **2005**, *7*, 1415–1417.
- [221] H. Zhang, M. Sridhar Reddy, S. Phoenix, P. Deslongchamps, *Angew. Chem. Int. Ed.* **2008**, *47*, 1272–1275.
- [222] M. E. Jung, Y.-G. Pan, M. W. Rathke, D. F. Sullivan, R. P. Woodbury, *J. Org. Chem.* **1977**, *42*, 3961–3963.
- [223] I. Ryu, S. Murai, Y. Hatayama, N. Sonoda, *Tetrahedron Lett.* **1978**, *19*, 3455–3458.
- [224] K. C. Nicolaou, D. L. F. Gray, T. Montagnon, S. T. Harrison, *Angew. Chem. Int. Ed.* **2002**, *41*, 996–1000.

## References

- [225] J. R. Hwu, M. L. Jain, S.-C. Tsay, G. H. Hakimelahi, *Tetrahedron Lett.* **1996**, *37*, 2035–2038.
- [226] T. Ho, J. Wang, C. Li, in *Encycl. Reagents Org. Synth.*, John Wiley & Sons, New Jersey, **2007**, pp. 1–7.
- [227] American Chemical Society Green Chemistry Institute’s Pharmaceutical Roundtable, “Deprotection by Lewis Acids,” can be found under <https://reagents.acsgcipr.org/reagent-guides/boc-deprotection/list-of-reagents/lewis-acids/>, **2024** (accessed 5 October 2024).
- [228] G. J. McGarvey, in *Encycl. Reagents Org. Synth.*, John Wiley & Sons, New Jersey, **2001**, pp. 1–4.
- [229] S. C. Nigam, A. Mann, C. Georges Wermutha, M. Taddei, *Synth. Commun.* **1989**, *19*, 3139–3142.
- [230] M. E. Jung, M. J. Martinelli, G. A. Olah, G. K. S. Prakash, J. Hu, in *Encycl. Reagents Org. Synth.*, John Wiley & Sons, New Jersey, **2005**, pp. 1–12.
- [231] G. A. Olah, S. C. Narang, B. G. B. Gupta, R. Malhotra, *Angew. Chem. Int. Ed.* **1979**, *18*, 612–614.
- [232] E. F. Evans, N. J. Lewis, I. Kapfer, G. Macdonald, R. J. K. Taylor, *Synth. Commun.* **1997**, *27*, 1819–1825.
- [233] W. Zhou, T. Zhou, M. Tian, Y. Jiang, J. Yang, S. Lei, Q. Wang, C. Zhang, H. Qiu, L. He, Z. Wang, J. Deng, M. Zhang, *J. Am. Chem. Soc.* **2021**, *143*, 19975–19982.
- [234] D. Caine, in *Encycl. Reagents Org. Synth.*, John Wiley & Sons, New Jersey, **2006**, pp. 1–16.
- [235] W. C. Hoffman, in *Encycl. Reagents Org. Synth.*, John Wiley & Sons, New Jersey, **2001**, pp. 1–3.
- [236] S. G. Newman, L. Gu, C. Lesniak, G. Victor, F. Meschke, L. Abahmane, K. F. Jensen, *Green Chem.* **2014**, *16*, 176–180.
- [237] MEGlobal, “Diethylene Glycol Physical Properties,” DOI 10.1007/978-3-319-55411-2\_17 can be found under <https://www.meglobal.biz/products/diethylene-glycol/physicalproperties/>, **2024** (accessed 5 October 2024).

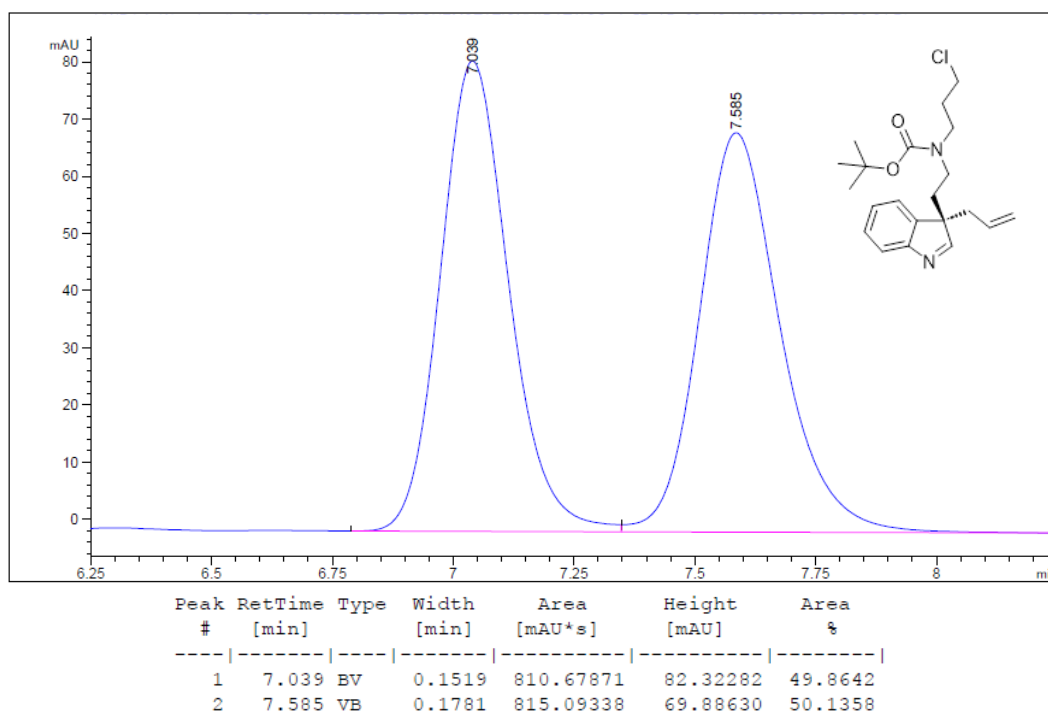
## References

- [238] T. Gaich, P. S. Baran, *J. Org. Chem.* **2010**, *75*, 4657–4673.
- [239] Y. L. He, W. M. Chen, X. Z. Feng, *J. Nat. Prod.* **1994**, *57*, 411–414.
- [240] W. R. Roush, B. B. Brown, *J. Org. Chem.* **1993**, *58*, 2151–2161.
- [241] M. Yoshida, Y. Katagiri, W. Bin Zhu, K. Shishido, *Org. Biomol. Chem.* **2009**, *7*, 4062–4066.
- [242] H. J. Jessen, A. Schumacher, F. Schmid, A. Pfaltz, K. Gademann, *Org. Lett.* **2011**, *13*, 4368–4370.
- [243] M. Frigerio, M. Santagostino, S. Sputore, *J. Org. Chem.* **1999**, *64*, 4537–4538.
- [244] M. Frigerio, M. Santagostino, *Tetrahedron Lett.* **1994**, *35*, 8019–8022.
- [245] D. B. Dess, J. C. Martin, *J. Org. Chem.* **1983**, *48*, 4155–4156.
- [246] C. T. Yang, Z. Q. Zhang, Y. C. Liu, L. Liu, *Angew. Chem. Int. Ed.* **2011**, *50*, 3904–3907.

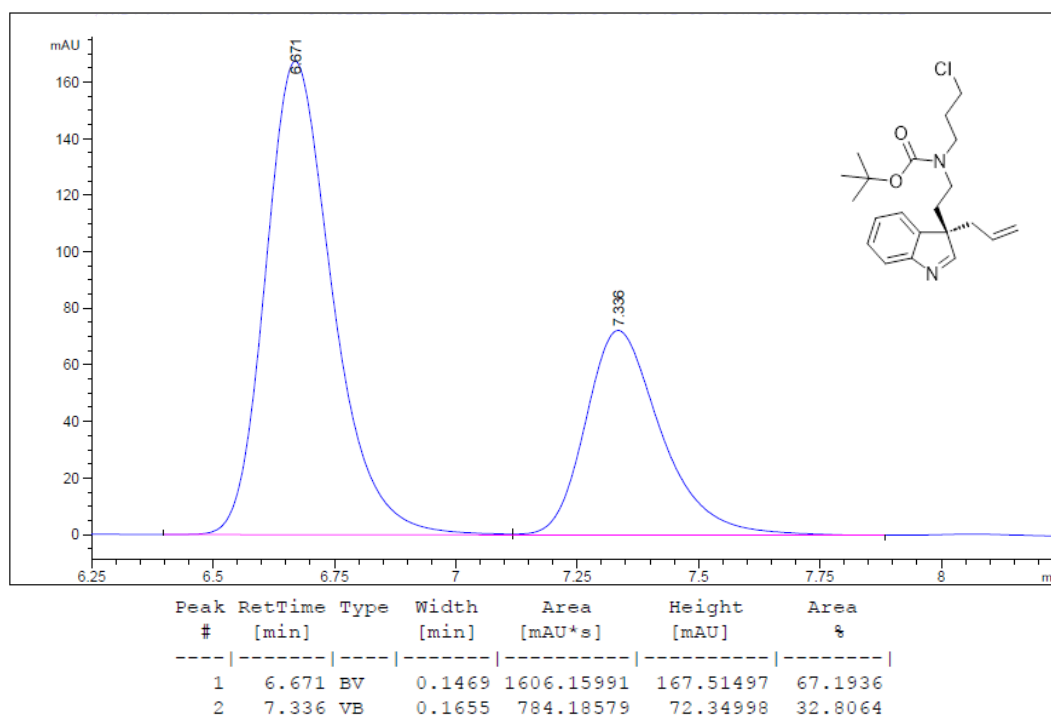
## 7 Appendices

### 7.1 Chiral HPLC Chromatograms

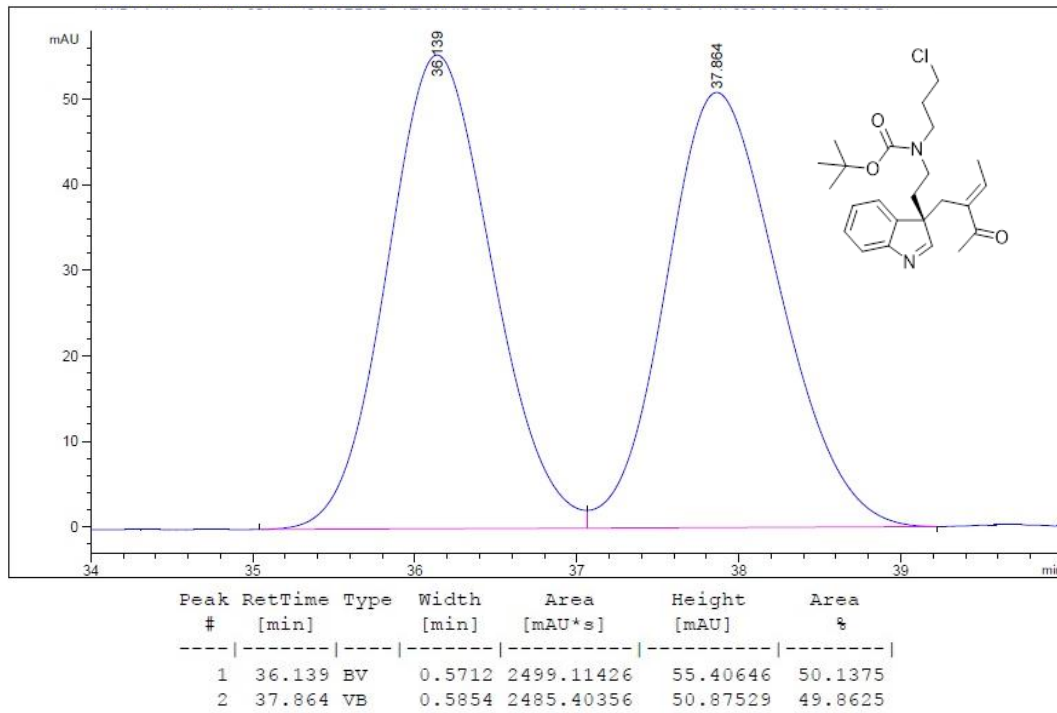
#### HPLC Chromatogram of Racemic Compound 162



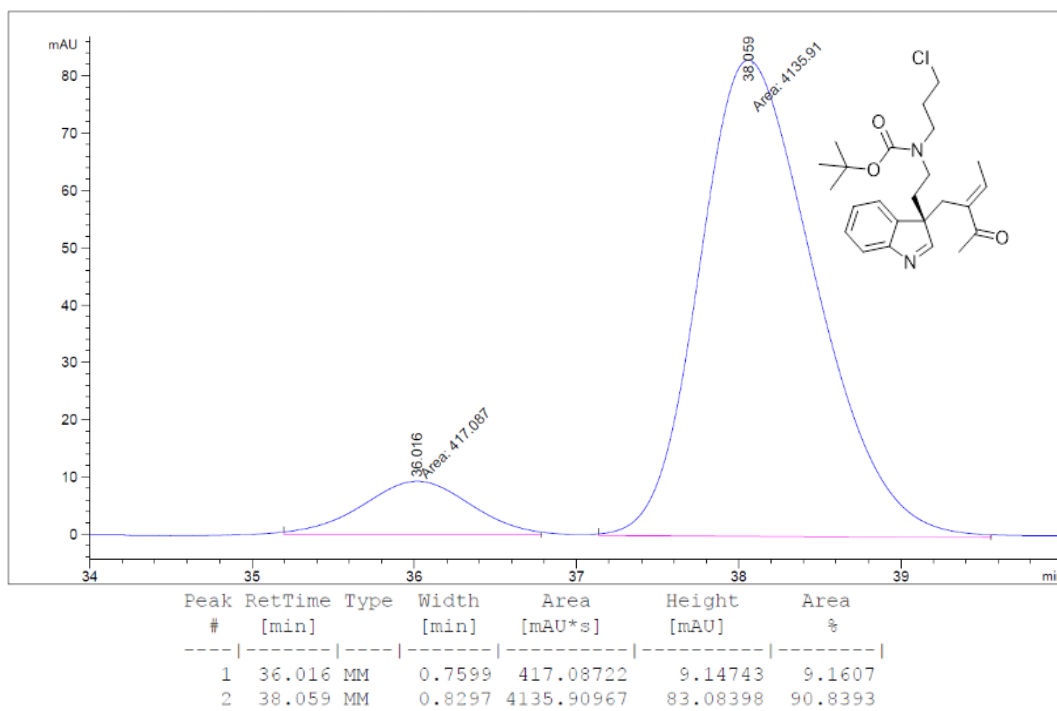
#### HPLC Chromatogram of Enantioenriched Compound 162



HPLC Chromatogram of Racemic Compound 164



HPLC Chromatogram of Enantioenriched Compound 164



## 7.2 List of Hazardous Substances

Substance Name (CAS Number)	GHS Code	Hazard Statements	Precautionary Statements
(±)-2,2'-bis(diphenylphosphino) 1,1'-binaphthyl (98327-87-8)	Not a hazardous substance		
(1 <i>S</i> )-(+)-10-Camphorsulfonic acid (3144-16-9)	GHS05	290, 314	260, 280, 303+361+353, 305+351+338, 310
(9-Fluorenylmethyl) chloroformate (28920-43-6)	GHS05	314	260, 280, 303+361+353, 304+340+310, 305+351+338, 363
( <i>R,R</i> )-DACH-phenyl Trost ligand (138517-61-0)	Not a hazardous substance		
( <i>S</i> )-(-)-1-Amino-2-(methoxymethyl)pyrrolidine (59983-39-0)	Not a hazardous substance		
( <i>S</i> )-Carreira ligand (942939-38-0)	Not a hazardous substance		
( <i>S,S</i> )-ANDEN-phenyl Trost ligand (138517-65-4)	Not a hazardous substance		
( <i>S,S</i> )-DACH-naphthyl Trost ligand (205495-66-5)	Not a hazardous substance		
( <i>S,S</i> )-DACH-phenyl Trost ligand (169689-05-8)	Not a hazardous substance		
Bis(1,5-cyclooctadiene)diiridium(I) dichloride (12112-67-3)	GHS07	302+312, 319, 315, 335	280, 261, 304, 340, 312, 301, 330, 305, 351, 338
1,1'-(Azodicarbonyl)dipiperidine (10465-81-3)	GHS07	315, 319, 335	261, 264, 271, 280, 302+352, 305+351+338
1,2-Bis(dimethylphosphino)ethane (23936-60-9)	GHS02, GHS07	225, 315, 319, 335	210, 302+352, 305+351+338
1,2-Dichloroethane (107-06-2)	GHS02, GHS06, GHS08	225, 302, 304, 315, 319, 331, 335, 350	210, 301+310, 303+361+353, 304+340+311, 331
1,4-Benzoquinone (106-51-4)	GHS02, GHS05, GHS06, GHS08, GHS09	228, 301+331, 314, 317, 335, 341, 410	210, 260, 280, 303+361+353, 304+340+310, 305+351+338
1,4-Bis(diphenylphosphino)butane (7688-25-7)	GHS07	315, 319, 335	261, 264, 271, 280, 302+353, 305+351+338
1,4-Diazabicyclo[2.2.2]octane (280-57-9)	GSH02, GSH07	228, 302, 315, 319, 335, 412	210, 261, 273, 305+351+338
1,4-Dioxane (123-91-1)	GSH02, GSH07, GSH08	225, 319, 335, 351	201, 210, 305+351+338, 308+313
1,5,7-Triazabicyclo[4.4.0]dec-5-ene (5807-14-7)	GHS05	314	260, 280, 301+330+331, 303+361+353, 304+340+310, 305+351+338
1,8-Diazabicyclo[5.4.0]undec-7-ene (6674-22-2)	GHS05, GHS06	290, 301, 314, 412	234, 273, 280, 303+361+353, 304+340+310, 305+351+338
1-Bromo-3-chloropropane (109-70-6)	GHS06, GHS08	302, 331, 335, 341, 350, 360FD, 412	201, 273, 301+312+330,

Appendices

			304+340+311, 308+313
1-Octanol (111-87-5)	GSH07	319, 412	273, 305+351+338
1-Octene (111-66-0)	GHS02, GHS08, GHS09	225, 304, 410	210, 233, 240, 273, 301+310+331
2,3-Dichloro-5,6-dicyano-1,4-benzoquinone (84-58-2)	GHS06	301	301+310
2,4,6-Trimethylbenzoic acid (480-63-7)	Not a hazardous substance		
2,6-Di- <i>tert</i> -butyl-4-methylpyridine (38222-83-2)	GHS07	302, 315, 319, 335	261, 264, 270, 301+312, 302+352, 305+351+338
2-Iodobenzoic acid (88-67-5)	GHS05, GHS07	302, 315, 318, 335	261, 280, 305+351+338
2-Methylbut-3-en-2-ol (115-18-4)	GHS02, GHS07	225, 302, 315, 319	210, 301+312+330, 302+352, 305+351+338
2-Propanol (67-63-0)	GHS02, GHS07	225, 319, 336	210, 233, 240, 241, 242, 305+351+338
3,5-Dimethylpyrazole (67-51-6)	GHS07, GHS08	302, 373	260, 264, 270, 301+312, 314, 501
4-Dimethylaminopyridine (1122-58-3)	GHS05, GHS06, GHS08, GHS09	301+331, 310, 315, 318, 370, 411	262, 273, 280, 301+310, 302+353+310, 305+351+338
4-Methoxypyridine- <i>N</i> -oxide hydrate (1122-96-9)	GHS07	315, 319, 335	302+352, 337+313, 304+340, 312, 280, 332+313
4-Nitrobenzoic acid (62-23-7)	GSH07	302, 319	305+351+338
9-Borabicyclo[3.3.1]nonane dimer (21205-91-4)	GHS02, GHS07	228, 261, 315, 319, 335	210, 231+232, 261, 305+351+338, 422
9-Borabicyclo[3.3.1]nonane solution (0.5 M in THF) (280-64-8)	GHS02, GHS07, GHS08	225, 260, 302, 319, 335, 336, 351	202, 210, 231+232, 301+312, 305+351+338, 308+313
Acetaldehyde (75-07-0)	GSH02, GSH07, GSH08	224, 319, 335, 341, 350	201, 210, 305+351+338, 308+313, 403+233
Acetic acid (64-19-7)	GHS02, GHS05	226, 314	210, 280, 301+330+331, 303+361+353, 305+351+338+ 310
Acetic acid (64-19-7)	GSH02, GSH05	226, 314	210, 280, 301+330+331, 303+361+353, 305+351+338+310
Acetic anhydride (108-24-7)	GHS02, GHS05, GHS06	226, 302, 314, 330	210, 280, 301+312, 303+361+353, 304+340+310, 305+351+338
Acetone (67-64-1)	GHS02, GHS07	225, 319, 336	210, 233, 240, 241, 242, 305+351+338
Acetonitrile (75-05-8)	GHS02, GHS07	225, 302+312+332, 319	210, 280, 301+312, 303+361+353, 304+340+312, 305+351+338

Appendices

Acrolein (107-02-8)	GHS02, GHS05, GHS06, GHS09	225 300+330, 311, 314, 410	210, 280, 301+310+ 330, 303+361+353, 304+340+310, 305+351+338+310
Allyl alcohol (107-18-6)	GHS02, GHS06, GHS09	225, 301+311+331, 315, 319, 335, 400	210, 273, 280, 301+310+330, 302+352+312, 304+340+311
Allyl chloroformate (2937-50-0)	GHS02, GHS05, GHS06	226, 301, 314, 330	210, 233, 280, 303+361+353, 304+340+310, 305+351+338
Allylpalladium(II) chloride dimer (12012-95-2)	GHS07	315	264, 280, 302+352, 332+313, 362+364
Aluminium oxide (1344-28-1)	Not a hazardous substance		
Ammonium cerium(IV) nitrate (16774-21-3)	GHS03, GHS05, GHS07, GHS09	272, 290, 302, 314, 317, 410	210, 260, 273, 280, 303+361+353, 305+351+338
Ammonium chloride (12125-02-9)	GHS07	302, 319	264, 280, 301+312, 305+351+338, 337+313, 501
<i>p</i> -Anisaldehyde dimethyl acetal (2186-92-7)	Not a hazardous substance		
Benzoic acid (65-85-0)	GSH05, GSH08	315, 318, 372	260, 280, 305+351+338+ 310
Benzyl chloromethyl ester (3587-60-8)	GHS05, GHS07, GHS08, GHS09	302+332, 315, 317, 318, 334, 335, 350, 373, 400	201, 261, 273, 280, 305+351+338, 308+313
Boron trifluoride ethyl etherate (109-63-7)	GSH02, GSH05, GSH06, GSH08	226, 302, 314, 330, 335, 373	210, 280, 303+361+353, 304+340+310, 305+351+338, 314
Bromine (7726-95-6)	GHS05, GHS06, GHS09	314, 330, 400	260, 273, 280, 303+361+353, 304+340+310, 305+351+338
Cerium(III) chloride heptahydrate (18618-55-8)	GHS05, GHS09	314, 410	260, 273, 280, 303+361+353, 304+340+310, 305+351+338
Cerium(IV) sulfate (13590-82-4)	GHS05, GHS09	314, 410	260, 273, 280, 303+361+353, 304+340+310, 305+351+338
Chlorobenzene (108 -90-7)	GHS02, GHS07, GHS09	226, 315, 332 411	210, 233, 240, 273, 303+361+353, 304+340+312
Chloroform (67-66-3)	GHS06, GHS08	302, 315, 319, 331, 336, 351, 361d, 372, 412	201, 273, 301+312+330, 302+352, 304+340+311, 308+313
Chloroform-d (865-49-6)	GHS06, GHS08	302, 315, 319, 331, 336, 351, 361d, 372	202, 301+312, 302+352, 304+340+311, 305+351+338, 308+313

Appendices

Chlorotrimethylsilane (75-77-4)	GHS02, GHS05, GHS07, GHS08	225, 301+331, 312, 314	210, 233, 280, 303+361+353, 304+340+310, 305+351+338
Chromium(VI) oxide (1333-82-0)	GHS03, GHS05, GHS06, GHS08, GHS09	270, 301+311, 314, 317, 330, 334, 335, 341, 350, 361f, 372, 410	210, 260, 280, 303+361+353, 304+340+310, 305+351+338
Cyclohexane (110-82-7)	GHS02, GHS07, GHS08, GHS09	225, 304, 315, 336, 410	210, 233, 273, 301+310, 303+361+353, 331
Cyclohexene (110-83-8)	GHS02, GHS07, GHS08, GHS09	225, 302, 304, 411	210, 233, 240, 273, 301+310, 331
Dess–Martin periodinane (87413-09-0)	GHS02	272, 315, 318, 335	210, 220, 221, 305+351+338, 370+378
Dichloromethane (79-09-2)	GSH07, GSH08	315, 319, 336, 351	201, 302+352, 305+351+338, 308+313
Diethyl ether (60-29-7)	GHS02, GHS07	224, 302, 336	210, 233, 240, 241, 301+312, 403+233
Diethylene glycol (111-46-6)	GHS07	302	264, 270, 301+312, 501
Diisobutylaluminium hydride solution (1191-15-7)	GSH02, GSH05, GSH07, GSH08	225, 250, 260, 304, 314, 336, 361d, 373, 412	210, 231+232+280+ 301+330+331, 303+361+353, 305+350+338+ 310, 370+378
Diisopropyl azodicarboxylate (2446-83-5)	GSH07, GSH08, GSH09	315, 319, 335, 351, 373, 411	201, 260, 264, 273, 280, 391
Diisopropylamine (108-18-9)	GSH02, GSH05, GSH06	225, 302, 314, 33	210, 280, 303+361+353, 304+340+310, 305+351+338, 403+233
Dimethyl carbonate (616-38-6)	GHS02	225	210, 233, 240, 241, 242, 243
Dimethyl sulfoxide (67-68-5)	Not a hazardous substance		
Dimethyl sulfoxide-d <sub>6</sub> (2206-27-1)	Not a hazardous substance		
Dimethylphenylphosphine (672-66-2)	GHS02, GHS07	226, 315, 319, 335	210, 302+352, 305+352+338
Di- <i>tert</i> -butyl dicarbonate (24424-99-5)	GHS02,GHS05, GHS06	226, 315, 317, 318, 330, 335	210, 233, 280, 303+361+353, 304+340+310, 305+351+338
Ethanol (64-17-5)	GHS02, GHS07	225, 319	210, 233, 240, 241, 242, 305+351+338
Ethyl acetate (141-78-6)	GHS02, GHS07	225, 319, 336	210, 233, 240, 241, 242, 305+351+338
Ethyl acetoacetate (141-97-9)	Not a hazardous substance		
Ethyl acrylate (140-88-5)	GSH02, GSH06	225, 302+312, 315, 317, 319, 331, 335, 412	210, 233, 261, 280, 370+378, 403+233
Ethyl diazoacetate (623-73-4)	GHS02, GHS07, GHS08	226, 242, 302, 315, 319, 336, 351	201, 210, 235, 308+313, 370+378, 403

*Appendices*

Ethyl triphenyl phosphonium bromide (1530-32-1)	GHS05, GHS06	301, 318, 412	264, 270, 273, 280, 301+310, 305+351+338
Ethylene glycol (107-21-1)	GHS07, GHS08	302, 373	260, 264, 270, 301+312, 314, 501
Formic acid (64-18-6)	GSH02, GSH05, GSH06	226, 302, 314, 331	210, 280, 301+312, 303+361+353, 304+340+310, 305+351+338
Hexamethyldisilazane (999-97-3)	GHS02, GHS06	225, 302+332, 311, 412	210, 273, 280, 301+312, 303+361+353, 304+340+312
Hydrazine monohydrate (7803-57-8)	GHS02, GHS05, GHS06, GHS08, GHS09	226, 301+311, 314, 317, 330, 350, 410	210, 273, 280, 303+361+353, 304+340+310, 305+351+338
Hydrochloric acid (37%) (76447-01-0)	GHS05, GHS07	290, 314, 335	234, 261, 271, 280, 303+361+353, 305+351+338
Hydrogen bromide solution (33 wt.% in acetic acid)	GHS05, GHS07	290, 314, 335	234, 261, 271, 280, 303+361+353, 305+351+338
Hydrogen fluoride pyridine (62778-11-4)	GSH05, GSH06	300+310+330, 314	260, 262, 280, 301+310+330, 303+361+353, 304+340+310, 305+351+338+ 310, 403+233
Hydrogen peroxide solution (30% wt.% in H <sub>2</sub> O)	GHS03, GHS05, GHS07	272, 302, 314, 335, 412	210, 273, 280, 301+312, 303+361+353, 305+351+338
Imidazole (288-32-4)	GSH05, GSH07, GSH08	302, 314, 360D	201, 260, 280, 303+361+353, 305+351+338+ 310, 308+313
Iodic acid (7782-68-5)	GHS03, GHS05	272, 314	210, 220, 260, 280, 303+361+353, 305+351+338
Iodotrimethylsilane (16029-98-4)	GHS02, GHS05	225, 314	210, 233, 240, 280, 303+361+353, 305+351+338
Isobutyl chloroformate (543-27-1)	GSH02, GSH05, GSH06	226, 302, 314, 331	210, 280, 301+310+330, 303+361+353, 304+340+311, 305+351+338
KHMDS solution (0.5M in toluene) (40949-94-8)	GHS02, GHS05, GHS07, GHS08	225, 304, 314, 336, 361d, 373, 412	210, 280, 301+310+331, 303+361+353, 305+351+338+ 310
Lithium (7439-93-2)	GHS02, GHS05	260, 314	223, 231+232, 260, 280, 303+361+353, 305+351+338
Lithium bis(trimethylsilyl)amide solution (1.0 M in THF)	GSH02, GSH05, GSH07, GSH08	225, 302, 314, 335, 336, 351	201, 210, 280, 303+361+353, 305+351+338+

Appendices

			310, 308+313
Lithium hydroxide (1310-65-2)	GHS05, GHS07	302, 314	260, 270, 280, 301+312, 303+361+353, 305+351+338
Lithium <i>tert</i> -butoxide (1907-33-1)	GHS02, GHS06, GHS07	251, 302, 314	235, 260, 280, 301+312, 303+361+353, 305+351+338
L-Selectride® solution (1.0 M in THF) (38721-52-7)	GHS02, GHS05, GHS07, GHS08	225, 250, 260, 314, 335, 351	210, 231+232, 280, 305+351+338, 370+378, 422
Magnesium sulfate (7487-88-9)	Not a hazardous substance		
Manganese(III) acetate dihydrate (19513-05-4)	Not a hazardous substance		
Manganese(IV) oxide (1313-13-9)	GHS07, GHS08	302+332, 373	260, 264, 270, 301+312, 304+340+312, 314
Methanol (67-56-1)	GSH02, GSH06, GSH08	225, 301+311+331, 370	210, 280, 301+310+330, 302+352+312, 304+340+311
Methanol-d (1455-13-6)	GHS02, GHS06, GHS08	225, 301+311+331, 370	210, 233, 280, 301+310, 303+361+353, 304+340+311
Methyl acrylate (96-33-3)	GHS02, GHS07	225, 302+312, 315, 317, 319, 331, 335, 412	210, 233, 261, 273, 280, 303+361+353
Methyl chloroformate (79-22-1)	GHS02, GHS05, GHS06	225, 302+312, 314, 330	210, 280, 301+312, 303+361+352, 304+340+310, 305+351+338
Methyl vinyl ketone (78-94-4)	GSH02, GSH05, GSH06, GSH09	225, 300+310+330, 314, 317, 410	210, 280, 301+310+330, 303+361+353, 304+340+310, 305+351+338+ 310
<i>N,N</i> -Diisopropylethylamine (7087-68-5)	GHS02, GHS05, GHS06	225, 302, 318, 331, 335	210, 261, 304+340, 305+351+338, 370+378, 403+233, 403+235, 501
<i>N,N</i> -Dimethylformamide (68-12-2)	GHS02, GHS07, GHS08	226, 312+332, 319, 360D	210, 280, 303+361+353, 304+340+312, 305+351+338, 308+313
Naphthalene (91-20-3)	GHS02, GHS07, GHS08, GHS09	228, 302, 351, 410	210, 273, 280, 308+313
<i>N</i> -Bromosuccinimide (128-08-5)	GHS03, GHS05, GHS07, GHS08, GHS09	272, 290, 315, 317, 319, 341, 400	210, 273, 280, 302+352, 305+351+338, 308+313
<i>n</i> -Butyllithium solution (1.6 M in hexanes) (109-72-8)	GSH02, GSH05, GSH07, GSH08, GSH09	225, 250, 261, 304, 314, 336, 361f, 373, 411	210, 222, 231+232, 261, 273, 422

Appendices

<i>N</i> -Chlorosuccinimide (128-09-6)	GHS05, GHS07, GHS09	290, 302, 314, 335, 410	260, 273, 280, 301+312, 303+361+353, 305+351+338
Nitrosobenzene (586-96-9)	GHS06	301, 312+332	261, 264, 280, 301+310, 302+352+312, 304+340+312
Oxone® (70693-62-8)	GHS05, GHS07, GHS09	302, 314, 411	260, 273, 280, 301+312, 303+361+353, 305+351+338
Oxygen (7782-44-7)	GHS03	270, 280	220, 410+403
Palladium hydroxide on carbon (20 wt.%) (12135-22-7)	Not a hazardous substance		
Palladium on carbon (10 wt.%) (Pd/C)	GHS02	228	210, 240, 241, 280, 370+378
Palladium(II) acetate (3375-31-3)	GHS05, GHS07, GHS09	317, 318, 410	261, 272, 273, 280, 302+353, 305+351+338
Petroleum ether 40–65 (64742-49-0)	GHS02, GHS07, GHS08, GHS09	225, 304, 315, 336, 411	210, 280, 301+310, 331, 303+361+353, 304+340
Phosphomolybdic acid hydrate (51429-74-4)	GHS03, GHS05	272, 314	210, 220, 260, 280, 303+361+353, 305+351+338
Phosphorus tribromide (7789-60-8)	GHS05, GHS07	314, 335	261, 280, 305+351+338, 310
Potassium carbonate (584-08-7)	GHS07	315, 319, 335	305+351+338
Potassium hydroxide (1310-58-3)	GHS05, GHS07	290, 302, 314	234, 260, 280, 301+312, 303+361+352, 305+351+338
Potassium permanganate (7722-64-7)	GHS03, GHS05, GHS07, GHS08, GHS09	272, 302, 314, 361d, 373, 410	210, 260, 273, 280, 303+361+353, 305+351+338
Potassium phosphate monobasic (7778-77-0)	Not a hazardous substance		
Potassium <i>tert</i> -butoxide (865-47-4)	GHS02, GHS05	228, 260, 314	210, 231+232, 260, 280, 303+361+353, 305+351+338
Potassium thioacetate (10387-40-3)	Not a hazardous substance		
Propane-1,3-dithiol (109-80-8)	GHS02, GHS06	226, 301, 315	210, 233, 240, 241, 301+310, 303+361+353
<i>p</i> -Toluenesulfonic acid monohydrate (6192-52-5)	GHS05	290, 314, 412	234, 260, 273, 280, 303+361+353, 305+351+338
Pyridine (110-86-1)	GHS02, GHS07	225, 302+312+332, 315, 319	210, 280, 301+312, 303+361+353, 304+340+312, 305+351+338
Rhodium(II) acetate dimer (15956-28-2)	GHS07	315, 319	302+352, 305+351+338
Rhodium(III) chloride trihydrate (13569-65-8)	GHS05, GHS07, GHS08, GHS09	290, 302, 318, 341, 410	202, 273, 280, 301+312, 305+351+338, 308+313

*Appendices*

Scandium(III) triflate (144026-79-9)	Not a hazardous substance		
Selenium dioxide (7446-08-4)	GHS06, GHS08, GHS09	301+331, 373, 410	260, 264, 273, 301+310, 304+340+311, 314
Silica gel (7631-86-9)	Not a hazardous substance		
Sodium (7440-23-5)	GHS02, GHS05	260, 314	223, 231+232, 260, 280, 303+361+353, 305+351+338
Sodium periodate (7790-28-5)	GSH03, GSH05, GSH08, GSH09	290, 314	260, 280, 303+361+353, 305+351+338, 310
Sodium borohydride (16940-66-2)	GHS02, GHS05, GHS06, GHS08	260, 301, 314, 360FD	231+232, 260, 280, 303+361+353, 304+340+310, 305+351+338
Sodium carbonate (497-19-8)	GHS07	319	264, 280, 305+351+338, 337+313
Sodium chloride (7647-14-5)	Not a hazardous substance		
Sodium hydride (60% dispersion in mineral oil) (7646-69-7)	GHS02, GHS05	228, 260, 290, 314	210, 231+232, 260, 280, 303+361+353, 305+351+338
Sodium hydrogen carbonate (144-55-8)	Not a hazardous substance		
Sodium hydroxide (1310-73-2)	GHS05	290, 314	234, 260, 280, 303+361+353, 304+340+310, 305+351+338
Sodium iodide (7681-82-5)	GHS07, GHS08, GHS09	315, 319, 372, 400	260, 264, 273, 302+352, 305+351+338, 314
Sodium phosphate dibasic (7558-79-4)	Not a hazardous substance		
Sodium sulfate (7757-82-6)	Not a hazardous substance		
Sodium thiosulfate (7772-98-7)	Not a hazardous substance		
Sulfuric acid (min. 95%) (7664-93-9)	GHS05	290, 314	234, 280, 303+361+353, 304+340+310, 305+351+338, 363
<i>tert</i> -Butyl acetate (540-88-5)	GSH02	225	210
<i>tert</i> -Butyl hydroperoxide solution (5.0–6.0 M in decane) (75-91-2)	GHS02, GHS05, GHS06, GHS08, GHS09	226, 242, 302, 304, 311, 314, 317, 330, 335, 341, 411	210, 280, 301+330+331, 303+361+353, 304+340+310, 305+351+338, 370+378
<i>tert</i> -Butyl hydroperoxide solution (70 wt.% in H <sub>2</sub> O) (75-91-2)	GHS02, GHS05, GHS06, GHS08, GHS09	226, 242, 302, 311, 314, 317, 330, 335, 341, 411	210, 280, 303+361+353, 304+340+310, 305+351+338, 370+378
<i>tert</i> -Butyl methyl ether (1634-04-4)	GHS02, GHS07	225, 315	210, 233, 240, 241, 242, 303+361+353
<i>tert</i> -Butyldimethylsilyl chloride (18162-48-6)	GSH02, GSH05, GSH09	228, 314, 411	210, 260, 273, 280, 303+361+353, 305+351+338+310
Tetrabutylammonium fluoride solution (429-41-4)	GSH02, GSH05, GSH07, GSH08	225, 314, 335, 351	201, 210, 233, 280, 303+361+353, 305+351+338

*Appendices*

Tetrahydrofuran (109-99-9)	GSH02, GSH07, GSH08	225, 302, 319, 335, 351	201, 210, 301+312+330, 305+351+338, 308+313
Tetrakis(triphenylphosphine) palladium(0) (14221-01-3)	None	302, 317, 413	261, 264, 273, 280, 301+312, 302+352
Thionyl chloride (7719-09-7)	GHS05, GHS07	302+332, 314, 335	261, 280, 301+312, 303+361+353, 304+340+310, 305+351+338
Tin(II) chloride (7772-99-8)	GHS05, GHS07, GHS08	290, 302+332, 314, 317, 335, 373, 412	260, 273, 280, 303+361+353, 304+340+312, 305+351+338+310
Toluene (108-88-3)	GSH02, GSH07, GSH08	225, 304, 314, 336, 361d, 373, 412	201, 210, 273, 301+310+331, 302+352, 308+313
Tri(2-furyl)phosphine (5518-52-5)	Not a hazardous substance		
Trichloroacetic acid (76-03-9)	GHS05, GHS09	314, 410	260, 273, 280, 303+361+353, 304+340+310, 305+351+338
Triethylamine (121-44-8)	GHS02, GHS05, GHS06	225, 302, 311+331, 314, 335	210, 280, 301+330+331, 303+361+353, 304+340+311, 305+351+338+ 310
Triethylborane solution (1.0 M in hexanes) (97-94-9)	GHS02, GHS05, GHS07, GHS08, GHS09	225, 304, 314, 336, 361f, 373, 411	210, 280, 301+310+331, 301+330+331, 303+361+353, 305+351+338+ 310
Triethylborane solution (1.0 M in THF) (97-94-9)	GHS02, GHS05, GHS07, GHS08	225, 250, 261, 302, 314, 335, 336, 351	210, 231+232, 280, 303+361+353, 305+351+338, 370+378
Triethylsilane (617-86-7)	GHS02, GHS07	225, 315, 319, 335	210, 233, 240, 241, 303+361+353, 305+351+338
Trifluoroacetic acid (76-05-1)	GHS05, GHS07	314, 332, 412	261, 273, 280, 303+361+353, 304+340+310, 305+351+338
Triisopropylsilane (6485-79-6)	GHS02	226	210, 233, 240, 241, 242, 243
Trimethyl orthoformate (149-73-5)	GHS02, GHS07	225, 319	210, 233, 240, 214, 242, 305+351+338
Trimethylphosphine solution (1.0 M in toluene) (594-09-2)	GHS02, GHS07, GHS08	225, 304, 315, 336, 361d, 373, 412	201, 210, 273, 301+310+331, 302+353, 308+313
Tri- <i>n</i> -butylphosphine (998-40-3)	GHS02, GHS05, GHS07, GHS09	251, 302, 314, 411	235, 273, 280, 301+312, 303+361+353, 305+351+338
Triphenyl phosphite (101-02-0)	GHS07, GHS08, GHS09	302, 315, 317, 319, 373, 410	273, 280, 301+312, 302+352, 305+351+338, 314

## Appendices

Triphenylphosphine (603-35-0)	GSH02, GSH05, GSH07	302, 317, 318, 372	280, 301+312+330, 302+352, 305+351+338+ 310, 314
Tris(dibenzylideneacetone) dipalladium(0) (51364-51-3)	GHS07, GHS09	317, 411	261, 272, 273, 280, 302+352, 333+313
Tris(dibenzylideneacetone) dipalladium(0)-chloroform adduct (52522-40-4)	GHS07, GHS08	302, 315, 351	201, 202, 264, 301+312, 302+353, 308+313
Tris(hydroxymethyl) aminomethane hydrochloride (1185-53-1)	GHS07	315, 319	264, 280, 302+352, 305+351+338, 332+313, 337+313, 362+364
Tris(triphenylphosphine) rhodium(I) chloride (14694-95-2)	GHS07	317, 413	261, 272, 273, 280, 302+353, 333+313
Trityl chloride (76-83-5)	GHS05	314	260, 280, 303+361+353, 304+340+310, 305+351+338, 363
Tryptamine (61-54-1)	GHS05, GHS07	302, 314, 335	260, 280, 301+312+330, 301+330+331, 303+360+353, 305+351+338+ 310
Vinyl acetate (108-05-4)	GHS02, GHS07, GHS08	225, 332, 335, 351, 412	202, 210, 233, 273, 304+340+312, 308+313
Zinc bromide (7699-45-8)	GHS05, GHS07, GHS09	302, 314, 317, 411	260, 273, 280, 301+312, 303+361+353, 305+351+338

### GHS Hazard Pictograms:



GHS01



GHS02



GHS03



GHS04



GHS05



GHS06



GHS07



GHS08



GHS09

### **7.3 Acknowledgments**

I would like to thank Prof. Dr. Christian B. W. Stark for the opportunity to work on this project and in his group. I am grateful for the support during manuscript preparation and the opportunity to participate in conferences and workshops.

I would also like to thank Prof. Dr. Chris Meier for taking the time to evaluate this thesis and Prof. Dr. Ralph Holl and Prof. Dr. Louisa Temme for serving on the examination committee.

I would like to thank Dr. Gunnar Ehrlich, Dr. Katie Grant, Finni Speckenheuer, Lukas Paffrath, Markus Winkler and Dr. Jelena Berl for the time and effort that they have devoted to proofreading this thesis.

I would also like to thank all members of the Stark Group, past and present, for their advice and suggestions and for creating such a welcoming and friendly work atmosphere. I would like to pay special thanks to Dr. Matthias Böge for his generosity with his time and knowledge and to Lilia Marcinkiewicz for her practical support and patience with my German. I would also like to acknowledge my fellow members of 'Team Prenylierung' for the insightful and helpful discussions on the topic of allylic substitution. Particularly Leon Sander, who has taken the time to share his expertise on this topic. I would also like to thank the students who have worked with me on this project: Ben Bimberg and Marie Bode.

I would like to acknowledge the technical staff at Universität Hamburg, in particular Claudia Wontorra for her assistance with the high-temperature NMR measurements.

I would also like to thank my fellow ISP-assistants for the time spent together inside and outside of the teaching course.

Finally, I would like to thank my family and friends, near and far, for their moral support throughout. I would like to pay special tribute to Moritz for his understanding, for always lending an ear and for making Hamburg home these past few years.

#### **7.4 Statutory Declaration**

I hereby declare and affirm that this doctoral dissertation is my own work and that I have not used any aids and sources other than those indicated. If electronic resources based on generative artificial intelligence (gAI) were used in the course of writing this dissertation, I confirm that my own work was the main and value adding contribution and that complete documentation of all resources used is available in accordance with good scientific practice. I am responsible for any erroneous or distorted content, incorrect references, violations of data protection and copyright law or plagiarism that may have been generated by the gAI.

Hamburg, the 30<sup>th</sup> of December 2024

A handwritten signature in black ink, appearing to read 'codameu', written in a cursive style.

MChem Charlotte O'Donnell